CARBONIC ANHYDRASE ACTIVITY AND ITS ROLE IN MEMBRANE H^+-EQUIVALENT TRANSPORT IN MAMMALIAN VENTRICULAR MYOCYTES

Francisco C. Villafuerte

Exeter College

University of Oxford

Thesis submitted for the degree of Doctor of Philosophy

Michaelmas Term 2007

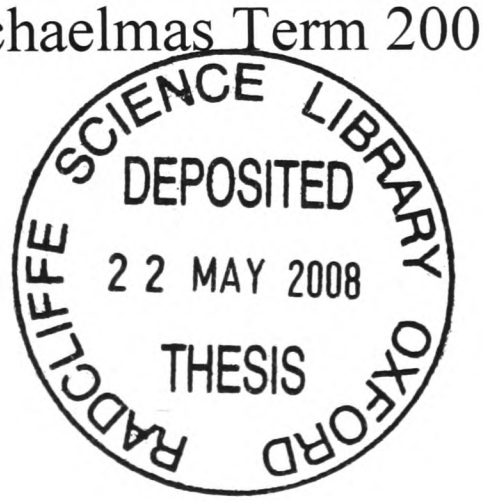

Abstract

Carbonic anhydrase activity and its role in membrane H^+-equivalent transport in mammalian ventricular myocytes

Francisco C. Villafuerte
Exeter College, Oxford
Doctor of Philosophy (D.Phil.) Thesis, Michaelmas Term, 2007

Carbonic anhydrases (CAs) are fundamental and ubiquitous enzymes that catalyse the reversible hydration of CO_2 to form HCO_3^- and H^+ ions. Evidence derived from heterologous expression systems has led to the proposal of a novel role for CA in intracellular pH regulation, where its physical and functional coupling to membrane H^+-equivalent transport proteins appears to enhance their activity. It has yet to be established whether such a functional association occurs naturally in wild-type cells. Additional evidence on CA activity *in-vitro*, has also suggested that certain CA isoforms are regulated by physiological changes of pH, an effect that may then affect their ability to enhance H^+-equivalent transport. No information, however, exists on the pH sensitivity of CA in intact cells. Finally, pharmacological inhibition of CA activity has been reported previously for various compounds, in addition to those designed specifically as CA inhibitors. It is possible that some compounds, currently used to inhibit membrane H^+ transport, may also target CA. The present work has examined functional aspects of CA activity in ventricular myocytes isolated enzymically from rat heart, focusing on the potential role of CA in controlling sarcolemmal Na^+/H^+ exchange (NHE) and sarcolemmal Na^+-HCO_3^- cotransport (NBC). NHE and NBC activity were estimated from the rate of recovery of intracellular pH (pH_i), following an intracellular acid load in myocytes loaded with carboxy-SNARF-1 (a pH-sensitive fluorescent dye, used to measure pH_i). In other experiments, *in-vitro* CA activity was assessed from the time-course of pH change after addition of CO_2-saturated water to a buffered solution containing either CA II or a cardiac homogenate. In further experiments, intracellular CA activity was assessed from the rate of CO_2-induced fall of pH_i. Three major results emerged. (i) In intact myocytes, CA activity doubles acid extrusion on sarcolemmal NBC, but has no effect on NHE activity. Facilitation of NBC activity by CA is likely to be mediated by an intracellular CA isoform. (ii) *In-vitro* and intracellular CA activity displays strong pH-dependence within the physiological pH range, activity declining with a fall of pH. (iii) The NHE inhibitor, cariporide, the bicarbonate transport inhibitors DIDS (4,4'-diisothiocyanatostilbene-2,2'-disulphonic acid) and S0859 (an experimental compound from Sanofi-Aventis), and the aquaporin blocker, pCMBS (p-chloromercuribenzene sulphonate), all showed strong inhibitory activity towards CA *in-vitro*, but had no effect on intracellular CA activity.

Overall, the work provides the first clear demonstration of a functional role of CA activity in H^+-equivalent transport in a wild-type cell. CA thus represents an important regulatory mechanism of H^+-equivalent transport. The pH sensitivity displayed by *in-vitro* and intracellular CA activity may also have significant functional consequences for pH_i regulation. CA inhibition by various membrane transport inhibitors highlights the need for careful drug and experimental design, to avoid secondary inhibition of CA activity and its side-effects. The present work thus provides insight into the functional roles of CA, plus important new information on the enzyme's pharmacological properties.

ACKNOWLEDGEMENTS

Firstly, I would like to thank Professor Richard Vaughan-Jones for his supervision and guidance during my time in Oxford. I am grateful for his support, objectivity, encouragement and patience, and for the opportunity to work in his laboratory. I also have greatly appreciated his advice, comments, and help on the early versions of this manuscript.

I would like to thank the members of the group, particularly Dr. Pawel Swietach and Mr. Philip Cobden for their friendship and support during these years. A special thanks to Pawel for all his help with the experimental techniques and analysis of data. To both of them, thanks for such an enjoyable time at work.

I am grateful to Professor Kenneth W. Spitzer at the University of Utah, USA, for his kindness, patience, and useful advice during my electrophysiology training at CVRTI, Utah and also in Oxford.

I would like to thank my family, specially my parents. Mom and Dad were always there to give me their support, love, and encouragement during these years away from home. I cannot recall a single day Mom did not talk to me over the phone or the internet!

I would also like to thank all my close friends in Lima and the USA for showing care and support at all times.

This work was possible thanks to the generous support of The Wellcome Trust and the Overseas Research Student (ORS) Award Scheme.

Contents

Abbreviations

AE	Anion (Cl^-/HCO_3^-) Exchange
AQP	Aquaporin
ATZ	Acetazolamide
CA	Carbonic Anhydrase
CAPSO	3-(Cyclohexylamino)-2-hydroxy-1-propanesulphonic acid
CHE	Cl^-/OH^- Exchange
DIDS	4,4'-diisothiocyanatostilbene-2,2'-disulphonic acid
DMA	5-(N,N-dimethyl)amiloride
EGTA	Ethylene glycol-bis(2-aminoethylether)-*N,N,N',N'*-tetraacetic acid
EIPA	5-(N-Ethyl-N-isopropyl) amiloride
E_{NBC}	NBC equilibrium potential
ETZ	Ethoxyzolamide
GPI	Glycosylphosphatidylinositol
Hepes	4-(2-Hydroxyethyl)piperazine-1-ethanesulphonic acid
HOE 642	4-isopropyl-3-(methylsulphonyl)benzoyl guanidine methanesulphonate
HOE-694	3-methylsulphonyl-4-piperidinobenzoyl guanidine methanesulphonate
I_{NBC}	NBC current
J^H	Acid efflux
J_{NBC}	NBC-mediated acid efflux
J_{NHE}	NHE-mediated acid-efflux
MCT	Monocarboxylate Transporter
MES	2-(N-Morpholino) ethanesulphonic acid
NBC	Na^+-HCO_3^- co-transport
NHE	Na^+/H^+ exchange
NMDG	N-Methyl-D-Glucamine
pCMBS	p-chloromercuribenzene sulphonate
pH_i	Intracellular pH
pH_o	Extracellular pH

PKA	Protein kinase A
PKC	Protein kinase C
SR	Sarcoplasmic reticulum
β	Buffering capacity
β_{CO2}	CO_2-dependent buffering capacity
β_{int}	Intrinsic buffering capacity
β_{tot}	Total intracellular buffering capacity
$[Ca^{2+}]_i$	Intracellular Ca^{2+} concentration
$[K^+]_o$	Extracellular K^+ concentration
$[Na^+]_i$	Intracellular Na^+ concentration

CHAPTER 1

GENERAL INTRODUCTION

1.1. Importance of Intracellular pH

A basic property of life is the ability of an organism to regulate its internal environment to maintain a stable, constant condition. Multiple dynamic equilibrium adjustments and regulation mechanisms make this possible. This property of living organisms is known as homeostasis. Among the most important cellular homeostatic mechanisms are those which regulate intracellular pH (pH_i). pH_i is defined as the negative logarithm of the activity of hydrogen (H^+) ions and is given by the following equation:

$$pH_i = -\log_{10} a_{H^+} = -\log(\gamma_{H^+}[H^+]_i)$$

where a_{H^+} is H^+-ion activity, γ_{H^+} the H^+ activity coefficient, and $[H^+]_i$ is the concentration of H^+-ions in the cytosolic space.

pH_i influences the activity of virtually all cellular functions. Metabolic reactions can be significantly affected by pH_i because of its influence on both protein conformation and enzyme activity (Andres et al., 1990; Bock & Frieden, 1976a; Bock & Frieden, 1976b; Dobson et al., 1986; Erecinska et al., 1995; Hochachka & Mommsen, 1983; Miccoli et al., 1996; Roos & Boron, 1981). Ion channel conductivity (Bear et al., 1988; Blatz, 1984), cell-cell coupling (Francis et al., 1999; Sorgen et al., 2004; Spray & Burt, 1990; Swietach et al., 2007a), intracellular signalling and cell cycle (Busa & Nuccitelli,

1984), structure and function of the cytoskeleton (De Brabander et al., 1982; Sampath & Pollard, 1991), gene expression (Isfort et al., 1993), cell survival and apoptosis (Shrode et al., 1997) are all modulated by pH_i.

pH_i also plays a particularly important role in the modulation of cardiac function as it has significant effects on Ca^{2+}-signalling, contractility, excitability and rhythm (Orchard & Cingolani, 1994; Orchard & Kentish, 1990). Several mechanisms account for the effect of pH_i on cardiac function. Intracellular acidosis for example, affects Ca^{2+}-signalling by decreasing ionic currents through voltage-gated Ca^{2+} channels (Blanchard et al., 1984; Blanchard & Solaro, 1984; Irisawa & Sato, 1986; Sato et al., 1985), reducing Ca^{2+} release through ryanodine receptors in response to sarcolemmal depolarisation (Balnave & Vaughan-Jones, 2000; Choi et al., 2000a; Xu et al., 1996), and by reducing the activity of Ca^{2+}-ATPase, hence transiently reducing SR loading (Orchard & Kentish, 1990). Mechanisms related to reduced contractility caused by intracellular acidosis include reduced myosin ATPase activity (Kentish & Nayler, 1979), diminished binding of Ca^{2+} to myofilaments (Allen & Orchard, 1983; Fabiato & Fabiato, 1978), or more specifically, to Troponin C (Blanchard et al., 1984; Blanchard & Solaro, 1984), and Ca^{2+}-independent reduction in actin-myosin cross-bridge formation (Swartz et al., 1999). Also, acidosis can affect cardiac excitability and rhythm by decreasing voltage-gated Na^+ channel current (Zhang & Siegelbaum, 1991), retarding the spread of the action potential through gap-junctions to neighbouring ventricular myocytes (Spray et al., 1985), and also lengthening of action potential duration (Janse & Wit, 1989) probably due to inhibition of repolarising K^+ currents (Komukai et al., 2002).

This list of mechanisms, although not exhaustive, is sufficient to illustrate the powerful and multifaceted influence pH_i has on cell and, in particular, cardiac myocyte function, and therefore the fundamental significance of efficient pH_i regulatory mechanisms. These mechanisms are particularly important since changes in pH_i occur during normal activity, e.g. during whole-body acid-base disturbances such as changes in ventilation (Roos & Boron, 1981), or in response to changes in the metabolic work-load placed on the heart (Bountra *et al.*, 1988; Elliott *et al.*, 1994). Events that affect extracellular pH (pH_o) would also result in a change of pH_i, and thus of cellular function.

It has been shown that in the physiological range, pH_i is almost linearly related to pH_o, with a 1 unit change in pH_o resulting in a 0.3-0.4 unit change in pH_i (Ellis & Thomas, 1976; Sun *et al.*, 1996; Vaughan-Jones, 1986). Since it is essential to maintain a constant pH_i, major homeostatic mechanisms cells have evolved to counterbalance any rise or fall in pH_i created by these internal and external events.

1.2. Regulation of Intracellular pH

In the event of an intracellular acid or alkali load, changes in pH_i are minimised by intracellular buffers. Any displacements of pH_i then stimulate surface membrane acid/base transporters to add or remove H^+ (or their ionic equivalents), thereby restoring a favourable resting pH_i. The steady-state level to which pH_i is regulated depends on the balance between acid-equivalent extruders and acid-equivalent loaders. In mammalian cardiac cells, pH_i is normally controlled by four sarcolemmal H^+-equivalent transport processes. Na^+/H^+ exchange (NHE) and Na^+-HCO_3^- co-transport (NBC) are activated at low pH_i to extrude acid (Dart & Vaughan-Jones, 1992; Lagadic-Gossmann *et al.*, 1992).

High pH_i, on the other hand, activates Cl^-/HCO_3^- (anion) exchange (AE) and Cl^-/OH^- exchange (CHE) that engage in H^+-equivalent loading (Sun *et al.*, 1996; Vaughan-Jones, 1979). Extracellular pH (pH_o) also allosterically regulates the activity of these sarcolemmal ionic transporters but in a manner opposite to pH_i (Leem *et al.*, 1999; Wu & Vaughan-Jones, 1997). The activity of all four sarcolemmal transporters working in concert determines steady-state pH_i. Additionally, a reversible monocarboxylate transporter (MCT) which co-transports H^+ with anions such as lactate also participates in pH_i regulation under post-ischaemic or hypoxic conditions when lactic acid production is raised (Halestrap *et al.*, 1997; Vandenberg *et al.*, 1993) (Figure 1).

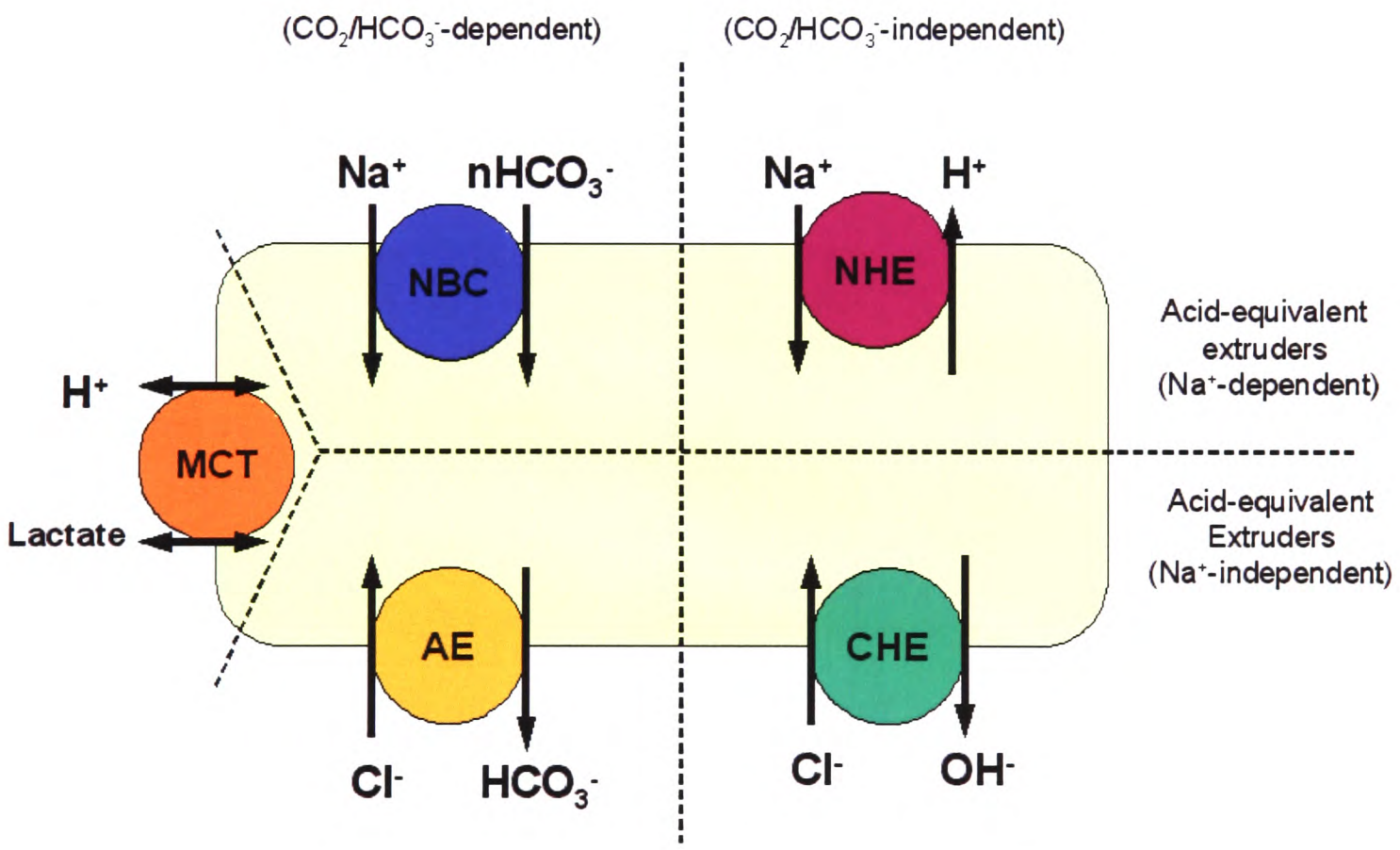

Figure 1. Control of pH_i in mammalian ventricular myocytes. pH_i is mainly regulated by four sarcolemmal transporters. There are two acid-equivalent extruders, Na^+/H^+ exchange (NHE) and Na^+-HCO_3^- cotransporter (NBC), and two acid-equivalent loaders Cl^-/HCO_3^- exchange (anion exchange or AE) and Cl^--OH^- exchange (CHE) (Leem *et al*, 1999). A reversible lactic acid transporter (Monocarboxylate transporter; MCT) may also be involved in acid extrusion under hypoxic/ischaemic conditions.

The contribution of each of the four main sarcolemmal transporters to transmembrane H^+-equivalent flux is illustrated in Figure 2. The central coloured region represents a permissive pH_i range within which small pH_i displacements are tolerated, at least transiently. The low transporter fluxes imply that small acid/base loads or small shifts in the pH_i sensitivity of an individual acid/base transporter will relatively easily produce displacements of pH_i. Such an arrangement could provide a control system that permits some forms of pH_i signalling in the cardiac cell while still, in the longer term, overseeing pH_i regulation. Outside these limits, net acid-equivalent flux activates steeply, thus safeguarding the cell from extreme acidosis or alkalosis.

Figure 2. H^+-equivalent fluxes in mammalian cardiac myocytes. Fluxes calculated for NHE, NBC, AE and CHE plotted as a function of pH_i, obtained from Leem *et al.* 1999. Near to resting pH_i (6.9-7.2; pink) flux rates are low and give rise to a "permissive range" where small deviations of pH_i are countered by only a small transmembrane H^+-flux (modified from Vaughan-Jones *et al.* 2006).

NHE and NBC are the main acid extrusion mechanisms in cardiac myocytes. In the present Thesis, the modulation of the activity of these transporters by the enzyme carbonic anhydrase is investigated. Thus, a more detailed description of their function, structure and regulation is given in the following section.

1.2.1 Na^+/H^+ Exchange (NHE)

The transmembrane exchange of protons for Na^+ is ubiquitous in organisms across all phyla and kingdoms, and underlies fundamental homeostatic mechanisms to control these ions (Brett et al., 2005). The mammalian NHE is an integral membrane protein that mediates the electroneutral exchange of one intracellular proton for one extracellular Na^+ ion. NHEs are classified as secondary active transporters since the driving force for catalysis is not coupled directly to ATP hydrolysis, but instead is derived from the inwardly-directed Na^+ electrochemical gradient established by the Na^+/K^+-ATPase pump (Orlowski & Grinstein, 2004; Wakabayashi et al., 1997).

1.2.1.1 NHE isoforms in mammals

To date, nine mammalian NHE isoforms (NHE1 – NHE9) have been identified (Nakamura et al., 2005; Orlowski & Grinstein, 2004; Orlowski & Grinstein, 1997). The isoforms share 25–70% amino acid identity, with calculated relative molecular masses ranging from approximately 74 to 93 kDa (Khadilkar *et al.*, 2001; Orlowski & Grinstein, 2004; Orlowski & Grinstein, 1997).

The NHE1 isoform is the 'housekeeping' isoform of the exchanger and is expressed in the plasma membrane of virtually all tissues (Orlowski & Grinstein, 2004; Orlowski & Grinstein, 1997; Putney *et al.*, 2002). NHE1 plays a central role in the

regulation of pH_i and cellular volume (Counillon & Pouyssegur, 2000; Orlowski & Grinstein, 2004; Orlowski & Grinstein, 1997; Putney *et al.*, 2002), and it is the dominant isoform in the mammalian myocardium and the only expressed at the sarcolemma (Karmazyn *et al.*, 1999; Orlowski & Grinstein, 1997).

Similarly to NHE1, NHE2 – NHE5 isoforms also localize to the plasma membrane, but have more restricted tissue distributions. NHE2 and NHE3 are predominantly located in the apical membrane of epithelia and are highly expressed in kidney and intestine (Noel *et al.*, 1996; Orlowski & Grinstein, 2004; Orlowski *et al.*, 1992). NHE4 is most abundant in stomach, but is also expressed in intestine, kidney, brain, uterus and skeletal muscle (Orlowski *et al.*, 1992). NHE5 is expressed predominantly in brain, but may also be present at low levels in other non-epithelial tissues, including spleen, testis and skeletal muscle (Attaphitaya *et al.*, 1999; Baird *et al.*, 1999). The isoforms NHE6-NHE9 are ubiquitously expressed and are present in intracellular compartments and are presumed to regulate luminal pH and cation concentration (Nakamura *et al.*, 2005). NHE6 expression is highest in heart, brain and skeletal muscle and is localized to early recycling endosomes (Brett *et al.*, 2002; Nakamura *et al.*, 2005). The NHE7 isoform is localized predominantly to the *trans*-Golgi network, and differs from the other NHE isoforms in that it mediates the influx of either Na^+ or K^+ in exchange for H^+ (Numata & Orlowski, 2001). The highest levels of NHE8 expression are found in skeletal muscle and kidney, and this isoform is mainly localized to the mid- to *trans*-Golgi compartments (Nakamura *et al.*, 2005). The recently identified NHE-9 isoform is localized to late recycling endosomes (Nakamura *et al.*, 2005).

1.2.1.2. NHE Structure and Membrane Topology

The structure of NHE1 is one of the best characterized within the NHE family. The protein is 815 amino acids in length, comprising the membrane domain and the cytoplasmic tail (Putney *et al.*, 2002). The membrane domain of NHE1 is both necessary and sufficient for ion transport, whereas the cytosolic domain is involved in regulation of the activity of the exchanger (Fliegel & Frohlich, 1993; Wakabayashi *et al.*, 1992). Prediction of the membrane topology of the NHE family suggests a similar arrangement for all isoforms with an N-terminal membrane domain consisting of twelve membrane-spanning segments and a more divergent C-terminal cytoplasmic tail (Orlowski & Grinstein, 2004) (Figure 3).

Figure 3. Membrane topology of NHE1. The NHE1 molecule comprises 12 membrane-spanning, a short N-terminal cytoplasmic domain and a large C-terminal cytoplasmic domain which contains regulatory sites. C-terminal sites for interaction with several signalling molecules are shown, including calmodulin (CaM), calcineurin homologous protein (CHP), PIP_2 and carbonic anhydrase (CA) II binding sites. Phosphorylation sites are shown in yellow. Kinases that up-regulate NHE activity include CamKII, ERK1/2, p90 ribosomal kinase, the Rho-associated kinase $p160^{ROCK}$, and Nck-interacting kinase, NIK. P38 MAPK inhibits NHE1 activity in response to angiotensin II via inhibition of ERK1/2. Protein kinases C and D are also able to regulate the exchanger (Reproduced from Slepkov *et al.* 2007).

1.2.1.3. NHE Activity and Regulation

Ion flux via NHE is driven by the transmembrane Na^+ gradient and requires no direct metabolic energy input. The exchanger mediates the electroneutral extrusion of H^+ in exchange for Na^+ influx with 1:1 stoichiometry. NHE1 exhibits Michaelis–Menten dependence on extracellular Na^+, with a reported apparent *K*m of 3–50 mM (Levine *et al.*, 1993; Orlowski, 1993). In contrast with the simple Michaelis–Menten dependence on extracellular Na^+, intracellular acidification allosterically increases the activity of NHE.

NHE activity is primarily controlled by pH_i. NHE is minimally active at resting pH_i but it is steeply activated upon an increase in $[H^+]_i$. The regulation of NHE by H^+-ions appears to be mediated by allosteric control. H^+-ions bind to an intracellular modifier site distinct from the intracellular H^+-ion transporter site, displaying co-operative behaviour with a Hill coefficient of 1.5-2.0 (Aronson, 1985). NHE activity is also sensitive to pH_o since extracellular acidosis inhibits Na^+-binding and transport rate (Aronson *et al.*, 1983; Wu & Vaughan-Jones, 1997). A rise in intracellular Na^+ can also inhibit NHE activity, due to a decrease in the thermodynamic driving force (Green *et al.*, 1988; Grinstein *et al.*, 1984; Grinstein & Furuya, 1986), yet fluctuations in intracellular Na^+ within the physiological range have been shown to have no significant effect (Wu & Vaughan-Jones, 1997).

NHE1 is also modulated by phosphorylation at its cytosolic C-terminus, which increases the sensitivity of the H^+ modifier site and therefore increases NHE activity. All phosphorylation sites of NHE1 are located in the cytoplasmic tail (Wakabayashi *et al.*, 1994; Wakabayashi *et al.*, 1992). The phoshorylation cascade includes phosphoinositide hydrolysis and subsequent activation of protein kinase C (PKC), via activation of the

mitogen activated protein (MAP) kinase pathway. Many external stimuli, including endothelin-1 (Khandoudi *et al.*, 1994), angiotensin II (Matsui *et al.*, 1995), α_1-adrenergic agonists (Lagadic-Gossmann & Vaughan-Jones, 1993; Wallert & Frohlich, 1992), thrombin (Yasutake *et al.*, 1996), and growth factors (Rosoff *et al.*, 1984), affect NHE activity via phosphorylation cascades.

In addition, there are factors which regulate NHE1 via phosphorylation-independent mechanisms. ATP depletion has been shown to inhibit NHE activity (Goss *et al.*, 1994). It is thought that this may be mediated by an unidentified co-factor which can only interact with NHE1 when ATP levels are above a threshold level (Aharonovitz *et al.*, 1999; Wu & Vaughan-Jones, 1994). Cell volume and osmotic changes can affect NHE-1 independently of phosphorylation (Grinstein *et al.*, 1992). A regulatory site located close to the N-terminal domain has been postulated to mediate the effect of cell volume changes (Bianchini *et al.*, 1997). Intracellular Ca^{2+} bound to calmodulin also regulates NHE1. Calmodulin sites have been identified on the C-terminal domain of NHE1 (Bertrand *et al.*, 1994). Occupation of these sites is thought to reverse the autoinhibitory state (Bertrand *et al.*, 1994; Wakabayashi *et al.*, 1994). Recently, the enzyme carbonic anhydrase (CA) II has been shown to bind and influence NHE1 transport efficiency through a direct interaction with a cluster of acidic residues at the C-terminus of the NHE1 protein (Li *et al.*, 2002).

1.2.1.4. NHE Pharmacological Inhibition

The first class of NHE inhibitors developed included amiloride and its 5' alkyl-substituted derivatives such as 5-(N-Ethyl-N-isopropyl)amiloride (EIPA), 5-(N,N-dimethyl)amiloride (DMA), and 5-N-(methylpropyl)amiloride (MPA). First synthesised

in 1965 (Bickling *et al.*, 1965), amiloride was developed as a K^+-sparing diuretic due to its ability to inhibit both the epithelial Na^+ conductive ion channel (E_{NaC}) and NHE in the kidney. In the case of NHE, amiloride is believed to competitively inhibit close to or at the extracellular Na^+ binding site (Counillon *et al.*, 1993; Kinsella & Aronson, 1981). Wakabayashi *et al* (2000) demonstrated that amino acid residues in transmembrane domains 4 and 9 were important for amiloride binding. Amiloride and related compounds have been used clinically, to treat hypertension and congestive heart failure (Antcliff *et al.*, 1971; Ramsay *et al.*, 1980). These agents, however, are relatively non-specific protein inhibitors, affecting also Na^+/K^+-ATPase (Soltoff and Mandel, 1983), protein kinase C (Besterman *et al.*, 1985), Na^+/Ca^{2+} exchange (Kaczorowski *et al.*, 1985), and voltage-gated Ca^{2+} current (Takahashi *et al.*, 1989). Amiloride has also been shown to increase significantly action potential duration, possibly by inhibiting K^+ currents (Marchese *et al.*, 1984).

A second class of NHE inhibitors, more recently developed, comprises benzoylguanidines and their derivatives, for example HOE 694 (Counillon *et al.*, 1993) and HOE 642 (cariporide) (Scholz *et al.*, 1995; Scholz *et al.*, 1999). Such compounds display a ~10^3-10^5-fold higher specificity for NHE1 than NHE3, compared to amiloride compounds which only have a 10^2-fold higher specificity for NHE1. Due to this greater specificity for the NHE1 isoform and the fact that they do not appear to inhibit other ion transporters (Scholz *et al.*, 1995; Scholz *et al.*, 1993) or other pH regulatory systems (Loh *et al.*, 1996), compounds such as HOE 694, cariporide (HOE 642) and the more recently developed quinoleine, zoniporide (Guzman-Perez *et al.*, 2001; Knight *et al.*, 2001) have become valuable experimental tools for cardiac pH research. They are also

being developed clinically as treatments for NHE1-mediated ischaemia/reperfusion injury. These compounds exhibit powerful cardioprotective properties in animal models of myocardial ischaemia/reperfusion (Clements-Jewery *et al.*, 2004; Scholz *et al.*, 1993) and may even attenuate or reverse features of myocardial hypertrophy (Yoshida & Karmazyn, 2000), although their therapeutic potential in a clinical setting has so far proved inconclusive (for review, see Avkiran & Marber, 2002). The functional effects of these drugs are proposed to be related to their influence on cardiac pH_i, $[Na^+]_i$ and $[Ca^{2+}]_i$.

1.2.2. Na^+-HCO_3^- Co-transport (NBC)

Bicarbonate transporters are major pH_i regulation systems in animal cells and play vital roles in acid-base movement in a number of mammalian organs, including, pancreas (Abuladze et al., 1998; Marino et al., 1999), kidney (Abuladze et al., 2000; Schmitt et al., 1999; Wang et al., 2001), reproductive system (Jensen et al., 1999), central nervous system (Bevensee *et al.*, 2000; Brune *et al.*, 1994; Schmitt *et al.*, 2000), and heart (Choi *et al.*, 1999; Dart & Vaughan-Jones, 1992; Yamamoto *et al.*, 2005). Na^+-HCO_3^- co-transport (NBC) was first described in salamander (*Ambystoma tigrinum*) renal proximal tubule (Boron & Boulpaep, 1983). This transporter was also the first NBC to be cloned (Romero *et al.*, 1997) followed by subsequent clones obtained from human kidney (Abuladze *et al.*, 1998), rat kidney (Abuladze *et al.*, 1998; Sciortino & Romero, 1999), human retina (Ishibashi *et al.*, 1998), human pancreas (Abuladze *et al.*, 1998), human heart (Choi *et al.*, 1999), human skeletal muscle (Pushkin *et al.*, 1999a), rat aorta and pulmonary artery, and brain (Bevensee *et al.*, 2000). NBC has also been described in invertebrate species (Deitmer, 1991; Deitmer & Schlue, 1989; Piermarini *et al.*, 2007a).

NBC transporters mediate the co-transport of Na^+ and HCO_3^- ions (or CO_3^{2-}) using the driving force derived from the inwardly-directed transmembrane Na^+ gradient.

Depending on the flux of the net charge per transport cycle, these transporters are characterised as electroneutral, when the transported negative charge equals the transported positive charge; or electrogenic, when the transported negative charge exceeds the transported positive charge.

1.2.2.1. NBC isoforms in mammals

To date, three NBC isoforms, two electrogenic and one electroneutral, have been identified. NBC1 corresponds to the original electrogenic isoform discovered and cloned from salamander (Boron & Boulpaep, 1983; Romero *et al.*, 1997). NBC1 is also termed NBCe1 or SLC4A4 according to the new nomenclature based on membership of the solute carrier (SLC) family.

In humans, two major NBC1 variants, NBCe1-A (kNBC; first cloned from kidney) and NBCe1-B (pNBC; first cloned from pancreas and heart) are expressed (Abuladze *et al.*, 1998; Burnham *et al.*, 1997; Choi *et al.*, 1999). These transporters are differentially expressed in a cell-specific manner (Abuladze *et al.*, 1998). NBCe1-mediated transport can work with a stochiometry of $1Na^+:2HCO_3^-$ or $1Na^+:3HCO_3^-$.

NBCe2 (NBC4 or SLC4A5) was originally cloned from a human cardiac cDNA library (Pushkin *et al.*, 2000a). NBCe2 refers to the splice variant NBCe2-C. This transporter also works with a stochiometry of $1Na^+:2HCO_3^-$ or $1Na^+:3HCO_3^-$.

NBCn1 (NBC3 or SLC4A7), the electroneutral NBC, was originally cloned from human skeletal muscle (Pushkin *et al.*, 1999a). Later, the rat ortholog of the transporter was cloned from rat aorta (Choi *et al.*, 2000b). NBC3 protein is expressed in kidney

(Kwon *et al.*, 2000; Odgaard *et al.*, 2004; Praetorius *et al.*, 2004a; Pushkin *et al.*, 1999b; Vorum *et al.*, 2000), epidydimis (Pushkin *et al.*, 2000b), duodenum (Praetorius *et al.*, 2001), choroids plexus (Praetorius *et al.*, 2004b) and submandibular glands (Gresz *et al.*, 2002; Luo *et al.*, 2001).

In the heart, these three NBC isoforms have been detected at mRNA transcript and protein level (Choi *et al.*, 2000b; Choi *et al.*, 1999; Pushkin *et al.*, 1999a; Virkki *et al.*, 2002). There is clear evidence for the functional activity of electrogenic NBC in mammalian ventricular tissue with stochiometry of $1Na^+:2HCO_3^-$ (Aiello *et al.*, 1998; Yamamoto et al., 2005, Yamamoto et al., 2007), while a recent report also suggests functional activity from an electroneutral NBC (Yamamoto et al., 2005).

1.2.2.2. NBC Structure and Membrane Topology

Na^+-HCO_3^- co-transporters belong to the SLC4 family of H^+-equivalent transporters. Comparison of the primary structures of SLC4 transporters shows significant homology especially in putative membrane domains. To date, only the membrane topology of NBCe1 has been described (Tatishchev *et al.*, 2003). NBCe1 is 1035 amino acids in length and contains 10 transmembrane domains with cytoplasmic localization of the N-terminal and C-terminal hydrophilic domains (Figure 4).

Figure 4. Membrane topology of NBCe1-B. The membrane domain of the NBC1 protein mediates ion transport while the cytoplasmic N-terminal and C-terminal domains present phosphorylation regulatory sites. Yellow circles represent phosphorylation sites by PKC and purple circle represent phosphorylation site by PKA. Orange circles represent DIDS binding sites and red represents binding sites for CA (Based on Tatishchev *et al.* 2003, Romero, 1999, and Alvarez *et al,* 2003).

1.2.2.3. NBC Activity and Regulation

Similarly to NHE, NBC is also regulated by pH_i. Lagadic-Gossmann *et al* (1992) demonstrated that in guinea-pig ventricular myocytes NBC displays a similar pH_i dependency to NHE, activity increasing steeply as pH_i falls below 7.1 mediating approximately 40% of the total acid-equivalent efflux when pH_i was decreased from 7.15 to 6.95. Leem *et al* (1999) reported that, while NHE and NBC are equally stimulated by modest acid loads, greater activation of NHE occurs below a pH_i of 6.9. Below this pH_i, NBC is not activated to the same extent and the relationship between pH_i and NBC activity is approximately linear. A similar study on sheep Purkinje fibres revealed that

NBC accounts for 30% of total acid efflux at pH_i of 7.0 but only 20% at pH_i of 6.6 (Dart & Vaughan-Jones, 1992). NBC, like NHE, is inhibited by a fall in pH_o and this is thought to be mediated by extracellular H^+-ion (H^+_o) titration of an allosteric regulator site, since inhibition is largely independent of extracellular HCO_3^- (Ch'en & Vaughan-Jones, 2001).

NBC activity is also influenced by the concentration of Na^+ and HCO_3^-. Rat renal electrogenic NBC (rkNBC; NBCe1) displayed a K_m for extracellular Na^+ of 30mM at every test voltage (between -160mV and +60mV) when expressed in in *Xenopus* oocytes (Sciortino & Romero, 1999). The HCO_3^- dependency of NBC has also been explored yet whether the chemical form transported is HCO_3^-, CO_3^{2-} or $NaCO_3^-$ is yet to be fully established due to the interdependent reactions between H^+, CO_2 and HCO_3^-. Apparent affinity constants for HCO_3^- of 7-15mM have been reported in rabbit kidney cortical basolateral vesicles (Akiba *et al.*, 1986; Stim *et al.*, 1994). More recently, Boron and colleagues (Grichtchenko *et al.*, 2000) expressed both, the salamander and the rat renal NBCs in *Xenopus* oocytes and showed an apparent K_m for HCO_3, based on changes in membrane potential, of 10.6mM and 10.8mM, respectively. However, under voltage clamp conditions the K_m for HCO_3^- of the rat renal NBC was found to be 6.5 mM.

Regulation of NBC activity can also be mediated by phosphorylation of specific sites on the cytoplasmic C-terminal domain. A protein kinase A (PKA) phosphorylation site has been identified which is conserved in salamander, rat and human kidney clones. Tyrosine, PKC and casein kinase II phosphorylation sites have also been identified (Romero & Boron, 1999). Many external factors that acutely up or down regulate NBC activity via sarcolemmal receptors are upstream of these phosphorylation cascades. Up-regulating stimuli include PKC, angiotensin II, endothelin I, cholinergic, and β-

adrenergic stimulants (Eiam-Ong *et al.*, 1992; Lagadic-Gossmann & Vaughan-Jones, 1993; Ruiz *et al.*, 1997; Ruiz *et al.*, 1995; Ruiz *et al.*, 1996b). On the other side, down-regulating factors include PKA, calmodulin, and parathyroid hormone (Ruiz & Arruda, 1992; Ruiz *et al.*, 1996a). Cardiac NBC has also been shown to be activated by the MAPK-(ERK)-dependent pathway and arachidonic acid (Baetz *et al.*, 2002; Kohout & Rogers, 1995). Additionally, NBC regulation may also occur via the N-linked glycosylation sites. Also, chronic up-regulation of NBC can occur during metabolic acidosis and potassium depletion, while metabolic alkalosis can result in chronic down regulation (Akiba *et al.*, 1987; Alpern, 1990; Soleimani *et al.*, 1990; Soleimani *et al.*, 1991).

CA has been proposed to be another factor that modulates NBC activity. By physically and functionally interacting with NBC at intracellular and extracellular sites, CA has been shown to enhance NBC-mediated HCO_3^- transport when these proteins are co-expressed in heterologous transfection systems. The electrogenic and electroneutral NBC isoforms NBCe1-A, NBCe1-B, and NBCn1-A display a binding site for CA II in their C-terminus (Alvarez *et al.*, 2003; Gross *et al.*, 2002; Loiselle *et al.*, 2003; Loiselle *et al.*, 2004; Pushkin *et al.*, 2004). NBCe1-B has been proposed to also interact with CA IV at its fourth extracellular loop, but it is possible that additional portions of the NBCe1-B extracellular surface are also involved in the CA IV interaction (Alvarez *et al.*, 2003).

1.2.2.4. NBC Pharmacological Inhibition

Disulphonic stilbene compounds such as 4,4'-diisothiocyanatostilbene-2,2'-disulphonic acid (DIDS) are effective inhibitors of NBC in the majority of cell types and have been used to identify the transporter in many studies (Cabantchik & Greger, 1992). Stilbenes however, are not specific since they also inhibit AE and MCT (Leem & Vaughan-Jones, 1998b; Wang *et al.*, 1996). The stilbene disulphonate DBDS (4,4'-dibenzamidostilbene-2,2'-disulphonate) has also been shown to inhibit CHE (Sun *et al.*, 1996). More recently a putative specific inhibitor for NBC has been developed, S0859 ($C_{29}H_{24}ClN_3O_3S$; Sanofi-Aventis), which has been shown to inhibit cardiac NBC with an apparent K_i of 3.57μM, while having no effect on the other acid-equivalent transporters (Ch'en *et al.*, 2008). This NBC inhibitor has been successfully used to block NBC activity in cardiac (Yamamoto *et al.*, 2005) and epithelial (Schwab *et al.*, 2005) tissues.

1.3. Intracellular Buffering

Buffering represents the first line of defence of pH_i when an intracellular acid or alkali load occurs. Over a rapid time course, buffers can bind or release a significant amount of H^+, thus minimising pH_i fluctuations. The ability of a buffer to minimise a pH disturbance is described quantitatively by its buffering capacity. Intracellular buffering capacity (β_i) is defined as the amount of acid or base (in mmoles) that can be added to one litre of cytoplasm to change pH_i by one pH unit (Roos & Boron, 1981):

$$\beta_i\ (\mathrm{mM}) = \frac{\Delta[H^+]_i}{\Delta pH_i}$$

Total intracellular buffering power (β_{tot}) comprises both intrinsic, CO_2-independent buffering (β_{int}) and CO_2-dependent buffering (β_{CO2}). β_i consist of H^+/OH^--titratable groups on intracellular proteins and dipeptides, as well as titratable groups on other smaller molecules (Vaughan-Jones *et al.*, 2002; Zaniboni *et al.*, 2003). β_{int} has a fixed (β_{fix}) and mobile (β_{mob}) component. β_{fix} consist of imidazole groups and other H^+ titratable groups on cytoplasmic proteins. Macromolecules, such as proteins, are typically polyvalent and of high molecular weight, and therefore have low intracellular mobility, being effectively anchored within the cell, at least on a time scale of minutes. β_{mob}, in contrast, consists of smaller non-protein buffers such as taurine, inorganic phosphate, lactate, various amino acids and several derivatives of the histidine-based dipeptides carnosine, anserine and homocarnosine (Vaughan-Jones *et al.*, 2002). These relatively low molecular weight buffers (100–200 Da) diffuse two or three orders of magnitude faster than large proteins, and can reversibly bind and shuttle H^+-ions spatially within the cell. Spatial movement of H^+ is particularly important because it couples cytoplasmic pH_i to sarcolemmal regulatory transporters resulting in efficient pH_i control (Vaughan-Jones *et al.*, 2006).

Because the capacity of a cellular buffer is defined in part by its pK, cytoplasmic buffering power will vary as a function of pH_i. In mammalian cardiac myocytes, β_{int} increases with falling pH_i (within the physiological range) and varies in a manner consistent with at least two buffer populations (Figure 5), which are assumed to be the fixed and mobile buffer species (Leem *et al.*, 1999; Zaniboni *et al.*, 2003).

The pH-dependence of β_{int} is given by the following relationship:

$$\beta_{int} = \frac{\ln_{10} \times C_{fix} \times 10^{pH_i - pK_{fix}}}{(1+10^{pH_i - pK_{fix}})^2} + \frac{\ln_{10} \times C_{mob} \times 10^{pH_i - pK_{mob}}}{(1+10^{pH_i - pK_{mob}})^2}$$

where C_{fix} and C_{mob} are the total concentrations of fixed and mobile buffers, respectively. The fixed buffer population is assumed to be one relatively homogeneous of high concentration (~70mM) and a low average pK (~6.1). This pK value would be consistent with imidazole groups on histidine residues and, due to their effective concentration; these would most likely be components of intracellular proteins.

Figure 5. pH_i-dependence of intrinsic buffering capacity. Intrinsic buffering capacity (β_{int}; black) comprises two populations of buffers which represent the fixed (β_{fix}; red) and the mobile (β_{mob}; light blue) components. β_{fix} consist of imidazole groups and other H^+ titratable groups on high molecular weight and low intracellular mobility molecules such as cytoplasmic proteins. β_{mob} consists of smaller non-protein low molecular weight and higher intracellular mobility buffers such as the histidine-based dipeptides carnosine, anserine and homocarnosine (from Zaniboni *et al.* 2003).

On the other hand, the mobile component has been determined to be one of lower concentrtation (~13mM) and an average pK_a of 7.30-7.48 (Leem *et al.*, 1999; Swietach & Vaughan-Jones, 2005; Vaughan-Jones *et al.*, 2002; Vaughan-Jones *et al.*, 2006; Zaniboni *et al.*, 2003) (Figure 6).

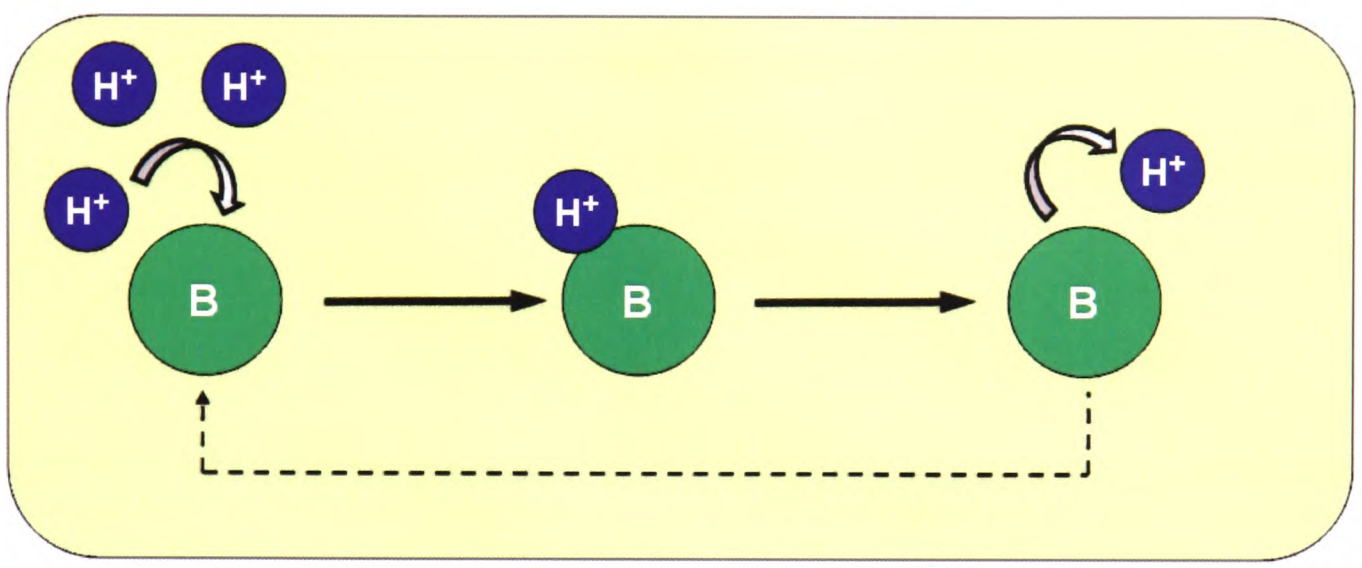

Figure 6. Facilitated spatial diffusion of protons. Low molecular weight buffers (B) mediate the spatial diffusion of H^+-ions within the cytoplasm. Mobile buffers shuttle protons from acidic regions to regions of higher pH_i.

The second component of β_{tot}, $\beta_{CO2,}$ relies on the CO_2/HCO_3^- buffer system or carbonic buffer. Buffering occurs via the reversible protonation of bicarbonate anions leading to the formation of carbonic acid which instantly dissociates into CO_2 and H_2O:

$$\mathbf{H^+ + HCO_3^- \Leftrightarrow H_2CO_3 \Leftrightarrow CO_2 + H_2O}$$

Intracellular buffering due to CO_2 is defined by the following expression, derived from a rearrangement of the Henderson-Hasselbach equation:

$$\beta_{CO_2} = 2.303 \times [HCO_3^-]_i = 2.303 \times [HCO_3^-]_o \times 10^{(pH_i - pH_o)}$$

In order for the β_{CO_2} expression to be valid, CO_2/HCO_3^- must be at equilibrium and the calculation of $[HCO_3^-]_o$ from the Henderson-Hasselbach equation should use an appropriate pK_a value taking into account the temperature and the effect of saturated water vapour pressure on the pK_a of CO_2/HCO_3^- (6.15 at 37°C) (Leem & Vaughan-Jones, 1998a).

In contrast to β_{int}, the equilibrium value of β_{CO_2} rises with rising pH_i for a fixed value of pH_o. The relative importance and contribution of β_{int} and β_{CO2} to β_{tot} therefore depends on pH_i (Figure 7).

Figure 7. pH-dependence of total buffering capacity (β_{tot}), intrinisc buffering (β_{int}), and CO_2-dependent buffering capacity (β_{CO2}) in mammalian ventricular myocytes. β_{tot} includes the intrinsic and CO_2-dependent buffering components. At a resting pH_i of 7.2, β_{CO2} represents approximately 40% of β_{tot} (reproduced from Leem *et al.* 1999).

Efficient buffering of H^+ by HCO_3^- ions requires rapid equilibration with CO_2 in solution. Without catalysis however, the equilibration of carbonic buffer occurs slowly. In unbuffered solutions the spontaneous CO_2 hydration reaction has a half-time of about 5 seconds (Forster, 1991). In a cell containing intrinsic buffers, however, carbonic buffer equilibration can take several minutes (Leem & Vaughan-Jones, 1998a). Cells express the enzyme carbonic anhydrase (CA) which is responsible for accelerating the equilibration of carbonic buffer ensuring adequate and rapid provision of HCO_3^- to buffer H^+-ions. At the concentration found inside erythrocytes, CA can accelerate the uncatalysed hydration reaction rate by 17000-fold at 37°C (Itada & Forster, 1977). In cardiac myocytes, CA has been shown to accelerate intracellular CO_2 hydration at a more modest level (~3-fold) (Lagadic-Gossmann *et al.*, 1992; Leem & Vaughan-Jones, 1998a)

Similarly to intrinsic mobile buffers, carbonic buffer can also shuttle protons within the cytoplasm and contribute to pH_i control. The mechanism by which this "carbonic shuttle" facilitates proton mobility relies on diffusion and hydration of intracellular CO_2, leading to the formation of H^+ and HCO_3^- in regions distal to the local acid load, with back diffusion of HCO_3^- to neutralize some of the original acid load. The shuttle thus effectively mediates a passive spread of intracellular H^+-ions from proximal to distal regions within the cell. CA plays a key role in this mechanism. Because efficient function of the shuttle relies on the rapid equilibration between the carbonic buffer components, CA is required for maximal turnover of the shuttle (Figure 8).

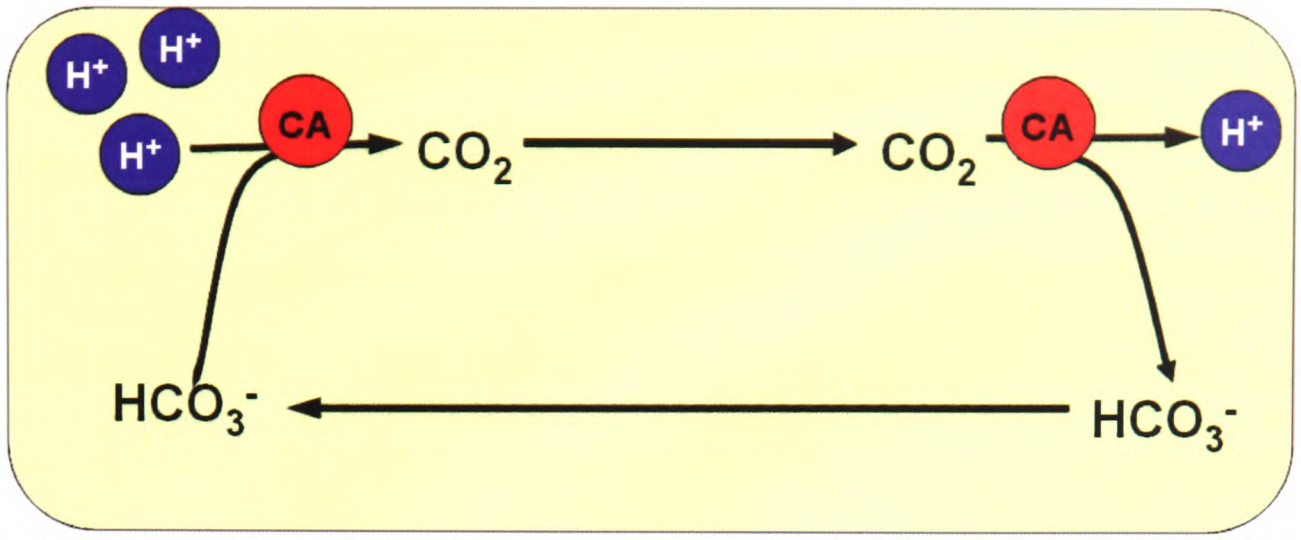

Figure 8. Intracellular carbonic buffer shuttle. In the event of a localized acid load, H^+-ions are buffered proximally by HCO_3^- and converted by CA into CO_2 which can then diffuse to more distal intracellular regions. There, CA catalyses the rehydration of CO_2 to form H^+ and HCO_3^-. Thus, effectively, H^+-ions have moved from a proximal to a distal region of the cell.

1.4. Carbonic Anhydrase

Carbonic anhydrase (CA; EC. 4.2.1.1) was first characterised from erythrocytes in 1933 directly as a result of a search for a catalytic factor that had been theoretically determined as necessary for rapid transit of HCO_3^- from the erythrocyte to the pulmonary capillary (Meldrum & Roughton, 1933). CAs are ubiquitous zinc metalloenzymes that catalyze the reversible hydration of CO_2 to form bicarbonate and H^+. These enzymes are present across the phylogenetic tree and are encoded by four distinct evolutionary unrelated gene families: α, β, γ and δ (Hewett-Emmett, 2000; Tripp *et al.*, 2001). The α-CAs are present in vertebrates, bacteria, algae and in the cytoplasm of plants, both mono- and dicotyledons. β-CAs are found predominantly in bacteria, algae and chloroplasts. The γ-CAs are present mainly in archaea and in some bacteria, and δ-CAs are found in some marine diatoms (Roberts *et al.*, 1997; Tripp *et al.*, 2001). There are no significant

homologies between representatives of the different CA families. Thus, this seems to be a good example of convergent evolution of catalytic function.

In mammals, 16 different α-CA isoforms of varying activity, tissue specificity, physiological role and sensitivity to pharmacological inhibitors have been reported (Chegwidden & Carter, 2000; Parkkila, 2000). Among them, the most studied are isozymes CA I, CA II, CA III, CA IV and CA IX; thus, most of the data available correspond to these isoforms. α-CAs can be classified into four broad groups:

(i) **Cytosolic CAs**. This group includes the cytosolic isozymes CA I, CA II, CA III, CA VII, and CA XIII. Among cytosolic CAs, CA II appears to have the most widespread distribution in mammalian tissues and is one of the fastest enzymes known with a K_{cat} of 1.4×10^6 s^{-1} and a K_m for CO_2 of ~10mM (K_{cat} = Vmax/total enzyme concentration). CA VII is the most highly conserved of the α-CA isozymes. This isoform also has a high catalytic activity, almost in the order of 10^6 s^{-1}, and is seemingly widely distributed, albeit at low concentrations. CA I and CA III seem to have a more restricted distribution pattern, and their Kcat values are in the order of 10^5 s^{-1} and 10^4 s^{-1}, respectively.

(ii) **Membrane-bound CAs**. Membrane-bound isozymes include CA IV, CA IX, CA XII, CA XIV and XV. Of these, three (IX, XII and XIV) are transmembrane proteins while two (IV and XV) are bound to membranes via a glycosylphosphatydlinositol (GPI) anchor. CA IV is a high activity isozyme (K_{cat} 1.1×10^6 s^{-1}; K_m ~22mM) with a widespread distribution, especially in the capillary endothelium. CA IX and CA XII are bitopic (single-pass) transmembrane proteins and have been identified in many normal

tissues (Karhumaa *et al.*, 2000; Parkkila, 2000) and particularly overexpressed in several human carcinomas and tumour cell lines (Parkkila *et al.*, 2000). Both proteins are hypoxia-inducible and are negatively regulated by the von Hippel-Lindau tumor-suppressor protein (Potter & Harris, 2004). Values of K_{cat} for CA IX and CA XII are in the order of 10^5 s^{-1}. CA XV is the latest membrane-bound CA isozyme to be described, and it is an exception to the other isozymes in the group in that it is the only with low catalytic activity.

(iii) **Mitochondrial CAs**. Two CA isozymes, CA VA and CA VB, have been identified in mitochondria. These unique mitochondrial isozymes are localized in the mitochondrial matrix and their catalytic activity is necessary in certain biosynthetic metabolic pathways (Chegwidden *et al.*, 2000; Dodgson, 1987; Dodgson & Forster, 1986a; Dodgson *et al.*, 1984; Forster *et al.*, 1984). CA VA was the first CA isoform determined to have a function in intermediary metabolism. Compared to other CAs, CA V isozymes have moderate catalytic activities with K_{cat} values around 3 x 10^5 s^{-1} (Chegwidden & Carter, 2000; Heck *et al.*, 1994). CA VA and CA VB have a different tissue-specific distribution. Studies in mouse tissues have shown that CAVB has a widespread expression pattern while CA VA expression appears to be limited to liver, skeletal muscle and kidney mitochondria (Shah *et al.*, 2000). The orthologue human genes of mouse CA V also show differences in tissue-specific expression (Fujikawa-Adachi *et al.*, 1999).

(iv) **Secreted CAs**. CA VI is the only secreted CA isozyme identified to date. Inmunohistochemical studies have demonstrated the presence of CA VI in the mammalian parotid and submandibular glands (Kadoya *et al.*, 1987; Ogawa *et al.*, 1992; Ogawa *et al.*, 1993; Parkkila *et al.*, 1990) from where it is secreted into saliva. More recent studies have also demonstrated the presence of CA VI in the mammary gland and its secretion in milk (Ichihara *et al.*, 2003; Karhumaa *et al.*, 2001; Nishita *et al.*, 2007) and in the lower airways and lungs (Leinonen *et al.*, 2004). CA VI was detected in the seromucous tracheobronchial glands and its secretion, the tracheobronchial surface epithelium, and the bronchiolar surface epithelium of rats. Also, CA VI was observed in acinar cells, in duct contents of the anterior gland of the nasal septum, and in the lateral nasal gland in mice (Kimoto *et al.,* 2004). Immunoreactivity was also observed in the mucus covering the respiratory and olfactory mucosa and in the lumen of the nasolacrimal duct. The catalytic activity of CA VI is moderate compared to other CA isozymes. Its K_{cat} is about 7×10^4 s^{-1} with a Km for CO_2 of about 4mM (Chegwidden & Carter, 2000).

(v) **CA-related proteins**. Along with the rest of active CA isozymes, evolutionarily conserved but acatalytic members of the CA family have been reported, and designated as CA-related proteins (CA-RPs). In the CA numbering system (the order of discovery), three isoforms, CA-RPs VIII, X and XI, have been described. These three isoforms appear to lack activity because of histidine residue substitutions in the active site. These molecules have been tightly conserved during evolution, suggesting important functions.

The exact biological function of the CA-RPs however, has not yet been elucidated (Tashian et al., 2000).

1.4.1. General Structure of α-CAs

α-CAs generally are monomeric metalloenzymes with a molecular weight in the range of 26kDa to 58kDa. The X-ray crystal structures for seven α-CA isozymes (CA I, II, II, IV, V, XII and XIV) have been resolved and all show structural homology and conservation of active site motifs (Stams & Christianson, 2000; Whittington *et al.*, 2004; Whittington *et al.*, 2001). The CA catalytic domain of α-CAs is nearly spherical, and the dominant secondary structure is a 10-stranded, twisted β-sheet, which divides the molecule into two halves (Figure 9).

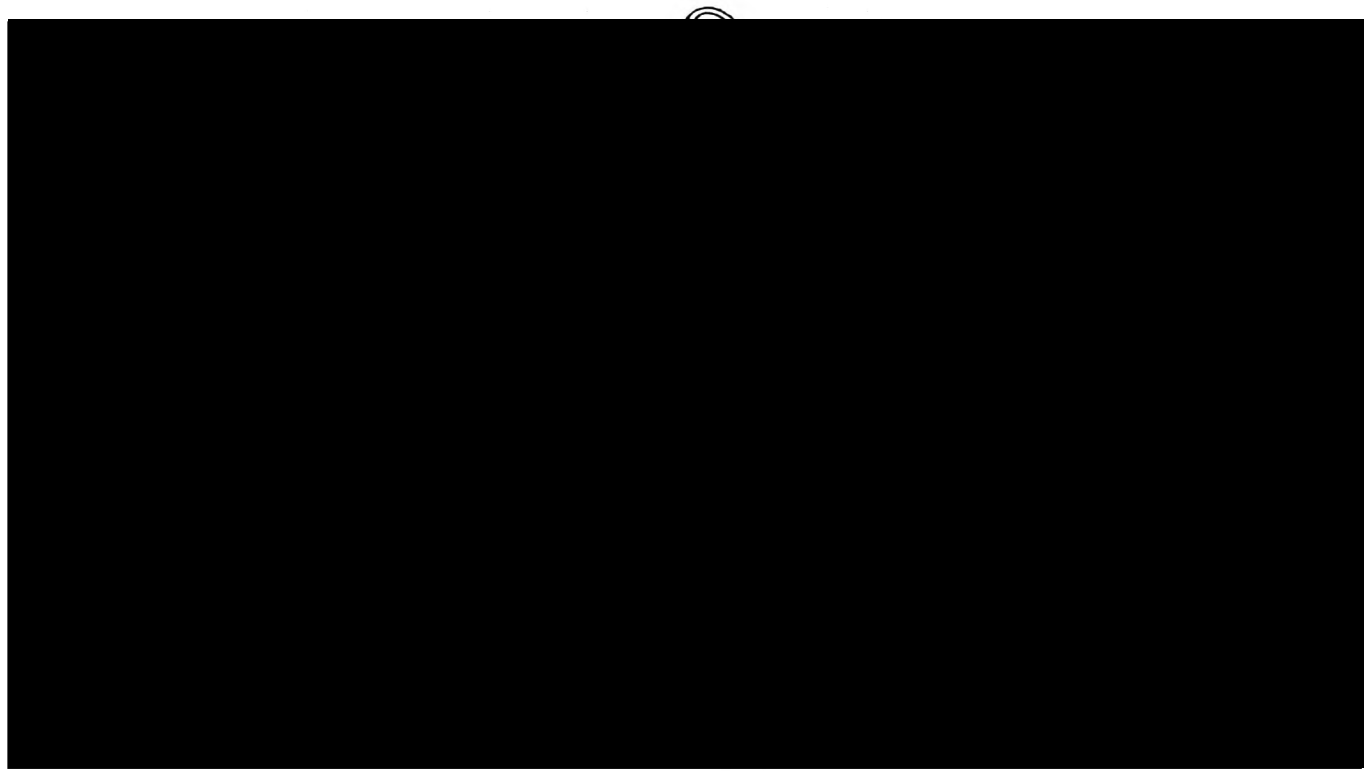

Figure 9. Sturcture of carbonic anhydrase. Consensus ribbon structure for the catalytic domain of α-carbonic anhydrases (reproduced from Chegwidden and Carter, 2000)

There are four important structural features of CAs within or interacting with the active site of the enzyme that are critical for catalysis: the Zn^{2+} binding site, the Thr-199 loop, the substrate association pocket, and the proton shuttle.

The active site is located in a roughly cone-shaped cavity that reaches almost to the centre of the CA molecule. It consists of a Zn^{2+} ion coordinated by three histidine residues (His-94, His-96 and His-119) and a hydroxyl ion (OH^-) in a roughly tetrahedral geometry. The zinc-bound OH^- acts as a potent nucleophile and is crucial in the catalytic process. Histidine ligands play important structural and functional roles in maintaining the stabilization of the zinc binding site and the reactivity of the zinc-bound OH^- for catalysis (Alexander *et al.*, 1993; Christianson & Fierke, 1996; Ippolito & Christianson, 1994; Kiefer & Fierke, 1994). These three histidine direct ligands are positioned by hydrogen bonds to other groups in the protein forming a sphere of "indirect ligands" (Christianson & Alexander, 1989). Both, the direct and indirect ligands are mostly conserved in all sequenced α-CAs (Figure 10).

Thr-199 is contained within a loop which connects the two strands of the central β-sheet. The zinc-bound OH^- interacts via a hydrogen bond with the hydroxyl side chain of Thr-199. This interaction is important because it orients the nucleophile for catalysis (Merz, 1990). Thr-199 in turn donates a hydrogen bond to the carboxylate side chain of Glu-106 (Hakansson *et al.*, 1992; Liljas *et al.*, 1972; Merz, 1990). In the absence of substrate, the zinc-bound OH- also establishes a hydrogen bond with a water molecule ("deep water") which in turn forms another hydrogen bond with the amino group of Thr-199.

Figure 10. Structure of the active site of carbonic anhydrase. The Zn^{2+} center is coordinated to three direct ligands, His-94, His-96 and His119. These in turn are stabilized by a "sphere" of indirect ligands, Gln-92, Glu-106 and Glu-117. Hydrogen bonds are indicated by dashed lines (reproduced from Coleman JE, 1998).

A hydrophobic pocket, which comprises amino acid residues Val-121, Val-143 and Leu-198, is located adjacent to the Zn^{2+} ion and it is believed to serve as a pre-catalytic association site for substrate CO_2 (Krebs *et al.*, 1993; Liljas *et al.*, 1972; Lindskog, 1986). The hydrophobic pocket participates in desolvating the CO_2 molecule, thus enhancing its reactivity, and also in channeling the substrate toward the nucleophilic zinc-bound OH^- (Liang & Lipscomb, 1990; Merz, 1991; Merz, 1990).

Another critical residue for catalysis in the CA molecule is the shuttle residue His-64, which is positioned between the zinc centre and the mouth of the active-site cavity. This residue facilitates an intramolecular proton transfer (proton shuttling) event

that is critical for catalysis and constitutes the rate-limiting step for CO2 hydration (Tu et al., 1989).

1.4.2. Carbonic anhydrase activity and function

CAs catalyze the reversible hydration of CO2 with high efficiency and are remarkable in that they posses some of the highest measured turnover rates among enzymes (Khalifah, 1971). The efficient regulation of acid–base balance mediated by CAs appears to be extremely important in biological processes, since numerous isozymes catalyse the same fundamental reaction across species and in different organs, tissues and cell compartments (Chegwidden & Carter, 2000; Parkkila, 2000). α-CAs can also catalyze a variety of other reactions, such as the hydrolysis of a range of ester substrates (Briganti *et al.*, 1999; Pocker & Storm, 1968; Supuran *et al.*, 2003). It is unclear however, whether the latter reactions are of physiological significance.

α-CAs play important physiological and pathophysiological functions in mammals. They are involved in processes related to respiration and transport of CO_2/HCO_3^- between metabolizing tissues and lungs, pH and CO_2 homeostasis, electrolyte secretion, biosynthetic reactions, bone resorption, calcification, tumorigenesis and many other physiological and pathophysiological processes (Chegwidden *et al.*, 2000; Geers & Gros, 2000; Maren, 1967; Parkkila, 2000; Swietach *et al.*, 2007b).

Probably the basic and most well known physiological role of CA is the regulation of acid-base homeostasis. CA isozymes I, II, and IV are normally involved in this process by participating in the interconversion and transport of CO_2 and HCO_3^- between tissues and excretion sites such as lungs and kidneys. CA activity facilitates elimination of CO_2 in capillaries and pulmonary microvasculature (Chegwidden &

Carter, 2000; Maren, 1967), and participates in the elimination of H^+-ions in the renal tubules and collecting ducts, as well as the reabsorption of HCO_3^- in the brush border of the proximal convoluted tubule and thick ascending Henle loop in kidneys (Chegwidden & Carter, 2000; Parkkila, 2000; Sly & Hu, 1995). CAs are also involved in the secretion of electrolytes in many tissues and organs. In the eye, for example, CA II and CA IV, participate in the formation of the bicarbonate-rich, aqueous humor secretion. Malfunctioning of this process leads to high intraocular pressure and glaucoma. CA is also involved in the formation of CSF by providing HCO_3^- and regulating pH in the choroid plexus (Maren, 1967).

The process of formation of many gastrointestinal tract secretions also involves the participation of CA. These include the production of saliva in acinar and ductal cells, of gastric acid in the stomach parietal cells, of bile and pancreatic juice (Parkkila, 2000; Parkkila & Parkkila, 1996; Parkkila *et al.*, 1994; Swenson, 1991). CAs also play an important role in ion and water transport in the intestines (Fleming *et al.*, 1995; Swenson, 1991).

In the reproductive tract, CA is involved in the regulation of pH and HCO_3^- of the seminal fluid (Cohen *et al.*, 1976; Goyal *et al.*, 1980; Kaunisto *et al.*, 1995; Kaunisto *et al.*, 1990; Parkkila *et al.*, 1993). CA is also involved in the development and function of bone by participating in differentiation of osteoclasts and providing H^+-ions for bone resorption (Chegwidden & Carter, 2000; Silverton, 1991; Vaananen & Parvinen, 1991). Some isozymes are involved in molecular signalling and metabolic processes. CA V, for example, participates in insulin secretion signalling in pancreas β cells (Parkkila *et al.*, 1998). CA II and CA V are involved in metabolic processes by providing HCO_3^- for

gluconeogenesis, fatty acids *de novo* biosynthesis, urea cycle, and pyrimidine base synthesis (Dodgson, 1991; Dodgson, 1987; Dodgson & Cherian, 1989; Dodgson & Forster, 1986a; Dodgson & Forster, 1986b; Dodgson *et al.*, 1983; Dodgson *et al.*, 1984; Dodgson *et al.*, 1993). Finally, some isozymes such as CA IX, CA XII, are highly expressed in tumors and are involved in oncogenesis and tumor progression (Dorai *et al.*, 2005; Hynninen *et al.*, 2006; Leppilampi *et al.*, 2003; Parkkila *et al.*, 2000; Pastorek *et al.*, 1994; Potter & Harris, 2004; Swietach *et al.*, 2007b; Ulmasov *et al.*, 2000).

Recently, a novel role for CA in acid-base homeostasis at the cellular level has been proposed. Based on evidence from heterologous transfection systems, CA has been proposed to interact functionally and physically with membrane pH_i regulatory transporters enhancing their activity (Alvarez *et al.*, 2003; Li *et al.*, 2002; Sterling *et al.*, 2002; Sterling *et al.*, 2001; Vince *et al.*, 2000; Vince & Reithmeier, 1998; Vince & Reithmeier, 2000). Reithmeier and colleagues (Vince *et al.*, 2000; Vince & Reithmeier, 1998; Vince & Reithmeier, 2000) have shown that the C-terminus of AE1 binds CA II, and that the enzyme enhances the transport function of AE1, AE2 and AE3 when these proteins are expressed in cultured embryonic renal-derived HEK 293 cells (Sterling *et al.*, 2001). These findings led to the proposal that the complex formed by AE and CA II functions as a bicarbonate transport metabolon (Sterling *et al.*, 2001). In this model, the efficiency of bicarbonate transport is enhanced by the intracellular intermolecular shuttling of HCO_3^- between CA II and AE (McMurtrie *et al.*, 2004). On the extracellular side, CA IV has been shown to interact with an extracellular loop of the AE1 protein (Sterling *et al.*, 2002). This arrangement would facilitate the conversion of transported HCO_3^- ions into CO_2, thereby accelerating the rate of AE-mediated bicarbonate transport.

Recently, the physical and functional interaction of CA IX with AE1, AE2, and AE3 when coexpressed in HEK 293 cells has also been reported (Morgan *et al.*, 2007).

The C-terminus of the electrogenic transporter kNBC (NBCe1-A or SLC4A4) has also shown to bind CA II *in vitro* with high affinity (Gross *et al.*, 2002), and that the complex formed by these two proteins when expressed in the mouse proximal tubule (mPCT) cell line, resulted in the enhancement of HCO_3^- transport (Pushkin *et al.*, 2004). pNBC, the other electrogenic isoform of the transporter (NBCe1-B), has been reported to interact at intracellular and extracellular sites with CA II and CA IV, respectively, when these proteins are expressed in transfected HEK293 cells (Alvarez *et al.*, 2003). The C-terminus of the electroneutral NBCn1 (NBC3 or SLC4A7) has also been shown to bind CA II with high affinity on *in vitro* studies (Loiselle *et al.*, 2003). These findings have been supported by results obtained in different expression system. A recent functional study in which NBCe1 was expressed in *Xenopus* oocytes, showed that co-expressing or injecting CA II enhanced NBC activity, and that this effect can be abolished by pharmacological CA inhibition (Becker & Deitmer, 2007).

There are, however, studies that do not support the proposal of the bicarbonate transport metabolon, and that find no effect of CA on NBC activity (Lu *et al.*, 2006; Piermarini *et al.*, 2007b).

The formation of transport metabolons involving CA and membrane H^+-equivalent transporters seems not to be restricted to only members of the SLC4 family. Fliegel and colleagues (Li *et al.*, 2002) have shown that CA II binds and intracellular motif in the C-terminus of the NHE1 protein, and enhances its transport rate when these proteins are heterologoulsy expressed in a cultured cell line. These findings led to the

proposal that CA might facilitate NHE-mediated acid extrusion by providing H^+-ions (arising from the hydration of CO_2) for transport. Thus, it is possible that the functional interactions of CA and membrane H^+-equivalent transporters represent a widespread additional controller of pH_i regulatory mechanisms. It is noteworthy to mention that CA has been also proposed to interact with other membrane transporters such as MCT1 (Becker *et al.*, 2005) and the glutamine transporter SNAT3 (Weise *et al.*, 2007), and modulate their activity. There is, however, not yet evidence of a functional H^+-equivalent transport metabolon in intact wild-type cells.

1.4.3. Inhibitors of CA activity and their use in physiology and clinic

CA inhibitors have been very important in determining the physiological function of CA isozymes in organs, cells and organelles. Most CAs are strongly inhibited by aromatic and heterocyclic sulphonamides as well as by inorganic, metal complexing anions (Lindskog, 1997; Supuran *et al.*, 2003).

Sulphonamides are powerful CA inhibitors and have been classically used in physiological studies and in the clinic. In 1940, sulphanilamide was the first sulphonamide described to act as a potent and specific inhibitor of CA activity (Mann & Keilin, 1940). This very simple monocyclic sulphonamide molecule afforded the development of a wide spectrum of sulphonamide pharmacological agents with a variety of biological actions, among others, the antibacterial agent sulfathiazole, the widely used diuretic furosemide, the hypoglycaemic agent glibenclamide, the anticancer sulphonamide indisulam, the aspartic HIV protease inhibitor amprenavir, and the potent CA inhibitor acetazolamide (ATZ).

At present, CA inhibitors are widely used clinically as antiglaucoma agents, diuretics and antiepileptics, and as agents for the management of acute mountain sickness, gastric and duodenal disorders, and osteoporosis (Supuran *et al.*, 2003). Extensive research on structure-activity correlations has been carried out leading to the development of a wide range of specific sulphonamide and modified sulphonamide CA inhibitors aimed to target intracellular as well as extracellular CA isozymes (Supuran *et al.*, 2004).

Two of the most well-known sulphonamide drugs, ATZ and ethoxyzolamide (ETZ), have been clinically used as systemic antiglaucoma agents. Systemic inhibitors are useful in reducing the elevated intraocular pressure characteristic to this disease, as they represent the most efficient physiological treatment for glaucoma. This is achieved by reducing the rate of HCO_3^- and aqueous humour secretion due of the inhibition of CA II and IV. The systemic administration of these drugs however, results in the inhibition of various CA isozymes present in tissues other than the eye leading to a range of side effects (Maren, 1967; Supuran & Scozzafava, 2000). Topical administration of these drugs however, proved not to be effective. In order to avoid these complications, more recently, novel topically acting CA sulphonamides have been developed. The first such drug, dorzolamide, entered the clinic in 1995 (Sugrue, 2000) and the second one, brinzolamide, in 1999 (Silver, 2000). These two drugs showed much less side effects compared to the systemically administered ones, and inhibited all the physiologically relevant CA isozymes.

CA inhibitors have been also used in the treatment of neurological conditions. For decades, acetazolamide has been used to treat epilepsy (Reiss & Oles, 1996). Topimarate,

a sulphamate fructopyranose derivative, is currently used in the treatment of epileptic seizures in adults and children (Bialer *et al.*, 1999; Lyseng-Williamson & Yang, 2007). Interestingly, topimarate shares with other sulphamate or sulphonamide derivatives the ability to act as a potent inhibitor of CA activity (Casini *et al.*, 2003; Dodgson *et al.*, 2000; Supuran & Scozzafava, 2000).

Acetazolamide has been also used for the treatment of Acute Mountain Sickness (AMS) (Leaf & Goldfarb, 2007) and also of High Altitude Cerebral Edema (HACE) secondary to AMS (Hackett & Roach, 2001). Recently the use of ATZ for the treatment of Chronic Mountain Sickness has been proposed (Richalet *et al.*, 2005; Rivera-Ch *et al.*, 2007).

Other drugs, not originally designed to target CA, can also act as inhibitors of the enzyme. Some of these compounds such as the non-steroidal anti-inflammatory drugs celecoxib and valdecoxib designed as cyclo-oxygenase-2 inhibitors or the antipsychotic sulpiride design as a postsynaptic dopamine (D2) receptor antagonist, have a sulphonamide group in their molecules and thus can act as CA inhibitors (Weber *et al.*, 2004).

Recently, some non-sulphonamides have shown to inhibit CA activity suggesting that some chemical groups different from the classic sulphonamide o sulphonamide derivatives can affect CA activity (Iyer et al, 2006). CA inhibition by non-sulphonamide groups could be useful in the design of new drugs but also a potential problem to take into consideration when designing experimental protocols because of potential secondary effects (see Chapter 3).

In the present work, the functional relationship between intracellular and extracellular carbonic anhydrase activity and sarcolemmal H^+-equivalent transport mediated by the acid extruders NHE and NBC was investigated in isolated cardiac myocytes as a model of a wild-type intact cellular system. Because the study of membrane transport mechanisms requires the use of selective pharmacological inhibitors, the effect of these on *in vitro* and intracellular carbonic anydrase activity was also investigated, and possible inhibition mechanisms and potential repercussions on H^+-equivalent transport discussed. Some inhibition of sarcolemmal H^+-transport by these drugs may be secondary to inhibition of CA. Finally, the pH-dependence of *in vitro* and intracellular CA activity was examined and its possible implications for sarcolemmal H^+-equivalent transport also discussed.

CHAPTER 2

GENERAL METHODS

2.1. Ventricular Myocyte Isolation

Single ventricular myocytes were isolated from the hearts of Sprague-Dawley rats (~300-350g) stunned and killed by cervical dislocation according to UK Home Office regulations. Following rapid opening of the chest cavity, the aorta was sectioned and the heart was then quickly removed and placed into ice-cold (4-8°C) Solution A containing 16 IU/mL of heparin. After remaining connective tissue was removed, the heart was placed in a warmed water-jacketed chamber at 37°C and connected to a Langendorff system through a glass cannula inserted into the aorta and securely fastened with surgical thread.

In the Langendorff preparation, the heart is perfused in a retrograde direction down the aorta. This forces the aortic valves to shut and the perfusion fluid is directed into the coronary arteries thereby perfusing the entire ventricular mass of the heart, draining into the right atrium via the coronary sinus.

The cannula and all the tubing in the Langendorff system were pre-filled with Solution A plus 750μM $CaCl_2$ plus heparin (~4 IU/mL) before the heart was cannulated in order to avoid air-bubbles in the system. The heart could be perfused with three solutions maintained at 37°C in heated water-jacketed chambers of the Langendorff system. Three-way plastic valves were used to control the flow of the selected solution from one of the three chambers. The solutions were continuously bubbled with 100% O_2

and were supplied to the heart by a persitaltic pump (Gilson, Minipulse 3) to ensure tight control of flow and pressure. Flow rate was maintained at 14.5 mL min^{-1}. The perfusate flowed through a heating coil and bubble trap before reaching the heart to prevent bubbles from entering and blocking perfusion. A Hg-filled manometer was connected to the side-arm of the cannula for continuous monitoring of aortic pressure as a measure of the progress of digestion.

The heart was first perfused with Solution A plus 750μM $CaCl_2$ and heparin until it had regained a regular and stable beat. At this point, the perfusate was changed to Ca^{2+}-free solution (Solution A plus 1 mM EGTA). Under these conditions, the heart beat decreased gradually until stopping completely. The time between switching solution and the heart beat stopping (ie. the time for the Ca^{2+}-free solution to reach the heart) was recorded (T ~80 secs). Two minutes after switching to Ca^{2+}-free solution, the manometer was opened so pressure, which gives an indication of coronary resistance, could be monitored. After three minutes, the perfusate was switched to enzyme solution which consisted of Solution A plus Liberase Blendzyme 3 (a mixture of collagenase I and II, and protease; 0.2 mg/mL; Roche Diagnostics, UK) for ~12 min. Pressure was recorded and was usually between 40 and 80 mmHg. Once the enzyme solution had reached the heart (time T plus 10 seconds), it was collected (after passing through the heart) by closing off the line to waste at the bottom of the chamber that surrounded the heart. The collected enzyme solution was immediately bubbled with 100% O_2. When all the original enzyme solution had been used, the collected enzyme solution was recirculated. Pressure was recorded just after the beginning of recirculation and was, on average, 60 mmHg. Total time of perfusion with enzyme, including re-circulation, was 12 minutes.

After enzymic digestion, the heart was transferred from the Langendorff system to a Petri dish and the cannula removed from the aorta. The atria were cut away and discarded, and the remaining digested ventricles were finely cut up and flushed into a stirring chamber with 10mls of collected enzyme solution. The contents were then mechanically dispersed by slow stirring and constantly bubbled with 100% O_2 at 37°C.

After 5 minutes of mechanical dispersion, the cell suspension was filtered through a nylon mesh (aperture 250μm), and the filtrate collected in a beaker and subsequently centrifuged at 100g for 1 minute in 10mL Falcon tubes. The residual, undigested tissue that remained on the nylon mesh was then flushed back to the mechanical dispersion chamber, together with another 10mL of enzyme solution. This procedure was repeated once or twice more, or until no more undigested tissue remained.

After settling down, the supernatant in all three centrifuged tubes was pipetted off and discarded. The pellet of cells settled at the bottom of the tube was re-suspended in Solution A plus 500μM $CaCl_2$, and centrifuged for another minute. Again the cell suspension was left to stand so the cells could settle to the bottom, then they were resuspended, this time in Hepes-buffered Dulbecco's modified Eagle's medium (DMEM, Sigma, UK) at pH 7.4 and kept at room temperature, and away from light until use. The gradual re-addition of calcium prevents cell death from calcium overload.

Only rod-shaped myocytes, which were calcium-tolerant and did not contract spontaneously, were used in experiments. An example of a healthy myocyte is illustrated in Figure 1.

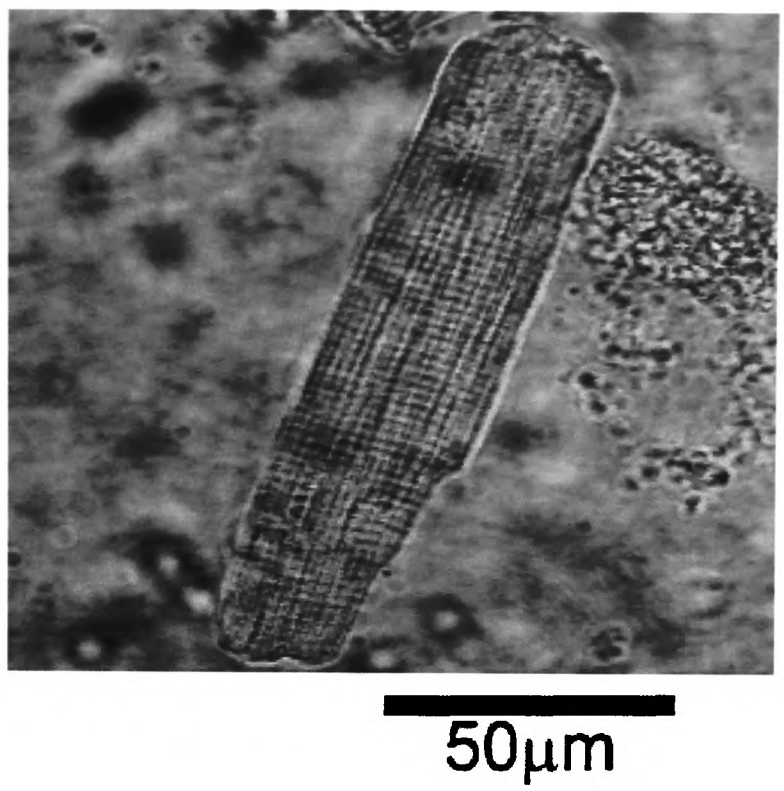

Figure 1. Transmission image of a healthy single rat ventricular myocyte.

2.2. Solutions and ventricular myocyte superfusion

2.2.1. Solutions

The amounts in brackets refer to concentrations, in mM, unless otherwise stated. All solutions, except those used for calibration, had a pH of 7.4 and an average osmolarity of 300mOsm.

Hepes-buffered Tyrode: NaCl (135), Hepes (20), KCl (4.5), $MgCl_2$ (1), $CaCl_2$ (2), glucose (11). pH was adjusted to 7.4 at 37°C with 4N NaOH.

CO_2/HCO_3^--buffered Tyrode: NaCl (125), KCl (4.5), $MgCl_2$ (1), $CaCl_2$ (2), glucose (11), $NaHCO_3$ (22). pH was adjusted to 7.4 by bubbling with 5% CO_2/air at 37°C for at least one hour before starting the experiments.

Ammonium Tyrode, Hepes-buffered: NaCl (115), NH_4Cl (20), Hepes (20), KCl (4.5), $MgCl_2$ (1), $CaCl_2$ (2), glucose (11). pH was adjusted to 7.4 with 4N NaOH at 37°C.

Acetate Tyrode, Hepes-buffered: Na^+-acetate (80), NaCl (55), Hepes (20), KCl (4.5), $MgCl_2$ (1), $CaCl_2$ (2), glucose (11). pH was adjusted to 7.4 with 4N NaOH at 37°C.

High [K^+] CO_2/HCO_3^- -buffered Tyrode (iso-osmotic): NaCl (85), KCl (4.5), $MgCl_2$ (1), $CaCl_2$ (2), glucose (11), $NaHCO_3$ (22). pH was adjusted to 7.4 by bubbling with 5% CO_2/air at 37°C for at least one hour before starting the experiments.

Na^+-free Hepes-buffered Tyrode: N-Methy-D-Glucamine (NMDG; 140), KCl (4.5), $MgCl_2$ (1), $CaCl_2$ (2), Hepes (20), glucose (11). pH was adjusted at 37°C using 5N HCl.

Na^+-free CO_2/HCO_3^--buffered Tyrode: NMDG (135), KCl (4.5), $MgCl_2$ (1), $CaCl_2$ (2), glucose (11). pH was adjusted to 7.4 by bubbling with either 5% CO_2/air or 20% CO_2/air at 37°C for at least two hours before starting the experiments.

Cl^--free Hepes-buffered Tyrode: Na^+-gluconate (135), K^+-gluconate (4.5), Mg^{2+}-gluconate (1), Ca^{2+} -gluconate (8.5), Hepes (20), glucose (11), 2,3-butanedione monoxime (20). pH was adjusted to 7.4 at 37°C with 4N NaOH.

Cl^- -free CO_2/HCO_3^- buffered Tyrode: Na^+-gluconate (118), K^+-gluconate (4.5), Ca^{2+}-gluconate (8.5), Mg^{2+}-gluconate (1), $NaHCO_3$ (22), Glucose (11), 2,3-butanedione monoxime (20). pH was adjusted to 7.4 at 37°C by bubbling with 5%CO_2/air.

Calibration solution for pH 5.5: KCl (140), MgCl2 (1), EGTA (0.5), nigericin (0.01), MES (20), pH balanced to 5.5 with NaOH and HCl.

Calibration solution for pH 6.5 or 7.0 or 7.5: KCl (140), MgCl2 (1), EGTA (0.5), nigericin (0.01), Hepes (20), pH balanced with NaOH and HCl.

Calibration solution for pH 8.5: KCl (140), MgCl2 (1), EGTA (0.5), nigericin (0.01), CAPSO (20), 2,3-butanedione monoxime (11), pH balanced to 8.5 with NaOH and HCl.

Solution 'A' for cell isolation: NaCl (128), KCl (2.6), Hepes (10), Taurine (20), $MgSO_4$ (1.18), glucose (11), KH_2PO_4 (1.18). pH was balanced to 7.4 with NaOH and bubbled with 100% O_2. All the solutions for myocytes isolation were prepared using ultrapure deionised water.

Storage solution, Dulbecco's Modified Eagle Medium (DMEM): NaCl (15), Hepes (20), 50U/ml penicillin, 50μg/ml streptomycin, pH balanced to 7.48 at room temperature with NaOH.

Reaction medium (RM) for CA assay: NaCl (15), KCl (35) , Hepes (20), K^+-gluconate (105). The medium was adjusted with 4N NaOH at 2°C to the desired pH value. The ionic strength (I) of the solution was calculated as $I = 0.5\Sigma (C_i z_i^2)$ where C_i is the concentration of i^{th} ion present in the solution and z_i its charge. The summation, Σ, is taken over all the ions in the solution. The ionic strength component due to the charged species of buffer was calculated using the pK_a value at the desired temperature and pH.

Double-buffered reaction medium: NaCl (15), KCl (35), Hepes (20), MES (20), K^+-gluconate (105). The medium was adjusted with 4N NaOH to pH 8.0, 7.5, 7.0 and 6.5 at 2°C.

High buffering capacity reaction medium: Hepes (130), NaCl (50). The medium was adjusted with 4N NaOH to pH 8.0, 7.5, 7.0 and 6.5 at 2°C, 12°C, and 22°C.

Saturated CO_2 solution for CA assay

A saturated CO_2 solution was obtained by bubbling 99.9% CO_2 into ultrapure, deionized water. Water was bubbled in a water-jacketed glass vessel, and temperature was kept constant using a thermostated water recirculator (Grant LTD6G, Cambridge). The final CO_2 concentration in solution was calculated from previously published CO_2 solubility data (Gevantman, 1995).

2.2.2. Superfusion chamber for cardiac myocytes

Experiments in which living isolated cardiac myocytes were used, involved myocyte superfusion in specially designed chambers. Perspex chambers (volume ~200μL) were made specifically to fit onto the stage of a microscope. Solution was delivered through tubes, driven by a peristaltic pump at 3mL/min. Experiments were carried out at 37°C and solutions were warmed to this temperature by pre-heating the bottles in a water bath and by warming solution just before it entered the superfusion chamber using a miniaturized feedback resistance heater (25W, RS components, UK). A metal tubing piece, connected in series with the line that feeds the solutions to the chamber, passed across the heater ensuring that the solutions were warmed and had the appropriate temperature on entering the chamber. The resistance heater was controlled by a feedback circuit, sampling the chamber temperature through a thermocouple probe.

A suction tube, fixed to the opposite end of the chamber, removed excess solution to keep a low level at steady state. The bottom of the chamber was sealed by a number 1 coverslip (Chance Proper, UK). The transparency and thickness of the coverslip would minimise light aberrations and absorption. The underside of the coverslip made contact

with the x40 objective lens of the viewing microscope through a thin layer of oil (Cargille oil, type DF; Cargille Laboratories, USA), applied before experiments. Oil has a similar refractive index to glass, i.e. the objective lens. Therefore, light passing through the coverslip to the lens, was not refracted greatly and the numerical aperture of the microscope (related to the resolving power) was increased.

In order to perform solution changes, two lines of solution were run simultaneously. A two-way tap was installed near the chamber. This tap diverted one solution to the superfusion chamber and the other solution to a waste reservoir. The tap can slide to a second mode, reversing the diversion. The continuous supply and removal of solution to the superfusion chamber permitted rapid solution change. To avoid loss of cells with the bulk flow of solution, the coverslip was treated with 100μL of poly-L-lysine (Sigma, UK). After washing the poly-L-lysine, cells could be applied. The charge deposited by poly-L-lysine on the coverslip helps cells to adhere.

2.3. Drugs

NHE inhibitors: In this thesis three NHE inhibitors were used. Two of them were the pyrazine-derived generic inhibitors 5-(N,N-dimethyl)amiloride (DMA) and 5-(N-Ethyl-N-isopropyl)amiloride (EIPA). Another class of inhibitor, Cariporide (HOE-642), a benzoylguanidine compound with high specificity for the NHE-1 isoform, was also used. Cariporide was kindly provided by Sanofi-Aventis (Germany). DMA and EIPA were purchased from Sigma (Sigma-Aldrich, UK).

NBC inhibitors: Two NBC inhibitors were used in the experiments of this thesis. One was the non-selective anion transport inhibitor 4,4'-diisothiocyanatostilbene-2,2'-

disulphonic acid (DIDS). The other was S0859, a selective, high-affinity generic NBC inhibitor. S0859 was kindly provided by Sanofi-Aventis, Germany, and DIDS was purchased from Sigma (Sigma-Aldrich, UK).

CA inhibitors: In this thesis three CA inhibitors were used, acetazolamide (ATZ; K_i for human CA II = 10nM), ethoxozolamide (ETZ; K_i for human CA II = 1nM) and the compound "14v" (1-[5-sulfamoyl-1,3,4-thiazol-2-yl-(aminosulphonyl-4phenyl)]-2,6-dimethyl-4-phenyl-pyridinium perchlorate) (Alvarez *et al.*, 2003; Supuran *et al.*, 2004). ATZ and ETZ are uncharged, membrane-permeant sulphonamides and when applied to an isolated cell, will inhibit both intra- and extracellular CA isoforms. "14v" is a positively-charged heterocyclic sulphonamide that is membrane-impermeant, and will only inhibit membrane-associated CA isoforms with active sites oriented towards the extracellular space (Supuran *et al.*, 2004). The affinity of this compound for CA IV and CA II is in the nanomolar range (Scozzafava *et al.*, 2000; Supuran *et al.*, 2004). ATZ and ETZ were purchased form Sigma (Sigma-Aldrich, UK). 14v was kindly provided by Dr. Claudiu T. Supuran, Laboratorio di Chimica Bioinorganica, Universita degli Studi di Firenze, Firenze, Italy.

2.4. Enzyme and ventricular tissue preparation

2.4.1. CA II

CA II purified from bovine erythrocytes (Sigma-Aldrich, UK), was dissolved in RM at a concentration of 1mg/mL and kept on ice until use.

2.4.2. Cardiac ventricular homogenates for CA activity assay

Cardiac ventricular tissue was obtained by a procedure similar to the one used for isolating ventricular myocytes (see Ventricular Myocyte Isolation), with slight modification. Briefly, once the heart had been removed from the animal, it was placed in a warmed water-jacketed chamber and connected to the Langendorff system through the aorta where it was perfused with Solution A plus 750μM $CaCl_2$ and 16 IU/mL heparin.

Solution A, was continuously bubbled with 100% O_2 and maintained at 37°C by heated water-jacketed chambers before being supplied to the heart. After 10 minutes of retrograde perfusion, the heart was removed from the Langendorff apparatus and placed in an ice-cold petri dish. The heart was rinsed with ice-cold RM, and the atria and any remaining connective tissue were removed.

The excised ventricles were then finely chopped in the cold petri dish kept on ice, and quickly weighed. The tissue was placed in a round-bottom plastic tube and suspended in ice-cold RM plus 0.5% (v/v) Triton-X-100 to give a 1/10 (w/v) dilution. The tube was placed on ice and the suspension was homogenised using a Polytron homogenizer (Polytron® Kinematica AG, Switzerland) with four bursts of 10s each. Protein concentration in cardiac homogenates was quantified spectrohotometrically using the Bradford's assay (QuickStart, BioRad). Absorbance values were calibrated to protein content using different dilutions of bovine serum albumin (BSA) as standard. A 20μL sample of a 1/100 (v/v) homogenate dilution was used to determine protein content. Final protein concentration in the assay was 2.8mg/mL.

2.5. Assay of carbonic anhydrase activity

The uncatalysed reaction of reversible hydration-dehydration of CO_2 yields H_2CO_3 as an intermediate which instantly dissociates into HCO_3^- and H^+-ions:

$$\mathbf{CO_2 + H_2O \Leftrightarrow H_2CO_3 \Leftrightarrow HCO_3^- + H^+}$$

In the presence of CA, the reaction proceeds without the formation of H_2CO_3 as intermediate. In this case, CO_2 undergoes nucleophilic attack by an hydroxyl ion (OH^-) bound at the active centre of the enzyme, resulting in the formation of a HCO_3^- ion. A water molecule displaces the HCO_3^- and undergoes protolysis yielding a H^+ and regenerates the OH^- ion at the active site (see Chapter 3 for a detailed description of the reaction mechanism). The reaction can be expressed in two steps as:

$$\mathbf{E\text{-}OH^- + CO_2 \Leftrightarrow E\text{-}(OH^-)CO_2 \Leftrightarrow E\text{-}HCO_3^- \overset{H_2O}{\Leftrightarrow} E\text{-}H_2O + HCO_3^-} \quad \textbf{(i)}$$

$$\mathbf{E\text{-}H_2O \Leftrightarrow H^+\text{-}E\text{-}OH^- \Leftrightarrow E\text{-}OH^- + H^+} \quad \textbf{(ii)}$$

where E represents the enzyme, the first step (i) corresponds to the formation of HCO_3^-, and the second (ii) to the regeneration of OH^- and release of a H^+-ion.

For simplicity, the uncatalysed and catalysed reactions can be reduced to:

$$\mathbf{CO_2 + H_2O \Leftrightarrow HCO_3^- + H^+}$$

Because H^+-ions are produced in the course of the reaction for CO_2 hydration, either catalysed or uncatalysed, the rate of change of pH provides a measured index of

the reaction velocity. Therefore, CA activity can be measured by following the rate of fall in pH when CO_2 is added to a solution containing the enzyme (Figure 2).

The reaction set-up consisted of a combination digital mini pH-electrode (Biotrode, Hamilton, Switzerland) incorporated in a 4 mL water-jacketed borosilicate glass reaction chamber, mounted on a magnetic stirring plate to provide continuous mixing throughout the assay. The temperature throughout the assay period was kept constant (typically 2°C unless otherwise stated) by using a thermostated water recirculator.

For the assay of CA II activity, a volume of 1.5mL RM plus 0.5μL of CA II dilution were placed in the reaction chamber and the pH was recorded. Once the pH had stabilized, 500μL of CO_2-saturated solution were added to start the reaction giving an initial CO_2 concentration of 15.6mM and a final reaction volume of 2mL. The final [CA II] in the reaction mixture was 7.75nM.

For measuring CA activity in ventricular cardiac homogenates, 600μl RM and 400μL of homogenate were placed in the reaction chamber and, once the pH had stabilised, the reaction was started by adding 333μL of CO_2-saturated water.

After starting the reaction, the time-course of pH change was recorded until equilibrium was reached. The uncatalyzed rate of reaction was measured by recording the time-course of change of pH after addition of the appropriate volume of CO_2-saturated solution to RM (Figure 2).

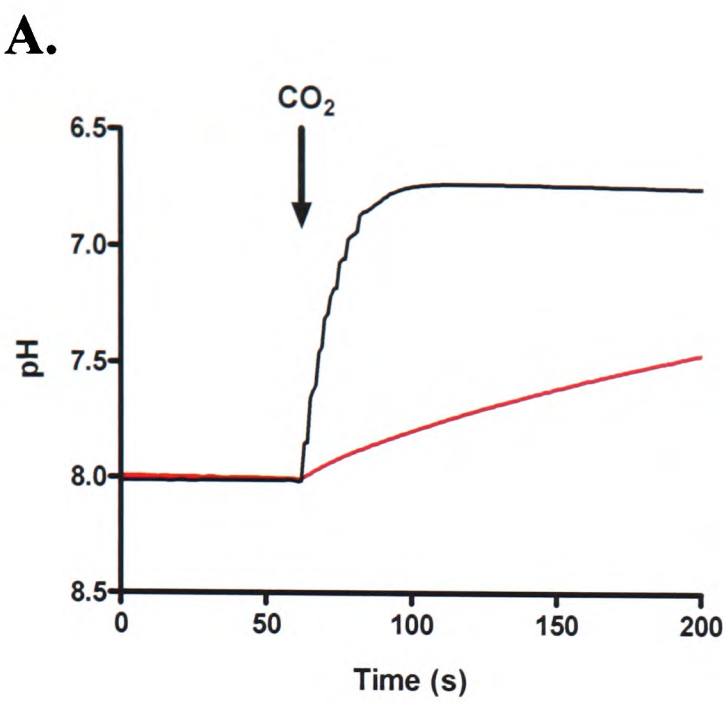

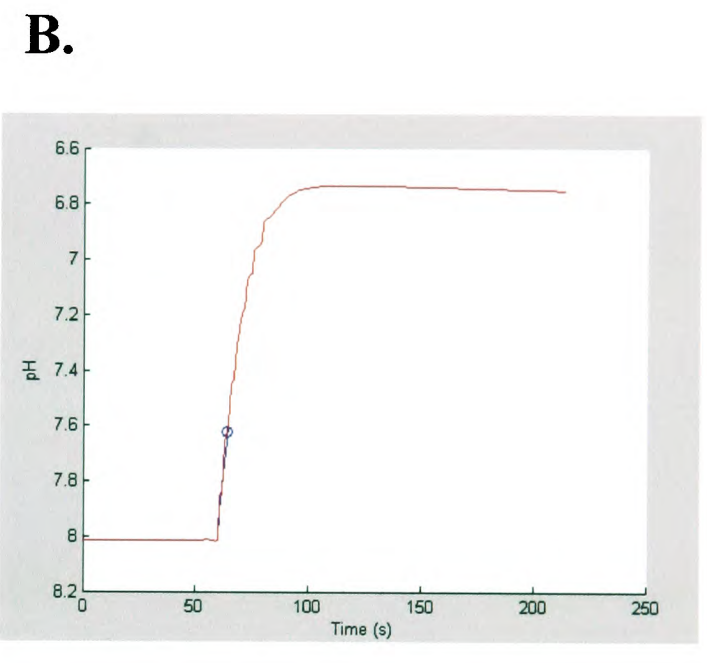

Figure 2. Assay of carbonic anhydrase activity. Panel A shows a typical experiment recording of the time-course of pH change after addition of an aliquot of CO_2-saturated deionized water in the presence (black) or absence (red) of 7.75nM CA II at 2°C, and at a buffer concentration of 15mM (Hepes). Data obtained in the absence of CA was used to obtain the uncatalysed rate of reaction. Panel B shows the best-fit to data predicted by a kinetic model (blue) during the initial 0.25 pH unit drop (see page 52). The best-fit was used to estimate k_f. The blue circle indicates the end of the fitting interval.

Solution pH was recorded at 1 Hz and the CO_2 hydration rates were expressed as a first-order forward hydration constant k_f (s^{-1}). The value for k_f was estimated by fitting a kinetic model to the pH time-course data. The model simulates the time-course of pH change on CO_2 addition and compares it with experimental data. The algorithm solves a

three-component reaction system of ordinary differential equations for pH, [HCO_3^-] and [CO_2]. Changes in pH are induced by the hydration reaction CO_2, yielding H^+ and HCO_3^-.

Due to the presence of buffer, the change in pH is given by the change in [H^+] divided by the buffering capacity of the reaction medium. In the case of CA II and CA activity in cardiac homogenates assays (*in-vitro* assays), the equations solved are:

$$\frac{dpH}{dt} = -\frac{1}{\beta(pH)} \cdot (\gamma \cdot k_f{}^0 \cdot [CO_2] - \gamma \cdot k_r{}^0 \cdot 10^{-pH} \cdot [HCO_3^-]) \quad (1)$$

$$\frac{d[HCO_3^-]}{dt} = \gamma \cdot k_f{}^0 \cdot [CO_2] - \gamma \cdot k_r{}^0 \cdot 10^{-pH} \cdot [HCO_3^-] \quad (2)$$

$$\frac{d[CO_2]}{dt} = -\frac{d[HCO_3^-]}{dt} \quad (3)$$

where β(pH) is the buffering capacity of the sample solution, determined by the physico-chemical properties of the buffer species ie. Hepes $(\ln 10 \times [buffer] \times 10^{(pH-pKa)})/(1+10^{(pH-pKa)})^2$. Typically the concentration of buffer in the reaction chamber was 16mM unless otherwise stated. In the case of *in-vitro* assays of cardiac homogenates, the dilution of with RM sanctions the assumption that the contribution of homogenate buffering capacity to total buffering capacity is negligible.

Gamma (γ) is a dimensionless factor that quantifies the acceleration of CO_2 hydration in the presence of CA. γ value was derived by best-fitting data with the model. Constants k_f^0 and k_r^0 are the spontaneous reaction rate constants for CO_2 hydration (forward) and dehydration (reverse), respectively. Constants k_f and k_r are expressed as multiples of the spontaneous rates, k_f^0 and k_r^0, and a non-dimensional multiplier γ, thus

k_f=$\gamma \times k_f^0$ and k_r=$\gamma \times k_r^0$ (for spontaneous CO_2 hydration, γ=1). The ratio of k_f/k_r is equal to, the equilibrium constant for carbonic buffer. Note that k_f and k_r are constrained such that $k_f/k_r = K_{CO2} = [H^+] \times [HCO_3^-]/[CO_2]$. It is therefore sufficient to fit only one parameter to the data. The spontaneous rate of hydration k_f^0 is determined from experiments performed in the absence of CA activity e.g. enzyme-free runs or runs performed in the presence of CA inhibitors such as ATZ.

The initial conditions for the simulations were determined by the starting pH of the assayed solution, assuming $[CO_2]$ = 0mM and $[HCO_3^-]$ = 0mM. Differential equations were solved using MATLAB ODE15s. The initial conditions for the simulations are determined by the starting pH of the in vitro assayed solution. It is assumed that there is nil CO_2 and nil HCO_3^-.

The simulations were performed for a range of multipiers γ varying between 1 (uncatalysed rate) and 1000 (1000-fold acceleration by CA). The goodness of fit between data and simulation was determined by the least squares method:

Error = Σ(data-simulation)^2

Chi-squared testing was used to identify significant fits. The level of significance judged worthy of a good fit was 5% and below. Most fits produced good or very good fits with errors not larger than 0.05 pH units over the fitting time-course.

The period over which best-fitting was delimited depended on the fitting protocol. If fitting was performed over the entire time course, least squares was applied throughout the time course. If the fitting interval was limited to a given fall in pH e.g. by 0.2 units, the errors were summed for the relevant time period only.

2.6. Measurement of intracellular pH: Whole-cell Epifluorescence Microscopy

One of the most widely used techniques for measuring pH_i employs pH-sensitive fluorescent indicators or fluorophores. Fluorescence is a physical phenomenon by which a substance absorbs light at a certain frequency and emits light at a lower frequency. A photon of energy of a certain wavelength is supplied by an external source and absorbed by the fluorophore, creating an excited electronic state within the molecule. The excited state exists for a finite time after which, another photon of energy is emitted returning the fluorophore to its original state. Due to energy dissipation during the excited-state lifetime, the energy of this photon is lower, and therefore of longer wavelength, than the excitation photon.

Fluorescent dyes can be used in biology to quantify intracellular ions, such as Ca^{2+}, Na^+ or H^+. The binding of such an ion produces a change in either the absorption spectrum (e.g. SBFI used to measure Na^+) or the excitation spectrum (e.g. Fluo-3 used to measure Ca^{2+}). The advantage of using fluorescence to measure pH_i is that they can be used to study small cells, even organelles, with great spatial and temporal resolution.

Fluorophores have been developed that have excellent pH sensitivity, have the ability to diffuse across the cell membrane and once hydrolysed inside the cell are membrane-impermeant such that they are trapped inside the cell. Such a compound is carboxy-seminaphthorhodafluor-1 (carboxy-SNARF-1; Molecular Probes, USA). In this thesis, the acetoxymethyl (AM) ester form of SNARF-1 was used. The ester form of SNARF is uncharged, and highly lipid soluble and therefore membrane permeant. Inside the cell esterases hydrolyse the ester bond producing the membrane-impermeant carboxylic acid.

The pKa of carboxy-SNARF-1 falls within the range 7.4-7.6 (Haugland, 2002), which makes it a suitable fluorophore for physiological studies. Carboxy-SNARF-1 is a single excitation and dual emission dye and therefore, a signal ratio output can be obtained. Measurement of a signal ratio eliminates the potential artefacts from changes in dye concentration, path-length and excitation intensity. Excitation at 540nm results in the emission of two strong, inversely related fluorescence signals at 580nm and 640nm. The two wavelengths correspond to the protonated (580nm) and unprotonated (640nm) forms of the dye, the ratio of which can be converted to a linear pH scale using a standard in situ nigercin calibration technique (see Calibration section). The emission spectra for carboxy SNARF-1 are given in Figure 3.

Figure 3. Emission spectra of carboxy-SNARF-1 excited at 534nm. From (Haugland, 2002).

SNARF-1 has many advantages over other pH-sensitive dyes including strong intensity at both emission wavelengths. Its long excitation wavelength also permits its use with certain drugs (such as amiloride and its derivatives, and also with stilbene

compounds such as DIDS) that would otherwise emit fluorescence themselves if exposed to shorter wavelength light.

In order to load the cells with SNARF-1, rat cardiac myocytes suspended in DMEM were mixed with 1-2μL of stock solution of the AM ester form of carboxy-SNARF-1 dissolved in dimethyl sulphoxide (DMSO; Sigma, UK) (1mg/mL). After an 8 minute loading period in darkness at room temperature, most of the dye that has passively entered the cell would have been hydrolysed and trapped inside the cell.

In this thesis, pH_i was measured using the epifluorescence technique. This particular style of fluorescence microscopy uses the microscope objective to illuminate the sample and the fluorescent signal is then collected, using the same objective, from an entire cell. In order to measure this, an inverted microscope (Nikon, Telford, UK) is coupled to a pair of bialkali photomultiplier tubes (PMTs, Thorn EMI, UK) for detection of emitted light, and to a source of excitation light from a 100W xenon lamp. Light from the xenon lamp first passes a 0.2% transmission neutral density filter to prevent phototoxicity and dye photobleaching.

Afterwards, the light of reduced intensity passes the 540nm interference filter (Glen Spectra Ltd, UK) and then reflected off a long-pass dichromatic mirror at 560nm (Glen Spectra Ltd, UK) into a Nikon Ph4DL x40 oil-immersion objective focused on the cell under observation.

A diaphragm is used to limit the area over which fluorescence will be measured. This ensures that fluorescence is recorded from the desired regions of the field of view, and prevents possible damage to the PMTs. The emitted light, together with the excitation light, then passes through another long pass dichromatic mirror at 610nm

(Glen Spectra Ltd, UK). This ensures the emitted light is separated into two beams, so that the PMTs can detect the signal from the protonated and unprotonated forms of the dye independently. To filter out light of unwanted wavelengths, light passes through interference 580 ± 5nm and 640 ± 5nm filters before it reaches the PMTs.

The current signals from the two PMTs are converted into a voltage signal, filtered at 10Hz and digitised at 0.5 kHz for collection on a computer drive. A sampling program records and ratios the digitized PMT outputs at 5Hz (Spike 4, Cambridge Electronic Design, UK).

A tungsten light bulb provides a concurrent beam of light that illuminates the cells for purposes of visualisation. A filter which transmits wavelengths above 650nm (red filter) was placed in the light path of this in order to avoid interference with fluorescence images. The transmission image is collected by a camera and displayed on a monitor. Figure 4 shows a schematic representation of this epifluorescence set-up.

2.6.1. Calibration of pH

In this thesis, data obtained from intracellular recording of SNARF-1 epifluorescence are in the form of the ratio of the intensities of two wavelengths detected independently by two photomultiplier tubes. This ratio is independent of light-path, dye concentration, photobleaching and most importantly, it is dependent on pH. Calibration of the ratiometric signal was performed using the nigericin method (Thomas *et al.*, 1979; Buckler & Vaughan-Jones, 1990). Nigericin is a membrane-soluble ionophore, which exchanges H^+ for K^+ across the cell membrane. If the intracellular and extracellular $[K^+]$ are equal, i.e. around 140mM, the intracellular pH should be constrained to equal the pH

of the bathing solution. Thus, by superfusing the cells with solutions of different pH and recording the intracellular fluorescence ratio (R), a relation between the intracellular pH (equal to extracellular pH) and fluorescence can be obtained and fitted to a sigmoidal function

$$\mathbf{pH = pKa + \log_{10}[(R_{max}-R)/(R-R_{min})] + pF}$$

where R_{max} is the maximum fluorescence ratio corresponding to an overwhelming ratio of protonated to unprotonated dye (normally detected at pH 5), R_{min} is the minimum fluorescence ratio corresponding to an overwhelming ratio of unprotonated to protonated dye (normally detected at pH 9), pK_a is the apparent dissociation constant for the protonated dye, and pF, the negative logarithm of the ratio of fluorescence at pH 9 to pH 5, measured at 640nm.

In order to obtain a sigmoid fit to data, a three-parameter sigmoid fit was performed for R_{max}, R_{min} and the sum of pK_a and pF under a single fitting variable.

Calibration experiments are carried out on cells loaded with fluorescent dye. The superfusate is changed to one of the calibration solutions listed in the Solutions section of this chapter. In a series of solution changes, the extracellular pH was changed from 5.5 to 8.5 in any pattern. The use of solutions with pH 5 and 9 was avoided in order to improve the survival of cells.

As the steady-state level approaches, R is acquired and plotted as a function of the pH of the bathing solution. Calibration was performed every six months and consecutive estimates of calibration parameters did not varied significantly between calibrations.

It is known that nigericin contaminates experimental apparatus due to its persistence in tubing and in the Perspex superfusion chamber (Richmond & Vaughan-Jones, 1997).

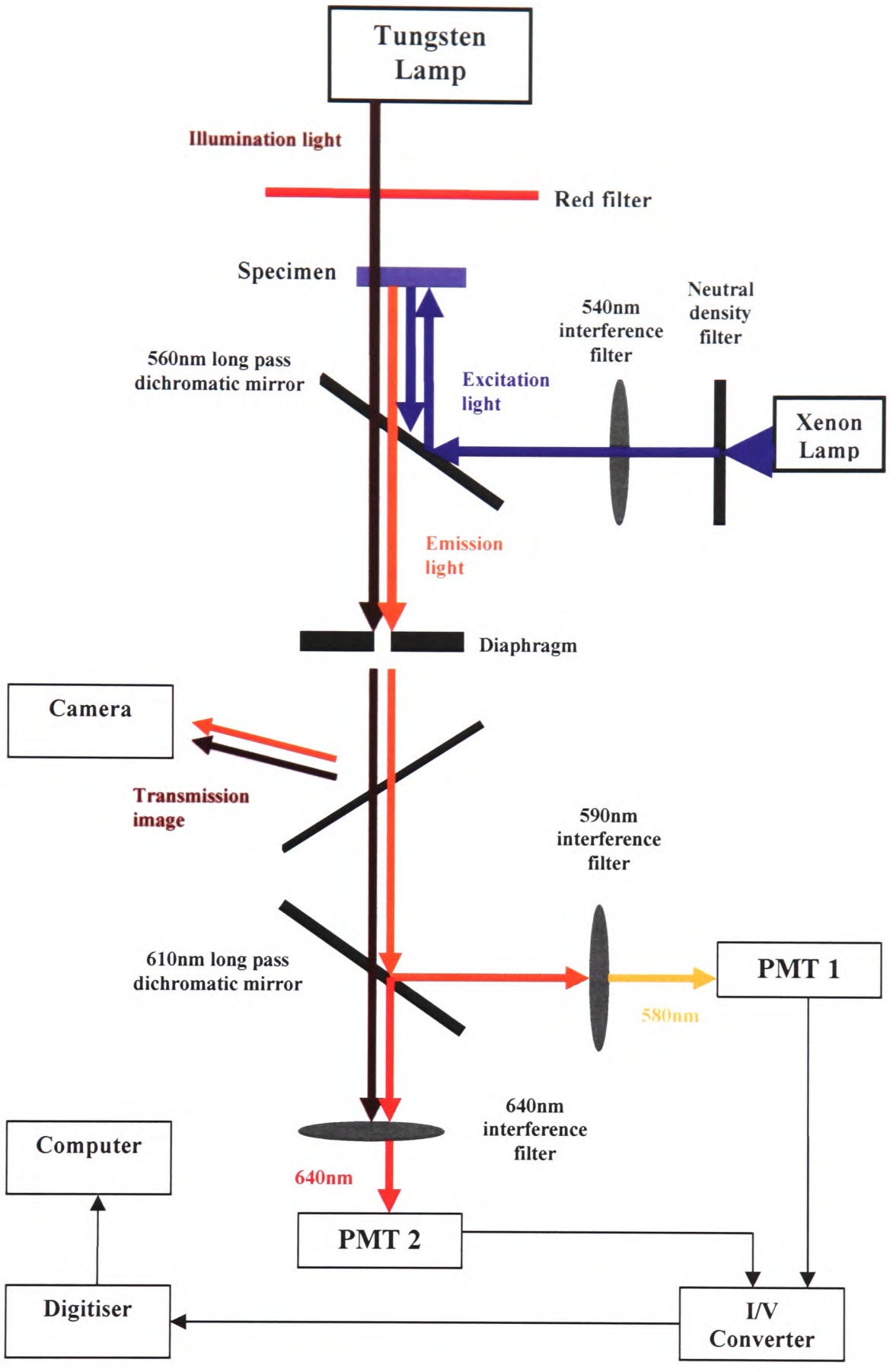

Figure 4. Schematic representation of the epifluorescence set-up for carboxy-SNARF-1. The specimen under a x40 objective lens is excited with light from a Xenon lamp. Light is then passed through a series of filters and mirrors to eliminate the excitation light and extract light of wavelengths around 580nm and 640nm for independent measurement of intensity by two PMTs.

To avoid contamination and detrimental consequences on subsequent experiments, the apparatus was cleaned by washing tubing and the superfusion chamber with 100mL of 2% bovine serum albumin (Sigma, UK) at 37°C, 2l of 20% Decon 75 (Decon Labs, UK) at 60°C, 100mL of ethanol at room temperature and finally with 3L of distilled water. Figure 5 shows a typical calibration curve performed on rat myocytes loaded with carboxy-SNARF-1.

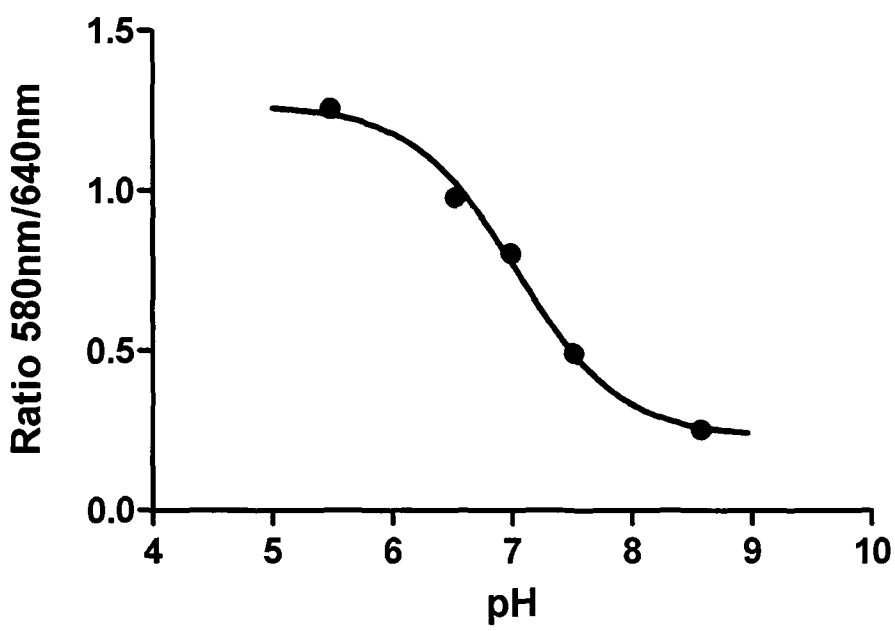

Figure 5. Typical calibration curve for carboxy-SNARF-1-loaded isolated rat myocytes. Error bars (SE) fall within the size of averaged data points (n=10).

2.7. Measurement of the reversible intracellular CO_2 hydration in intact myocytes

To quantify the kinetics of CO_2 hydration in intact myocytes, pH_i was measured while the superfusion solution was changed from Hepes-buffered (nominally CO_2-free) to CO_2/HCO_3^--buffered Tyrode at constant pH_o. The reverse solution change was performed to estimate the kinetics of CO_2 dehydration. On raising extracellular CO_2, rapid permeation of CO_2 into the cell drives the CA-catalysed reaction in the direction of

H^+-ion generation, producing a fall of pH_i. Conversely, when extracellular CO_2 is lowered, CO_2 is driven out of the cell driving the CA-catalysed reaction in the direction of intracellular H^+ consumption and thus rising pH_i (Figure 6).

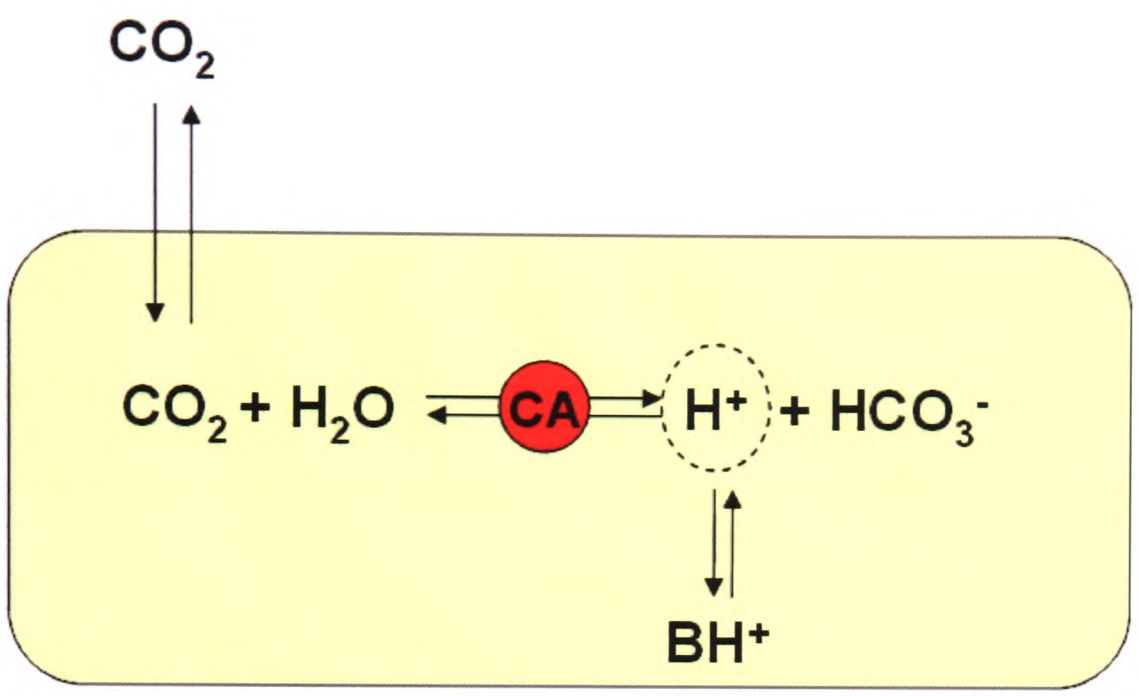

Figure 6. Schematic diagram illustrating the reversible intracellular hydration of CO_2. When the superfusate bathing the myocyte is switched from nominally CO_2-free Hepes-buffered to CO_2/HCO_3^- buffered Tyrode, CO_2 rapidly permeates the sarcolemma. The intracellular hydration of CO_2 catalysed by CA generates H^+, part of which are buffered instantaneously by intrinsic buffers. The unbuffered free H^+-ions cause pH_i to fall. When the superfusate is switched back to Hepes-buffered Tyrode, HCO_3^- ions combine with H^+ to generate CO_2 and water, causing pH_i to rise.

The rate of pH_i change on CO_2 addition/removal was used to assess the degree of CA catalysis. Na^+-free superfusates or pharmacological inhibitors were used in order to block Na^+-dependent acid extrusion transporters (NHE and NBC) during the CO_2-induced acid load, which would otherwise alter the kinetics of pH_i change. To estimate the uncatalysed rate of intracellular CO_2 hydration, switching between Hepes and CO_2/HCO_3^--buffered superfusates was also carried out in the presence of 100μM ATZ. Figure 7A shows a representative experiment in which a cardiomyocyte superfusate was

switched from Hepes to CO_2/HCO_3^- buffered solution ("ON") and then after 2 minutes, switched back to Hepes ("OFF"). The time-course of change of pH_i during CO_2 addition was used to calculate the intracellular hydration reaction constant (k_{fi}). When drugs were added, cells were superfused with drug-containing solution for at least 2 minutes before CO_2-containing buffer addition.

Reaction constants for the intracellular CA-catalysed reaction were estimated by simultaneously solving a set of differential equations that simulate the change of pH_i after switching from Hepes to CO_2/HCO_3^--buffered superfusates, and back. The equations were similar to those used previously for calculating the rate constants in the *in-vitro* enzyme assay, with modifications to comply with the conditions in an intact cell (permeation across a membrane and the intracellular buffering environment):

$$\frac{dpH_i}{dt} = -\frac{1}{\beta(pH_i)} \cdot (\gamma \cdot k_{fi}^{\,0} \cdot [CO_2]_i - \gamma \cdot k_{ri}^{\,0} \cdot 10^{-pH_i} \cdot [HCO_3^-]_i) \qquad (4)$$

$$\frac{d[HCO_3^-]_i}{dt} = \gamma \cdot k_{fi}^{\,0} \cdot [CO_2]_i - \gamma \cdot k_{ri}^{\,0} \cdot 10^{-pH_i} \cdot [HCO_3^-]_i \qquad (5)$$

$$\frac{d[CO_2]_i}{dt} = \rho \cdot P_{CO_2} \cdot ([CO_2]_o - [CO_2]_i) - \frac{d[HCO_3^-]_i}{dt} \qquad (6)$$

Here, ρ represents the surface/volume ratio of the cell and equals $0.68 \cdot 10^5$ dm^{-1}. P_{CO2} is the membrane permeability to CO_2, 0.058 dm/s (Forster, 1969). $\beta(pH_i)$ represents the intrinsic buffering capacity (β_{int}) and its value for rat was obtained from previous work (Zaniboni *et al.*, 2003). The initial conditions when switching solutions from Hepes to HCO_3^-/CO_2-buffered solution were: pH_i = steady-state starting pH_i, determined independently for each experiment; $[CO_2]_i$=0mM and $[HCO_3^-]_i$=0mM (Figure 7B). When

switching solutions from to HCO_3^-/CO_2 to Hepes, the initial conditions were: pH_i = steady-state pH_i after the CO_2-induced acid load, $[CO_2]_i=[CO_2]_o=1.16mM$ (5% CO_2 at 37°C) and $[HCO_3^-]_i=[HCO_3^-]_o\times10^{pHi-pHo}$ (Figure 7C). The short time-course of simulations sanctions the assumption that HCO_3^- membrane permeability is nil.

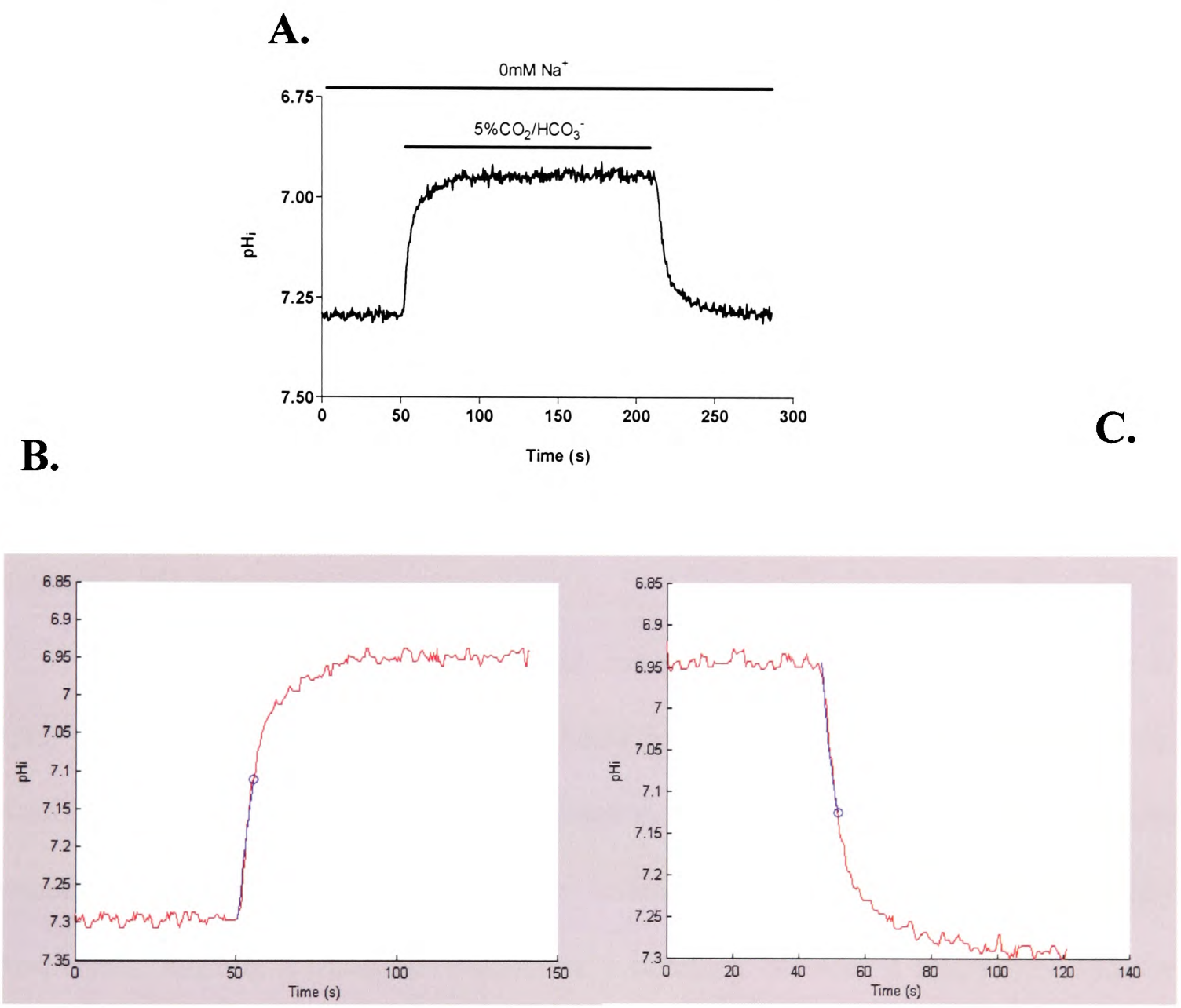

Figure 7. Panel A shows a typical experiment in which the superfusate was switched from Hepes- to CO_2/HCO_3^--buffered solutions, and back to Hepes under Na^+-free conditions. Panel B shows the best-fit predicted by the kinetic simulation to the first 0.2 pH unit drop induced by CO_2. Data is shown in red and the prediction in blue. The blue circle indicates the end of the fitting interval. The best-fit was used to estimate k_{fi}. Panel C shows the best-fit predicted by the simulation to the first 0.2 pH units of rise in pH_i on CO_2 removal. Graphs from Matlab macro output.

CHAPTER 3

EFFECT OF MEMBRANE TRANSPORT INHIBITORS ON CARBONIC ANHYDRASE ACTIVITY

3.1. Introduction

The study of the mechanisms underlying intracellular pH (pH_i) regulation requires physiological and kinetic characterization of the different H^+-equivalent membrane transporters. A common approach involves pharmacological dissection through selective transporter inhibition. This approach, however, requires that the inhibitors be specific for their target transporters, without side effects on other processes involved in pH_i regulation.

In order for membrane H^+-equivalent transporters to work efficiently, the rate of supply or removal of substrate or products should not be rate-limiting. It has recently been proposed that CA can modulate H^+ translocation or its equivalents (ie. HCO_3^-) across membranes by physically and functionally interacting with membrane pH_i regulatory transporters, forming a transport metabolon: a complex between a transporter and the enzyme that produces or consumes the transport substrate (Alvarez *et al.*, 2003; Alvarez *et al.*, 2005; Li *et al.*, 2002; Loiselle *et al.*, 2004; McMurtrie *et al.*, 2004; Sterling *et al.*, 2002; Sterling *et al.*, 2001a; Sterling *et al.*, 2001b). Because the reversible CA-catalyzed reaction produces and consumes H^+ and HCO_3^- it can facilitate the provision or removal of substrates or products associated with H^+-equivalent membrane transporter (see Chapter 4). These associations have been described in heterologous transfection systems

for CA II and NHE1 (Li *et al.*, 2002), for CA II and IV and NBC (Alvarez *et al.*, 2003), for CA II and IV with AE1 (Sterling *et al.*, 2002; Sterling *et al.*, 2001b), and for CA IX and AE1, AE2, and AE3 (Morgan *et al.*, 2007)

In the case of HCO_3^- transporters, activity can be hindered by the slow kinetics of spontaneous equilibration of CO_2 and HCO_3^-. Without enzymatic catalysis, the CO_2 hydration reaction is very slow, equilibration taking up to 30 seconds in unbuffered solution and several minutes in buffered cytoplasm (Leem & Vaughan-Jones, 1998a), therefore a HCO_3^- transport event may drive the buffer system out-of-equilibrium for several seconds, with a subsequent impediment to further HCO_3^- transport. Under physiological conditions CA is responsible for catalysing the interconversion of CO_2 and HCO_3^-, thus ensuring rapid attainment of chemical equilibrium. Rapid equilibration of the carbonic buffer system is also important for facilitation of intracellular H^+ mobility (Spitzer *et al.*, 2002; Swietach *et al.*, 2007) to ensure pH_i uniformity and efficient coupling between sub-membrane domains and the bulk cytoplasm.

Pharmacological inhibition of membrane pH_i regulatory transporters has been achieved by using drugs that target Na^+/H^+ exchange (NHE), and bicarbonate transport such as Na^+-HCO_3^--cotransport (NBC) and anion exchange (AE; Cl^-/HCO_3^- exchange).

Investigations on the contribution of NHE to pH_i regulation have been aided by a range of these inhibitors. Two major classes of pharmacological agents are currently used to inhibit NHE activity. One class includes amiloride and its 5'alkyl-substituted derivatives (Counillon *et al.*, 1993; Masereel *et al.*, 2003) such as 5-(N,N-dimethyl)amiloride (DMA) and 5-(N-Ethyl-N-isopropyl)amiloride (EIPA). DMA and EIPA are much more effective than amiloride on each studied NHE isoform and have

low inhibitory potency on Na^+ channels and Na^+/Ca^+exchange. Another class of NHE inhibitors includes the benzoylguanidines and its derivatives. This group comprises compounds such as 3-methylsulphonyl-4-piperidinobenzoyl-guanidine methanesulphonate (HOE-694) (Scholz *et al.*, 1993), 4-isopropyl-3-(methylsulphonyl)benzoyl-guanidine methanesulphonate (cariporide; HOE-642) (Scholz *et al.*, 1995), eniporide (Baumgarth *et al.*, 1997) and BIIB-513 (Gumina *et al.*, 1999) which completely lack the Na^+/Ca^+ exchanger inhibitory potency as well as the ability to block Na^+-channels (Figure 1). Later, some bicyclic selective NHE-1 inhibitors such as the quinoleine, zoniporide were developed (Guzman-Perez *et al.*, 2001).

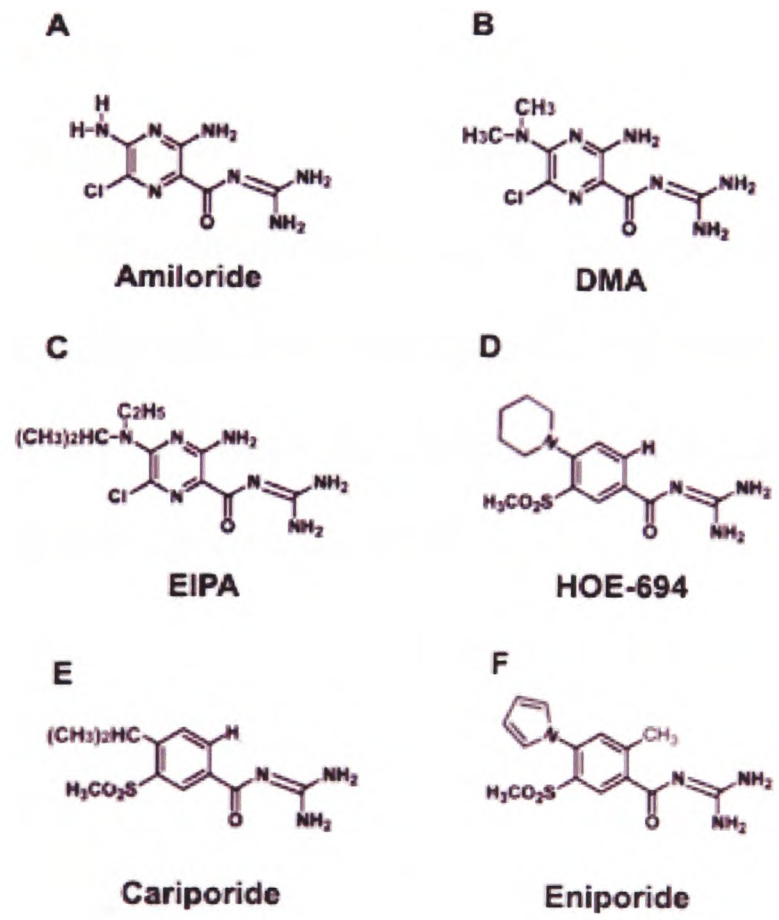

Figure 1. Structure of some Na^+/H^+ exchange (NHE) inhibitors. Two major classes of NHE inhibitors are shown. Pyrazine derivatives include Amiloride (A) and its related compounds, DMA (B) and EIPA (C). Benzoylguanidines include HOE-694 (D), cariporide (E), and eniporide (F).

Stilbene drugs have been widely used for studying the role of HCO_3^- transporters in pH_i regulation (Cabantchik & Greger, 1992). Disulphonic stilbenes are among the most potent HCO_3^- transport inhibitors and include the commonly used compounds 4,4'-diisothiocyanatostilbene-2,2'-disulphonic acid (DIDS; Figure 2A), and 4-acetamido-4'-isothiocyanostilbene-2,2'-disulphonic acid (SITS; Figure 2B).

DIDS has been widely used on studies investigating Cl^-/HCO_3^- exchange (AE) and Na^+-HCO_3^- cotransport (NBC) (Brune *et al.*, 1994; Dart & Vaughan-Jones, 1992; Deitmer, 1991; Eladari *et al.*, 1998; Lagadic-Gossmann *et al.*, 1992; Leem *et al.*, 1999; Leem & Vaughan-Jones, 1998b; Munsch & Deitmer, 1994). DIDS, however, as well as all disulphonic stilbenes, is not specific and thus will cause the non-selective inhibition of many types of bicarbonate transport. Recently, some more specific inhibitors have been developed. One example is S0859 ($C_{29}H_{24}ClN_3O_3S$; Sanofi-Aventis), a putative specific inhhibitor for NBC. In cardiac myocytes, for example, S0859 (Figure 2C) has been shown to block completely NBC activity in the micromolar range (30μM), with no pharmacological activity on other sarcolemmal H^+-equivalent transporter normally involved in pH_i regulation (Ch'en *et al.*, 2008).

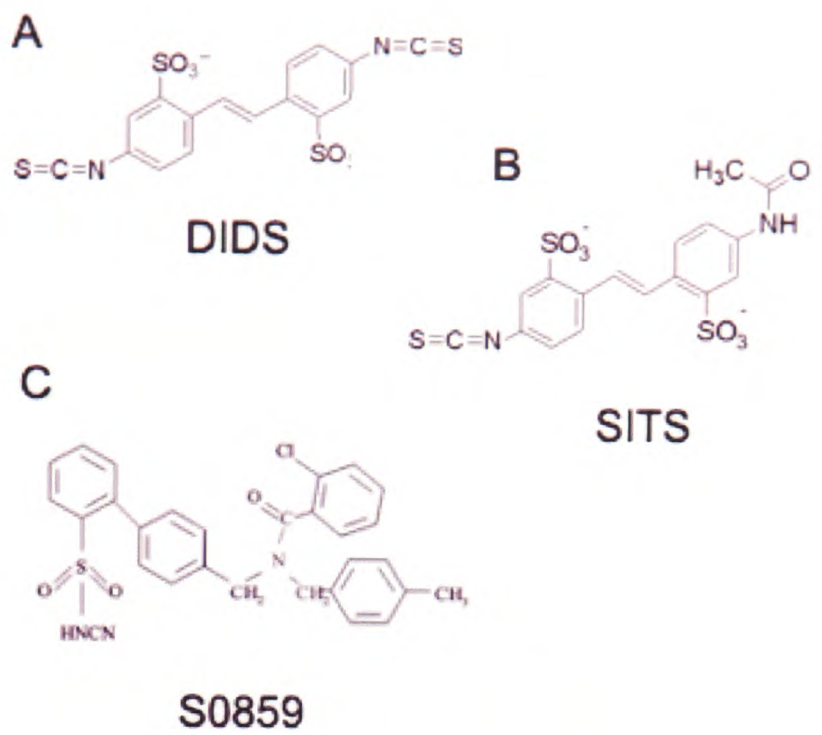

Figure 2. Structure of some bicarbonate transport inhibitors. Disulphonic stilbenes such as DIDS (A) and SITS (B) are non-selective inhibitors of bicarbonate transport. S0859 is a Na^+-HCO_3^- cotransport (NBC) selective inhibitor.

It is well known that CA activity is inhibited by sulphonamides ($R\text{-}SO_2NH_2$; Figure 3) and monovalent anions (Lindskog, 1997b; Supuran *et al.*, 2003). Although structurally different, both share common inhibition kinetics, behaving as noncompetitive inhibitors of the CA-catalysed reaction.

Variations on the sulphonamide structure have yielded additional CA inhibitors such as sulphamates ($R\text{-}OSO_2\text{-}NH_2$), hydroxysulphonamides ($R\text{-}SO_2NH(OH)$), and hydroxamates (R-CO-NH-OH) (Ilies & Banciu, 2004b; Supuran *et al.*, 2004). For example, steroidal and non-steroidal sulphamates, used as steroid sulphatase inhibitors to reduce estrogen levels in the tratment of hormone-dependent breast cancer, have been shown to inhibit CA *in vitro* (Abbate *et al.*, 2004b; Ho *et al.*, 2003; Vicker *et al.*, 2003).

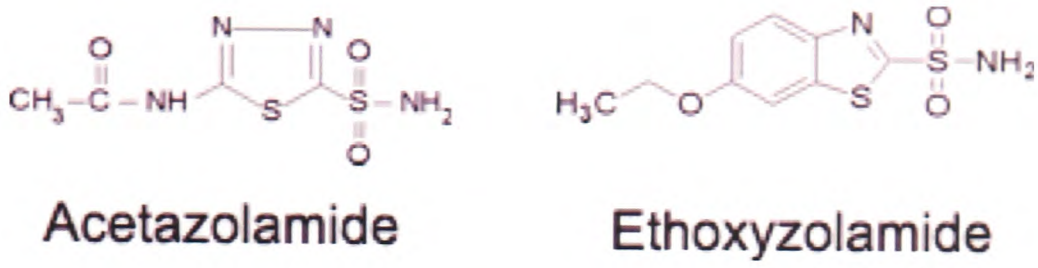

Figure 3. Sulphonamide CA inhibitors. Unsubstituted sulphonamides such as acetazolamide (ATZ) and Ethoxyzolamide (ETZ) are very powerful and widely used CA inhibitors.

Monovalent anions inhibit the enzyme with sufficient potency to generate significant physiological consequences. CN^-, HS^-, SCN^-, CNO^- and Cl^- are among the most potent anionic CA inhibitors described (Ilies & Banciu, 2004a).

Other drugs, originally not classified or intended as CA inhibitors, such as the cyclo-oxygenase-2 inhibitors celecoxib and valdecoxib (Weber *et al.*, 2004), the anticonvulsants topiramate (Maryanoff *et al.*, 2005) and zonisamide (Morgan *et al.*, 2004), and the antiphyschotic sulpiride (Abbate *et al.*, 2004a) also show inhibitory activity against CA.

Although membrane transport inhibitors used in pH_i regulation studies are not known CA inhibitors, some of them contain chemical moieties that may potentially affect CA activity. The compound S0859, for example, presents a cyanide-substituted sulphonamide group ($-SO_2NH(CN)$; Figure 2C). Therefore, it is important to determine if the drugs used for inhibiton of membrane transporters in pH_i studies have non-specific effects on CA activity that could, in turn, affect pH_i regulation, either by affecting the

kinetics of CA-coupled membrane transporters or the intracellular CA-facilitated mobility of H^+-ions.

3.1.1. Catalytic mechanism of carbonic anhydrase

Despite some differences between α-CA isoforms, all of them share basic catalytic features of hydration-dehydration of CO_2. Most of the work on the catalytic mechanism of CA derives from studies on the high-activity cytosolic isozyme CA II.

There is enough evidence, however, that indicates that all α-CAs share the same general mechanism (Liljas *et al.*, 1994; Lindskog, 1997a; Lindskog & Liljas, 1993; Silverman & Lindskog, 1988). The catalytic mechanism for CO_2 hydration can be divided in two major steps: i) the nucleophilic attack of the CO_2 molecule by the zinc-bound OH^- with the formation of a coordinated HCO_3^-, followed by the displacement of HCO_3^- by a water molecule, and ii) the transfer of an H^+-ion from the zinc-bound water molecule to bulk solvent, thereby regenerating the nucleophilic zinc-bound OH^-:

$$\mathbf{EZn\text{-}OH^- + CO_2 \Leftrightarrow EZn\text{-}(OH^-)CO_2 \Leftrightarrow EZn\text{-}\overset{H_2O}{HCO_3^-} \Leftrightarrow EZn\text{-}H_2O + HCO_3^-} \quad \mathbf{(i)}$$

$$\mathbf{EZn\text{-}H_2O \Leftrightarrow H^+\text{-}EZn\text{-}\underset{BH^+}{\overset{B}{OH^-}} \Leftrightarrow EZn\text{-}OH^-} \quad \mathbf{(ii)}$$

Figure 4 shows a schematic representation of the catalytic mechanism of CA in which the reaction intermediates are shown. The interaction of the substrate CO_2 with the CA active site is the first event in the catalytic cycle of CO_2 hydration. The CO_2 molecule, located in the hydrophobic association pocket, undergoes nucleophilic attack by the zinc-bound OH^--ion to generate a zinc-coordinated HCO_3^- (B and C). This HCO_3^-

is also positioned by accepting a hydrogen bond from the NH moiety of Thr-199 (D). HCO_3^- is then displaced from the active-site by a water molecule and liberated into solution (E).

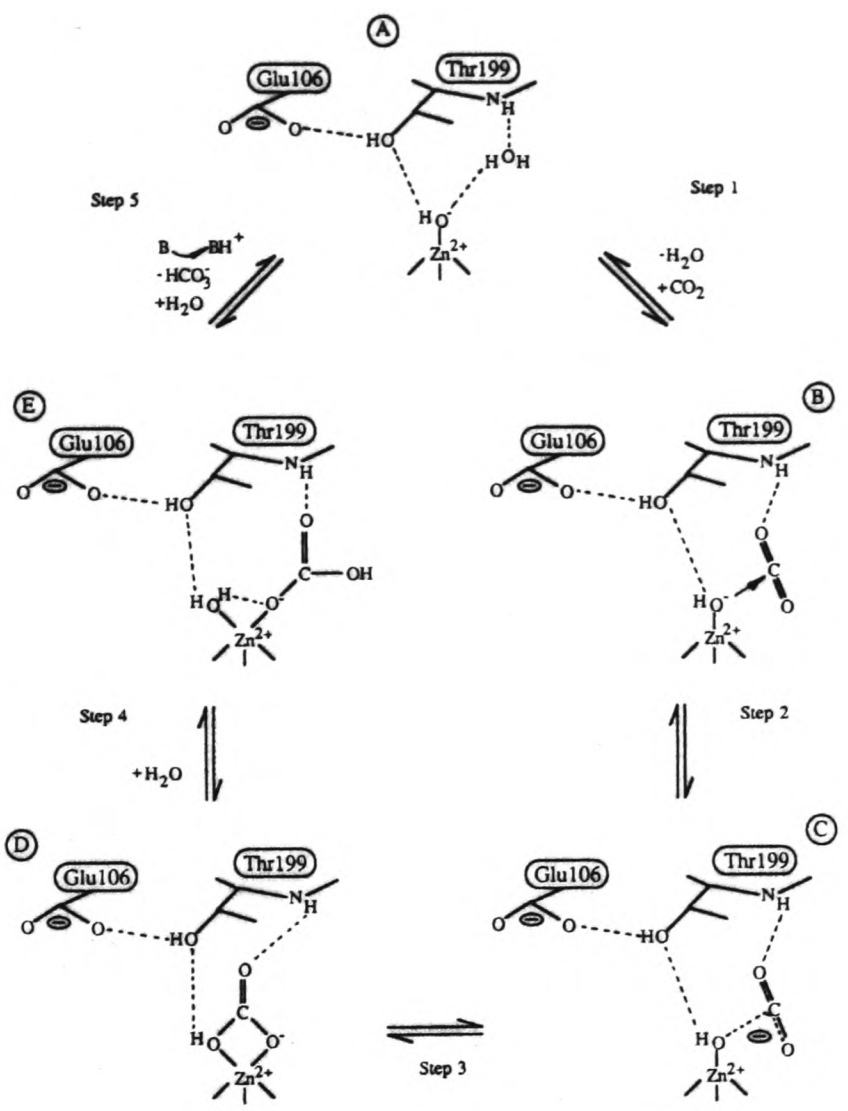

Figure 4. The catalytic mechanism of carbonic anhydrase. In the absence of substrate, the "deep water" molecule establishes hydrogen bonds with the nuclophile OH- and with the amino group of Thr-199 (A). The catalytic process in the direction of CO_2 hydration begins with the positioning of the substrate CO_2 in the hydrophobic pocket and subsequent nucleophilic attack by the zinc-bound OH^- (B). This causes a charge delocalization from the oxygen of the hydroxyl ion to the proximal CO_2 oxygen atom (C) leading to the formation of a HCO_3^- ion. The HCO_3^- remains bound to the Zn^{2+} ion through its two oxygens, giving the metal a penta-coordinated conformation (D). The HCO_3^- ion is also positioned by hydrogen bonds with the hydroxyl group and amide nitrogen ofThr-199. The bond between the Zn^{2+} ion and the hydroxyl moiety of HCO_3^- breaks, and a water molecules moves into its place (Step 4, E). The final step includes the release of the HCO_3^- from the active site, addition of a water molecule at the deep water site, and transfer of a H^+ from the zinc-bound water to a buffer molecule via a shuttling mechanism involving His-64. Hydrogen bonds are indicated by dashed lines (Taken from Eriksson and Liljas, 1991).

The regeneration of the zinc-bound OH^- from the zinc-bound water is considered to be the rate-limiting step, and it can be divided in two sequential events: an intramolecular and an intermolecular proton transfer (Khalifah & Silverman, 1991; Lindskog & Silverman, 2000). The intramolecular step consists of proton transfer from the zinc-bound water molecule to the His-64 residue. Because of the distance from the imidazole ring of His-64 to the Zn^{2+} ion, a direct proton transfer from the zinc-bound water molecule to His-64 is not possible.

The transfer occurs through two bridging hydrogen-bonded water molecules forming a "proton wire" (Hakansson *et al.*, 1992). This step is better described as a proton "translocation" and not a single proton transfer. The actual proton inmediately transferred away from the zinc-bound water does not diffuse to His-64, instead, this proton is transferred to a hydrogen bonded water, which in turn transfers a different proton to another hydrogen bonded water molecule, which in turn transfers a different proton to the imidazole moiety of His-64 (Figure 5). If the "proton wire" is disrupted, the rate of proton transfer will be substantially diminished.

Figure 5. Intramolecular proton transfer. In order to regenerate the nucleophile (OH^-), a proton is translocated via two hydrogen bonded water molecules from the Zn^{2+}-bound water to His-64 (Taken from Stams and Christianson, 2000).

The intermolecular step consists of proton transfer from the His-64 residue to the buffer species in the bulk solution (Khalifah, 1973; Lindskog & Coleman, 1973; Silverman & Lindskog, 1988). The rate of proton transfer depends on the difference in pKa of the enzyme as proton donor with a pKa about 7 and the buffer as acceptor (Silverman & Lindskog, 1988; Silverman & Vincent, 1983).

At high buffer concentrations (above 5mM), the intramolecular proton transfer step limits the maximal rate of catalysis. The intermolecular transfer step is buffer-dependent and becomes rate limiting at very low buffer concentrations (Silverman, 1995).

3.1.2. Inhibition of carbonic anhydrase activity

Carbonic anhydrase inhibitors interfere with the catalytic mechanism of the enzyme in different ways, depending on their nature, the properties of the reaction environment (ie. pH, ionic strenght), and the isozyme type.

Typically, CA inhibitors can be classified into two broad groups: monovalent anions and unsubstituted sulphonamides. Despite major structural differences, they share common inhibition kinetics, behaving as noncompetitive inhibitors with CO_2 (Bertini & Luchinat, 1983; Coleman, 1975; Mansoor *et al.*, 2000; Maren & Sanyal, 1983); they do not dock within the hydrophobic pocket and usually bind directly to the Zn^{2+} ion in the active site. Additionally, divalent metal ions like Cu^{2+} and Hg^{2+} also inhibit CA activity (Tu *et al.*, 1981). Crystallographic evidence has shown that these ions bind to both nitrogens of His-64 and thus prevent the rapid transfer of protons from the zinc-bound water molecule to the buffer (Eriksson *et al.*, 1988).

3.1.2.1. Inhibition by anions

Most monovalent anions inhibit CA activity, but their apparent K_i values vary considerably (Ilies & Banciu, 2004b). Also, the different CA isozymes display diverse susceptibility to anionic inhibitors. For example, CA I is more susceptible to inibition by anions than CA II (Maren *et al.*, 1976). CA IV (Baird *et al.*, 1997; Maren & Conroy, 1993; Maren *et al.*, 1993) and CA V (Heck *et al.*, 1994) behave similarly to CA II. CA III, VI, and IX show intermediate sensitivity towards anionic inhibition (Engberg & Lindskog, 1984; Murakami & Sly, 1987; Rowlett *et al.*, 1991; Wingo *et al.*, 2001).

Early studies of the effect of anions on CA activity concluded that the anionic inhibition is non-competitive for the hydrase activity of the enzyme (Pocker & Stone, 1968), but competitive with regard to the anionic product HCO_3^- (Lindskog *et al.*, 1971).

Monovalent anion inhibitors can be classified into three groups. The first group comprises anions with a protonated ligand. These inhibitors replace the zinc-bound OH^- ion without distorting the tetrahedral coordination geometry and maintain the hydrogen bond with the hydroxyl group of Thr-199. Examples of this group of inhibitors are HSO_3^- and HS^- (Hakansson *et al.*, 1992; Mangani & Hakansson, 1992). HSO_3^- also displaces the deep water molecule establishing an hydrogen bond to the NH group of Thr-199 through one of its oxygen atoms (Figure 6A).

A second group comprises anions lacking a protonated ligand. Most of these anions do not remove the zinc-bound hydroxyl and bind close to the metal ion displacing the deep water molecule and, in several cases, hydrogen bond to the NH group of Thr-199. The metal ion is pentacoordinated in these complexes with a trigonal bipyramidal

geometry. SCN^-, formate and acetate belong to this group of anionic inhibitors (Figure 6B). CN^- and NCO^- are also believed to belong to this group (Lindahl *et al.*, 1993).

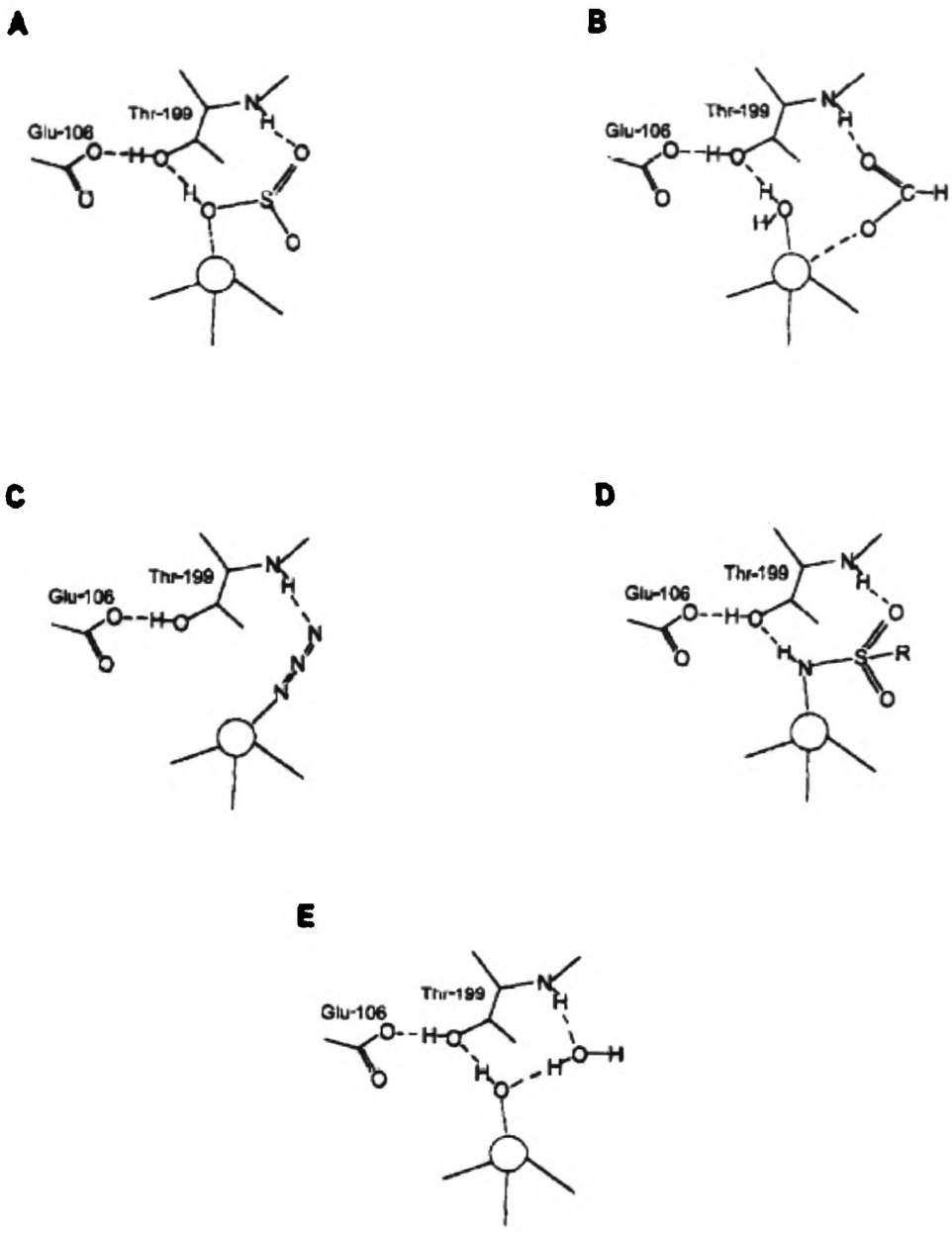

Figure 6. Structural representation of the binding of different inhibitors to the active site of the CA molecule. Figure 1A shows the mode of binding of bisulfite (HSO_3^-) as an example of the first group of inorganic anionic inhibitors. The binding of the second group of anionic inhibitors is exemplified by formate ($HCOO^-$) in Figure 1B. Azide (N_3^-) is shown in Figure 8C as an example of the third group of inhibitors. Figure 8D depicts the binding of a sulphonamide. The structure of the active site of the unihnibited enzyme is shown in Figure 8E.

The third group of anions corresponds to those that coordinate to the metal ion and displace the zinc-bound OH^- ion, but do not form a hydrogen bond to Thr-199. The resulting coordination geometry is still tetrahedral, but it is rather distorted (Figure 6C). Examples of anions in this group are the halides Br^- and I^-. Azide (N_3^-) also belongs to this group but, in this particular case, an hydrogen bond is established with the NH group of Thr-199.

3.1.2.2. Inhibition by Sulphonamides

The discovery of CA inhibition by sulfanilamide, a monocyclic sulphonamide, by Mann and Keilin (Mann & Keilin, 1940) led to the development of important drugs used to treat or prevent several diseases and to a wide variety of CA inhibitors (Supuran & Scozzafava, 2000; Supuran *et al.*, 2003). Sulphonamide compounds bind to the metal ion within the active site of the enzyme as anions via the nitrogen atom of the sulphonamide group. The NH^- group of the ionized sulphonamide replaces the zinc-bound OH^- and hydrogen bonds to the hydroxyl group of Thr-199. One of the sulphonamide oxygen atoms forms a hydrogen bond, with the peptide NH of Thr-199 displacing the deep water molecule, while the second oxygen points toward the Zn^{2+} ion but has no direct contact with the protein (Figure 6D). Because the NH^- of the sulphonamide group has the same position as the zinc-bound OH^- in the native structure (Figure 6E), the zinc coordination remains tetrahedral upon sulphonamide binding. The interaction of the rest of the sulphonamide molecule with the enzyme depends on which subtituents are situated at various locations on the aromatic or heterocyclic part of the inhibitor, which would interact with hydrophilic and hydrophobic residues within the cavity.

In the present study, the effect of the selective NHE inhibitors DMA, EIPA and cariporide, the bicarbonate transport inhibitors DIDS and S0859, and the organic mercurial compound p-chloromercuribenzene sulfonate (pCMBS, an aquaporin inhibitor), on the activity of the purified enzyme (CA II), total CA activity in cardiac homogenates, and CA-catalysed intracellular CO_2 hydration in intact cardiac myocytes have been investigated.

3.2. Methods

3.2.1. CA activity assay

Details of the reaction medium (RM), CA enzymatic assay and the quantification of the first-order CO_2 hydration rate constant (k_f) have been fully described in the General Methods chapter (Chapter 2). Protein content in the homogenates was quantified spectrophotometrically using the Bradford assay (QuickStart, BioRad).

3.2.2. Measurement of intracellular reversible CO_2 hydration in intact myocytes

Details of measurement of intracellular CO_2 hydration and dehydration, and quantification of the intracellular CO_2 hydration rate constant (k_{fi}; s^{-1}) have been fully described in the General Methods chapter (Chapter 2). All superfusates used were Na^+-free.

3.2.3. Drugs

The following drug stock solutions for the CA assay were prepared in DMSO and stored at 4oC on the same day of the experiments (in mM): ATZ 100, S0859 40, cariporide 39.8, DMA 79, EIPA 40, DIDS 400, pCMBS 391.

In order to obtain the desired drug concentration during the assay, 5μL of the stock solution or its appropriate dilution were added in the reaction tube. The final DMSO concentration was kept at 0.25%(v/v). For single cell epifluorescence experiments, drugs were dissolved in the superfusates. Final concentration of drugs were (in μM): cariporide 30, S0859 15, DIDS 100, pCMBS 250.

3.3. Results

3.3.1. Effect of ATZ on CA II and endogenous CA activity in cardiac homogenates

In order to confirm the presence of CA activity in cardiac homogenates, and to compare the inhibitory potency of the widely used sulphonamide CA inhibitor acetazolamide (ATZ) on purified CA II and endogenous CA in cardiac ventricular homogenates, a dose-response analysis was performed in CA activity assays. Figure 7A shows the effect of increasing doses of ATZ on the rate of change of pH due to CO_2 hydration in the presence of CA II. Similarly, increasing the concentration of ATZ caused significant slowing of CO_2-induced rate of acidification. The highest dose of ATZ resulted in a rate similar to that corresponding to the spontaneous reaction in the absence of CA II (CA-free blank shown in red).

Figure 7B shows a similar experiment but this time in the presence of cardiac homogenate. Increasing concentrations of ATZ also resulted in significant slowing of acidification induced by CO_2 hydration. Figure 7C shows the dose-response curves for ATZ on CA II and endogenous CA activity in cardiac homogenates. A four-parameter sigmoidal best-fitting procedure (Prism 4, GraphPad Software, Inc.) was used to obtain IC_{50} values. Doses of ATZ used were: 0.1, 1, 10, 100nM, 1 and 10mM. The dose-response curve (Figure 1C) shows IC_{50} values of 7.3nM and 3.3nM for CA II (n=4) and cardiac homogenates (n=8), respectively. The value of IC_{50} for ATZ on CA II activity is in agreement with previously published data (~10nM) (Khobzaoui *et al.*, 2004; Maren & Sanyal, 1983; Supuran, 2004).

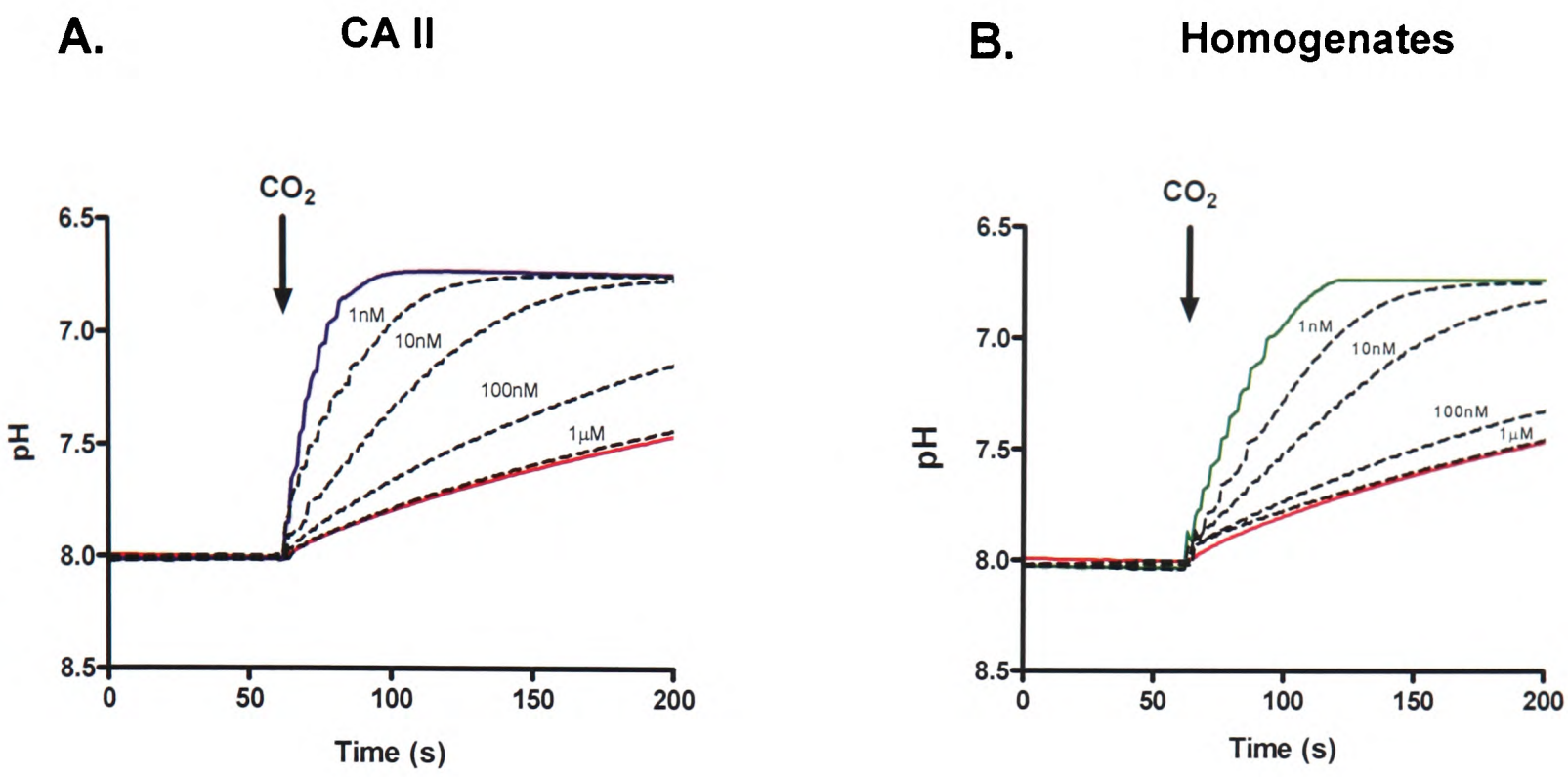

Figure 7. Dose-dependent inhibition of CA activity by ATZ. After starting the reaction, the time-course of pH change in the presence of CA II (A, blue) or cardiac homogenate (B, green) was recorded until equilibrium was reached. The uncatalysed rate of reaction was measured by recording the time-course of change of pH after addition of CO_2-saturated water to CA-free blanks (panels A and B, red). CA activity was confirmed by including acetazolamide (ATZ) in the reaction media containing cardiac homogenate (panel B) or CA II (A). Doses of ATZ used were: 0.1 (not shown), 1, 10, 100nM, 1 and 10µM (not shown). The dose-response curve (C) results in IC_{50} values of 7.3nM (n=4) and 3.3nM (n=8) for CA II and cardiac homogenates, respectively.

3.3.2. Screening the effect of membrane transport inhibitors on carbonic anhydrase activity

Six different membrane transport inhibitors were screened for their ability to inhibit CA II activity. The compounds used were the generic NHE inhibitors DMA and EIPA, the selective NHE1 isoform inhibitor cariporide, the non-selective/generic bicarbonate transport inhibitor DIDS, the selective NBC inhibitor S0859, and the aquaporin (AQP) inhibitor pCMBS. The inhibitor concentration employed in the screening was in the range of those used commonly in cellular experiments: DMA 200μM (Leem et al., 1999; Loh et al., 1996), EIPA 30μM (Bagnis et al., 2001; Bevensee et al., 1999), cariporide 30μM (Ch'en et al., 2003; Russ et al., 1996; Stuwe et al., 2007; Swietach & Vaughan-Jones, 2005), DIDS 100μM (Brune et al., 1994; Leem & Vaughan-Jones, 1998b; Schwiening & Boron, 1994), S0859 15μM (Ch'en *et al.*, 2008; Schwab *et al.*, 2005; Yamamoto *et al.*, 2005), and pCMBS 500μM (Cooper & Boron, 1998; Endeward et al., 2006).

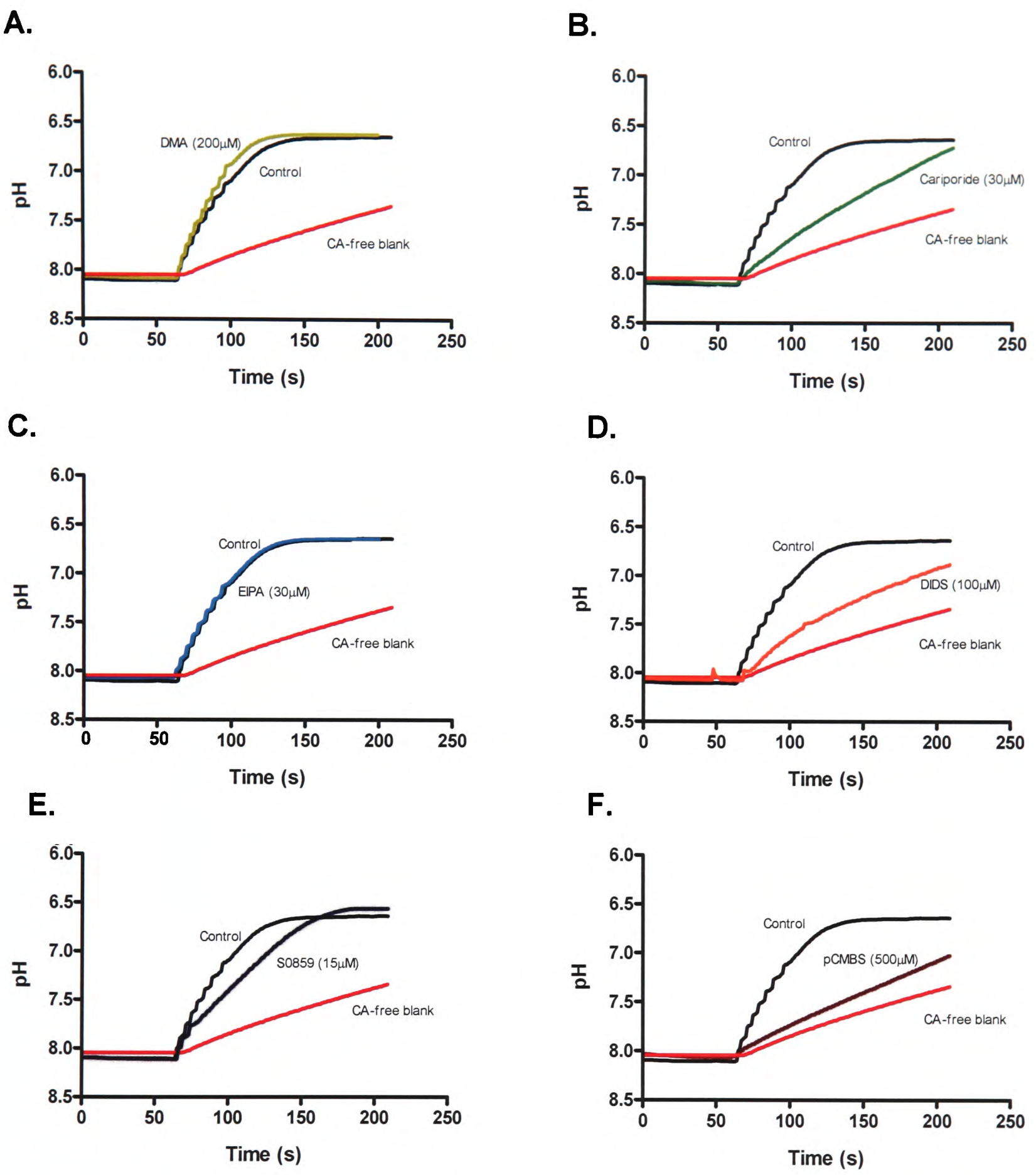

Figure 8. Six different membrane transport inhibitors were screened for their ability to inhibit CA II activity. The panels show typical pH experimental recordings of the different drugs tested at concentrations commonly used in cellular experiments (in μM): DMA 200 (A), cariporide 30 (B), EIPA 30 (C), DIDS 100 (D), S0859 15 (E), and pCMBS 500 (F). Only DMA and EIPA had no effect on CA II activity.

Figure 8 shows typical experimental recordings of the effect of the different inhibitors on the *in vitro* rate of acidification induced by CO_2 hydration. The experimental traces reveal that neither of the generic NHE inhibitors DMA (Figure 8A) nor EIPA (Figure 8C) inhibited CA II activity. In contrast, cariporide (Figure 8B), used at a concentration of 30μM, inhibited CA by 75%. Both bicarbonate transport inhibitors, DIDS (100μM; Figure 8D) and S0859 (15μM; Figure 8E), inhibited CA II activity by 68% and 50%, respectively. pCMBS at 500μM (Figure 8F) inhibited CA II activity by 88.5%. Figure 9 shows a comparison of the effect of the different transport inhibitors on normalised CA II activity.

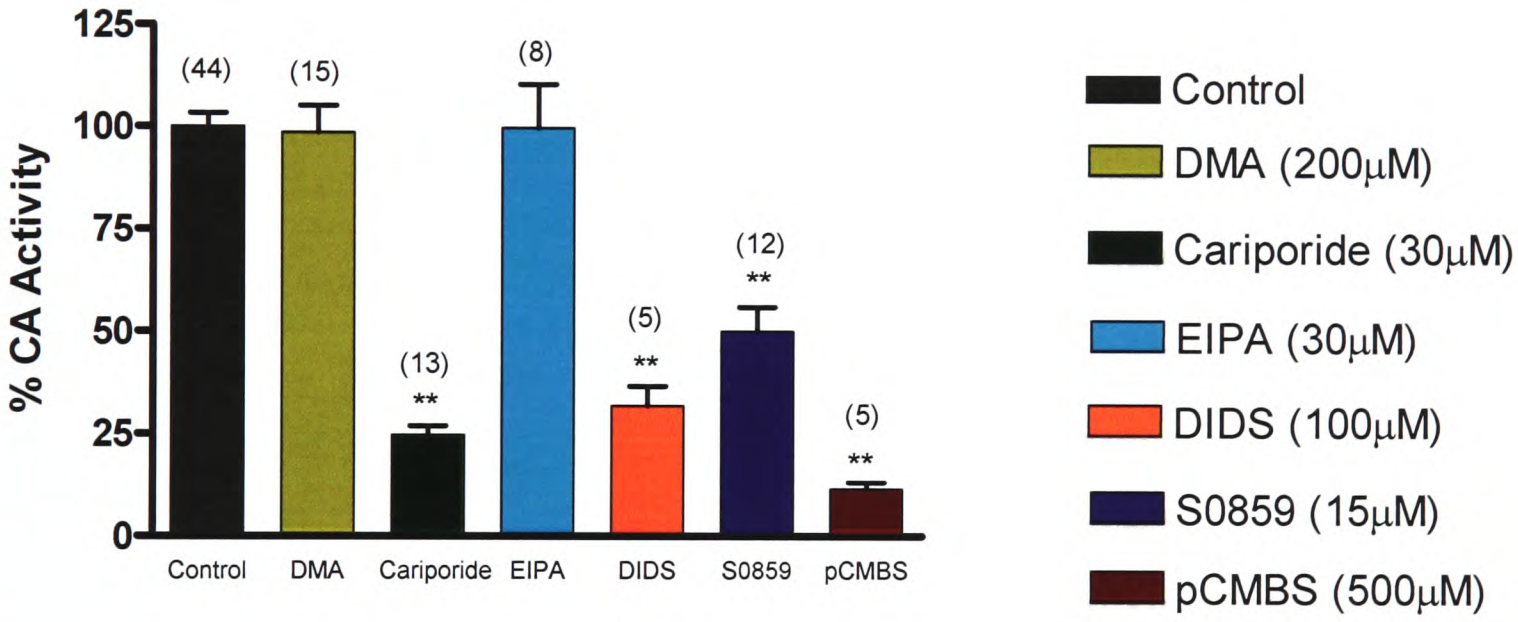

Figure 9. Comparison of the effect of membrane transport inhibitors on CA II activity. Neither DMA nor EIPA inhibited CA II activity. At 30μM, cariporide inhibited CA by 75%. DIDS at 100μM inhibited CA II activity by 68% and 15μM S0859 by 50%. pCMBS at 500 μM inhibited CA II activity by 88.5% (**$p<0.001$). The bars represent best-fit k_f values normalised to the k_f of the uncalaysed reaction.

A dose-response analysis of those membrane transport inhibitors that had an effect on CA II activity was carried out. A sigmoidal best-fitting procedure (Prism 4, GraphPad Software, Inc.) was used to obtain IC_{50} values, for each drug, for CA II and total CA activity in cardiac homogenates. Figure 10A shows the experimental recordings of the effect of increasing concentrations of cariporide on the rate of CO_2-induced acidification in the presence of CA II. Figure 10B shows the comparison of dose-response curves of the effect of cariporide on CA II and endogenous CA activity in cardiac homogenates. The IC_{50} on purified CA II and cardiac homogenates was 12.4 ± 7.31μM and 60 ± 2.61μM, respectively.

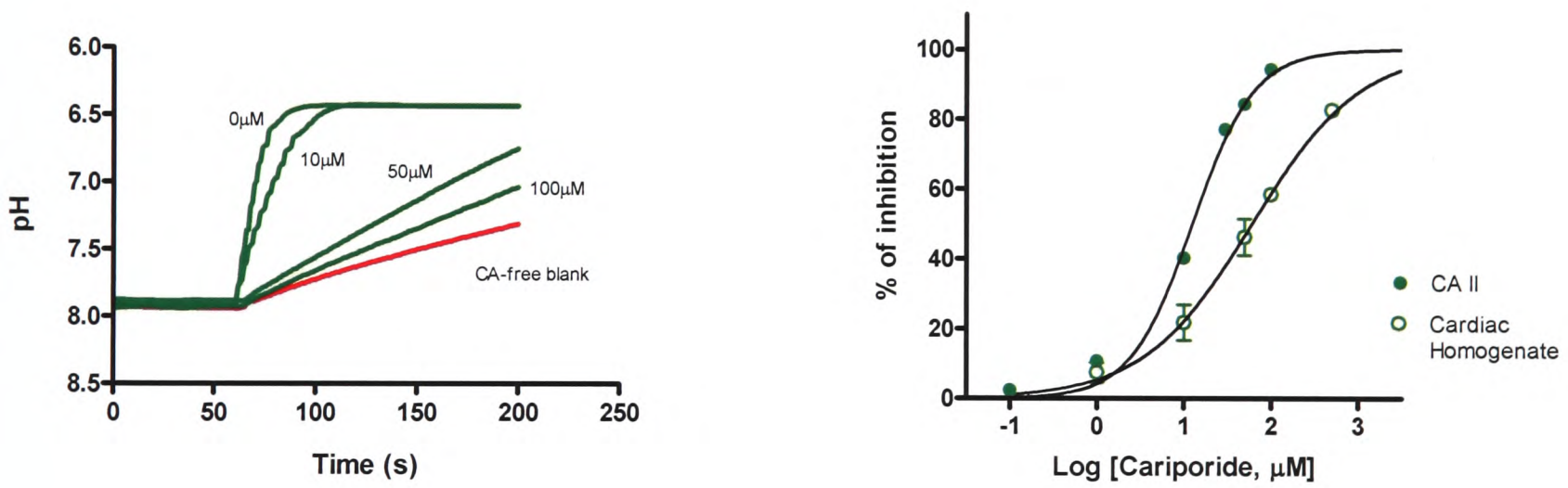

Figure 10. Dose-dependent CA-inhibition by cariporide. Panel A shows typical experimental recordings of the effect of increasing concentrations of cariporide on CA II activity. Panel B shows a comparison of dose-response curves of cariporide on CA II (IC_{50}=12.4 ± 7.31μM) and total CA activity in cardiac homogenates (IC_{50}=60 ± 2.61μM).

Figure 11 shows the dose-dependency of bicarbonate transport inhibitors on CA activity. Panels A and B show experimental recordings of the effect of increasing doses of S0859 and DIDS on the rate of CO_2-induced acidification, respectively. Panels C and D show a comparison of dose-response curves for S0859 (C) and DIDS (D) on CA II and total CA activity in cardiac homogenates. For S0859, IC_{50} values were 17 ± 8.1 μM for CA II and 64± 15.8 μM for cardiac homogenates Values of IC_{50} for DIDS were 42 ± 2.2μM and 316.5 ± 32μM, respectively.

Figure 12 shows the effect of increasing doses of the AQP inhibitor pCMBS on CA activity. Panel A shows the effect of increasing concentrations of the inhibitor on the CO_2-induced rate of acidification activity. Panel B shows a comparison of dose-response curves of pCMBS on CA II and cardiac homogenates. The IC_{50} values were 63.6 ± 18.6μM and 389.7 ± 38.6μM, respectively. Values for IC_{50} are given ± 95% confidence intervals.

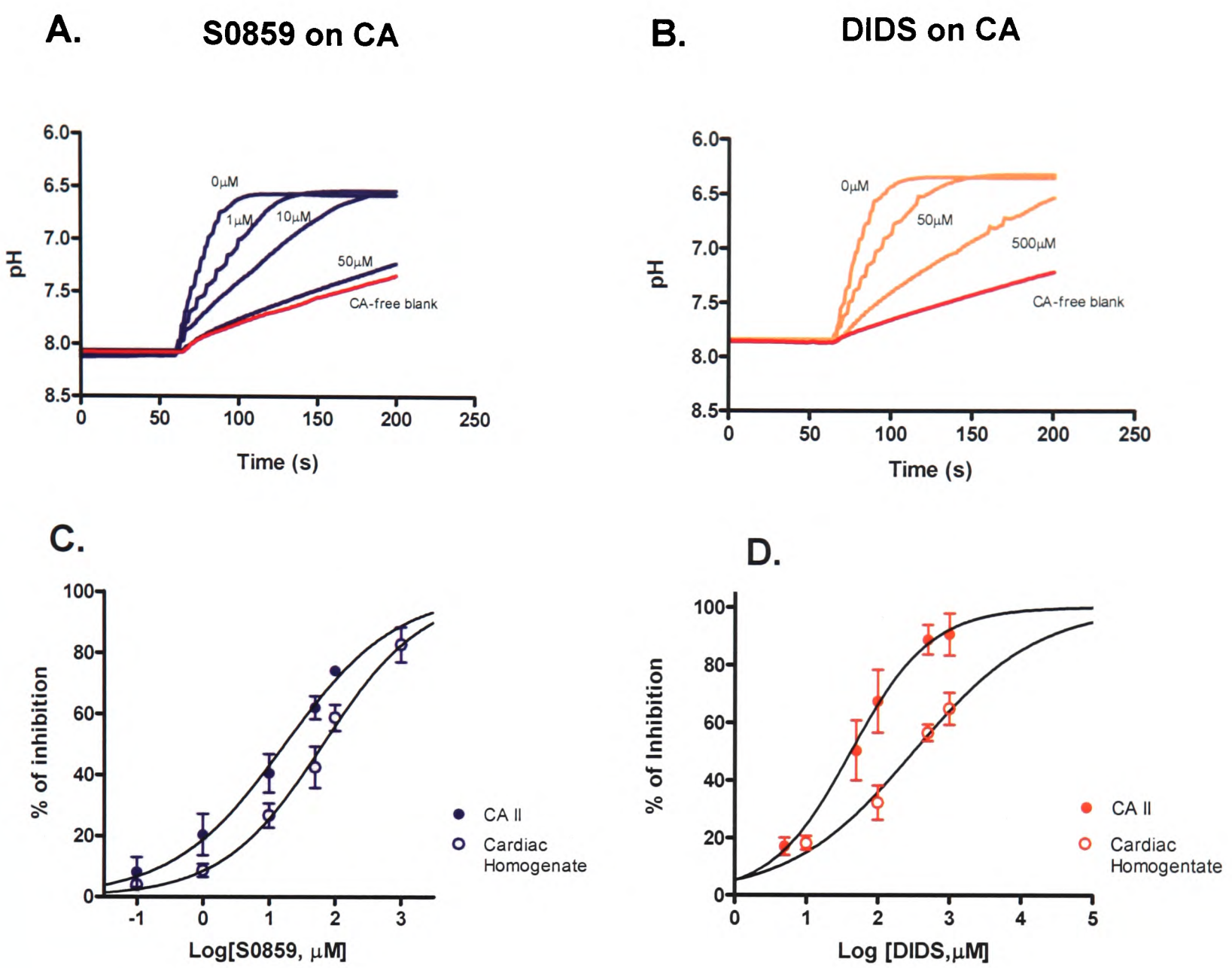

Figure 11. Dose-dependent inhibition of CA activity by bicarbonate transport inhibitors. Panels A and B show typical experimental recordings of the effect of S0859 and DIDS respectively, on CA II activity. Panels C and D show dose-response curves of S0859 and DIDS respectively, on CA II and endogenous CA activity in cardiac homogenates. (DIDS: IC_{50}=42 ± 2.2μM for CA II and 316.5 ± 32μM for homogenates; S0859: IC_{50}=17 ± 8.1 μM for CA II and 64± 15.8 for homogenates).

The higher IC_{50} values observed for each drug in the homogenates probably reflects the preferential binding to their target transporters, or the different sensitivities of the various CA isozymes expressed in heart to inhibition by these drugs. Because of the

presence of the different H^+equivalent transporters in cardiac homogentes, it is likely that the inhibitors will bind to them with greater affinity than to CA. Therefore, for obtaining the same amount of inhibition on CA II and cardiac homogenates, a higher concentration of the drug is required on the later, resulting in a higher IC_{50} value. Higher IC_{50} values in homogenates could also be the reflection of the IC_{50} of CA IV, IX and XIV, the other CA isoforms present in cardiac myocytes besides CA II (Alvarez *et al.*, 2006; Scheibe *et al.*, 2006).

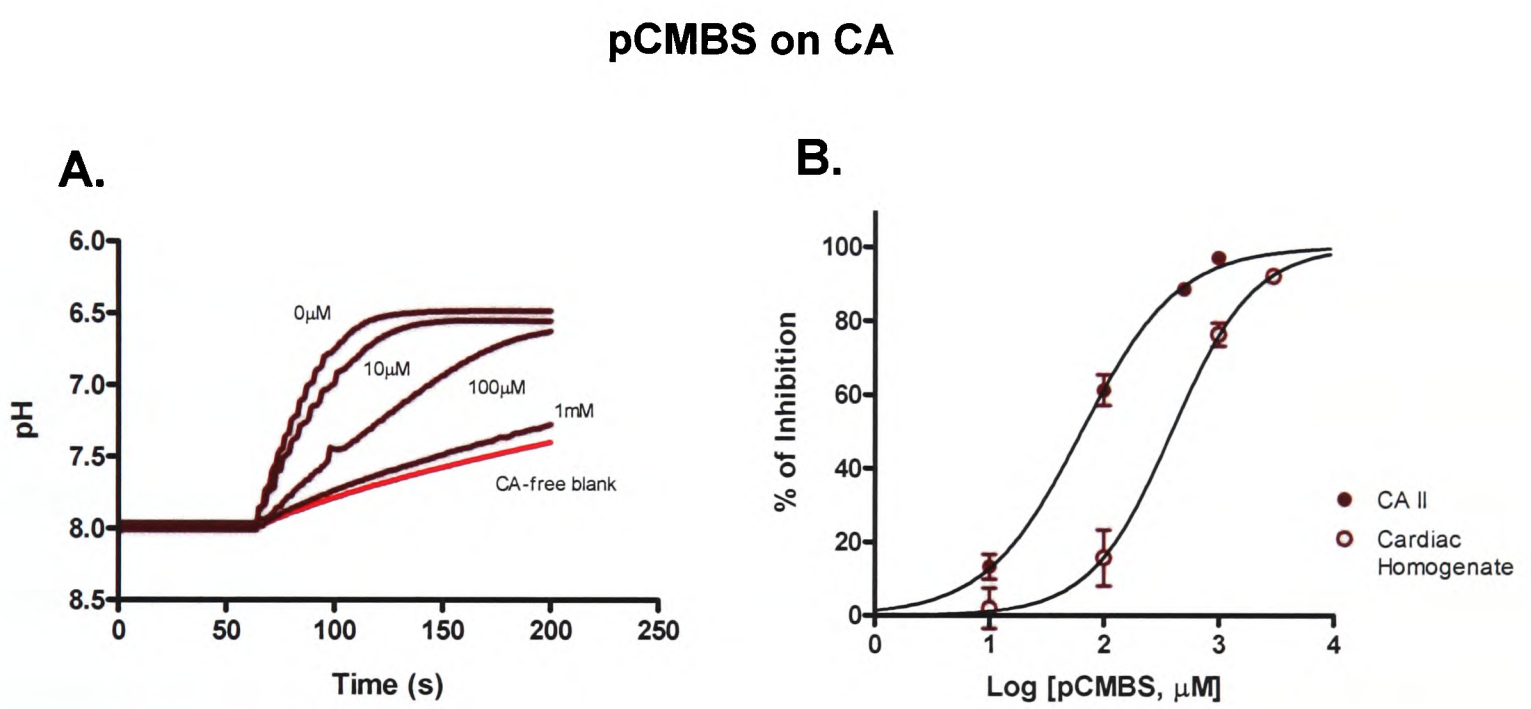

Figure 12. Dose-dependent inhibition of CA activity by pCMBS. The figure shows dose-response curves of pCMBS on CA II (IC_{50}=63.6 ± 18.6μM) and total CA activity in cardiac homogenates (IC_{50}=389.7 ± 38.6μM).

3.2.3. Effect of membrane transport inhibitors on intracellular carbonic anhydrase activity in intact cardiac myocytes

Although, several of the membrane transport inhibitors tested inhibited CA *in vitro* (i.e. where they had direct contact with the enzyme) it was necessary to investigate whether the same drugs are able to cross the sarcolemma and inhibit intracellular CA activity in intact cardiac myocytes.

In order to asses the effect of membrane transport inhibitors on the rate of the CA-catalyzed reversible hydration of intracellular CO_2 in cardiac myocytes, paired experiments were performed where the time-course of change of pH_i was recorded on switching from Hepes to 5% CO_2/HCO_3^--buffered superfusate ("ON"), and then back to Hepes ("OFF") (all solutions Na^+-free), in the absence and presence of the transport inhibitors. In order to confirm the presence of CA activity in cardiac myocytes, paired experiments were performed in the absence and presence of 100μM of the membrane-permeant CA inhibitor ATZ. Panel A of Figure 13 shows superimposed traces of such a experiment. In the presence of ATZ the rate of change of pH_i is reduced significantly for both the "ON" and the "OFF" phases, which confirms the presence of active CA. Panel B compares the intracellular CO_2 hydration rate constant (k_{fi}) values estimated from the initial change in pH_i obtained on switching the superfusate. 100μM ATZ resulted in a significant reduction of k_{fi}. This k_{fi} value ($k_{fi\ ATZ}$) represents an estimate of the uncatalysed rate of reversible intracellular CO_2 hydration.

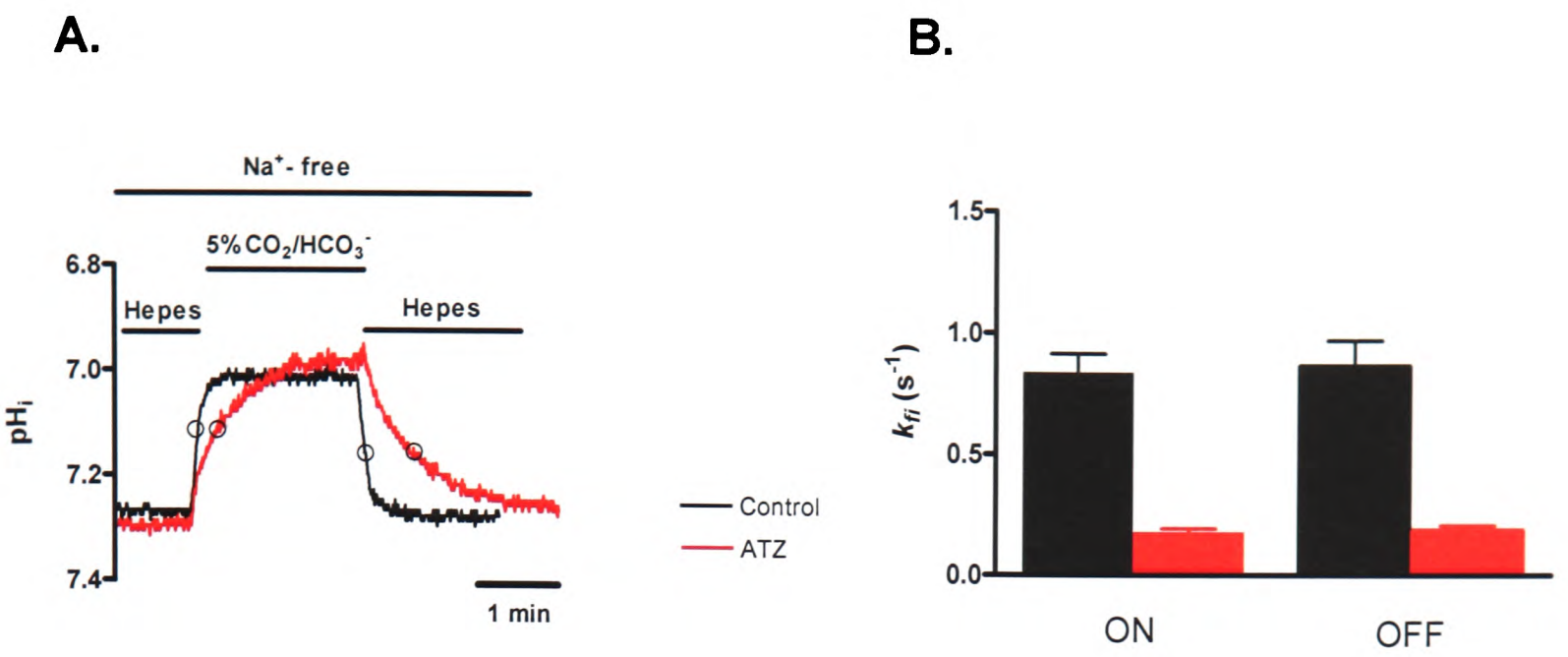

Figure 13. Effect of ATZ on the reversible hydration of intracellular CO_2. Panel A shows superimposed traces of a typical paired experiment where the time-course of change of pH_i was recorded on switching the superfusate bathing a cardiac myocyte from Hepes to 5% CO_2/HCO_3^--buffered solution and back to Hepes (all solutions Na^+-free) in the absence (control) and presence of 100μM ATZ. The rate of change of pH_i in the presence of ATZ was significantly slowed down. The corresponding k_{fi} values are shown in the Panel B (n=15). k_{fi} values were estimated from the best-fit of the kinetic algorithm to pH_i data obtained during the initial 0.2 pH_i unit drop after CO_2 addition. Circles on the traces shown in Panel A indicate the end of the fitting interval.

Switching to CO_2/HCO_3^- superfusate containing 30μM cariporide had no effect on the rate of intracellular CO_2-induced acidification or om the rate of alkalinisation on switching from CO_2/HCO_3^--buffered to Hepes-buffered superfusate (Figure 14A). This is reflected in the normalised k_{fi} values obtained in the presence of cariporide compared to controls (Figure 14B). k_{fi} was normalized to $k_{fi\ ATZ}$ ($k_{fi}/k_{fi\ ATZ}$).

Similarly, DIDS (100μM; Figure 14C and 14D), S0859 (15μM; Figure 14E and 14F), or pCMBS (250μM; Figure 14G and 14H) also had no effect at the exposure times employed.

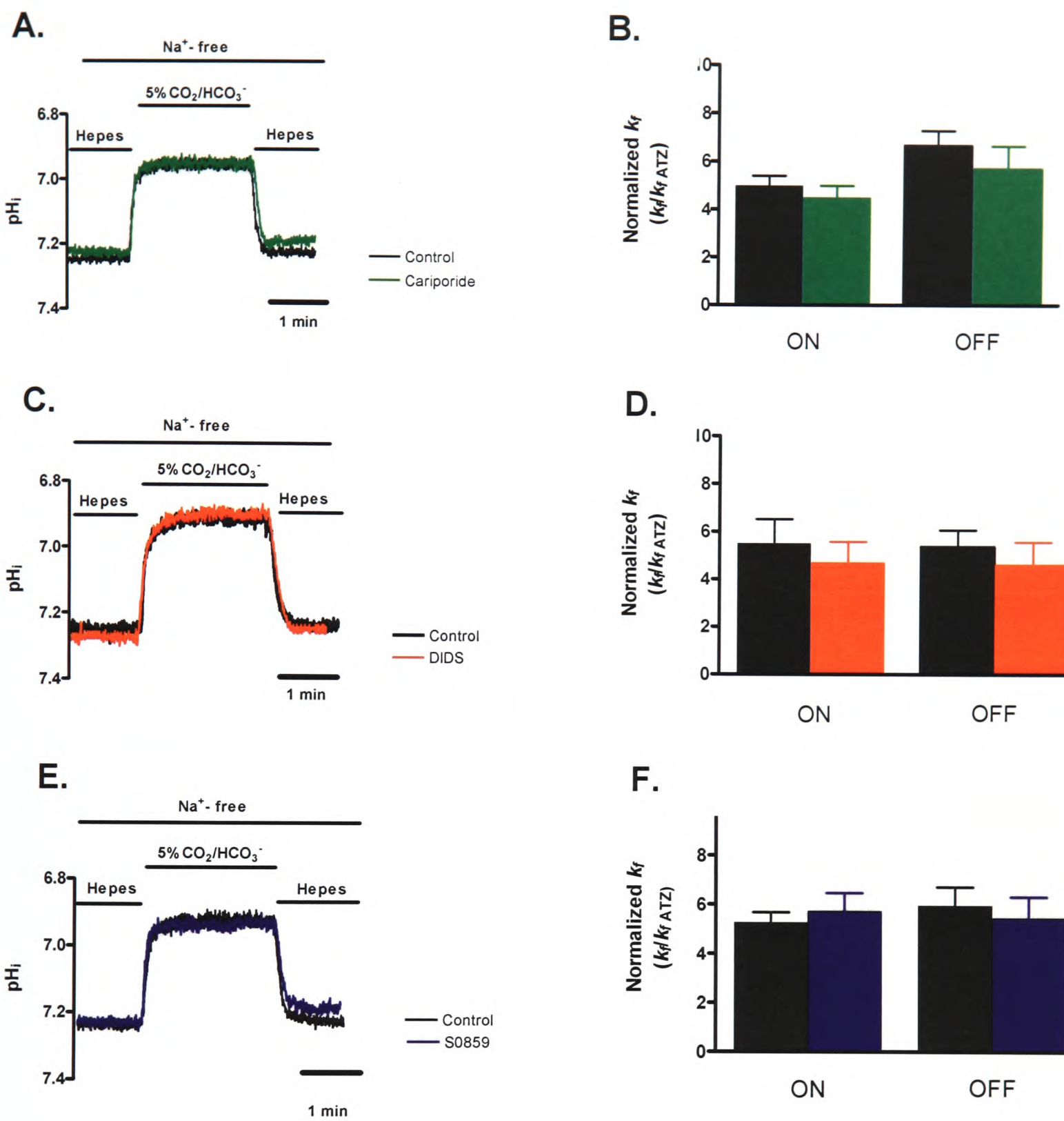

Figure 13. Effect of membrane transport inhibitors on the reversible hydration of intracellular CO_2. Left panels show superimposed traces of typical paired experiments where the time-course of change of pH_i was recorded on switching from Hepes to 5% CO_2/HCO_3^--buffered solution and back to Hepes (all solutions Na^+-free). **Continue on the next page.**

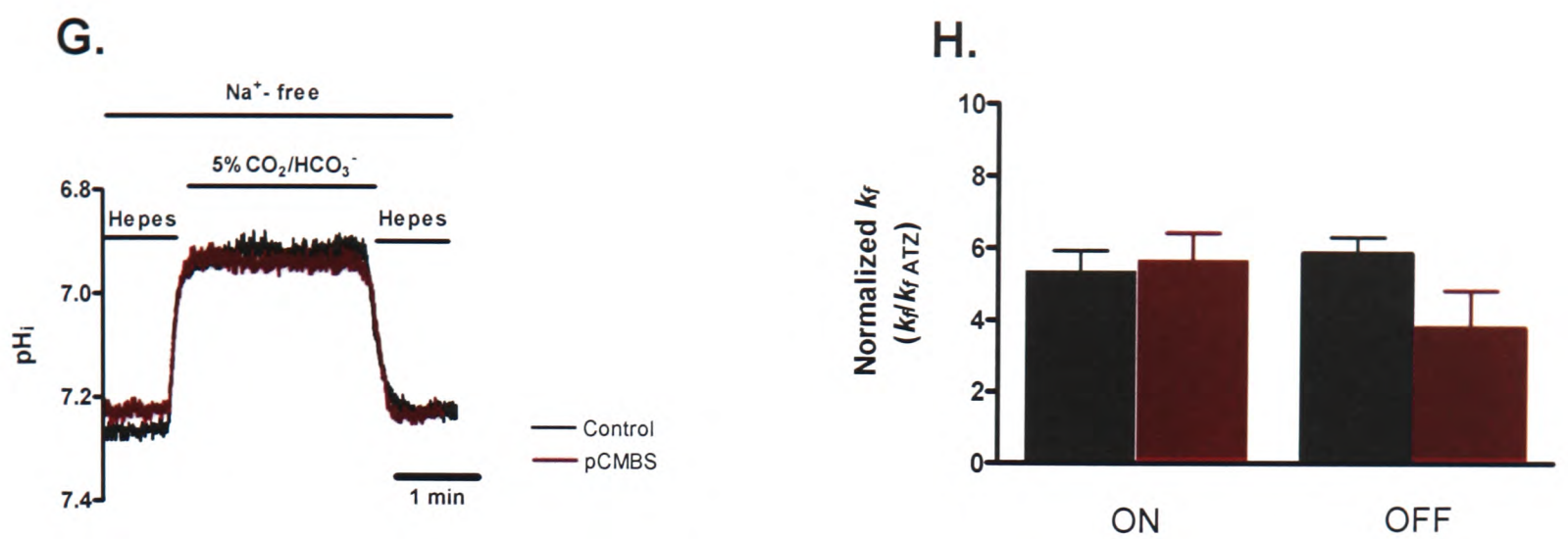

Figure 13 continued. Cariporide (30μM, A), DIDS (100μM, C), S0859 (15μM, E) or pCMBS (250μM, G) had no significant effect on the rate of intracellular CO_2-induced acidification (ON) or recovery (OFF) at the concentrations and exposure times employed. Corresponding averaged normalized k_f ($k_f/k_{f\ ATZ}$) values obtained from paired experiments are shown in the panels on the Right (B, D, F and H; n>4).

Therefore, although the transport inhibitors used inhibit CA activity *in vitro*, they do not affect intracellular CA activity, possibly because these drugs are membrane impermeant and therefore cannot interact with intracellular CA isoforms.

3.4. Discusson

The proposed participation of CA in H^+-equivalent transport (Alvarez *et al.*, 2003; Becker & Deitmer, 2007; Li *et al.*, 2002; Loiselle *et al.*, 2004; Sterling *et al.*, 2002; Sterling *et al.*, 2001a; Sterling *et al.*, 2001b) and its role in the facilitation of intracellular H^+ mobility (Spitzer *et al.*, 2002; Stewart *et al.*, 1999; Swietach *et al.*, 2007) raises the question of whether some compounds that are known to block pH_i regulatory transporters do so by acting directly on the carrier molecule or indirectly by acting on an associated CA molecule.

3.4.1. Many membrane transport inhibitors affect CA activity *in vitro*

Experimentally, when studying the kinetics of an acid extrusion mechanism, specific inhibitors are often used selectively to block membrane transporters. For example, NHE inhibitors are used to dissect the activity of NBC (Lagadic-Gossmann *et al.*, 1992; Leem *et al.*, 1999). Conversely, NBC inhibitors can be used to study contributions from NHE during pH_i recovery from an intracellular acid-load, a process in which both transporters normally participate. It is interesting that, among the inhibitor compounds tested, only those with chemical side-groups capable of establishing hydrogen bonds or coordination bonds, affected CA in the activity assay.

3.4.1.1. Effect of Na^+/H^+ Exchange Inhibitors

In the present study, three specific NHE inhibitors have been tested. None of these compounds is related to a sulphonamide compound. The amiloride derivatives DMA and EIPA did not affect CA activity. In contrast, the benzoylguanidine, cariporide,

inhibited CA activity with IC_{50} values in the micromolar range. Structurally, amiloride derivatives and benzoylguanidines differ in the cyclic part of their molecules and their side chemical moieties. In the case of amiloride derivatives, the cyclic nucleus of the molecule derives from pyrazine whereas, in the case of cariporide, the aromatic nucleus is a phenyl derivative. The main subtitutions in the phenyl ring of the cariporide molecule are an isopropyl group and a sulphomethyl group. The latter group is capable of establishing hydrogen bonds through its two oxygen atoms. Thus, this group represents a potential candidate for interacting with the hydrogen bond system in the active site of the enzyme, and thereby affecting catalysis. One possible mode of interaction may be that the sulphomethyl group in the cariporide molecule establishes hydrogen bonds with the amino group of Thr-199, disrupting the hydrogen bond network or, alternatively, that it establishes hydrogen bonds with other residues in the protein, and hence affects its catalytic activity.

In contrast to cariporide, amiloride and its derivatives, DMA and EIPA, do not include any group in their molecules that is capable of establishing hydrogen bonds. Substitutions in the amiloride molecule include two methyl groups in the DMA molecule, and one ethyl and one isopropyl group in the EIPA molecule. Therefore, these compounds are less likely to interfere with the catalytic process.

3.4.1.2. Effect of HCO_3^- Transport Inhibitors

In the case of bicarbonate transport inhibitors, both drugs tested (DIDS and S0859) inhibited CA activity. Structurally, these compounds are very different, but both include chemical groups that can potentially inhibit CA activity. DIDS is a disulphonic

stilbene compound, and contains isothiocyanate functional groups. It has been shown that incorporating an isothiocyanate group in place of the amino group in known arylamido-sulphonamide CA inhibitors results in IC_{50} values two orders of magnitude lower than their corresponding amines (Khobzaoui *et al.*, 2004). Isothiocyanate groups can react with amino acid, hydroxyl, sulfhydryl, tyrosyl, amino, and histydyl side chain groups forming transient adducts (Maddy, 1964). This suggests that isothiocyanate can potentially interact with the amino group of Thr-199 or interfere with H^+ shuttling at histidines residues. Thiocyanate (SCN^-) has also been reported to have inhibitory activity against CA, with K_i values almost in the millimolar range for different CA isozymes (Eriksson *et al.*, 1988; Ilies & Banciu, 2004b; Lindskog, 1997a; Supuran *et al.*, 2004). This anion displaces the deep water molecule and establishes a hydrogen bond with the amino group of Thr-199.

The N-cyanosulphonamide NBC inhibitor, S0859, might inhibit CA activity by interacting at the active site of the enzyme in a similar way to that of unmodified sulphonamides. In the S0859 molecule, a CN^- group replaces one of the hydrogen atoms on the original sulphonamide group. Studies on the development of modified sulphonamides have shown that the presence of an inorganic anion as an N-substituent led to compounds with appreciable CA inhibitory properties (Supuran *et al.*, 2004). The CN^- group in S0859 can functionally replace the sulphonamide NH^- group and establish a hydrogen bond with the hydroxyl group of Thr-199 or interact with the the NH group of Thr-199.

As with the unmodified sulphonamide, the oxygen atoms in the N-cyanosulphonamido group can also establish a hydrogen bond with the NH group of Thr-

199, thus potentially affecting CA-mediated catalysis. CN^- by itself is a known inhibitor of CA activity (Ilies & Banciu, 2004b; Lindahl *et al.*, 1993; Lindskog, 1997a) and interacts with the active site of CA in a similar way to SCN^- (Lindahl *et al.*, 1993), but with much lower K_i values (Ilies & Banciu, 2004b; Innocenti *et al.*, 2005).

3.4.1.3. Effect of Aquaporin Inhibitors

The mercurial compound pCMBS, an AQP blocker, was also tested for its effects on CA activity. Although this compound is not a membrane H^+ transporter inhibitor, it was chosen because it has recently been proposed that AQPs are an important route for gas molecules such as CO_2 to cross cell membranes (Cooper *et al.*, 2002; Endeward *et al.*, 2006). Because CO_2 can be reversible hydrated by CA to H^+ and HCO_3^-, its movement across the cell membrane is equivalent to transporting H^+-ions.

The results of the present work show that pCMBS inhibits CA activity with an IC_{50} values in the micromolar range, 64μM for CA II and 390μM for CA activity in cardiac homogenates. Thus, in addition to preventing transmembrane H^+ movement by blocking CO_2 membrane permeation, pCMBS may also hamper H^+ generation or consumption by inhibiting the reversible hydration of CO_2 mediated by CA.

Inhibition of CA activity by mercurial pCMBS might be explained in terms of the effect of Hg^{2+} on the enzyme. Hg^{2+} blocks intramolecular H^+ transfer steps by binding to His-64 (Eriksson & Liljas, 1991). Crystallographic evidence (Eriksson *et al.*, 1988; Eriksson & Liljas, 1991) has shown that in the Hg^{2+}-CA II complex both imidazolic nitrogens atoms in His-64 bind the metal with equal affinity, thereby eliminating the possibility for His-64 to participate in proton transfer. In addition, the common finding

that the use of mercuric ions or mercury-containing compounds (such as $HgCl_2$, pCMBS or 4-hydroxymercuribenzoate) in crystallography, to avoid dimerization of cysteine residues of CA II (Eriksson *et al.*, 1988; Mangani & Liljas, 1993; Tilander *et al.*, 1965; Xue *et al.*, 1993) also enhances the quality of the crystal, occurs probably because mercurials block the very mobile His-64 in a fixed conformation.

3.4.2. No Effect of membrane transport inhibitors on intracellular CA activity

Taking into consideration the findings discussed above, it was important to investigate whether the membrane transport inhibitors that affected CA activity in the enzymatic assay had an effect on the enzyme within an intact cell.

Isolated cardiac myocytes were used as the physiological model for this study. Several intracellular and extracellular CA isozymes have been identified in cardiac cells (Alvarez *et al.*, 2006; Knuppel-Ruppert *et al.*, 2000; Purkerson & Schwartz, 2005; Scheibe *et al.*, 2006). Intracellular CA isozymes include the soluble CA II and the sarcoplasmic reticulum (SR) membrane-bound isoforms CA IV, IX and XIV (Scheibe *et al.*, 2006). Extracellular facing CA isozymes at the sarcolemma include the isozymes CA IV, IX and XIV (Knuppel-Ruppert *et al.*, 2000; Scheibe *et al.*, 2006).

Addition of the membrane transport inhibitors with *in vitro* CA-inhibitory activity to superfusates did not affect CA-mediated intracellular hydration of CO_2 in cardiac myocytes. This may be explained in terms of the combined effect of the pK_a and the lipid solubility of the inhibitor. The undissociated (and hence uncharged) form of the drugs could potentially permeate via this route, but the lack of effect on the rate of hydration of

intracellular CO_2 suggests that, at least in the time-frame of our experiments, the uncharged fraction of the drugs does not permeate the sarcolemma.

In contrast to a lack of effect on intracellular CA isoforms, the activity of extracellular facing membrane-bound CA isozymes would potentially be affected by the inhibitors. In this case, the enzyme would be in direct contact with the superfusate. One physiological role for these CA isozymes is believed to be the accelerated equilibration of extracellular CO_2 and HCO_3^-, thus facilitating transmembrane efflux of CO_2. Therefore inhibition of extracellular-facing CA activity may have consequences for transmembrane CO_2 fluxes.

The results of the present work show that the presence of membrane transport inhibitors in the superfusates had no effect on the rate of hydration or dehydration of intracellular CO_2, events which are associated with CO_2 entry and exit, respectively. It is not possible, however, to conclude that the inhibitors do not affect extracellular CA activity. The continuous provision of CO_2 in the superfusate in single cell superfusion experiments, may be sufficient mantain CO_2/HCO_3^- buffering at equilibrium in the extracellular environment. There will therefore be no net activity of an extracellular CA isozyme. In contrast, the effect of extracellular CA inhibition may be more readily observed under conditions where significant unstirred layers surround the cells such as in poorly-vascularised multicellular preparations.

Thus, although membrane transport inhibitors had no effect on the intracellular hydration or dehydration of CO_2 in the well superfused myocytes used in the present study, an effect on extracellular CA activity by these compounds in less well perfused tissues cannot be excluded.

The lack of effect of pCMBS and DIDS on intracellular CO_2 hydration in cardiac myocytes has some important implications. If the hypothesis that AQPs serve as a dominant route for CO_2 movement across the membrane is accepted, addition of pCMBS to the superfusates should attenuate CO_2 permeation across the sarcolemma, and thus affect intracellular CO_2 hydration kinetics. Gros and colleagues (Endeward *et al.*, 2006) have shown that pCMBS reduces the permeability coefficient for CO_2 in red blood cells with a IC_{50} of 0.5M. Myocardial expression of various AQP isoforms has been reported in humans, rats and mice (Butler *et al.*, 2006). In rat heart, AQP-1, -6, -7, and -11 mRNAs were found as well as low levels of AQP-4 and -9. AQP-1 protein expression was confirmed by Western blot analysis.

The present work shows, however, that addition of 0.25mM pCMBS to superfusates had no effect on the intracellular hydration of CO_2. The K_i for inhibition of the AQP-1 water pathway expressed in *Xenopus* oocytes has been estimated as 0.13mM (Tsai *et al.*, 1991). Thus, pCMBS at 0.25 mM would have caused a noticeable inhibition of the AQP pathway in cardiac myocytes. It is possible, however, that the IC_{50} for pCMBS in myocytes has a higher value. Unfortunately, it was not possible to use higher concentrations because of an apparent toxic effect of pCMBS on cardiac myocytes.

Nevertheless, the results of the present work suggest that partial block of AQPs has no consequences on the kinetics of reversible CO_2 hydration within the cell. This in turn suggests that passive permeation of CO_2 across the lipid bilayer rather than through AQPs is an important route for CO_2 movement into or out of cardiac myocytes.

Gros and colleagues (Endeward *et al.*, 2006) reported that 100μM DIDS decreased CO_2 permeation by ~66% and suggest that this effect occurs by an action on both AQPs and an additional unknown permeation pathway in red blood cells.

The results obtained in intact cardiac myocyes in the present study show that 100μM DIDS had no effect on the kinetics of reversible intracellular hydration of CO_2. Since it has been proposed that DIDS inhibits AQPs, the lack of effect of DIDS on CO_2 reversible hydration again supports the idea that the AQP pathway is not rate limiting for CO_2 permeation in cardiac myocytes, confirming the findings with pCMBS.

In conclusion, the present work shows that several membrane transport inhibitors of H^+-equivalent transport affect CA activity when they are in direct contact with the enzyme. Under physiological conditions, however, these compounds cannot cross biological membranes, therefore preventing their interaction with intracellular CA isozymes. Extracellular-facing CA isozymes, however, are a potential target for these drugs. Although, in superfused single cell experiments, extracellular CA-isozyme activity is unlikely to facilitate CO_2 transfer accros the sarcolemma, in cell clusters or tissues where the extracellular space between cells is less well perfused, these enzymes are likely to become important for facilitating CO_2 movement. Therefore, membrane transport inhibitors with additional extracellular CA inhibitory activity, such as cariporide, which has been used in ischaemia-reperfusion studies (Avkiran & Marber, 2002; Scholz *et al.*, 1993; Theroux *et al.*, 2000; Wajima *et al.*, 2004), may have consequences on CO_2 washout and therefore on post-ischaemic pH_i recovery. Such consequenses would be independent of membrane transport inhibition and would therefore represent a novel pharmacological effect of these drugs.

CHAPTER 4

EFFECT OF CARBONIC ANHYDRASE ACTIVITY ON SARCOLEMMAL H^+-EQUIVALENT EXTRUSION

4.1. Introduction

In the event of an intracellular acid load, cardiac pH_i is normally restored by two sarcolemmal acid extrusion mechanisms, the Na^+-H^+ exchange (NHE) and the Na^+-HCO_3^- co-transport (NBC). The activity of these Na^+-dependent sarcolemmal acid extruders is allosterically controlled by intracellular $[H^+]$, being enhanced at low pH_i (Dart & Vaughan-Jones, 1992; Lagadic-Gossmann *et al.*, 1992).

Efficient function of acid/base membrane transporters depends on an appropriate supply and removal of substrates from their binding sites, and also on an adequate matching of bulk cytosolic $[H^+]$ to that surrounding any allosteric control sites on the protein.

For HCO_3^- transporters, substrate supply and removal may be hampered by the slow kinetics of spontaneous equilibration of CO_2 and HCO_3^-, two main components of carbonic buffering. In cells, the enzyme carbonic anhydrase (CA) accelerates the rate of attainment of equilibrium of the buffering reaction (Chegwidden *et al.*, 2000; Geers & Gros, 2000; Maren, 1967). At least 13 active mammalian CA isoforms have been identified, varying in activity and cellular localization. Some of these isozymes are cytosolic (CA I, II, III, VII, XIII), others are membrane-bound (CA IV, IX, XII, XIV, XV), CA VA and CA VB are mitochondrial isoforms whilst CA VI is secreted with saliva and milk.

Accelerated attainment of equilibrium between CO_2 and HCO_3^- may also facilitate pH_i regulation in other ways. High levels of intracellular pH buffers (Vaughan-Jones *et al.*, 2002; Zaniboni *et al.*, 2003), that protect against pH disturbances, reduce H^+-ion mobility by more than two orders of magnitude (Vaughan-Jones *et al.*, 2002). The reason for this is that many buffer molecules, in particular proteins, have low (sometimes nil) mobility. High buffering capacity will only allow a small fraction of H^+-ions to diffuse freely. A consequence of this reduction in mobility is an impediment of H^+ delivery to acid-extruders such as NHE, with subsequent development of pH_i non-uniformity during acid-extrusion (Swietach & Vaughan-Jones, 2005). Cells, however, posses a significant fraction of lower molecular weight buffers, which salvages diffusive H^+-coupling between bulk cytoplasm and the H^+ transporters at the surface membrane.

Such 'mobile' buffers will include low molecular weight endogenous histidyl dipeptides (Vaughan-Jones *et al.*, 2002) and also CO_2/HCO_3^- buffer (Spitzer *et al.*, 2002; Stewart *et al.*, 1999). In the case of the latter, efficient facilitation of H^+ mobility depends on CA activity (Spitzer *et al.*, 2002; Stewart *et al.*, 1999; Swietach *et al.*, 2007). Under physiological conditions, and at resting pH_i, carbonic buffer (5% CO_2/22mM HCO_3^-) at equilibrium accounts for around half of the total intracellular buffering capacity (β_{tot}) of a cardiac myocyte (Leem *et al.*, 1999).

Previous studies on the heart have suggested a modulatory role for CA in pH_i regulation (Lagadic-Gossmann *et al.*, 1992; Vandenberg *et al.*, 1996). In ferret heart, CA inhibitors have been shown to slow pH_i recovery during post-ischaemic reperfusion (Vandenberg *et al.*, 1996). These findings were explained in terms of a slowing of the rate of CO_2 efflux and a reduction in NBC-mediated HCO_3^- influx across the sarcolemma

of cardiac muscle cells. Other studies, this time on isolated guinea-pig myocytes (Lagadic-Gossmann *et al.*, 1992; Leem & Vaughan-Jones, 1998) have shown that CA inhibition with acetazolamide (ATZ) slows the rate of intracellular CO_2 hydration, assessed by the rate of pH_i change following addition of CO_2 in the bathing medium. This finding suggests that the rate of hydration of intracellular CO_2, and subsequent pH_i acidification, is limited by the CO_2 hydration reaction catalyzed by CA rather than membrane CO_2 permeation.

Functional coupling involving both extracellular and intracellular CA isoforms and a membrane transporter such as AE, NHE and NBC has been hypothesised to occur physiologically in cells such as erythrocytes, renal tubular cells and epidydimal cells (Pastor-Soler *et al.*, 2005; Romero *et al.*, 2004). For example, the co-localisation of NBCe1, CA II, and CA IV in epidydimal proximal cells (Jensen *et al.*, 1999a; Jensen *et al.*, 1999b; Kaunisto *et al.*, 1995; Kaunisto *et al.*, 1990; Parkkila *et al.*, 1993) has led to the proposal of a functional coupling of these two proteins to enhance the reabsortion of HCO_3^- (Pastor-Soler *et al.*, 2005).

Recent work on heterologous transfection systems has even suggested a physical association between certain CA isoforms (e.g. CA II, IV) and membrane H^+-equivalent transporters (AE1, NHE-1 and NBCe-1) (Alvarez *et al.*, 2003; Li *et al.*, 2002; Sterling *et al.*, 2001a; Sterling *et al.*, 2001b). The physical and functional association between CA and membrane H^+-equivalent transporters was first described for the bicarbonate-transporting AE1 and CA isoforms II and IV (Sterling & Casey, 2002; Sterling *et al.*, 2001b; Vince *et al.*, 2000; Vince & Reithmeier, 1998; Vince & Reithmeier, 2000), and the term "bicarbonate transport metabolon" was coined to describe this relationship. The term

'metabolon' has been used to describe a supra-molecular complex of sequential enzymes within a metabolic pathway (Ovadi & Srere, 2000; Srere, 1987; Srere, 2000). The close proximity of enzymes responsible for catalyzing consecutive steps of a metabolic pathway may be used to increase the metabolic flow by assuring the channeling of intermediates (Ovadi & Srere, 2000; Srere, 2000). Thus, similarly, a bicarbonate transport metabolon may result in facilitated HCO_3^- transport across AE. Intracellular CA (e.g. CAII) may streamline the rate of supply of HCO_3^- (generated from CO_2) at the substrate site and extracellular CA (e.g. CAIV) may remove HCO_3^- from the transporter, once the substrate has been transferred across the membrane. CA may thereby maintain a steep outward HCO_3^- gradient which would otherwise be shallower with slower carbonic buffer equilibration kinetics.

CA isoforms may also be useful in rapidly bringing carbonic buffer closer to equilibrium for the purpose of facilitating H^+ mobility for transporters using H^+-ions as substrate or allosteric regulator (Vaughan-Jones *et al.*, 2002). This concept was tested in AP1 cells transfected with CAII and the bicarbonate-independent transporter, NHE-1 (Li *et al.*, 2002). This study demonstrated that the intracellular C-terminal domain of NHE-1 can bind CA II and that, when both molecules are expressed in a heterologous system, the latter can significantly stimulate the activity of the transporter. It was also shown that NHE-1-mediated recovery of pH_i following an acid load was slowed in the presence of 100μM ATZ. Since hydration of CO_2 produces H^+, the proposed role for CA II in this particular case was hypothesized to be the facilitation of H^+ supply to NHE-1 for extrusion, which would otherwise be impaired by slow diffusion from bulk cytosol.

A direct interaction between NBCe1 and intra- and extracellular CA has also been demonstrated (Alvarez *et al.*, 2003). It was observed that co-expression of NBCe1, CA IV and CA II in HEK293 cells resulted in binding of CAIV and CAII to extra- and intracellular sites on NBC, respectively. That study also showed that NBCe1-mediated flux in this heterologous transfection system was dependent on CA activity. There is some controversy, however, about the extent to which CA can facilitate NBC activity.

Recent work (Lu *et al.*, 2006) has shown that injecting recombinant human CA II into *Xenopus* oocytes expressing NBCe1-A does not enhance HCO_3^- transport, measured in terms of the NBC current (I_{NBC}). While CA II accelerated the intracellular hydration of CO_2, it had no effect on I_{NBC}. Addition of ethoxzolamide (ETZ), a membrane-permeant CA inhibitor, prevented the effect on intracellular CO_2 hydration without affecting I_{NBC}. Contrary to these findings, using a similar experimental approach, Becker and Deitmer (Becker & Deitmer, 2007) found that NBC activity was enhanced by the catalytic activity of CA II. The activity of NBCe1-A expressed in *Xenopus* oocytes was quantified by measuring $I_{NBC,}$ and also the rate of change of intracellular $[H^+]$ and $[Na^+]$ following an acid load. The study showed that injecting CA II significantly increased NBCe1-A activity and that ETZ reversed this effect.

So far, the functional and/or physical association involving H^+-equivalent membrane transporter and different CA isozymes in a "transport metabolon" arrangement has only been shown in transfection cellular systems. It is not yet established if CA can influence the activity of membrane H^+ transport in an intact wild-type cell.

In order to assess the role of CA on membrane H^+-equivalent transport under physiological conditions, in the present study, rat ventricular myocytes were used as a model of an intact cellular system to investigate the role of intracellular and extracellular CA on NHE and NBC activity.

4.2. Methods

4.2.1. General methods

The intracellular pH of isolated rat ventricular myocytes was measured using the dual emission pH-sensitive fluorescent dye carboxy-SNARF-1. Full details of the cell isolation procedure, epifluorescence measurements, and calibration are described in Chapter 2.

4.2.2. Drugs

NHE and NBC inhibitors. Cariporide (NHE inhibitor) and S0859 (NBC inhibitor) were kindly provided by Sanofi Aventis (Germany) and were added to solutions just prior to use (from stock in aqueous solution). Dimethylamiloride (DMA; NHE inhibitor) was purchased from Sigma (Sigm-Aldrich). Doses of 30μM for cariporide or DMA and 15μM for S0859 were chosen since they had been shown effectively to inhibit NHE (cariporide; Scholz et al, 1995, DMA; (Loh et al., 1996) or NBC (S0859) (Ch'en *et al.*, 2008) without affecting other aspects of cell function such as electrically-evoked contraction.

CA inhibitors. ATZ and the recently developed compound 14v (1-[5-sulphamoyl-1,3,4-thiazol-2-yl-(aminosulphonyl-4phenyl)]-2,6-dimethyl-4-phenyl-pyridinium perchlorate) (Alvarez *et al.*, 2003; Supuran *et al.*, 2004) were used in this study. ATZ is an uncharged, membrane-permeant sulphonamide and will inhibit both intra- and extracellular CA isoforms. 14v is a positively-charged heterocyclic sulphonamide that will only inhibit membrane-associated CA isoforms with active sites oriented towards the extracellular

space (Supuran *et al.*, 2004). The affinity of this compound for CA IV and CA II is in the nanomolar range (Scozzafava *et al.*, 2000; Supuran *et al.*, 2004). Also, the potent membrane permeable CA inhibitor ETZ was used in some experiments.

4.2.3. CA activity assay

Details of the CA enzymatic assay and the quantification of the first-order CO_2 hydration rate constant (k_f) have been fully described in the General Methods chapter (Chapter 2). In order to asses the possible role of intracellular and extracellular CA activity in facilitating NHE- and NBC-mediated H^+-equivalent flux, CA was differentially inhibited using a combination of ATZ (a membrane-permeant) and 14v (a membrane-impermeant) inhibitors. First, it was necessary to determine the inhibitory potency of 14v on CA activity of cardiac homogenates, to test whether the drug is active on cardiac CA isoforms. CA activity was assayed in cardiac homogenates using a 14v concentration previously used for cardiac myocytes (100nM; (Alvarez *et al.*, 2003). The effect of 14v was compared with ATZ at the same concentration. To determine the IC_{50} for 14v, a dose-response analysis was performed on purified CA II and on total CA activity in ventricular homogenates, and the IC_{50} value has been determined from a four parameter sigmoidal fit to the data. Protein content in the homogenates was quantified spectrophotometrically using the Bradford assay (QuickStart, BioRad).

4.2.4. NHE and NBC-mediated acid efflux measurement

Acid-equivalent efflux through NBC (J_{NBC}) and NHE (J_{NHE}) was quantified by measuring pH_i-recovery following an intracellular acid-load, achieved by pre-pulsing the

cells with solutions containing 20mM NH_4Cl for 3-4 minutes (Roos & Boron, 1981). An equimolar amount of NaCl was omitted in NH_4Cl-containing solutions in order to maintain constant osmolarity.

Acid efflux (J^H) was calculated using the following equation:

$J^H = -\beta_{tot} \times dpH_i/dt$

where dpH_i/dt is the rate of change of pH_i driven by transmembrane acid-equivalent flux and β_{tot} is total intracellular buffering power in the rat ventricular myocyte.

Three protocols were performed to measure J_{NHE}.

(i) Cells were superfused in Hepes-buffered normal Tyrode to inactivate NBC, i.e. $J^H=J_{NHE}$; (Figure 3A)

(ii) Cells were superfused in CO_2/HCO_3^--buffered Tyrode in the presence or absence of 30μM DMA. Recovery of pH_i in the presence of CO_2/HCO_3^--buffered Tyrode is mediated by both NHE and NBC ($J^H=J_{NBC}+J_{NHE}$; Figure 3B). J_{NHE} can be isolated by subtracting the acid efflux in the presence of DMA ($J^H=J_{NBC}$ only; Figure 3C) from total acid efflux ($J^H=J_{NBC}+J_{NHE}$).

(iii) Cells were superfused with CO_2/HCO_3^--buffered Tyrode plus 15μM S0859, a selective inhibitor of NBC (Ch'en *et al.*, 2008), i.e. $J^H=J_{NHE}$; (Figure 4A)

To measure J_{NBC}, cells were superfused with CO_2/HCO_3^--buffered Tyrode in the presence of either 30μM DMA or 30μM cariporide ($J^H=J_{NBC}$; $J_{NHE}=0$; Figures 3C and 5A, respectively).

To eliminate all CA activity (both intracellular and extracellular), 100μM ATZ or 100μM ETZ was added to superfusates. To eliminate only extracellular CA activity, 100nM 14v was used.

4.2.5. Measurement of intracellular reversible CO_2 hydration in intact myocytes

Details of measurement of intracellular CO_2 hydration and dehydration, and quantification of the intracellular first-order hydration rate constant (k_{fi}) have been fully described in the General Methods chapter (Chapter 2).

The rate of initial pH_i change on switching the superfusate from Hepes-buffered to CO_2/HCO_3^--buffered Tyrode ("ON") and then back to Hepes ("OFF") was used to assess the degree of CA catalysis. 30μM cariporide plus 15μM S0859 were added to the superfusates to prevent sarcolemmal acid extrusion which would otherwise affect the initial pH_i change. As has been shown in Chapter 3 of this thesis, although cariporide and S0859 at these concentrations can partially inhibit CA activity *in vitro*, neither of these drugs affects the reversible intracellular hydration of CO_2 in single cardiac myocytes most probably because of its inability to cross the sarcolemma and have direct contact with the enzyme. Therefore, inhibition of membrane transport using these drugs can be achieved without affecting cytosolic CA activity. We have also shown that any possible effects of cariporide and S0859 on extracellular CA activity do not affect the kinetics of pH_i-change due to transmembrane CO_2 flux in well-superfused isolated cardiac myocytes.

To assess the effect of intracellular and extracellular CA inhibition, switching between Hepes and CO_2/HCO_3^--buffered solution was carried out in the presence of 100μM ATZ or 100nM 14v. Cells were superfused with drug-containing solution for at least 2 minutes before adding CO_2-containing buffer. Switching back from CO_2/HCO_3^--buffered to Hepes-buffered superfusates was carried out in the presence of the drug.

4.3. Results

4.3.1. Effect of the membrane-impermeable inhibitor 14v on CA activity

Figure 1A shows superimposed experimental recordings comparing the effect of 100nM of 14v (green) and 100nM ATZ (red) on the rate of acidification induced by CO_2 addition cardiac homogenates. Both drugs reduced the rate significantly, down to the level of uncatalysed CO_2 hydration (grey). CA activity, expressed as k_f is shown in Figure 1B. Addition of ATZ or 14v resulted in k_f values similar to the uncatalysed values. k_f was normalised to final protein concentration in the assay (per mg/ml). Figure 1C shows a comparison of the dose-response curves for CA II and cardiac homogenates. The IC_{50} for CA II and CA activity in the homogenates was 0.6 and 2.4nM, respectively. This IC_{50} difference between cardiac homogenates and CA II may be a consequence of the mixture of CA isozymes present in cardiac myocytes (Alvarez *et al.*, 2006; Scheibe *et al.*, 2006). For example, CA IV and CA IX have shown higher K_i values for sulphonamides than CA II (Supuran, 2004). Since these isozymes are present in cardiac myocytes, it is possible that the IC_{50} values obtained in the present study reflect to some extent the values of the isozymes with less sensitivity to inhibition by sulphonamides.

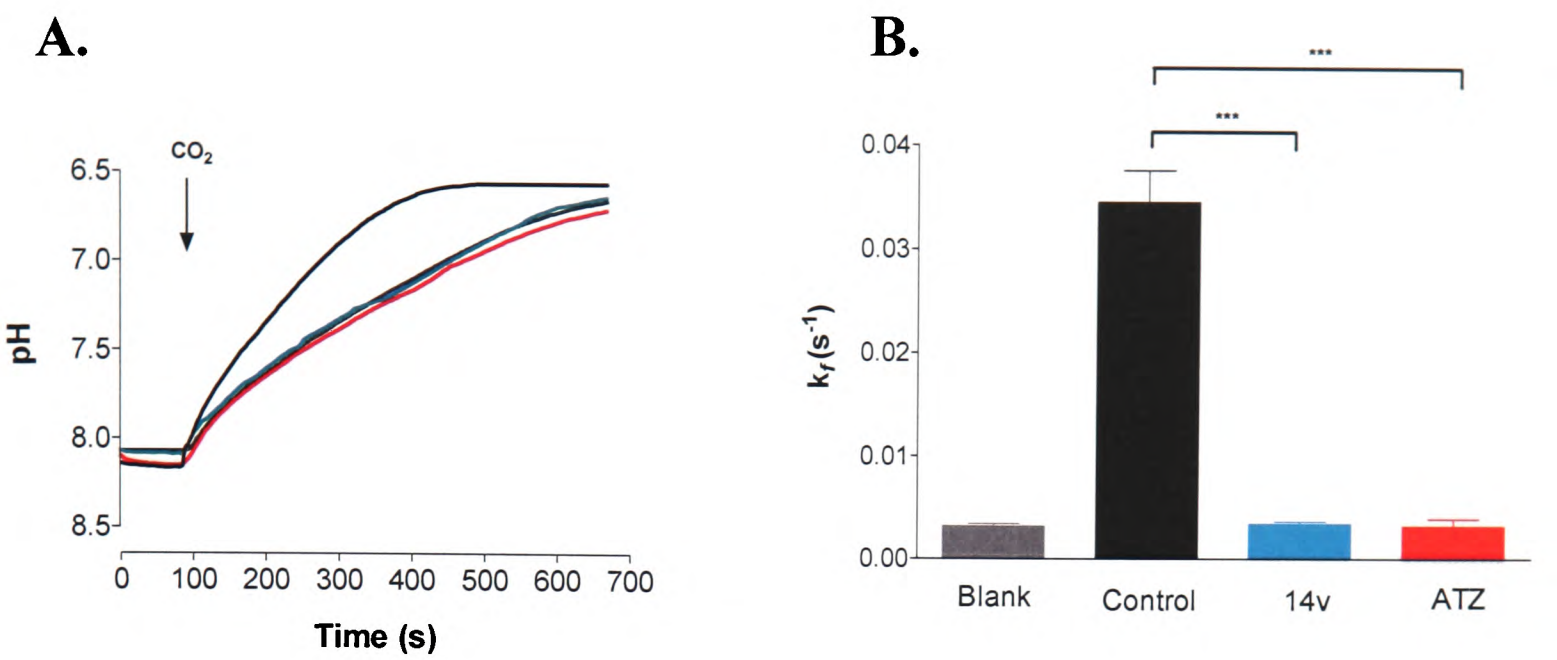

Figure 1. Assay of CA activity in ventricular myocyte lysates. Panel A shows a time-course of change of pH after CO_2 addition to cardiac homogenate (—), homogenate + 100nM ATZ (—), homogenate + 100nM "14v" (—) and to Hepes-buffered solution. B. CA activity, expressed as k_f, was significantly reduced in the presence 100nM ATZ (■) or 100nM "14v" (■) resulting in complete inhibition in both cases. C. Dose-response curve for 14v on the activity of CA II (●) and cardiac homogenates (○). IC_{50} values of 0.6±0.08 and 2.4±0.62 nM for CA II and CA activity in cardiac homogenates respectively were determined from a four parameter sigmoidal fit to data. Values for IC_{50} are given ± 95% confidence intervals.

4.3.2. Effect of CA inhibitors on intracellular reversible CO_2 hydration rates

Figure 2A shows a time-course of the CO_2-induced change of pH_i upon myocyte superfusion with HCO_3^-/CO_2-buffered Tyrode and subsequent switching back to Hepes-buffered Tyrode under control conditions and in the presence of ATZ. Under control conditions, rapid changes in pH_i were observed when switching between Hepes and CO_2/HCO_3^--buffered superfusates. In the presence of ATZ, changes in pH_i were significantly slowed. Figures 2B and 2C superimpose, on an expanded time-scale, the changes in pH_i on CO_2 addition or removal, in the presence and absence of CA inhibitor drugs. Addition of ATZ significantly slowed these pH_i changes. In contrast, the extracellular CA inhibitor 14v had no effect on pH_i kinetics. The rate of intracellular reversible CO_2 hydration, expressed as k_{fi}, is shown in Figure 3D. The k_{fi} value in the presence of ATZ ($k_{fi\ ATZ}$) was taken as an estimate for the uncatalyzed reaction rate.The extracellular CA-inhibitor 14v (100nM) had no significant effect on the estimates of k_{fi}.

These results suggest that an intracellular CA isoform catalyses the reversible CO_2 hydration in the cytoplasm of cardiomyocytes as proposed previously (Lagadic-Gossmann *et al.*, 1992; Leem & Vaughan-Jones, 1998). In contrast, extracellular CA activity appears not to be required, at least not either for membrane permeation of CO_2 or its intracellular hydration in well perfused single cells.

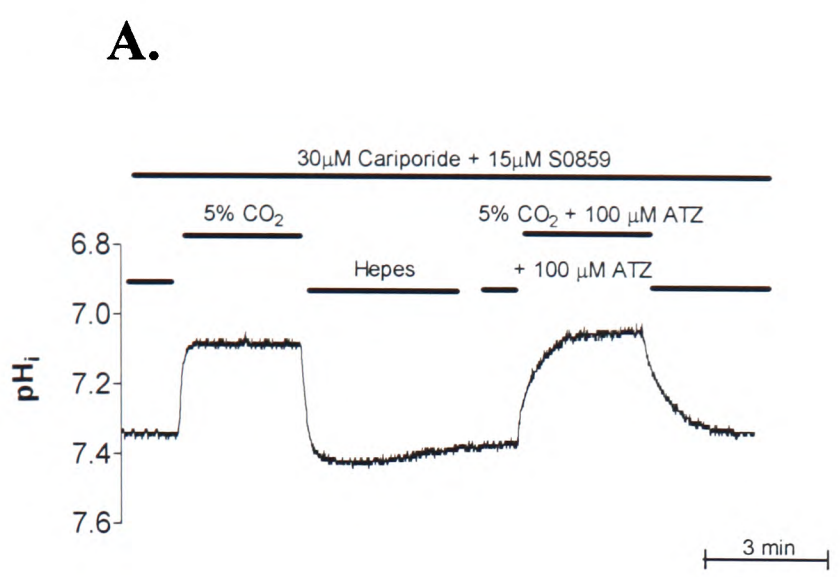

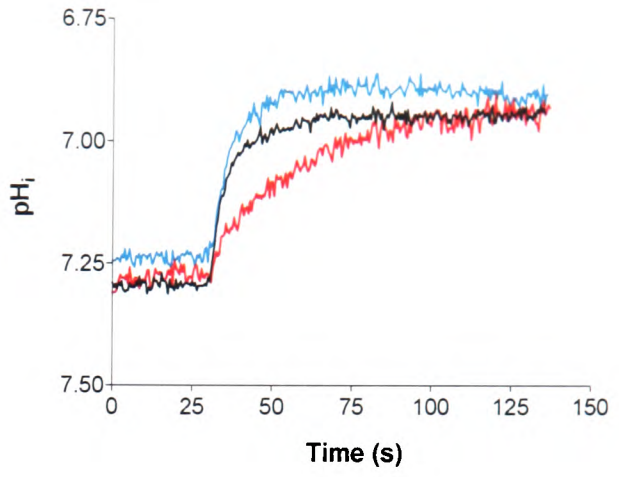

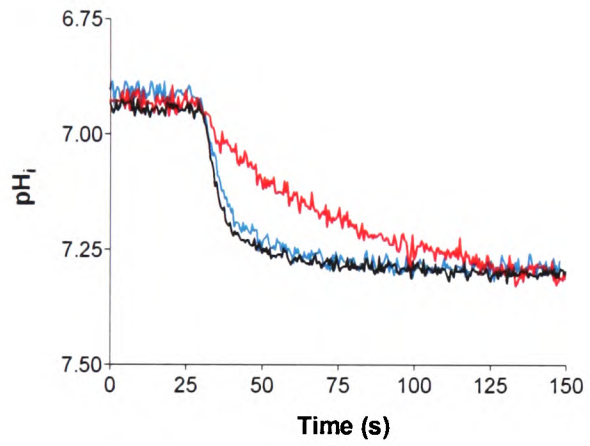

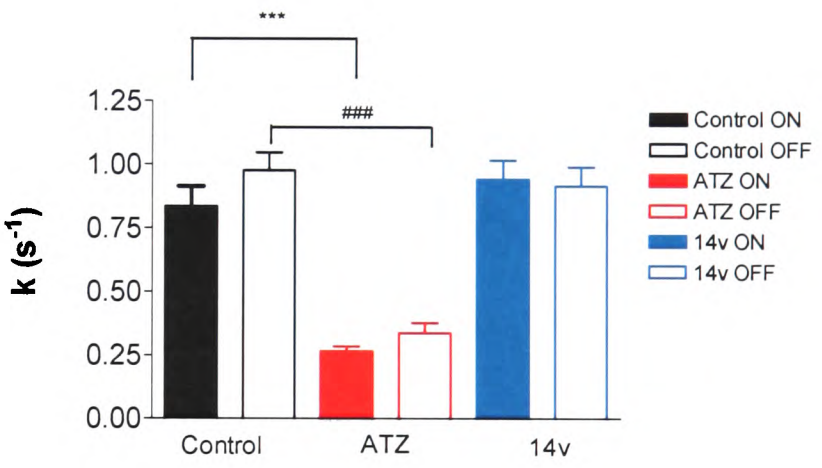

Figure 2. CA activity in intact ventricular myocytes A. Time-course of change of pH after switching from Hepes-buffered solution to CO_2/HCO_3^- -buffered solution and back to Hepes. The acid load and recovery were carried out in the presence of 30μM cariporide and 15μM S0859 to prevent acid extrusion on NHE and NBC, respectively. The figure shows a typical experiment in which after addition of ATZ the rate of acid load and recovery is significantly reduced. Similar results were obtained using Na^+-free superfusates to block sarcolemmal acid extrusion **B.** Comparison of the time-courses of intracellular acidification after switching from Hepes-buffered to CO_2/HCO_3^--buffered solution (ON) under control conditions (—), 100μM ATZ (—), and 100nM of 14v (—). **C.** Comparison of the time-courses of recovery of pH_i after switching from CO_2/HCO_3^- -buffered to Hepes-buffered solution (OFF) under control conditions (—), 100μM ATZ (—), and 100nM of 14v (—). **D.** CO_2 k_f from the CA-catalysed reaction. Addition of ATZ resulted in a significant slowing down of the forward (■) and reverse (□) reactions. The extracellular CA inhibitor 14v resulted in no change in k_f calculated either from ON or OFF.

4.3.3. Effect of CA inhibitors on sarcolemmal acid efflux

4.3.3.1. Role of CA in NHE-mediated acid extrusion

The effect of CA activity on NHE-mediated acid-efflux (J_{NHE}) was investigated. As mentioned in the Methods section, J_{NHE} was measured using three approaches. The first approach is illustrated in Figure 3A. Recovery of pH_i from an intracellular acid load in Hepes-buffered superfusate (nominally CO_2-free) is mediated by NHE ($J^H=J_{NHE}$).

Providing pCO_2 in the Hepes-buffered solution is close to zero, CA will be inactive because of the absence of substrate. The second approach includes Figures 3B and 3C, and consists of an indirect method to measure J_{NHE} in the presence of carbonic buffer, where CA will be active. Figure 3B shows a typical experimental recording performed in CO_2/HCO_3^--buffered Tyrode, where recovery of pH_i is known to be mediated by both NHE and NBC ($J^H=J_{NBC}+J_{NHE;}$ (Leem *et al.*, 1999). Figure 3C also shows recovery of pH_i in CO_2/HCO_3^--buffered Tyrode, but in the presence of 30μM DMA to inhibit NHE. Under these conditions, pH_i-recovery is mediated by NBC only ($J^H=J_{NBC}$). J_{NHE} in the presence of carbonic buffer can then be estimated by subtracting the acid efflux in the presence of DMA ($J^H=J_{NBC}$) from total acid efflux ($J^H=J_{NBC}+J_{NHE}$).

Figure 3D compares the pH_i-dependence of J_{NHE} in Hepes, the dependence of combined $J_{NBC}+J_{NHE}$, and the pH_i-dependence of J_{NBC} (pH_i range 6.6-7.25). These results were obtained from experiments similar to those illustrated in Figures 3A, 3B and 3C. A comparison of J_{NHE} obtained experimentally in Hepes-buffered and in CO_2/HCO_3^--buffered Tyrode is shown in Figure 3E. Over the pH_i range investigated, J_{NHE} is similar in the presence and absence of CO_2/HCO_3^- buffer. This suggests that, assuming that CA is inactive when myocytes are superfused with Hepes-buffered solution, CA plays no

role in facilitating NHE activity. To investigate whether there is some residual CA activity that can be affecting NHE in Hepes, additional experiments were performed in which recovery of pH_i in Hepes-buffered Tyrode was recorded in the presence and absence of 100μM ATZ. As shown in Figure 4A, ATZ had no effect on NHE-mediated acid extrusion, ruling out the possibility of NHE facilitation by residual CA activity. The third approach for assessing J_{NHE} is illustrated in Figure 4B. This shows the effect of 100μM ATZ on pH_i-recovery from an acid load induced by a 20mM ammonium pre-pulse. The experiment was performed in CO_2/HCO_3^--buffered Tyrode containing 15μM S0859 to inhibit NBC. As has been shown in Chapter 3, although this concentration of S0859 could partially inhibit any extracellular CA activity, it will exert no effect on the activity of intracellular CA isozymes. Since the intracellular CA isoform, CA II, has been suggested to facilitate NHE-mediated acid extrusion, thus it is unlikely that S0859 will affect NHE by inhibiting cytosolic CA. It has also been shown that S0859 has no direct effect on NHE activity in doses up to 30μM (Ch'en *et al.*, 2008). Therefore, S0859 can be safely used without any inhibitory effects on NHE or intracellular CA in intact myocytes. As shown in Figure 4B, ATZ had no effect on NHE-mediated recovery of pH_i. Figure 4C plots J_{NHE} as a function of pH_i and shows that inhibition of CA with 100μM ATZ had no effect on J_{NHE}.

Thus, the fact that similar results were obtained on J_{NHE} in the presence or absence of carbonic buffer or in the presence of carbonic buffer plus ATZ and S0859, suggests that CA has no role facilitating acid extrusion on NHE in intact cardiac myocytes.

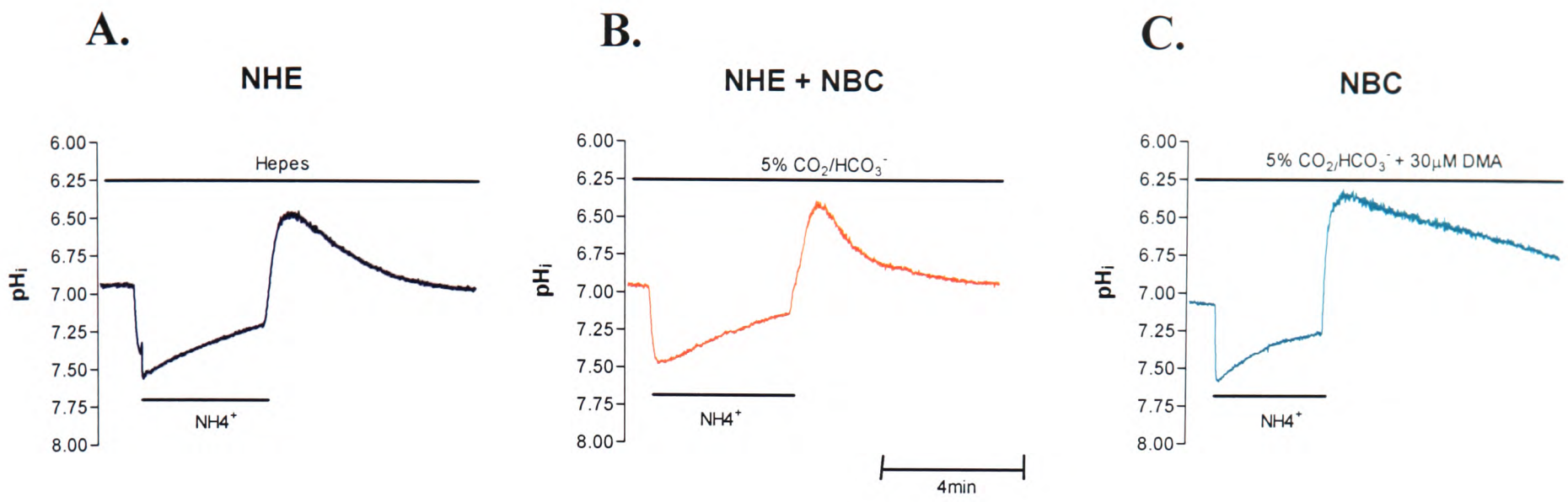

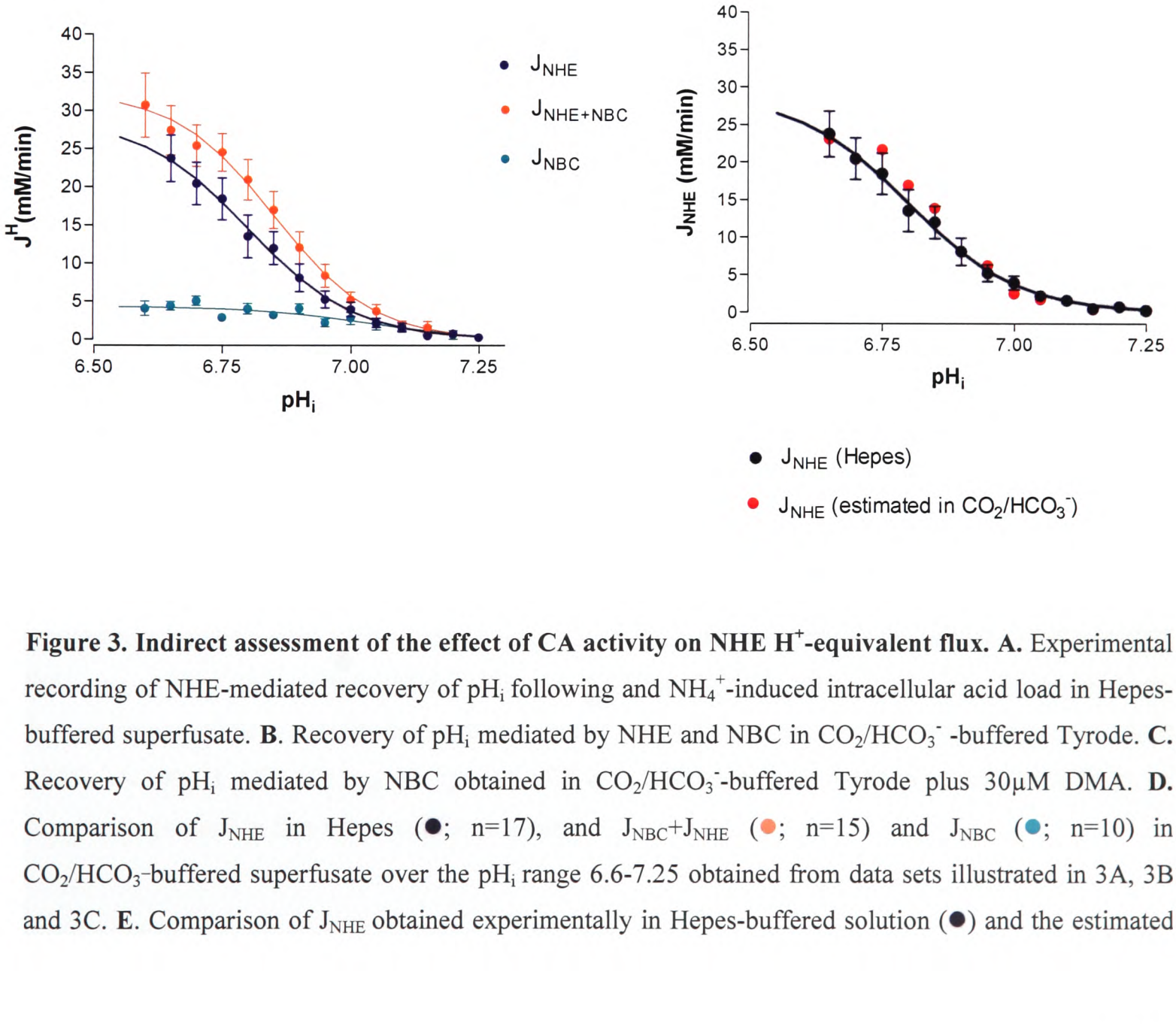

Figure 3. Indirect assessment of the effect of CA activity on NHE H^+-equivalent flux. A. Experimental recording of NHE-mediated recovery of pH_i following and NH_4^+-induced intracellular acid load in Hepes-buffered superfusate. **B**. Recovery of pH_i mediated by NHE and NBC in CO_2/HCO_3^- -buffered Tyrode. **C.** Recovery of pH_i mediated by NBC obtained in CO_2/HCO_3^--buffered Tyrode plus 30μM DMA. **D.** Comparison of J_{NHE} in Hepes (●; n=17), and $J_{NBC}+J_{NHE}$ (●; n=15) and J_{NBC} (●; n=10) in CO_2/HCO_3^-buffered superfusate over the pH_i range 6.6-7.25 obtained from data sets illustrated in 3A, 3B and 3C. **E.** Comparison of J_{NHE} obtained experimentally in Hepes-buffered solution (●) and the estimated

J_{NHE} in CO_2/HCO_3^--buffered Tyrode (●). Over the whole pH_i range investigated, 6.6-7.25, J_{NHE} had similar values in the presence and absence of CO_2/HCO_3^- buffer.

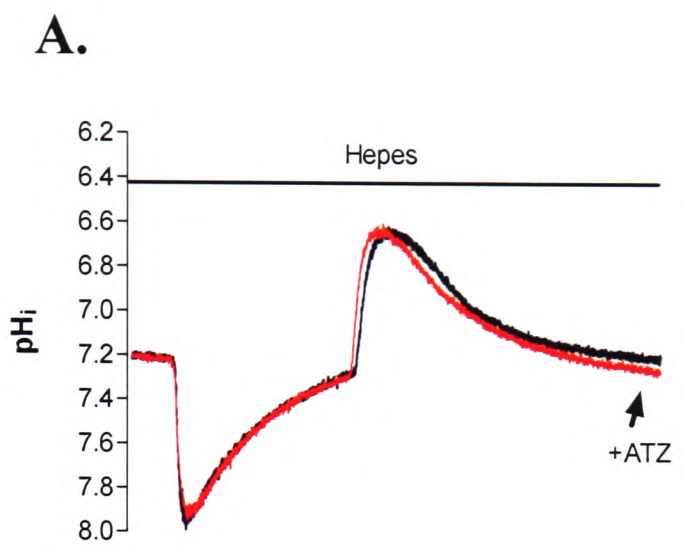

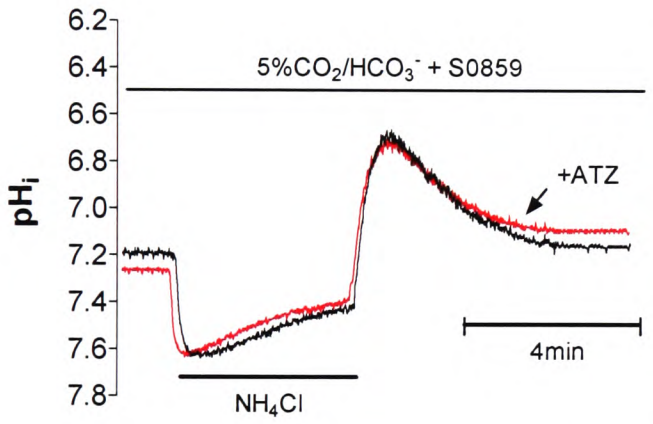

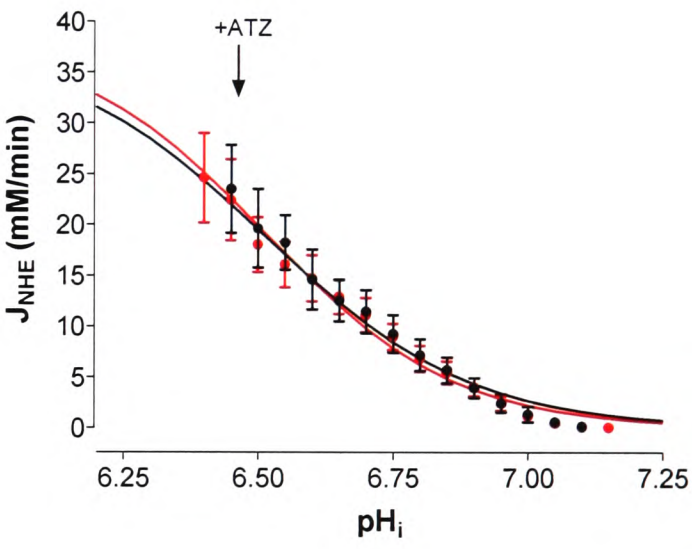

Figure 4. Direct assessment of the effect of CA activity on NHE H^+-equivalent flux. A. Supermiposed experimental recordings of NHE-mediated recovery of pH_i in Hepes-buffered superfusate +/-100μM ATZ following an NH_4^+-induced intracellular acid load. ATZ had no effect on the time-course of pH_i-recovery. **B**. Superimposed traces of NHE-mediated recovery of pH_i in CO_2/HCO_3^--buffered superfusate plus 15μM S0859 +/- 100μM ATZ. **C**. J_{NHE} +/- 100μM ATZ as a function of pH_i. Addition of 100μM ATZ to the superfusate resulted in flux values similar to control.

4.3.3.2. Role of CA in NBC-mediated acid extrusion

Initial evaluation of NBC-mediated pH_i recovery from an acid-load was carried out in CO_2/HCO_3^--buffered Tyrode, plus 30μM cariporide to inhibit NHE (Figure 5A). Recovery of pH_i appeared to be similar in the absence or presence of CA activity (+/- ATZ). When, however, NBC-mediated acid efflux (J_{NBC}) is plotted against pH_i, in the presence and absence of CA activity (Figure 5B), there appeared to be a trend, whereby ATZ reduced NBC activity, especially towards higher values of J_{NBC} (pH_i range 6.3-6.6). Nevertheless, over most of the pH_i range tested, the reduction of NBC activity was not statistically significant. Therefore, similar experiments were performed under conditions where of J_{NBC} was enhanced before addition of ATZ.

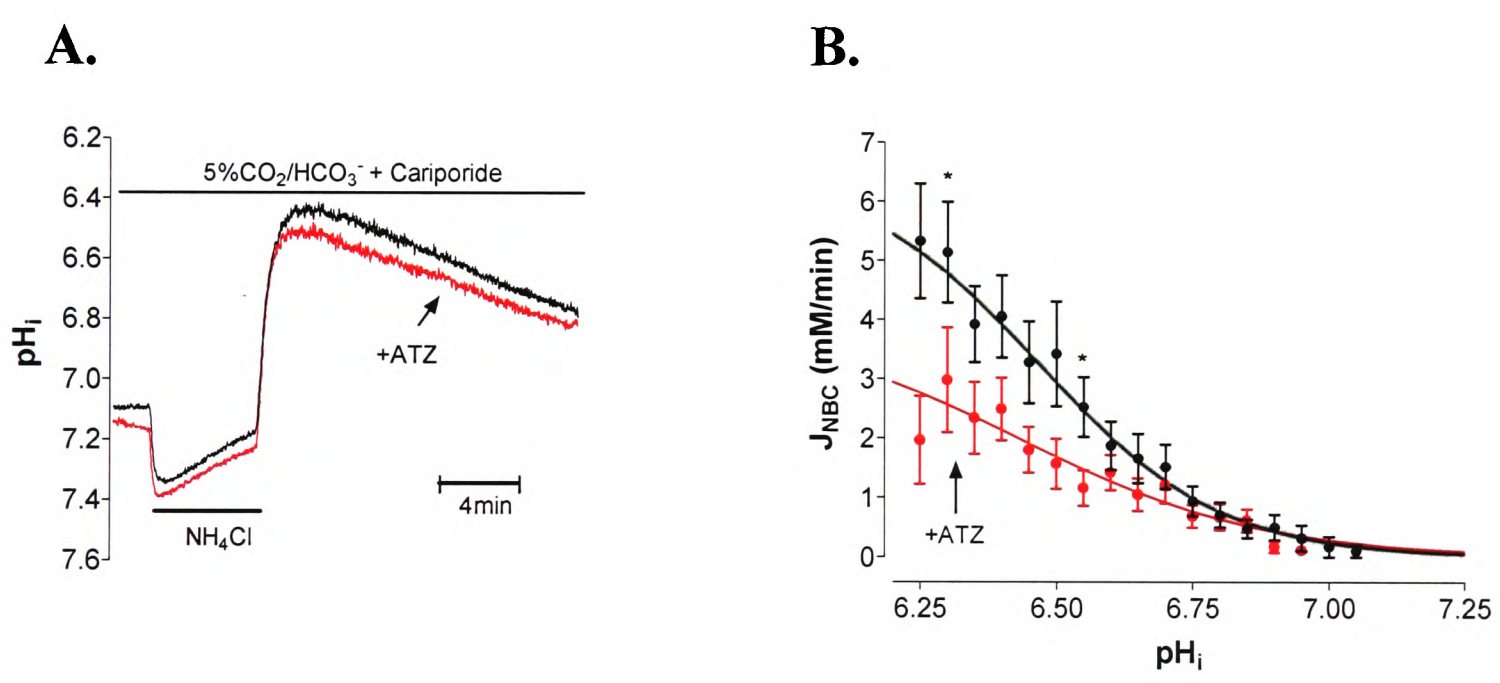

Figure 5. Effect of CA inhibition on NBC H^+-equivalent flux. **A.** Superimposed traces of NBC-mediated recovery of pH_i after an intracellular acid load +/- 100μM ATZ. 30μM cariporide was used to inhibit NHE activity. **B.** J_{NBC} as a function of pH_i. At a given pH_i value, J_{NBC} showed a tendency towards lower values in the presence of ATZ (n=8-26; *$p<0.05$)

Cardiac NBC, which in part is electrogenic (up to 60% of total J_{NBC} at pH_i 7.05), can be accelerated by depolarising the membrane potential (Yamamoto *et al.*, 2005). Experiments were performed under conditions of 10-fold elevated superfusate $[K^+]$ to depolarize the cardiac myocyte membrane potential to about -25mV (Figure 6A) (Yamamoto *et al.*, 2005). A membrane potential positive to rat cardiac electrogenic NBC equilibrium potential (at pH_i 7.05 E_{NBC}=-98mV) favours acid extrusion (i.e. HCO_3^- influx). Indeed, in high $[K^+]$ media, J_{NBC} is raised 3.4-fold over the pH_i range 6.40-6.85 (Figure 5B vs 6B). The addition of ATZ now caused a significant reduction in J_{NBC} by 51±2% over all of the pH_i range examined (Figure 6B).

It is important, however, to take into consideration that, although 30μM cariporide would not affect intracellular CA activity as has been shown in Chapter 3, partial inhibition of extracellular CA activity may influence the result. Since it has been proposed that J_{NBC} is enhanced by the activity of extracellular as well as intracellular CA isoforms (Alvarez *et al.*, 2003), it might be possible that cariporide affects NBC activity by acting on extracellular CA isozymes. This could result in partial inhibition of CA activity, and thus NBC. The subsequent inhibitory effect of ATZ on NBC would therefore be reduced, leading to an underestimate of the contribution of CA to J_{NBC}. In order to investigate this possibility, a different set of experiments under high $[K^+]$ conditions was carried out using 30μM DMA instead of cariporide. The results presented in Chapter 3 of this thesis showed that DMA has no effect on CA II activity or on endogenous cardiac CA activity in tissue homogenates. Therefore no inhibition of extracellular CA activity would be expected in isolated cardiac myocytes. Figure 6C shows a typical experimental recording of the effect of ATZ on NBC-mediated pH_i

recovery using 30μM DMA in the superfusates. Figure 6D compares J_{NBC} in the presence and absence of ATZ using DMA to inhibit J_{NHE}. ATZ resulted in an average reduction of 51±4% in J_{NBC} over the pH_i range 6.65-7.25, which is consistent with the results obtained in the presence of 30μM cariporide. Thus, regardless of the NHE inhibitor used (cariporide or DMA), blocking CA activity with ATZ caused a ~50% reduction of J_{NBC}.

A final question is whether ATZ has a direct inhibitory effect on NBC activity, independent of its inhibitory effect on CA. Unfortunately, in our experimental system, it is not possible to discriminate between the inhibitory effects of ATZ on CA and a possible direct effect on NBC. Both, Becker and Deitmer (Becker & Deitmer, 2007) and Boron and collaborators (Lu *et al.*, 2006), however, have shown recently that ETZ, another potent membrane-permeant sulphonamide CA inhibitor (with the same active chemical group), has no effect on NBCe1 activity expressed in *Xenopus* oocytes, provided it is expressed in the absence of CA II. This indicates that ETZ exerts no direct inhibitory effect on the transporter. Therefore, in the present work the effect of ETZ on cardiac NBC activity was evaluated.

Figure 6E compares typical experimental recordings of NBC-mediated recovery of pH_i. NHE was blocked with 30μM DMA, and NBC activity was enhanced by elevating $[K^+]_o$ to 45mM. In the presence of 100μM ETZ, recovery of pH_i was again significantly slowed. Figure 6F compares J_{NBC} as a function of pH_i with and without ETZ. Over the pH_i range measured (6.7-7.15), ETZ caused an average reduction of 45±3% on J_{NBC} which is similar to the inhibition obtained in the presence of ATZ. Since ETZ does not directly inhibit electrogenic NBC activity, the data presented here suggest that inhibition of NBC activity by ATZ and ETZ is secondary to inhibition of CA.

Figure 7 shows that, when plotting J_{NBC} (obtained using cariporide or DMA) in the presence of CA inhibition (ATZ or ETZ) versus control J_{NBC}, a constant fractional inhibition by the sulphonamides is observed. For low J_{NBC}, in the range from ~0.5 to 2 mM min^{-1}, inhibition of acid extrusion is not statistically significant, even though the trend was clear. For larger values of J_{NBC} the inhibition by ATZ or ETZ is clearly significant. At both, low and high J_{NBC} the trend towards inhibition is the same at ~50%. Thus, the facilitation of NBC activity by CA is likely to be constant, regardless of the H^+-equivalent flux carried by the transporter.

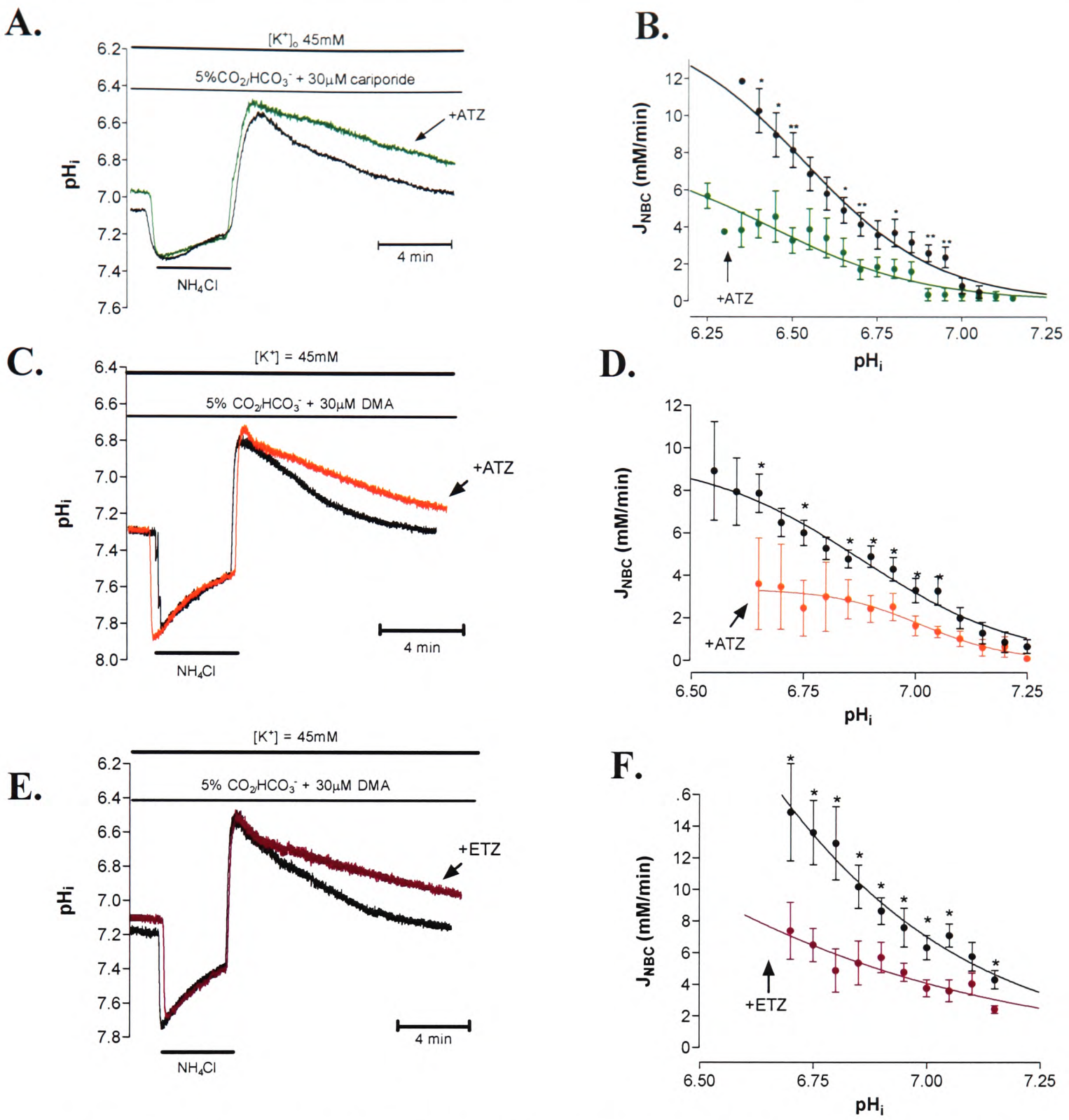

Figure 6. Effect of CA inhibition on NBC H^+-equivalent flux at $[K^+]_o$= 45mM. A. Superimposed traces of NBC-mediated pH_i-recovery ($[K^+]_o$ = 45mM) +/- 100μM ATZ. Elevated $[K^+]_o$ has been shown previously to double NBC flux (Yamamoto et al, 2005). 30 μM cariporide was used to inhibit NHE activity. **B.** ATZ caused a significant reduction by 51 ± 2% of NBC-mediated flux (n=3-12, *p<0.05, **p<0.01, ***p<0.001). **C.** Superimposed experimental recordings of NBC-mediated recovery of pH_i +/- 100μM ATZ using 30μM DMA to inhibit NHE-mediated acid extrusion. **D.** ATZ caused an average reduction of 51 ± 4% on J_{NBC} over most of the pH_i range investigated of 6.6-7.25 (n=3-20, *p<0.05). **E.** Superimposed experimental traces of NBC-mediated recovery of pH_i +/- 100μM ETZ using 30μM DMA to inhibit NHE activity. **F.** The presence of ETZ in the superfusates caused an average reduction by 45± 3% on J_{NBC} (n=7, *p<0.05).

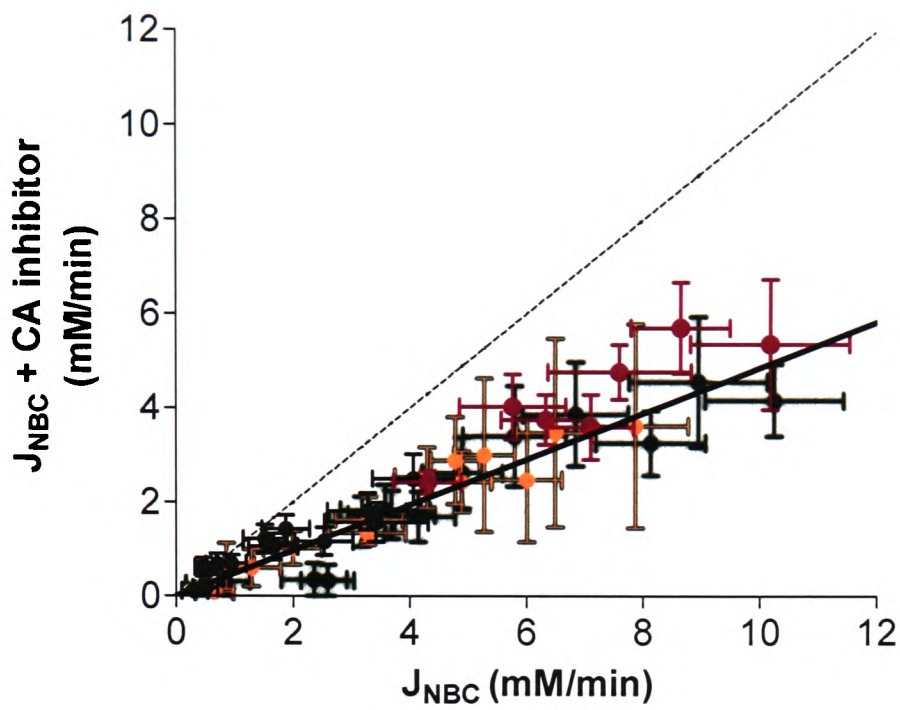

Figure 7. CA contribution to NBC activity. J_{NBC} data in the presence of the CA inhibitors ATZ and ETZ is shown as a function of the uninhibited J_{NBC} in order to illustrate the degree of contribution of CA to J_{NBC}. Data taken from Figure 5B (●), Figure 6B (●), Figure 6D (●) and Figure 6F (●). Inhibition of CA caused an averaged reduction of ~50% in J_{NBC} at low and high flux values. The dotted trace represents the identity line.

To investigate the site of CA activity, responsible for facilitating J_{NBC}, NBC-mediated pH_i recovery (measured using either cariporide or DMA) was evaluated in high $[K^+]_o$, CO_2/HCO_3^--buffered Tyrode containing 100nM 14v, a membrane-impermeant CA inhibitor (Figure 8A and 8C). Under these conditions, J_{NBC} was not affected by inhibition of extracellular CA (Figure 8B and 8D). This indicates that extracellular CA activity is not required for full activity of NBC.

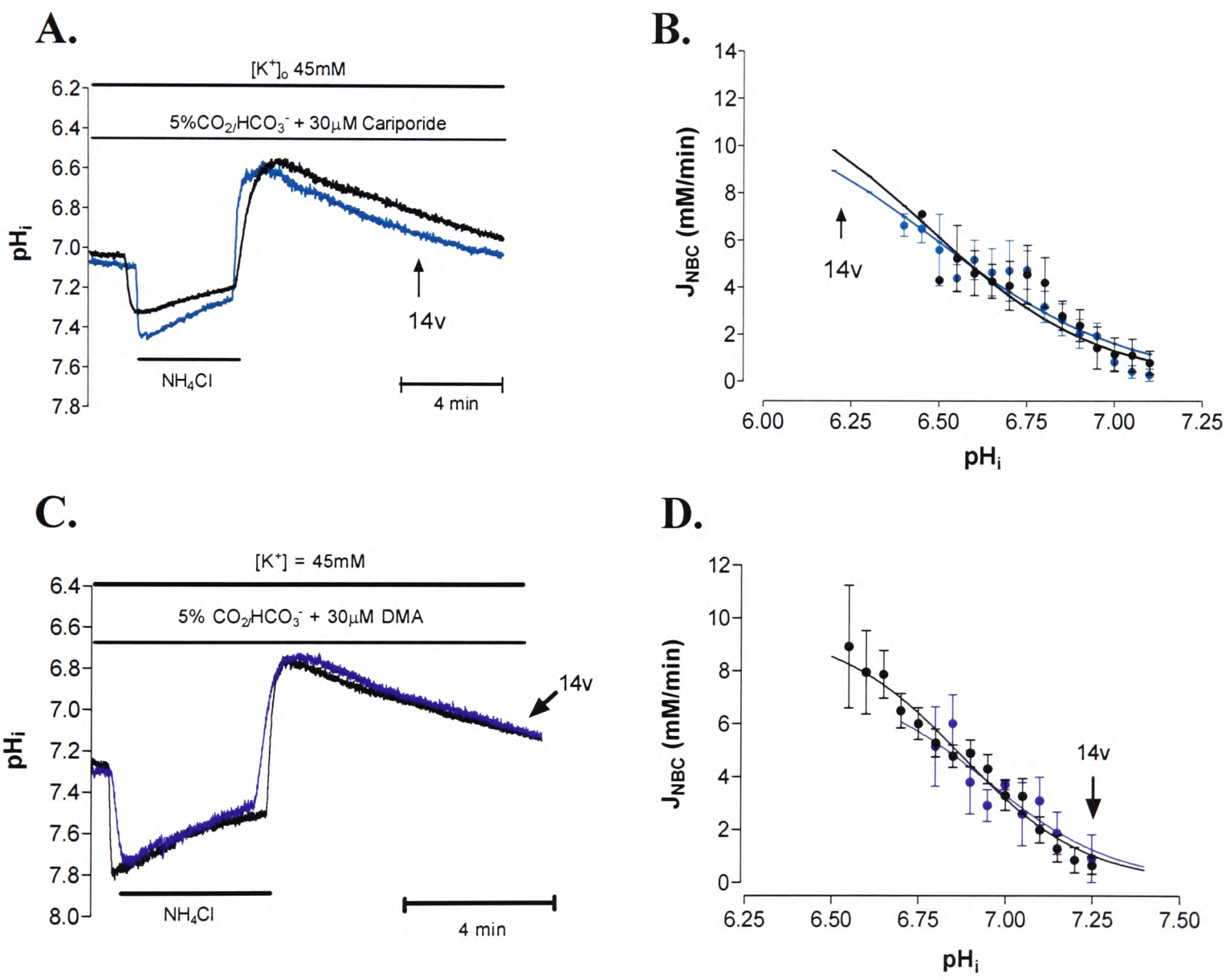

Figure 8. Effect of the extracellular CA inhibitor 14v on NBC H^+-equivalent flux at $[K^+]_o$= 45mM.
A. Superimposed traces of NBC-mediated recovery of pH_i +/- 100nM of the extracellular CA inhibitor 14v using 30μM cariporide to inhibit NHE activity. **B.** Plotting J_{NBC} as a function of pH_i shows that addition of 14v had no effect on NBC-mediated acid efflux in the presence of cariporide over the whole pH_i range examined. **C.** Superimposed experimental traces of NBC-mediated recovery of pH_i +/- 100nM 14v using 30μM DMA to inhibit NHE. **D.** 14v had no effect on J_{NBC} over the whole pH_i range investigated in the presence of DMA.

4.4. Discussion

In the present work, the physiological relevance of a functional relationship involving CA and the two major acid extruders in cardiac myocytes, NHE and NBC, was investigated. The results show that while CA activity has no effect on NHE-mediated H^+ extrusion, it facilitates NBC activity.

4.4.1. CA activity does not facilitate NHE-mediated acid efflux

Although it has been shown that CA can facilitate acid efflux on both NHE and NBC, when these transporters are expressed in heterologous transfection systems (Alvarez *et al.*, 2003; Loiselle *et al.*, 2004; Sterling & Casey, 2002; Sterling *et al.*, 2001a; Sterling *et al.*, 2001b), this is not evident for both transporters when physiologically expressed in the wild-type cardiac myocyte.

The present study shows that pharmacological inhibition of CA with ATZ did not affect NHE activity. This suggests that catalytic activity of CA is not necessary for NHE-mediated acid extrusion in isolated ventricular myocytes, even at flux-rates close to maximal NHE activity when pH_i is low. Furthermore, NHE activity was similar in the presence or absence of CO_2/HCO_3^- buffer. The finding of a lack of effect of CA on NHE activity is in contrast to a previous report (Li *et al.*, 2002) in which NHE-1 and CA II were overexpressed heterologously in HEK293 cells. That study showed addition of 100μM ATZ slowed NHE flux after induction of an acid-load (imposed by switching from CO_2-free to CO_2/HCO_3^- superfusate). It was suggested that CA II facilitated acid extrusion through NHE by providing intracellular H^+-ions arising from cytosolic CO_2 hydration. In order to attain a constant provision of H^+-ions to NHE, H^+-ions derived

from CO_2 hydration would have to diffuse fast enough via cytosolic mobile buffers from the active site of the enzyme to feed the transporter. It has been shown in epithelial and cardiac cells that intracellular H^+-ion mobility is enhanced/facilitated by means of a carbonic buffer "shuttle" (Spitzer *et al.*, 2000; Stewart *et al.*, 1999). The carbonic shuttle system depends on the reversible conversion of CO_2 to HCO_3^- and H^+ catalysed by CA.

According to this, H^+ extruded across the sarcolemma for example, would result in a local sub-sarcolemmal H^+ depletion, thus establishing an intracellular $[H^+]$ gradient. The lower sub-sarcolemmal $[H^+]$ would then drive the CA-reaction in the direction of CO_2 hydration, causing CO_2 to diffuse from the bulk cytoplasm to feed the reaction. Although the carbonic buffer shuttle has been shown to facilitate H^+ mobility in cardiac myocytes (Spitzer *et al.*, 2002), in the present study, the fact that no decrease of NHE-mediated acid extrusion occurred when inhibiting CA in the presence of a CO_2/HCO_3^- buffer system, suggests that H^+ provision to NHE by intrinsic mobile buffers (such as histidyl dipeptides) rather than CO_2/HCO_3^- is fast enough to sustain acid efflux.

Recently, Casey and colleagues have suggested that CA inhibition can prevent pharmacologically-induced cardiomyocyte hypertrophy by decreasing H^+ provision to NHE and thus reducing its activity (Alvarez *et al.*, 2006). Although that study showed the presence of NHE and CA II in cardiac myocytes, a functional demonstration and direct evidence for the requirement of CA II activity for full NHE flux in the intact ventricular myocyte was missing. The present work now shows that such a functional link cannot be demonstrated. This suggests that CA activity may contribute to hypertrophy through pathways other than NHE.

4.4.2. NBC-mediated acid extrusion is facilitated by CA activity

There are opposing views on whether CA facilitates NBC activity. Casey and co-workers (Alvarez *et al.*, 2003) showed that CA IV binds to human NBCe1 at an extracellular domain and enhances HCO_3^- transport when these two proteins are co-expressed in HEK293 cells. A similar association has been shown for NBCn1 and CAII co-expressed in the same renal cell line (Loiselle *et al.*, 2004). These studies have shown that CA can interact with NBC intracellularly and extracellularly, thereby facilitating acid efflux. Contrary to this, Boron and co-workers (Lu *et al.*, 2006) have recently shown that the activity of NBCe1-A expressed in *Xenopus* oocytes was not affected by injecting CA II or by subsequently inhibiting the enzyme with ETZ. Additionally, no effect of CA II on NBCe1-A activity was found when these molecules where expressed together as a fusion protein. With a similar experimental approach, however, Becker and Deitmer (Becker & Deitmer, 2007) showed that injecting or endogenously expressing CA II enhanced NBC-mediated acid extrusion in oocytes expressing NBCe1, and that the effect was reversed by treating the cells with ETZ. The study also showed that the enhancement of NBC activity was dependent on the concentration of CA II. The contribution of CA on NBC activity was assessed by measuring the slope conductance obtained from the I/V relationship of I_{NBC}, and also by measuring the rate of rise of $[Na^+]_i$ and $[H^+]_i$ upon introduction of CO_2/HCO_3^- in the presence and absence of CA. CA contributed ~30% to NBC activity. Additionally, because the activity of NBCe1 is dependent on membrane potential, increasing upon depolarization, the slope conductance and the contribution of CA was measured at two voltages, -40 and -80mV. At both potentials or, in other words, at low and high NBCe1 activity, CA increased NBC slope conductance by ~25%. The

study also showed that the effect of ETZ was specific on CA since addition of the drug had no effect on NBCe1 activity when this transporter was expressed alone in the oocytes in the absence of CA II.

Some possible explanations have been given for the discrepancy between results obtained by the research groups of Deitmer and Boron. Becker and Deitmer (Becker & Deitmer, 2007) suggest that the higher expression level of NBCe1 and higher CA II concentration in Boron and co-workers' study, and also some differences in the voltage-clamping protocol may account for the apparent lack of effect of CA on NBC activity. It is interesting, however, that even when reproducing Boron and co-workers' experiment in every detail, Becker and Deitmer still obtained a stimulatory effect of CA on NBC activity.

In order to avoid the complications that could arise from manipulating NBC and CA levels, in the present study, isolated cardiac myocytes were used to assess the physiological role of CA in an intact, wild-type cell. Also, instead of acid loading the cell by switching from Hepes to CO_2/HCO_3^- superfusate to assess NBC activity, intracellular acidosis was achieved by transiently exposing the cell to NH_4^+ (NH_4^+ prepulse), and NBC-mediated flux was quantified from the subsequent recovery of pH_i. This experimental procedure was used to prevent possible changes in the kinetics of NBC due to CO_2/HCO_3^- buffer equilibration.

The results of the present work suggest a functional association involving NBC and CA activity, inferred from the ATZ or ETZ-evoked reduction in NBC-mediated acid efflux, particularly clear at high extrusion rates. The effect of both sulphonamides, ATZ and ETZ, is likely to be specific to CA activity, without direct inhibitory effects on NBC,

given that ETZ has no effect on heterologously expressed NBCe1 in the absence of CA (Becker & Deitmer, 2007; Lu *et al.*, 2006). It is not yet clear, however, if this conclusion is valid for the NBCe2 isoform. Although transcripts of NBCe2 are expressed in cardiac tissue (Pushkin *et al.*, 2000; Virkki *et al.*, 2002), expression of the transporter at the protein level could not be detected in rat cardiac myocytes (Yamamoto *et al.*, 2007). This thus suggests that electrogenic NBC activity in the rat cardiac myocyte is mainly mediated by NBCe1 and therefore ATZ would not have any direct effect on the NBC protein.

Figure 5B shows that, at pH_i values where NBC flux is low, the inhibitory effect of ATZ failed to reach statistical significance, although an inhibition trend was evident. At more acidic pH_i values, when NBC-mediated acid extrusion is more active, addition of ATZ resulted in a significant reduction of NBC activity. Further stimulating NBC activity with high $[K^+]_o$ permitted to explore the effects of CA inhibition at higher NBC flux rates, over the same pH_i range. Figure 6B and 6D shows that, under these conditions, inhibition of CA resulted in a significant reduction of NBC activity over the pH_i range corresponding to H^+-equivalent flux values above 2mM min^{-1} using either cariporide or DMA to inhibit NHE. Similar results were obtained using 100μM ETZ (Figure 6F) instead of ATZ while inhibiting NHE with 30μM DMA. The effect of CA inhibition on NBC activity over a wide flux range is shown in Figure 7 in which NBC-mediated acid efflux in the presence of ATZ or ETZ, at low and high $[K^+]_o$, was plotted as a function of NBC flux. The curve shows that as NBC flux increases over the x-axis, the fractional reduction of 50% on NBC-mediated acid efflux caused due CA inhibition by ATZ or ETZ appears constant over the whole flux range. At low NBC-flux values however, it is

possible that the reduction of NBC activity does not reach statistical significance because, at such small fluxes, the resolution of J_{NBC} measurement in the present study becomes limiting. Nevertheless, the overall reduction obtained in the presence of ATZ or ETZ (Figure 7) is in agreement with the findings of Becker and Deitmer, suggesting a constant contribution of CA activity at both low and high NBC activity.

The mechanism by which CA activity may facilitate acid efflux on NBC could be by provision or removal of HCO_3^- or H^+, as suggested previously (Alvarez *et al.*, 2003; McMurtrie *et al.*, 2004). Alternatively, it may be by H^+ provision for allosteric regulation of the NBC transporter when diffusion is not rapid enough to match NBC demand. The latter possibility however, would not explain why NHE is not enhanced by the same mechanism in the presence of carbonic buffer and not affected by inhibition of CA. It is possible, however, that conformational differences between the NHE and NBC transport proteins may result in easier H^+ access to the transport and allosteric control-sites in the NHE protein, resulting in no requirement for CA to facilitate H^+ provision.

Recently, Deitmer and coworkers (Becker *et al.*, 2005) showed that CA-mediated facilitation of MCT-1 activity was a consequence of CA binding to MCT-1 and not a result of H^+ provision arising from CA catalytic activity. This study thus raises the possibility that CA may modulate H^+ transporters such as NHE but not NBC by physical binding rather than by its ability to enhance the reversible hydration of CO_2.

4.4.3. Intracellular CA activity facilitates NBC-mediated acid extrusion

Since CA has been reported to bind to NBC at extracellular and intracellular sites, its facilitation in cardiac myocytes may depend on both locations for CA. Because ATZ

and ETZ are both membrane-permeant CA inhibitors, they cannot be used to distinguish between these locations.

Although membrane-bound extracellular CA isoforms (CA IV, IX, XII and XIV) have been identified in cardiac myocytes (Knuppel-Ruppert *et al.*, 2000; Purkerson & Schwartz, 2005; Scheibe *et al.*, 2006; Sender *et al.*, 1998), extracellular faciltitation of HCO_3^- provision to NBC by CA seems unlikely in the present work because, in mammalian ventricular myocytes, the apparent K_m for HCO_3^- in NBC has been estimated as ~2mM (Ch'en & Vaughan-Jones, 2001). Low K_m for extracellular HCO_3^- has also been shown for NBC in other cell types (eg. (Deitmer & Schneider, 1998). During the experiments of the present study, the $[HCO_3^-]_o$ was kept constant at 22mM, and thus it seems unlikely that HCO_3^- provision would be a rate limiting factor for cardiac NBC. Furthermore, addition of the extracellular inhibitor, 14v, to the superfusates, had no effect on NBC-mediated acid efflux, suggesting that an extracellular CA isoform has little or no role in modulating NBC activity, at least in isolated ventricular myocytes.

Although, in the past, the identity of intracellular CA isoforms in the heart has remained elusive, several have recently been identified. Three sarcoplasmic reticulum (SR) membrane-bound CA isoforms, CA IV, IX and XIV, have been identified by immunostaining in adult mouse heart (Scheibe *et al.*, 2006). The study showed that CA XIV and CA IV are associated with the longitudinal SR membrane while CA IV and IX are associated with the terminal SR/t-tubule membranes. Because CA IV is a glycosylphosphatidylinositol (GPI)-anchored isozyme, it can be predicted that the orientation of its catalytic site is directed towards the lumen of the SR making unlikely a functional interaction with NBC. CA IX and XIV are transmembrane proteins, and when

they are expressed in the cell membrane their catalytic domain is oriented towards the extracellular space. Therefore, the predicted orientation of the catalytic activity of these isozymes in the SR will also be towards the luminal space. This orientation makes unfeasible an interaction of these isozymes and NBC within the cytosolic compartment of cardiac myocytes. A recent report (Alvarez *et al.*, 2006) however, has shown the presence of the cytosolic soluble isoform CA II in neonatal and adult rat cardiac myocytes. As mentioned earlier, since CA II has shown to be able to facilitate acid-extrusion when co-expressed with NBC in transfection systems (Alvarez *et al.*, 2003), this isoform, or other that might represent a potential candidate for interaction with NBC in intact cells.

Functional evidence for intracellular CA activity in cardiac myocytes has been provided by several studies (Lagadic-Gossmann *et al.*, 1992; Leem & Vaughan-Jones, 1998; Spitzer *et al.*, 2002). For example, Leem and Vaughan-Jones (Leem & Vaughan-Jones, 1998) showed that, in isolated guinea-pig ventricular cells, CA accelerates intracellular CO_2 hydration by ~2.6-fold at 37°C. Our results from the CA-activity assay in intact myocytes supports this finding, showing that the intracellular CO_2 hydration and dehydration rates are increased ~3-fold by CA at 37°C in rat myocytes. The fact that addition of the extracellular inhibitor, 14v, had no effect on CO_2 hydration or dehydration rates intact cells while ATZ or ETZ exerted clear inhibition, suggests that the CA activity responsible for these reactions in cardiac myocytes is intracellular.

In conclusion, the results of the present study suggest that NBC functionally interacts with an intracellular CA isoform, facilitating acid efflux (Figure 9).

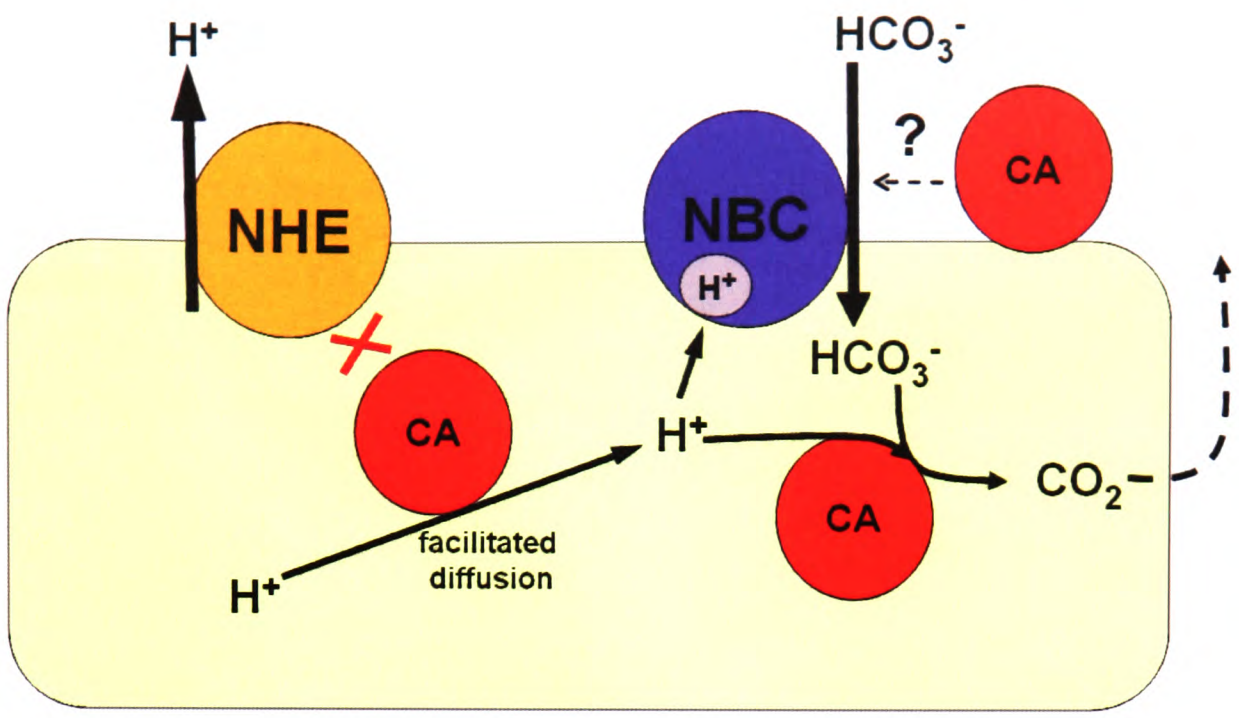

Figure 9. Schematic representation of the proposed role for CA on sarcolemmal acid extrusion. An intracellular CA isozyme enhances the activity of NBC but not of NHE. NBC functionally interacts with CA facilitating acid efflux by decreasing $[HCO_3^-]_i$ locally at the active transport site and thus enhancing NBC transport rate, or/and by facilitating H^+ diffusion to match bulk cytosolic pH to that of the H^+-allosteric regulatory site on the NBC protein. Both mechanisms could be related to the role of CA in the kinetics of the carbonic "shuttle". Although the CA isoform responsible for this effect has not been identified, intracellular CA isozymes, such as CA II, IX and XIV, have been detected in cardiac tissue. Although extracellular CA activity played no role in NBC-mediated acid extrusion in isolated cardiac myocytes, it cannot be discarded that in less well-perfused preparations or tissues, extracellular CA is necessary for transmembrane CO_2 movement and thus pH_i regulation.

CA may facilitate the intracellular conversion of transported HCO_3^- to CO_2 which then diffuses out of the cell. This would decrease $[HCO_3^-]_i$ locally at the active transport site and thus enhance NBC transport rate. Once in the extracellular space, CO_2 can be converted into HCO_3^- thus resulting in a net H^+ extrusion. CA may also enhance NBC-mediated acid extrusion by facilitating H^+ diffusion to match bulk cytosolic pH to that of

the H^+-allosteric regulatory site on the NBC protein. This mechanism would thus provide tight control for pH_i regulation. Although a physical association involving cardiac NBC and an intracellular CA isoform could not be proven, the evidence from this study shows a clear functional association.

CHAPTER 5

pH-DEPENDENCE OF CARBONIC ANHYDRASE ACTIVITY

5.1. Introduction

Proton concentration ($[H^+]$) affects the activity of most enzymes. The relationship between pH and the catalytic activity of any enzyme depends on the acid-base characteristics of the enzyme itself, and also of its substrates, products and co-factors.

Enzymes are amphoteric molecules containing a large number of acidic and basic groups. The charges on these groups will vary, according to their pK_a values, with the pH of their environment. This will affect the total net charge of the enzyme and the charge distribution, in addition to the reactivity of the catalytically active groups. These charge variations, plus any consequent structural alterations, may be reflected in changes in the binding of the substrate, the catalytic efficiency and the amount of active enzyme. Thus, the catalytic activity of enzymes varies over specific pH ranges, where the value at which the enzymes are most active is known as the optimum pH. Depending on the shape of the activity-pH relationship, even slight pH deviations can have a significant impact on the enzymatic rate of catalysis.

The enzyme carbonic anydrase (CA) plays an important role in acid-base homeostasis, and thus any factor affecting its activity may have important physiological consequences. CA accelerates the reversible hydration of CO_2, and thus it controls the effectiveness of carbonic buffering. Under physiological conditions, CO_2-dependent buffering (β_{CO2}) represents a significant component of total intracellular buffering capacity

(β_{tot}). At resting pH_i, β_{CO2} accounts for about half of β_{tot} when HCO_3^-/CO_2 buffer is fully equilibrated (Leem *et al.*, 1999).

Intracellular H^+ mobility and hence pH_i uniformity also depends partly on CA activity. Intracellularly, H^+-ions diffuse bound to intrinsic mobile buffers such as histidyl dipeptides (Vaughan-Jones *et al.*, 2002), and also by means of the "carbonic shuttle" using the carbonic buffer system (see Chapter 1). Thus, efficient function of the carbonic shuttle depends on CA activity (Spitzer *et al.*, 2002; Swietach *et al.*, 2007).

As discussed in Chapter 4, CA also appears to be involved in pH_i regulation by being physically or functionally coupled to membrane pH_i regulatory transporters in transport metabolons.

Thus, any effect of pH on CA activity is likely to affect physiological buffering, and intracellular H^+ diffusion. This, in turn, will affect spatial pH_i uniformity, and also the kinetics of pH_i regulation.

5.1.1. pH-sensitivity of CA

Early work by Kernohan (Kernohan, 1965) and Khalifah (Khalifah, 1971) on CA kinetics reported pH sensitivity of the isozymes CA I and CA II. These studies showed that the K_m for CO_2 is pH-insensitive but that K_{cat}/K_m varied as a function of pH, with a pK_a close to 7.0. Given that K_m is not dependent on pH, the pH-sensitivity of K_{cat}/Km reflects that of K_{cat}. K_{cat}, also called turnover number, is a general rate constant used to describe the limiting rate of any enzyme at saturation. It has reciprocal time units (s^{-1}) and can be calculated as the V_{max} of the enzyme divided by the total enzyme concentration ($K_{cat} = V_{max}/[E]_t$.

Another isozyme, CA III, however, has been shown to be insensitive to pH. Tu *et al* (Tu *et al.*, 1983) studied the activity-pH profile of CA III from cat muscle and showed that both K_m and K_{cat} were pH-insensitive.

Later, as more CA isozymes were discovered and kinetically characterized, the pH sensitivity profiles of some of these were also described (Baird *et al.*, 1997; Heck *et al.*, 1994; Ulmasov *et al.*, 2000; Wingo *et al.*, 2001). pK_a values of CA IV, CA V, CA IX and CA XII have been reported as 7.1, 7.4, 6.3, and 7.1, respectively. It has been also been shown that these pK_a values are consistent with a single ionizable group, which corresponds to the zinc-bound water molecule that originates the OH^--ion.

The relevance of pH sensitivity of CA however, had remained constrained to kinetic and pharmacological inhibition studies and not to its role under physiological conditions.

The aim of the present work was to re-investigate the pH-sensitivity of CA II, test the pH sensitivity of CA activity in cardiac homogenates and finally, investigate CA's pH sensitivity directly in a living cell.

5.2. Methods

5.2.1. CA Activity Assay

The activity of CA II and of endogenous CA in cardiac homogenates was assayed as previously described in Chapter 2 with some modifications in the buffering conditions of the reaction medium (RM). Since the protocol for assessing the pH sensitivity of the enzyme involves the use of a wide pH range, a double buffered reaction medium was used to maintain adequate buffering over the whole range. The double buffer RM consisted of a combination of Hepes and MES buffers which, due to their pK_a values, resulted in a roughly constant buffering capacity over the pH range 6.5 to 8.0. Figure 1 illustrates this by plotting the total and individual buffering capacity of each buffer as a function of pH.

The pH-dependence of the buffering capacity (β) of RM was calculated as:

$$\beta(\mathrm{mM}) = \frac{\ln_{10} \times [\mathrm{Hepes}] \times 10^{\mathrm{pH_i} - \mathrm{pK_{Hepes}}}}{(1 + 10^{\mathrm{pH_i} - \mathrm{pK_{Hepes}}})^2} + \frac{\ln_{10} \times [\mathrm{MES}] \times 10^{\mathrm{pH} - \mathrm{pK_{MES}}}}{(1 + 10^{\mathrm{pH} - \mathrm{pK_{MES}}})^2}$$

where each independent term of the equation defines the buffering capacity of the individual buffers, Hepes and MES, as a function of pH. At 2°C, the combination of 25mM of Hepes (pKa = 7.68) and 25mM MES (pKa = 6.25) resulted in a stable buffering capacity above 10mM in the reaction chamber over the pH range 6.5-8.0.

Sanyal and Maren (Sanyal & Maren, 1981) reported that the pK_a of CA II varied with temperature by a factor of 0.02 per degree. Therefore, it is possible that the apparent pK_a determined at 2°C differs at higher temperatures. In order to assess the extent to which temperature differences affect pK_a values in the enzymatic assay, CA activity was determined at 2 °C, 12 °C, and 22 °C using a high buffering capacity RM. The reaction

medium contained only Hepes and NaCl in order to maintain ionic strength and Cl^- concentration. Due to the high concentration of Hepes, it was unlikely that the concentration of buffer would become rate-limiting at acidic pH values during the course of the reaction. Therefore, MES was not included when Hepes was used at high concentration.

Due to the high turnover rate of the enzyme and also to the increased contribution of the uncatalysed reaction to the overall rate, it was not possible to measure CA activity at physiological temperatures (37°C) using this method.

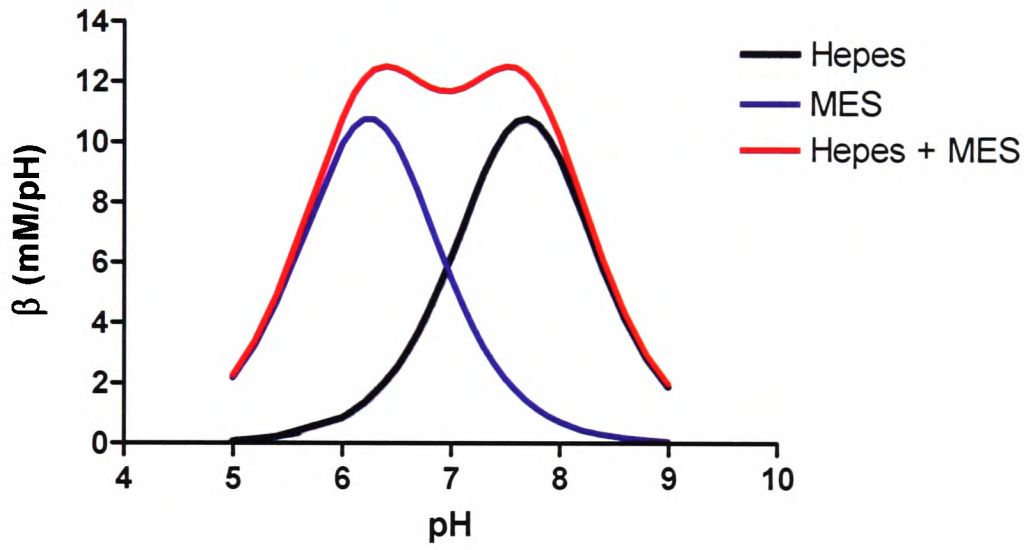

Figure 1. pH-dependence of buffering power in the reaction medium. A double-buffered medium was used to provide a stable buffering power during the course of the reaction. Hepes (25mM, pKa = 7.68; dark blue) or MES (25mM, pKa = 6.25; light blue) provided maximum buffering power only over a narrow pH range. The combination of both buffers (red) resulted in a stable buffering capacity above 10mM in the reaction chamber over the pH range 6.5-8.0.

CO_2 hydration rate was expressed as k_f (s^{-1}). The value for k_f was estimated by fitting the kinetic model described in Chapter 2 to the pH time-course data using two approaches. In one, the initial rate was estimated in RM of pH 8.0, 7.5, 7.0, and 6.5 by computing k_f

over the time interval for the pH to drop by 0.2 pH units after the addition of CO_2-saturated solution. Figure 2A shows a typical recording of such an experiment. Data are shown in red, and the prediction obtained from the best-fit of the model to data is shown in blue. The circle indicates the end of the fitting interval. If the fitting is performed over the whole pH range with a single average k_f value, the data appears to deviate from the model below pH ~7 suggesting that k_f values of the CA-catalysed reaction may decline with decreasing pH (Figure 2B).

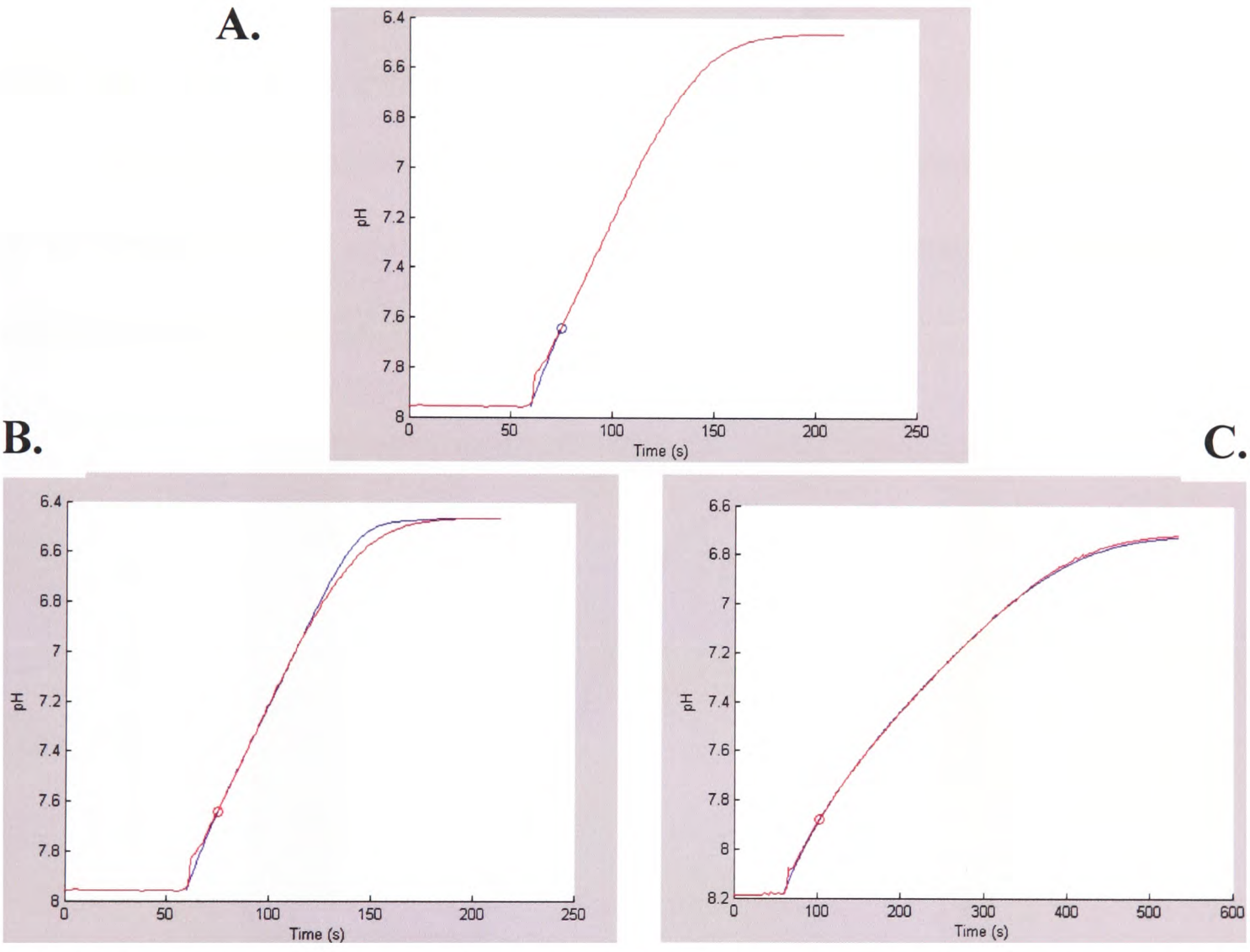

Figure 2. Typical experimental recording of CA II activity assay. Panel A shows original experimental recording (red) and the best-fit predicted by the model (blue) to the initial 0.25 pH unit drop. The blue circle indicates the end of the fitting interval. Panel B shows the same experimental trace as in Panel A, but the fitting was performed over the whole pH range of the reaction. A deviation from the prediction can be observed at pH below 7. Panel C shows an experimental recording of the time course of reaction in the absence of CA (uncatalysed reaction). In this case, no deviation from the prediction can be observed. Graphs from Matlab macro output.

In contrast, when the full-range fitting procedure is performed on data obtained from the reaction in the absence of CA (uncatalysed reaction; Figure 2C), no deviation was observed.

In order to estimate k_f over the whole pH range, an interval fitting procedure was used. This second approach consisted of computing k_f for intervals of 2 seconds, over the whole time-course of the reaction, using an RM of initial pH 8.0. The final values of $[CO_2]$, $[HCO_3^-]$, and pH of a given 2 second interval were used as the initial conditions for the next interval. The best-fitting k_f values were plotted as a function of mean pH within the interval. This approach provided k_f values over a wide pH range (Figure 3).

The two approaches were also used to obtain a spontaneous reaction k_f value (ie. in the absence of CA activity) using data obtained from blanks, or obtained in the presence of 10μM ATZ ($k_{f\,ATZ}$).

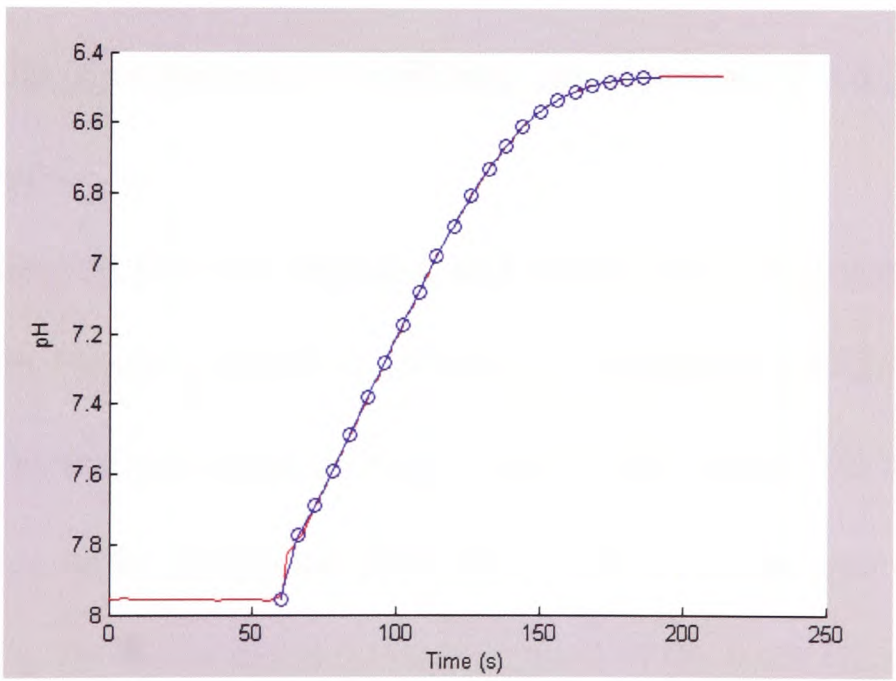

Figure 3. Typical experimental recording and piece-wise best-fit of CA II activity assay. A piece-wise fitting procedure (blue) to data (red) was used to estimate k_f over the whole pH range of the reaction. The fitting interval was set at 2 seconds. Graphs from Matlab macro output.

Several *in vitro* studies have previously shown that the pH profile of CA activity appears sigmoidal (Armstrong *et al.*, 1966; Donaldson & Quinn, 1974; Kernohan, 1965; Khalifah, 1971). Therefore, in the present work, data were fitted with a four-parameter, variable slope, sigmoidal function (Prism 4, Graphpad Inc), after subtracting the spontaneous reaction k_f. pK_a and Hill coefficient (n_H) values were obtained from the best-fit of the sigmoidal curve.

In order to compare the pH profile of CA at different temperatures, data were corrected by taking the difference obtained by subtracting the blank from the data and normalizing it to the same blank value (i.e. [data-blank]/blank).

5.2.2. pH-sensitivity of the intracellular reversible CO_2 hydration

In order to investigate the pH-sensitivity of intracellular CA activity, pH_i was preset to different values using the ammonium or acetate pre-pulse techniques (Roos & Boron, 1981) while simultaneously inhibiting sarcolemmal H^+-equivalent transport to prevent pH_i recovery.

Once the desired pH_i was obtained, and the pH_i recording was stable, superfusate was switched from Hepes-buffered to CO_2/HCO_3^- -buffered Tyrode at constant pH_o to measure the CO_2 hydration rate at different starting pH_i values. Na^+-free solutions were used in combination with ammonium pre-pulses when an acidic starting pH_i was desired (Figure 4A). Figure 4B shows the amplified sections of the trace shown in Figure 4A, on switching to CO_2/HCO_3^--buffered superfusate.

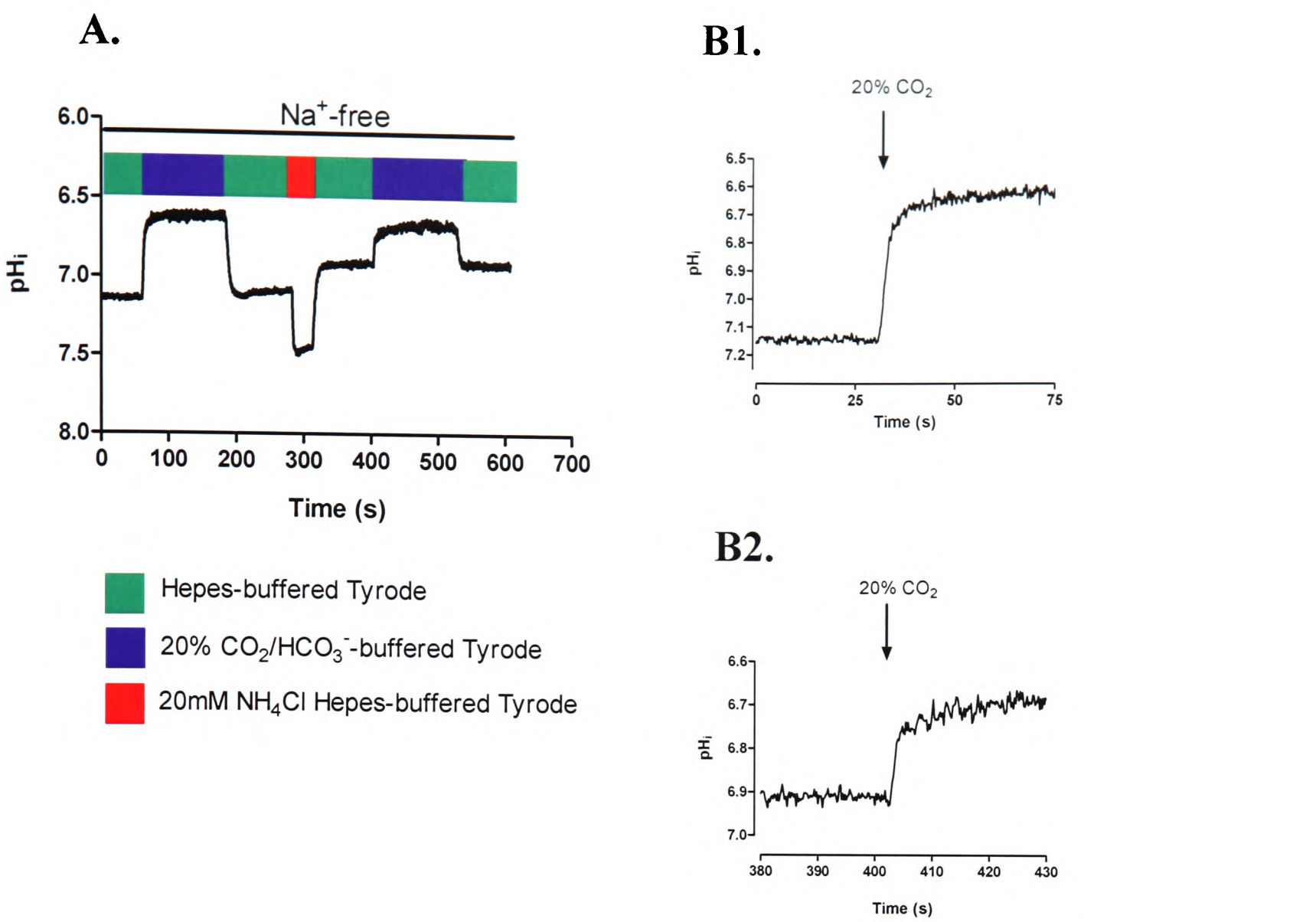

Figure 4. Typical experimental procedures used to investigate the pH_i-dependence of the intracellular CO_2 hydration rate and CA activity at acidic pH_i. After obtaining a stable resting pH_i, the rate of pH_i change on switching from Hepes- to CO_2/HCO_3^--buffered superfusates was used to assess the degree of CA catalysis. Panel A shows a typical experiment in which after switching from Na^+-free Hepes- to Na^+-free 20% CO_2/HCO_3^- -buffered solution and back, pH_i was reset to an acidic value using a 20mM NH_4^+ pre-pulse. Once the desired pH_i was obtained, and the recording stable, superfusate was switched to CO_2/HCO_3^- Tyrode to asses CA catalysis at acidic pH_i. Different levels of intracellular acid load were obtained by varying the time of exposure to the NH_4^+-containing solution. Panels B1 and B2 show the amplified sections of experimental trace shown in panel A on switching to CO_2/HCO_3^--buffered superfusate at resting (B1) and acidic (B2) pH_i in a faster time base.

Cl^--free solutions were used in combination with acetate pre-pulses when an alkaline starting pH_i was preferred (Figure 5A). Figure 5B shows the amplified sections of the experimental recordings shown in Figure 5A, on switching to CO_2/HCO_3^--buffered superfusate at resting and alkaline pH_i, on a faster time base.

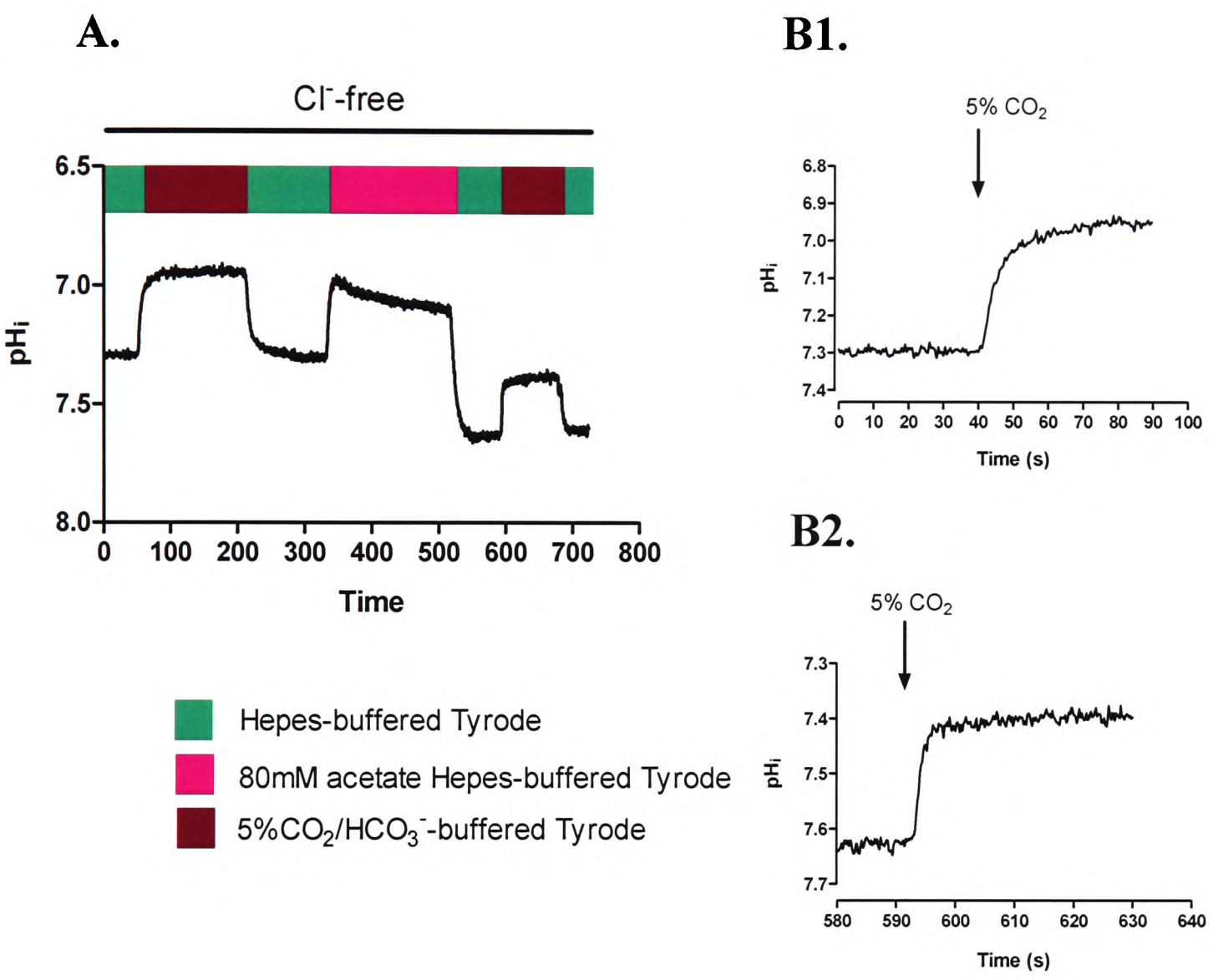

Figure 5. Typical experimental procedures used to investigate the pH_i-dependence of the intracellular CO_2 hydration rate and CA activity at alkaline pH_i. Panel A shows the experimental protocol for assessing the rate of CA catalysis at alkaline pH_i. In order to preset pH_i to alkaline values, an acetate pre-pulse was performed under Cl-free conditions. Once the new pH_i was obtained, superfusate was switched from Cl^--free Hepes- to Cl^- -free 5% CO_2/HCO_3^--buffered Tyrode. Panels B1 and B2 show the amplified sections of experimental trace shown in panel A on switching to CO_2/HCO_3^--buffered superfusate at resting (B1) and alkaline (B2) pH_i in a faster time base.

Different levels of intracellular acid or alkali load were obtained by varying the time of exposure to the ammonium or acetate-containing solutions, respectively.

The rate of pH_i change on CO_2 addition was used to assess the degree of CA catalysis. k_f for the intracellular CA-catalysed reaction (k_{fi}) was estimated by simultaneously solving the set of differential equations described in Chapter 2, modified for piece-wise fitting. k_{fi} was estimated in intervals of 1 second, and the final values of $[CO_2]_i$, $[HCO_3^-]_i$, and pH_i of an interval were used as the initial conditions for the next one (Figure 6). An estimate of the initial rate was obtained by using the first two intervals.

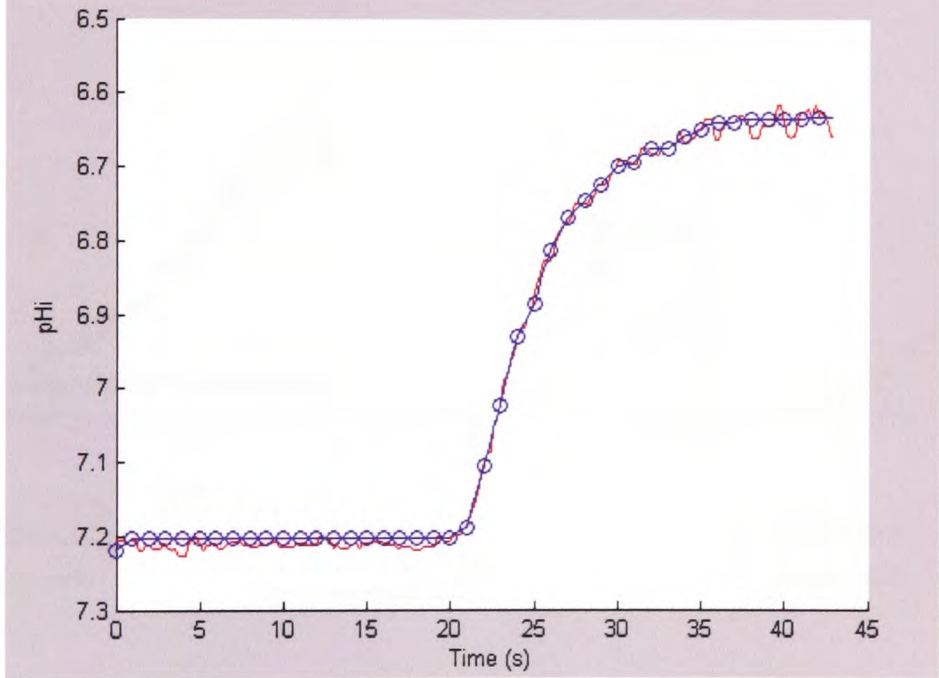

Figure 6. Experimental recording and piece-wise best-fit of intracellular hydration of CO_2. Piece-wise fit (blue) to data (red) was obtained in intervals of 1 second over the time course of pH change due to CA-catalysed intracellular CO_2 hydration . Graphs from Matlab macro output.

5.3. Results

Figure 7A shows a comparison of the pH profile of the k_f for CO_2 hydration obtained *in vitro* from initial rates of acidification and from the whole-range piece-wise fit, as described in the Methods section of this chapter. Clear pH-sensitivity was obtained using both procedures. Figure 7B shows that, at 2°C, apparent pK_a for CA II activity was 7.00 (using initial rates) and 6.99 (using the piece-wise approach). n_H values for the H^+-dependence of CA activity were 1.093 and 1.182, respectively. k_f values computed in the presence of ATZ or computed from blank data sets showed no variation over the whole pH range examined.

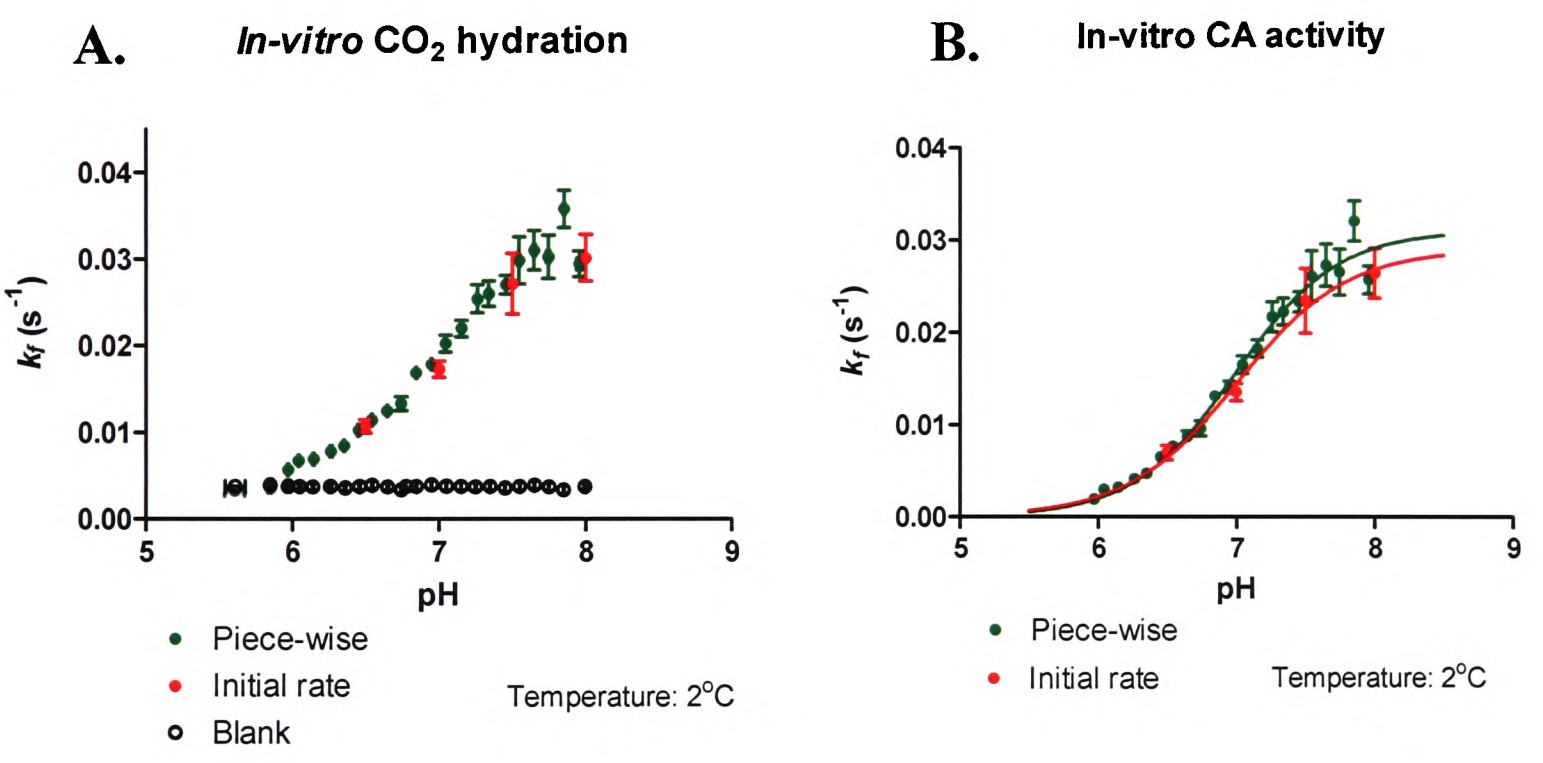

Figure 7. pH profile of CA II activity. Panel A shows a comparison of the pH dependence of k_f data obtained using the initial rate fit (●) and the whole-range piece-wise (●) fit approach at 2°C (n=8-104). k_f data obtained from blanks (○) showed no pH sensitivity over the same pH range (n=22-89). k_f values computed in the presence of ATZ or computed from blank data sets showed no variation over the whole pH range examined. Panel B shows the sigmoidal fits of the two data sets after subtraction of blanks. Apparent pKa for CA II was 7.00 ± 0.12 using initial rates and 6.99 ± 0.05 using the piece-wise approach. Hill coefficients (n_H) were 1.093 ± 0.10 and 1.182 ± 0.27, respectively.

A similar comparison was performed for CA activity in cardiac homogenates. Figure 8 shows pH-dependence of CA activity in cardiac homogenates using both approaches. k_f from blank sets or $k_{f\,ATZ}$ showed complete pH insensitivity and thus was subtracted from the overall value before applying the sigmoidal fit. Apparent pK_a for CA activity in cardiac homogenates was 7.145 using initial rates and 6.919 using the piece-wise approach. n_H values were 0.8 and 1.15, respectively.

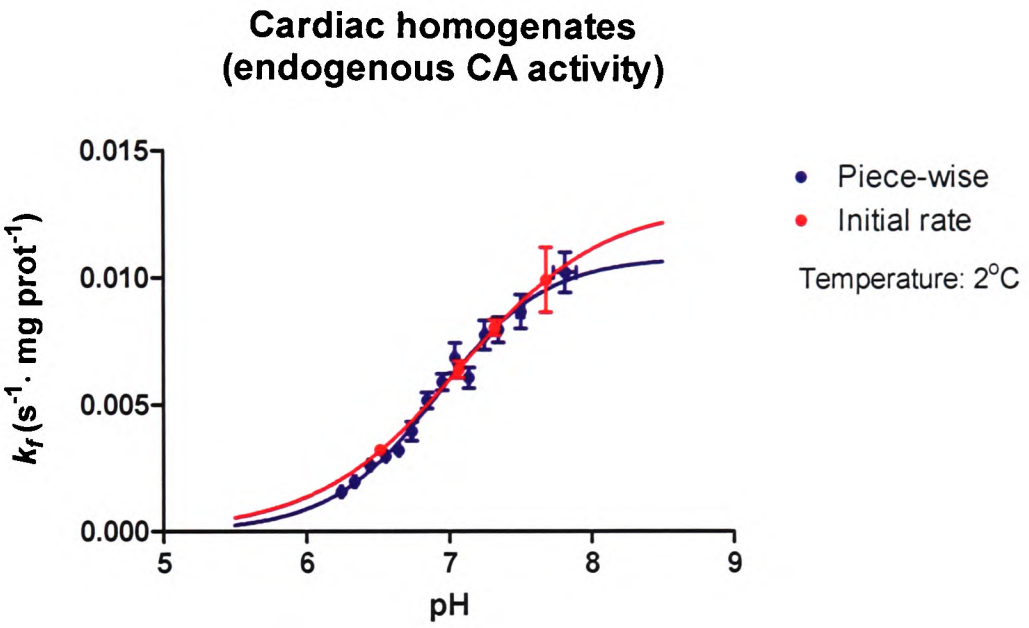

Figure 8. pH profile of CA activity in cardiac homogenates. After subtraction of blanks, sigmoidal fitting of data resulted in an apparent pKa of 7.145 using initial rates and 6.919 using the piece-wise approach. n_H values were 0.8 and 1.15, respectively (n=6-28).

Figure 9A shows the uncatalysed k_f at 2°C, 12°C and 22°C as a function of pH, which appears to be independent of pH within the each temperature data set. Note that, as expected, k_f increases with temperature. Figure 9B shows the k_f pH profile of CA II at 2°C, 12°C. At both temperatures CA activity was pH-sensitive and, as expected, k_f increased with temperature. k_f in the presence of CA at 22°C, however, was difficult to measure, due to the high catalytic activity of the enzyme at that temperature, and so has not been shown. Using a different methodology, Dodgson and Forster (Forster, 1991)

were able to measure CA activity up to 37°C. Unfortunately the assay method used in the present work did not have sufficient temporal resolution to detect the fast reaction rates attained in the presence of CA at temperatures above 12°C.

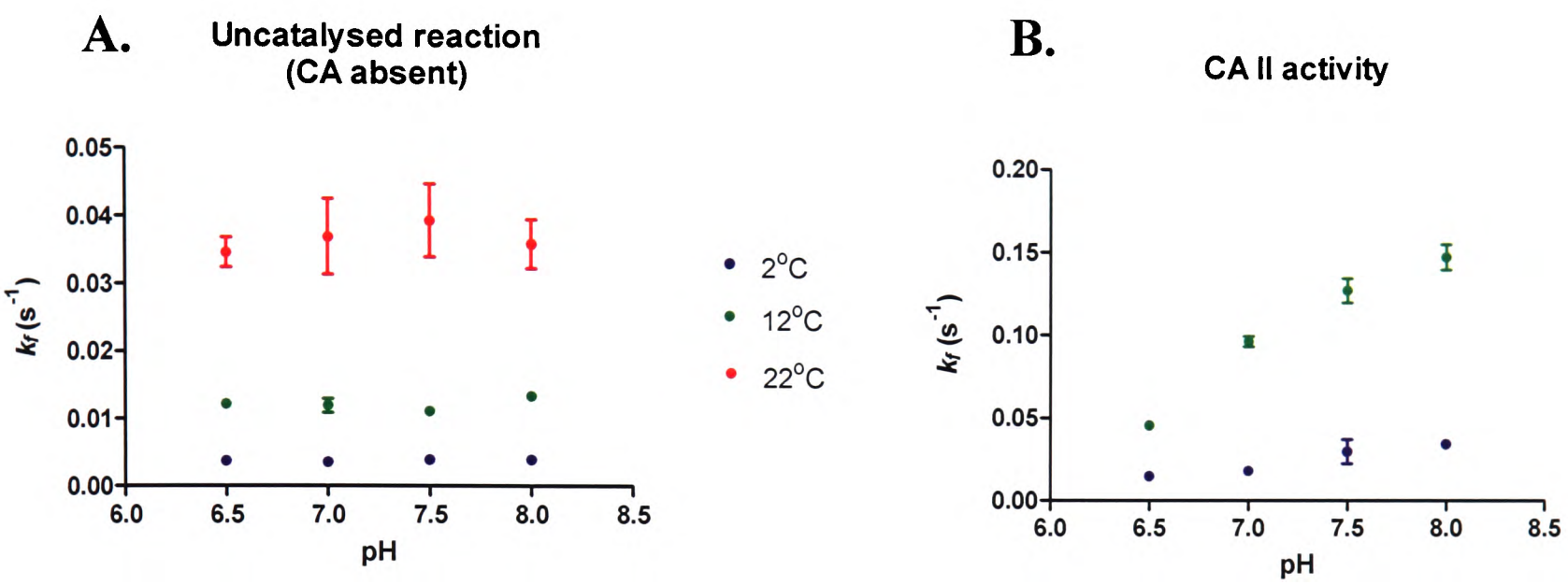

Figure 9. Temperature-dependence of CA II pH sensitivity. Panel A compares k_f obtained from blanks over the same pH range at 2°C (●), 12 °C (●), and 22 °C (●) (n=5 for each set). k_f of the uncatalysed reaction increased with temperature but within each temperature set k_f was invariable over the pH range. Panel B shows a comparison of k_f variation from pH 8.0 to 6.5 at 2°C (●) and 12 °C (●). Within each temperature set, k_f increased with pH (n=5 for each set). Panel C: After subtracting blank k_f, data obtained at 2°C and 12°C were fitted to a sigmoidal function. Resulting pK_a values at 2°C and 12°C were 7.248 ± 0.42 and 6.879 ± 0.034, respectively.

Thus, only data sets at 2°C and 12°C were obtained. After correction, using their respective blanks, a leftward shift was observed in the pH-sensitivity of CA, upon increasing temperature from 2 °C to 12°C. A four-parameter sigmoidal fit was performed on both data sets. Resulting apparent pK_a values at 2°C and 12°C were 7.248 ± 0.42 and 6.879 ± 0.034, respectively (Figure 9C). In this set of experiments, however, data obtained at 2°C did not show clear signs of saturation, and thus the sigmoid fit may not be completely reliable. This can be also noted from the larger confidence interval obtained at 2°C.

The problems of not working at 37°C *in vitro* were overcome by assessing the pH-sensitivity of CA under physiological conditions, inside a living myocyte. In this case, the high temporal resolution of pH_i measurement by using an intracellular pH-sensitive fluorophore, together with the modest expression of endogenous CA activity and the high intracellular intrinsic buffering, permitted resolution of the time course of CO_2-induced acidification of pH_i, even at body temperature.

Figure 10A shows the pH profile of k_f determined for intracellular CO_2 hydration (k_{fi}). The curve shows that k_{fi} increases with pH_i at 37°C showing clear pH-sensitivity of the hydration reaction. Addition of 100μM ATZ to superfusates resulted in non-variant k_f values over the whole pH_i range, which confirms pH sensitivity of intracellular CA activity and gives an estimate of the uncatalysed intracellular rate of hydration. Figure 10B shows the fitted data after subtraction of the uncatalysed k_f at each pH_i value. The fitting procedure resulted in an apparent pK_a of 7.17 ± 0.12 and a n_H for intracellular H^+-ions of 2.54.

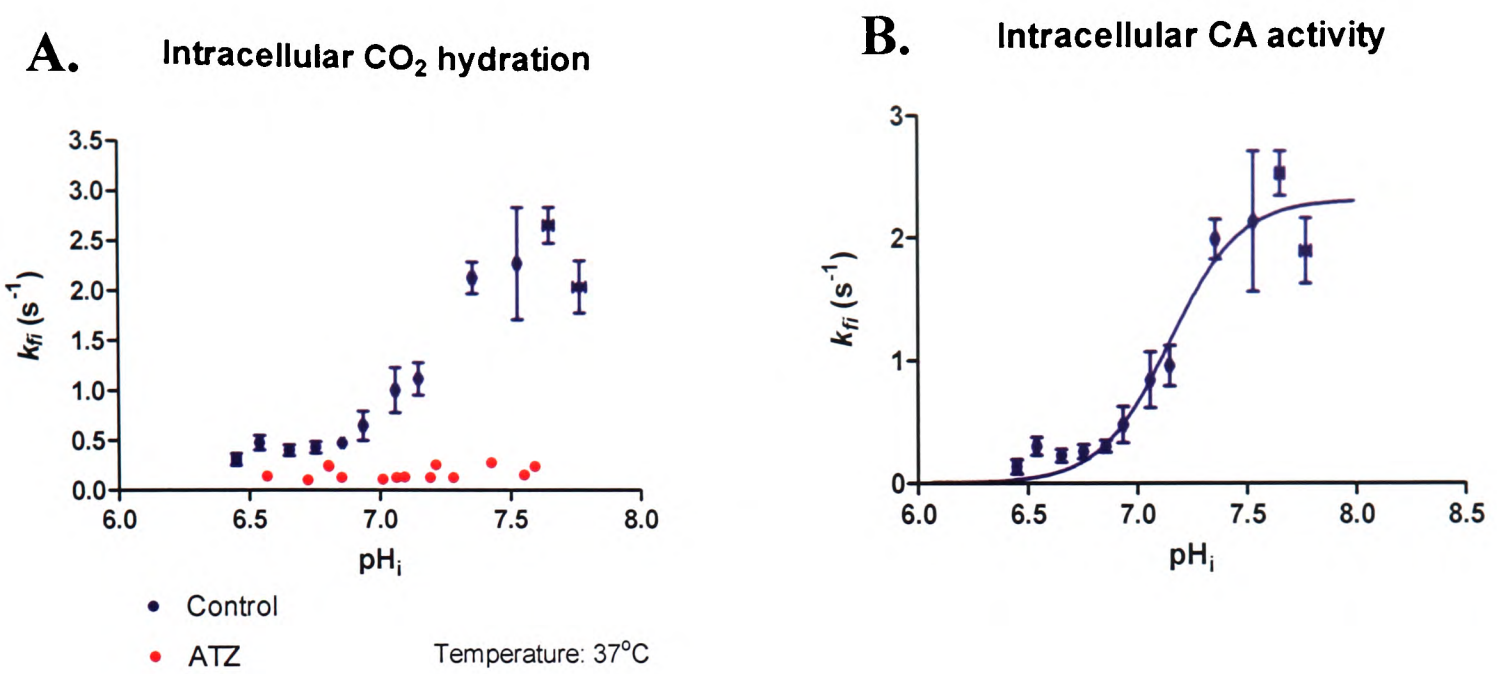

Figure 10. pH profile of intracellular CA activity. Panel A shows variation of k_{fi} with pH_i at 37°C in an intracellular environment (n=23). Addition of 100μM ATZ to superfusates significantly reduced k_{fi} and abolished pH dependence (n=6). This confirms pH sensitivity of intracellular CA activity and gives an estimate of the uncatalysed intracellular rate of hydration. Panel B shows the fitted data after subtraction of the uncatalysed k_{fi} at each pH_i value. The sigmoidal fitting procedure resulted in a pK_a of 7.17± 0.12 and an n_H of 2.54.

5.4. Discussion

The present work confirms that the activity of CA II *in vitro* is pH-sensitive, shows pH dependence of CA activity in cardiac homogenates and also, for the first time, demonstrates pH sensitivity of intracellular CA activity in cardiac myocytes as a model of an intact cell. CA activity showed to drop with decreasing pH.

Therefore carbonic anhydrase, an enzyme involved in physiological pH regulation, is itself regulated by pH. pH-dependence of CA activity has previously been reported in studies of different purified CA isozymes (Baird *et al.*, 1997; Engberg & Lindskog, 1984; Heck *et al.*, 1994; Kernohan, 1965; Khalifah, 1971; Wingo *et al.*, 2001) but not in cardiac homogenates or in intact cells.

pK_a values obtained from CA II and from cardiac homogenate activity assays fall within the same range of those previously published for purified CA isozymes (Baird *et al.*, 1997; Engberg & Lindskog, 1984; Heck *et al.*, 1994; Kernohan, 1965; Khalifah, 1971; Wingo *et al.*, 2001). In the case of CA II, for example, a pK_a of ~7 has been repeatedly reported (Baird *et al.*, 1997; Khalifah, 1971; Lindskog, 1963). In the present work, by using two different data fitting approaches for k_f determination, a pK_a of 7 was obtained for CA II (7.004 with initial rates and 6.990 with piece-wise approach). The pH profile of CA activity in cardiac homogenates determined over a similar pH range resulted in an apparent pK_a also close to 7 (7.071 using initial rates and 6.919 using piece-wise approach). In this case, however, it is not possible to say that this value corresponds to a single CA because several isoforms coexist in cardiac tissue (Alvarez *et al.*, 2006; Scheibe *et al.*, 2006). This value should be taken as an overall pK_a, which characterizes the pH profile of endogenous CA activity in cardiac tissue. Although there

are some studies where CA activity was determined in heart tissue (Bruns & Gros, 1992; Geers *et al.*, 1992), none of these characterized its pH-sensitivity.

One important difference between the kinetic studies, where CA pH-sensitivity was previously determined, and the present work is the temperature at which the activity assay was carried out. Most CA activity pH profiles have been determined at 25°C by different experimental methods (Baird *et al.*, 1997; Heck *et al.*, 1994; Kernohan, 1965; Khalifah, 1971; Wingo *et al.*, 2001). Therefore, a temperature correction should be applied in order to asses CA pH sensitivity at physiological temperature.

Sanyal and Maren (Sanyal & Maren, 1981) determined the temperature dependence of CA II, and showed that its pK_a decreased by 0.02 units per degree increment. In order to assess the extent to which pK_a is affected by temperature, in the present work, a pH profile of CA II was generated at two different temperatures. When the data and fits for these two sets were compared, a clear left shift is observed when the temperature is increased from 2°C to 12°C. The shift in pK_a is equivalent to 0.036 units per degree increment, a larger value than that expected from the data of Sanyal and Maren (Sanyal & Maren, 1981). Unfortunately, from only two temperature data sets it is not possible to extrapolate values and predict what the apparent pK_a of CA in the activity assay would be at 37°C. The assays, however, confirmed pH sensitivity of CA II, showed pH-sensitivity of CA activity in cardiac homogenates, and also that the CA II pH profile curve shifts to the left with increasing temperature.

In order to assess how this pH-sensitivity translates into a physiological situation, at 37°C and within a cellular environment, a pH profile of intracellular CA activity in cardiac myocytes was generated. CA activity obtained within a pH_i range between 6.45

and 7.76 showed clear pH dependence. This is confirmed by the fact that data obtained in the presence of 100μM ATZ appeared invariant within the same pH_i range. After subtracting $k_{f\,ATZ}$, an apparent pK_a of 7.17 and an n_H of 2.54 were obtained from the sigmoidal fit of data. The resulting apparent pK_a value is similar to that obtained in cardiac homogenates at 2°C (pKa = 6.919-7.14) in the present work. If the temperature correction factor obtained by Sanyal and Maren (Sanyal & Maren, 1981) were correct, pK_a at 37°C should be around 6.5. It is important however, to consider that intracellular conditions may be very different to those of an enzyme assay.

It is not unreasonable to suggest that the different conditions for catalysis and behavior of CA found inside cells could account for the difference between intracellular and *in vitro* estimates of CA's pK_a. It is possible that binding of electrolytes, of intracellular buffers, macromolecular crowding and electrostatic interactions with other proteins could result in a different pK_a value from that observed in *in-vitro* studies. Therefore, the results under physiological conditions in living cells should be favoured.

The apparent pK_a and n_H values estimated for intracellular CA activity represent global values which correspond to a mixture of CA isozymes found inside cardiac myocytes (Alvarez *et al.*, 2006; Scheibe *et al.*, 2006). For example, n_H values obtained *in-vitro* for the pH-dependence of CA II and cardiac homogenates total CA activity were closer to 1 while for intracellular CA activity was 2.54 which suggests the presence of at least two binding sites for H^+-ions per CA molecule or binding of H^+-ions to a CA dimer or trimer. CA IX (which is expressed in the cardiac myocytes) has been proposed to form trimers (Pastorekova *et al.*, 1992). Thus, it is possible that in intact myoctes CA IX is associated in trimers, and the n_H value above 2 may partly reflect CA IX pH-sensitivity.

The CA IX trimers might be disrupted during the homogenisation process and dilution of cardiac tissue. This will, in turn, result in n_H values closer to 1 for the pH-sensitivity of cardiac homogenates.

As shown in Figure 10B, the results of the present work suggest that at a resting pH_i of 7.25 for example, intracellular CA will be inhibited by H^+-ions by about 40%. Despite this, the remaining CA activity can still accelerate the spontaneous rate of CO_2 hydration by 6.6-fold. If pH_i falls, to 6.8 for example, CA-mediated acceleration of intracellular CO_2 hydration would be decreased by 4-fold.

5.4.1. Possible consequences of CA pH-sensitivity

5.4.1.1. Effect on buffering

Efficient physiological buffering requires rapid equilibration of carbonic buffer. In a well-buffered environment, such as the intracellular compartment, the uncatalysed reversible hydration of CO_2 can take up to several minutes. In cells, however, CA mediates the rapid equilibration of carbonic buffer. Thus, the efficiency of the CO_2/HCO_3^- buffer system depends on the catalytic activity of CA. Inhibition of CA by H^+-ions therefore implies that at low pH_i, apart from other factors such as decreased intracellular $[HCO_3^-]$, a decline in CA activity may contribute to less efficient physiological buffering.

5.4.1.2. Effect on intracellular H^+ mobility

Several studies have shown that in the presence of carbonic buffer, intracellular H^+ mobility is enhanced by ~50% (Spitzer *et al.*, 2002; Swietach *et al.*, 2007; Zaniboni *et*

al., 2003). This enhancement can be abolished by addition of ATZ, suggesting that CA is required for carbonic buffer-mediated H^+-mobility through the carbonic shuttle (see Chapter 1). Vaughan-Jones and co-workers (Swietach *et al.*, 2007) have shown that the contribution of carbonic shuttling is pH_i-dependent, decreasing about fivefold when pH_i drops from 7.5 to 6.1. Given that CA is pH sensitive, it is possible that the inhibition of CA activity by H^+-ions contributes in part to the decline in carbonic shuttling, and hence H^+ mobility. The decline in H^+-mobility may, in turn, give rise to spatial pH_i non-uniformity which may have important physiological consequences including disruption of Ca^{2+}-signalling and contraction (Dilworth *et al.*, 2006; Spitzer & Vaughan-Jones, 2006).

5.4.1.3. Effect on membrane H^+-equivalent transport

CA can be structurally and/or functionally coupled to membrane pH_i regulatory transporters (Alvarez *et al.*, 2003; Sterling *et al.*, 2002; Sterling *et al.*, 2001). The activity of CA in this particular arrangement facilitates transporter flux by substrate or product provision or removal, or by facilitating H^+ diffusion to the allosteric control site of the transporter and match it to that of the bulk cytosol in order to exert tight pH_i control.

Thus, the influence of pH on CA activity could also affect membrane transporter kinetics and hence pH_i regulation. As shown in Chapter 4, NBC-mediated transport is enhanced by intracellular CA activity in rat ventricular myocytes. In the event of an intracellular acid load, elevated $[H^+]_i$ activates NBC-mediated acid extrusion. As pH_i recovers, NBC activity decreases. Conversely, low pH_i decreases CA activity. Thus, the influence that H^+-ions appear to exert on NBC and CA is opposite. The enhancement provided by CA to NBC activity is by about 50% at every pH_i measured. This implies

that over the whole pH_i-recovery range, CA appears to act as a constant facilitator of NBC. Although at a low pH_i of for example 6.8, CA activity decreases by about 75%, the remaining enzyme activity would appear to be sufficient to enhance NBC-mediated transport. As pH_i recovers, CA activity increases but the facilitation on NBC activity remains constant, suggesting that only a fraction of intracellular CA activity is required for NBC-mediated flux facilitation in ventricular myocytes. Thus, paradoxically, although CA activity changes with pH_i, this effect is not reflected in the facilitation of NBC activity.

In summary, the present work confirms previous findings of CA's pH-sensitivity *in vitro*, it shows that CA activity in cardiac homogenates is pH-dependent, and it shows for the first time, that CA activity in an intact cell is strongly pH-sensitive. The pH-sensitivity of CA activity implies that the contribution of the enzyme to buffering and intracellular H^+ mobility, and overall pH_i regulation, could vary dynamically with local and global changes in intracellular $[H^+]$.

CHAPTER 6

GENERAL DISCUSSION

The enzyme carbonic anhydrase (CA) catalyses a very simple biological reaction, the reversible hydration of CO_2 to form HCO_3^- and H^+ ions. This reaction, however, is the basis for key physiological processes such as respiration, CO_2/HCO_3^- transport and overall acid-base balance.

6.1. Functional roles of CA

Throughout this thesis a number of functional roles of CA have been outlined. The widespread distribution of isoforms of the α-CA family among mammalian tissues is linked to a diversity of physiological processes as has been described in Chapter 1. In the heart, several CA isoforms have been described, and their particular spatial distribution within cardiac cells suggests specific functional roles. Intracellularly, soluble and membrane bound isoforms are expressed. CA II is present in the cytoplasm of cardiac myocytes (Alvarez *et al.*, 2006) and CA IV, CA IX, and CA XIV are expressed at the sarcoplasmic reticulum (SR) membrane (Scheibe *et al.*, 2006). SR-associated CA isozymes also display a differential spatial distribution. CA XIV is predominantly localized in the longitudinal SR, whereas CA IX is mainly expressed in the terminal SR/t-tubule region. CA IV is present in both SR regions possibly facing the SR-lumen. CA IV, CA IX, and CA XIV have been also shown to be expressed extracellularly associated to the sarcolemmal membrane.

The presence of CA in the cytosol and membranes within the cardiac myocyte suggests a role for global buffering in the cytoplasmic compartment. CA permits the CO_2/HCO_3^- system to act as a fast-reacting buffer, and thus the enzyme would play an important role in controlling the efficiency of physiological buffering even at tortuous intracellular sites, such as the invaginations of the t-system and of the SR. CA could be also relevant for H^+ mobility in ventricular myocytes and maintaining pH_i uniformity due to its role in controlling the effectiveness of the carbonic shuttle (Spitzer *et al.*, 2002; Stewart *et al.*, 1999). The presence of soluble CA activity and CA isozymes in the invaginations of the SR membrane and the t-system for example, would ensure rapid H^+-mobility preventing a rise in local $[H^+]$ and its inhibitory effects on Ca^{2+} channels and ryanodine receptors.

SR-associated CA isoforms may also be necessary for providing H^+-ions for counter-transport coupled with SR Ca^{2+} release and re-uptake by SERCA, as well as for intra-SR H^+-ion buffering (Wetzel & Gros, 2000). Thus, CA activity could be a factor that modulates excitation-contraction coupling in ventricular myocytes.

The presence of different CA extracellular isoforms also suggests relevant functional roles for these enzymes. Extracellular CA activity may play a role in increasing the availability of extracellular CO_2/HCO_3^- buffering (Vanheel *et al.*, 1986). Increased effective carbonic buffering capacity would prevent changes in sarcolemmal surface pH that could in turn affect pH_i, and consequently myocyte function. Accelerated extracellular equilibration of CO_2 and HCO_3^- is also relevant to CO_2 membrane permeation. The rapid equilibration of extracellular carbonic buffer facilitates CO_2

permeation by maintaining CO_2 gradients between the intracellular and extracellular compartments. Extracellular CA could be also relevant to substrate provision for myocyte metabolism since the extracellular hydration of CO_2 generates H^+-ions which are co-transported with lactate by MCT (Wetzel *et al.*, 2001).

Finally, intracellular and extracellular CA isoforms could be important in modulating/enhancing the activity membrane H^+ transporters such as NHE, NBC and AE as has been proposed based in evidence obtained in heterologous transfection systems (Alvarez *et al.*, 2003; Becker & Deitmer, 2007; Li *et al.*, 2002; Sterling *et al.*, 2002; Sterling *et al.*, 2001).

The aim of the present thesis has been to investigate the functional aspects of CA activity in ventricular myocytes, particularly focusing on its role membrane H^+-equivalent transport.

6.1.1. Functional bicarbonate transport metabolon in cardiac myocytes

One main finding of this work is the demonstration, for the first time, of a functional role of CA activity in H^+-equivalent transport in an intact living cell. A bicarbonate transport metabolon, involving an intracellular CA isoform and NBC is functional in cardiac myocytes. As shown in Chapter 4, CA doubles the rate of NBC-mediated transport at low and high NBC activity. Given that NBC co-transports HCO_3^- and Na^+-ions into the cell, CA is not only contributing to H^+ extrusion, but also to Na^+ influx into the myocyte. Since a rise in $[Na^+]$ is translated in to a rise in $[Ca^{2+}]$ through a

change in the driving forces of Na^+-Ca^{2+} exchange, CA would be also playing a role in modulating intracellular $[Ca^{2+}]$.

The enhancement of NBC-mediated transport by CA might thus represent a novel regulatory mechanism of NBC activity in wild-type cells.

The functional transport metabolon in cardiac myocytes, however, does not necessarily imply physical binding of CA II to NBC, as has been previously proposed. Although NBC has an intracellular binding site for the soluble cytosolic isoform, CA II, it is possible that other isoforms might also interact with the transporter in addition or instead of CA II. SR-membrane aasociated CA isoforms, such as CA IX and CA XIV, represent potential candidates for functionally interact with NBC.

In contrast to NBC, the present work has shown that NHE does not functionally interact with CA in cardiac myocytes. This suggests that although both transporters have CA II binding sites at intracellular domains, other factors, such as structural and conformational differences, may prevent the effect of CA II or other intracellular CA isoforms.

6.1.2. Inhibition of CA activity by various membrane transport inhibitors

Another important and also surprising finding of the present work is that CA showed high promiscuity towards inhibition by different pharmacological compounds. Four widely used membrane transport inhibitors also inhibit CA activity *in vitro*. The NHE inhibitor cariporide, the non-selective bicarbonate transport inhibitor DIDS, the putative NBC inhibitor S0859, and the aquaporin blocker pCMBS, all have been shown

to inhibit CA activity. This finding could have important implications in the design of selective H^+ transport inhibitors, and in general in drug design to avoid the potential side effects on acute or chronic CA inhibition.

This work points out some chemical characteristics that should be guarded against to prevent inhibition of CA activity. An insightful example is the case of NHE inhibitors. The sulphomethyl group present in cariporide, but absent in the amiloride derivatives DMA and EIPA, is likely to cause inhibition of CA activity by forming hydrogen bonds within the active site of the enzyme and disrupting critical interactions necessary for catalysis. Similarly, the N-cyanosulphonamide group in S0859, may disrupt interactions within the active site of the enzyme by hydrogen bonding to critical residues required for catalysis. Inhibition of CA by substituted sulphonamides has been previously reported. The inhibition caused by DIDS may be also due hydrogen bonding via the isothiocyanate groups in its molecule, or because of the reactivity of these with several side chain groups. In contrast to the other membrane transport inhibitors, the mercurial pCMBS may inhibit CA activity by blocking the intramolecular proton transfer requires for regenerating the active species (OH^-) at the catalytic centre of the enzyme.

These findings thus show that many membrane transport inhibitors are less selective than hitherto assumed, and that they can affect CA activity at least via two types of interaction with the catalytic mechanism of the enzyme. The potential CA-inhibitory chemical groups and their modes of interaction with the active site of the enzyme highlighted in this work will now have to be considered in drug and experimental design for improved selectivity (Figure 1).

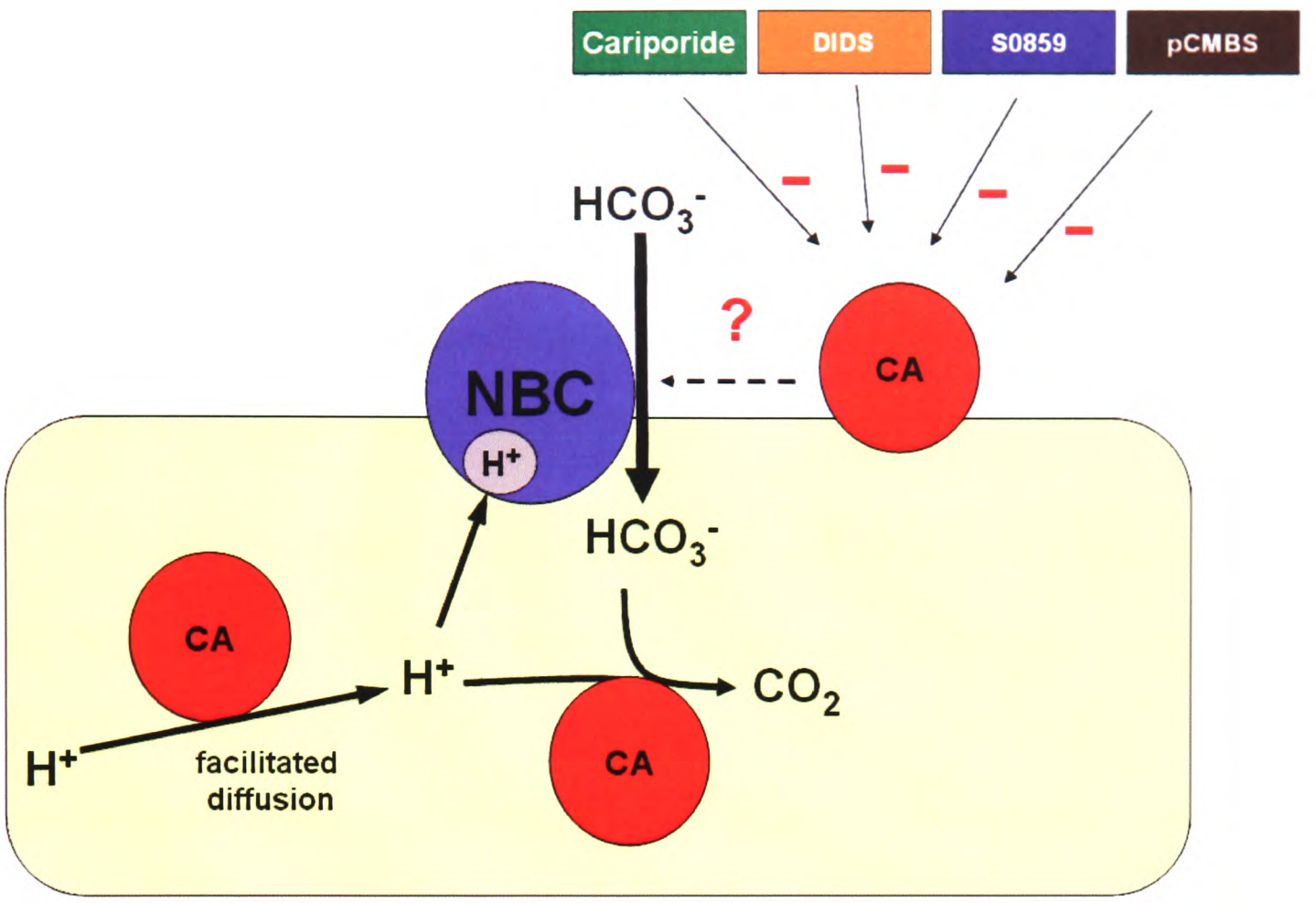

Figure 3. Potential effect of membrane transport inhibitors on extracellular CA activity. Extracellular CA isozymes are potential targets for some membrane transport inhibitors with CA-inhibitory activity. The inability of these drugs to cross the sarcolemma prevents them from interacting with intracellular CA isoforms and thus affecting CA-mediated facilitated diffusion of H^+-ions and facilitation of the activity of membrane transporters such as NBC.

6.1.3. Paradox of H^+-inhibition of CA activity

The present work also shows a paradoxical property of CA. Although the enzyme enhances many aspects of [H^+] regulation, it is, itself, *inhibited* by H^+-ions. The sigmoidal relationship of intracellular CA activity and pH shows that within the physiological pH range, CA is strongly pH sensitive. This is the first demonstration of

pH-dependence of CA activity inside a living cell. With a pK_a of 7.1, CA activity would be inhibited by 40% at resting pH_i. This suggests that CA does not operate physiologically at its "optimum pH" and thus its activity could be steeply increased or decreased by changes in pH_i. It is likely that the activity-pH relationship of intracellular CA represents the left limb of the classical bell-shaped relationship of pH-dependence of enzyme activity. This implies that besides declining at acidic pH, CA activity will be also inhibited at high non-physiological pH values.

Although the identity of the isoform/s conferring pH sensitivity is not known, it is likely that all of the isoforms present in myocytes are pH-sensitive. Several *in vitro* studies have shown that the activity of many CA isoforms, included those which are present in cardiac myocytes, such as CA II, CA IV, and CA IX is pH-dependent.

The consequences of this pH-sensitivity would be reflected for example in intracellular H^+ mobility (Figure 2A and 2B). Inhibition of CA activity by H^+ may partly explain the drop in H^+ mobility observed during intracellular acidosis in cardiac myocytes (Swietach *et al.*, 2007). The functional significance of this is not yet known, but it could be speculated that H^+-mediated decrease in CA activity and H^+ mobility might represent a mechanism to prevent spread of damaging acidosis to neighboring cells.

A.

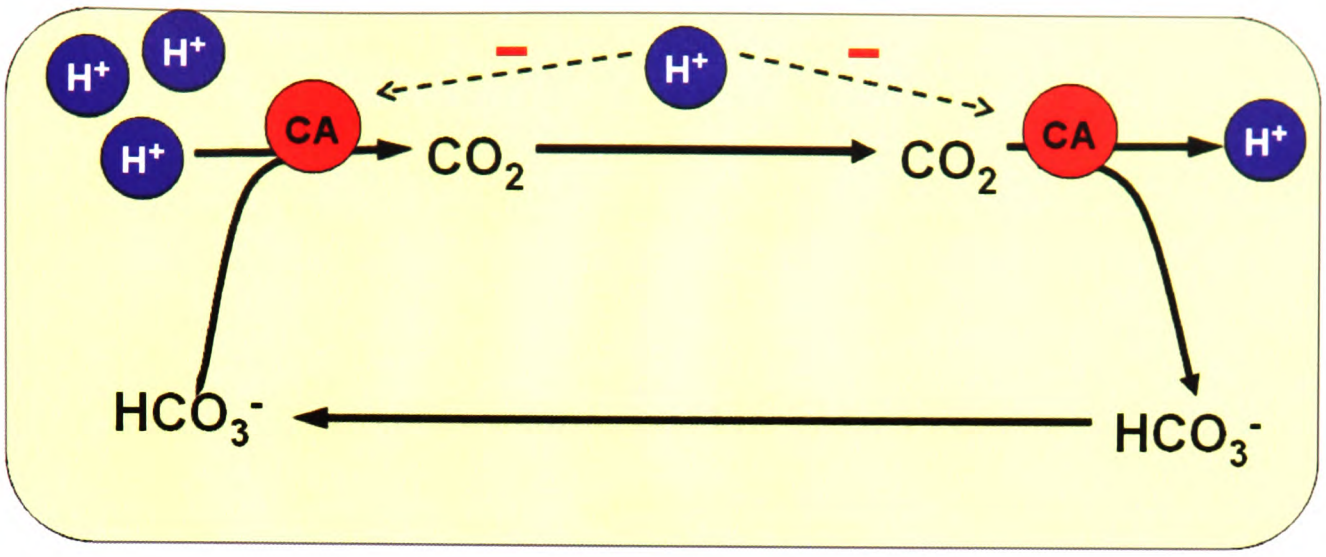

B.

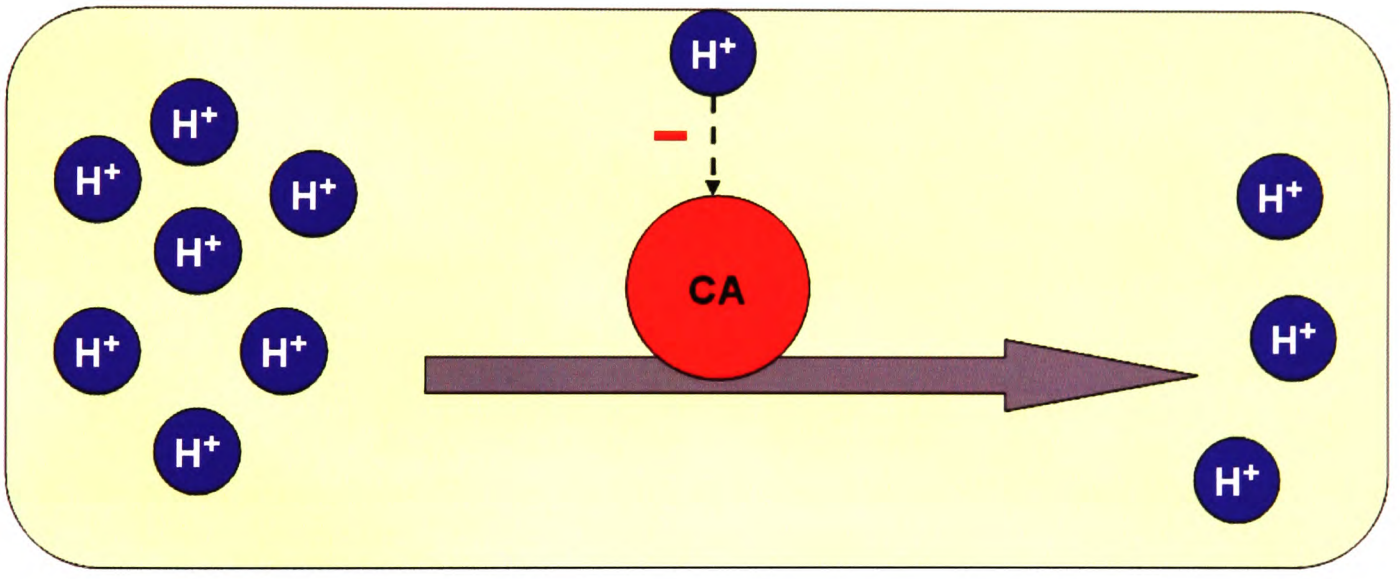

Figure 2. Effect of the pH-dependence of CA activity on H^+-mobility. A rise in intracellular [H^+] will inhibit CA activity and therefore decrease H^+-mobility through the carbonic shuttle (Panel A). The functional consequence is illustrated in Panel B; H^+-mobility is controlled by H^+-ions via CA.

The pH-dependence of CA activity may also influence the modulatory effect that the enzyme exerts on NBC activity. Given that the fractional contribution of CA to NBC activity is constant over a wide pH_i range, it is possible that the changes in the magnitude of the CA-mediated enhancement of NBC activity, consequence of the effects of pH_i on CA, may be obscured by H^+ stimulation of NBC-mediated transport (Figure 3).

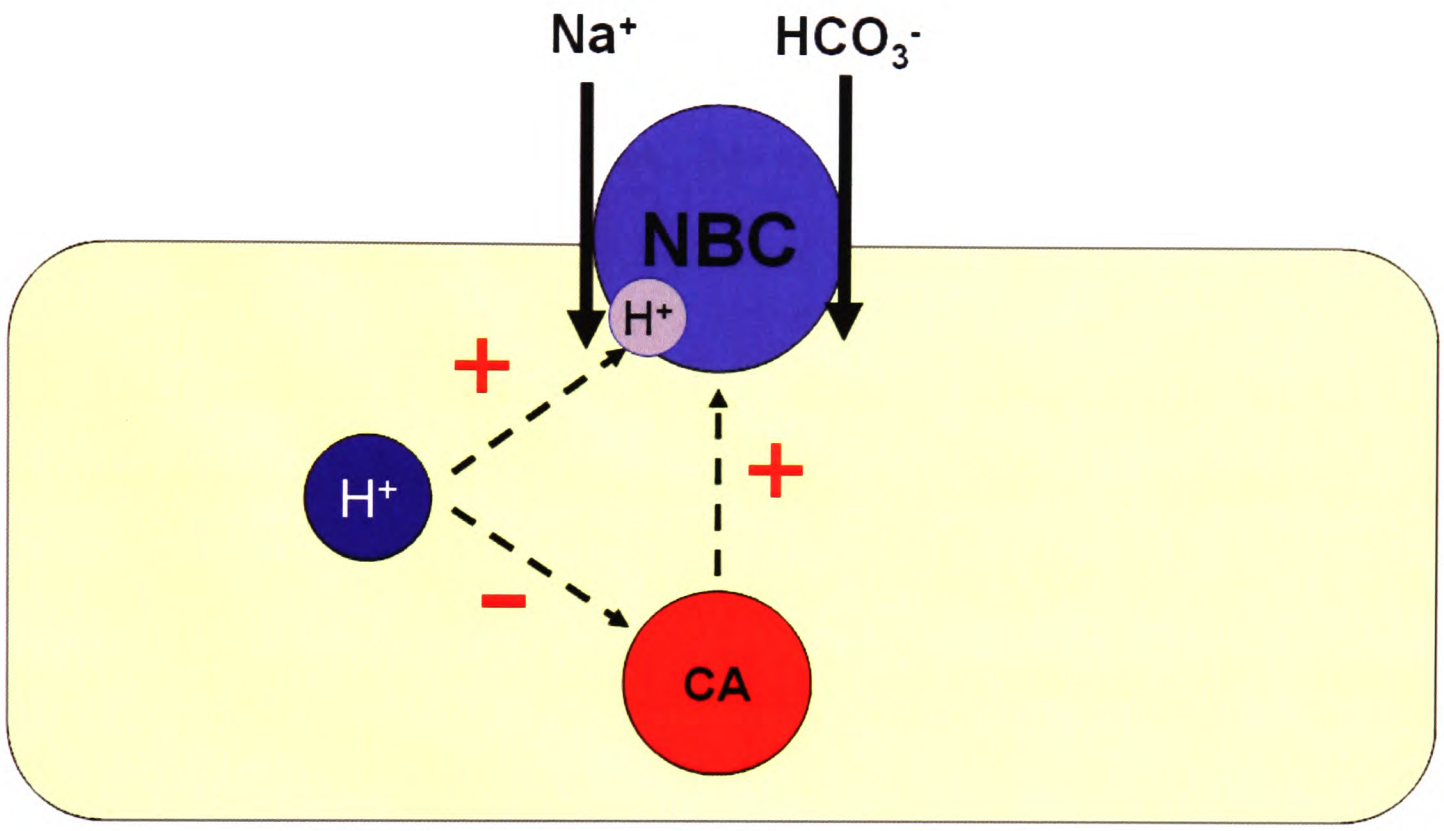

Figure 3. Effect of intracellular H^+-ions on NBC and CA. Intracellular H^+-ions stimulate NBC but at the same time inhibit CA activity. Thus, the expected modulation of NBC-mediated transport by CA due to changes in pH_i, might be obscured by a stronger influence of H^+-ions directly on NBC.

6.2. Conclusion

The present thesis has extended our understanding of the functional role of CA in cardiac myocytes by demonstrating for the first time, the functional coupling of CA and a membrane H^+-equivalent transport protein. The work also demonstrated that intracellular CA activity is strongly pH_i sensitive within the physiological range which may have important functional consequences for myocyte function. The novel finding of pharmacological inhibition of CA by various membrane transport inhibitors may have important implications for experimental and drug design in order to avoid secondary inhibition of the enzyme, and its acute and chronic effects.

The findings of the present work raise important questions on other roles of CA such as its functional effect on Ca^{2+}-signaling and regulation of contractility in cardiac myocytes, and also on the possible modulation of this effect by global and local disturbances in $[H^+]$. These questions will be experimentally addressed in future work.

References

ABBATE, F., COETZEE, A., CASINI, A., CIATTINI, S., SCOZZAFAVA, A. & SUPURAN, C.T. (2004a). Carbonic anhydrase inhibitors: X-ray crystallographic structure of the adduct of human isozyme II with the antipsychotic drug sulpiride. *Bioorg Med Chem Lett*, 14, 337-41.

ABBATE, F., WINUM, J.Y., POTTER, B.V., CASINI, A., MONTERO, J.L., SCOZZAFAVA, A. & SUPURAN, C.T. (2004b). Carbonic anhydrase inhibitors: X-ray crystallographic structure of the adduct of human isozyme II with EMATE, a dual inhibitor of carbonic anhydrases and steroid sulfatase. *Bioorg Med Chem Lett*, 14, 231-4.

ABULADZE, N., LEE, I., NEWMAN, D., HWANG, J., BOORER, K., PUSHKIN, A. & KURTZ, I. (1998). Molecular cloning, chromosomal localization, tissue distribution, and functional expression of the human pancreatic sodium bicarbonate cotransporter. *J Biol Chem*, 273, 17689-95.

ABULADZE, N., SONG, M., PUSHKIN, A., NEWMAN, D., LEE, I., NICHOLAS, S. & KURTZ, I. (2000). Structural organization of the human NBC1 gene: kNBC1 is transcribed from an alternative promoter in intron 3. *Gene*, 251, 109-22.

AHARONOVITZ, O., DEMAUREX, N., WOODSIDE, M. & GRINSTEIN, S. (1999). ATP dependence is not an intrinsic property of Na^+/H^+ exchanger NHE1: requirement for an ancillary factor. *Am J Physiol*, 276, C1303-11.

AIELLO, E.A., PETROFF, M.G., MATTIAZZI, A.R. & CINGOLANI, H.E. (1998). Evidence for an electrogenic Na^+-HCO_3^- symport in rat cardiac myocytes. *J Physiol*, 512 (Pt 1), 137-48.

AKIBA, T., ALPERN, R.J., EVELOFF, J., CALAMINA, J. & WARNOCK, D.G. (1986). Electrogenic sodium/bicarbonate cotransport in rabbit renal cortical basolateral membrane vesicles. *J Clin Invest*, 78, 1472-8.

AKIBA, T., ROCCO, V.K. & WARNOCK, D.G. (1987). Parallel adaptation of the rabbit renal cortical sodium/proton antiporter and sodium/bicarbonate cotransporter in metabolic acidosis and alkalosis. *J Clin Invest*, 80, 308-15.

ALEXANDER, R.S., KIEFER, L.L., FIERKE, C.A. & CHRISTIANSON, D.W. (1993). Engineering the zinc binding site of human carbonic anhydrase II: structure of the His-94-->Cys apoenzyme in a new crystalline form. *Biochemistry*, 32, 1510-8.

ALLEN, D.G. & ORCHARD, C.H. (1983). The effects of changes of pH on intracellular calcium transients in mammalian cardiac muscle. *J Physiol*, 335, 555-67.

ALPERN, R.J. (1990). Cell mechanisms of proximal tubule acidification. *Physiol Rev*, 70, 79-114.

ALVAREZ, B.V., JOHNSON, D.E., SOWAH, D., SOLIMAN, D., LIGHT, P.E., XIA, Y., KARMAZYN, M. & CASEY, J.R. (2006). Carbonic Anhydrase Inhibition Prevents and Reverts Cardiomyocyte Hypertrophy. *J Physiol*.

ALVAREZ, B.V., LOISELLE, F.B., SUPURAN, C.T., SCHWARTZ, G.J. & CASEY, J.R. (2003). Direct extracellular interaction between carbonic anhydrase IV and the human NBC1 sodium/bicarbonate co-transporter. *Biochemistry*, 42, 12321-9.

ALVAREZ, B.V., VILAS, G.L. & CASEY, J.R. (2005). Metabolon disruption: a mechanism that regulates bicarbonate transport. *Embo J*, 24, 2499-511.

ANDRES, V., CARRERAS, J. & CUSSO, R. (1990). Regulation of muscle phosphofructokinase by physiological concentrations of bisphosphorylated hexoses: effect of alkalinization. *Biochem Biophys Res Commun*, 172, 328-34.

ANTCLIFF, A.C., BEEVERS, D.G., HAMILTON, M. & HARPUR, J.E. (1971). The use of amiloride hydrochloride in the correction of hypokalaemic alkalosis induced by diuretics. *Postgrad Med J*, 47, 644-7.

ARMSTRONG, J.M., MYERS, D.V., VERPOORTE, J.A. & EDSALL, J.T. (1966). Purification and properties of human erythrocyte carbonic anhydrases. *J Biol Chem*, 241, 5137-49.

ARONSON, P.S. (1985). Kinetic properties of the plasma membrane Na^+-H^+ exchanger. *Annu Rev Physiol*, 47, 545-60.

ARONSON, P.S., SUHM, M.A. & NEE, J. (1983). Interaction of external H^+ with the Na^+-H^+ exchanger in renal microvillus membrane vesicles. *J Biol Chem*, 258, 6767-71.

ATTAPHITAYA, S., PARK, K. & MELVIN, J.E. (1999). Molecular cloning and functional expression of a rat Na^+/H^+ exchanger (NHE5) highly expressed in brain. *J Biol Chem*, 274, 4383-8.

AVKIRAN, M. & MARBER, M.S. (2002). Na^+/H^+ exchange inhibitors for cardioprotective therapy: progress, problems and prospects. *J Am Coll Cardiol*, 39, 747-53.

BAETZ, D., HAWORTH, R.S., AVKIRAN, M. & FEUVRAY, D. (2002). The ERK pathway regulates Na^+-HCO_3^- cotransport activity in adult rat cardiomyocytes. *Am J Physiol Heart Circ Physiol*, 283, H2102-9.

BAGNIS, C., MARSOLAIS, M., BIEMESDERFER, D., LAPRADE, R. & BRETON, S. (2001). Na^+/H^+-exchange activity and immunolocalization of NHE3 in rat epididymis. *Am J Physiol Renal Physiol*, 280, F426-36.

BAIRD, N.R., ORLOWSKI, J., SZABO, E.Z., ZAUN, H.C., SCHULTHEIS, P.J., MENON, A.G. & SHULL, G.E. (1999). Molecular cloning, genomic organization, and functional expression of Na^+/H^+ exchanger isoform 5 (NHE5) from human brain. *J Biol Chem*, 274, 4377-82.

BAIRD, T.T., JR., WAHEED, A., OKUYAMA, T., SLY, W.S. & FIERKE, C.A. (1997). Catalysis and inhibition of human carbonic anhydrase IV. *Biochemistry*, 36, 2669-78.

BALNAVE, C.D. & VAUGHAN-JONES, R.D. (2000). Effect of intracellular pH on spontaneous Ca^{2+} sparks in rat ventricular myocytes. *J Physiol*, 528 Pt 1, 25-37.

BAUMGARTH, M., BEIER, N. & GERICKE, R. (1997). (2-Methyl-5-(methylsulfonyl)benzoyl)guanidine Na^+/H^+ antiporter inhibitors. *J Med Chem*, 40, 2017-34.

BEAR, C.E., DAVISON, J.S. & SHAFFER, E.A. (1988). Intracellular pH influences the resting membrane potential of isolated rat hepatocytes. *Biochim Biophys Acta*, 944, 113-20.

BECKER, H.M. & DEITMER, J.W. (2007). Carbonic anhydrase II increases the activity of the human electrogenic Na^+/HCO_3^- cotransporter. *J Biol Chem*, 282, 13508-21.

BECKER, H.M., HIRNET, D., FECHER-TROST, C., SULTEMEYER, D. & DEITMER, J.W. (2005). Transport Activity of MCT1 Expressed in Xenopus Oocytes Is Increased by Interaction with Carbonic Anhydrase. *J Biol Chem*, 280, 39882-9.

BERTINI, I. & LUCHINAT, C. (1983). Cobalt(II) as a probe of the structure and function of carbonic anhydrase. *Accounts of Chemical Research*, 16, 272-279.

BERTRAND, B., WAKABAYASHI, S., IKEDA, T., POUYSSEGUR, J. & SHIGEKAWA, M. (1994). The Na^+/H^+ exchanger isoform 1 (NHE1) is a novel member of the calmodulin-binding proteins. Identification and characterization of calmodulin-binding sites. *J Biol Chem*, 269, 13703-9.

BESTERMAN, J.M., MAY, W.S., JR., LEVINE, H., 3RD, CRAGOE, E.J., JR. & CUATRECASAS, P. (1985). Amiloride inhibits phorbol ester-stimulated Na^+/H^+ exchange and protein kinase C. An amiloride analog selectively inhibits Na^+/H^+ exchange. *J Biol Chem*, 260, 1155-9.

BEVENSEE, M.O., BASHI, E., SCHLUE, W.R., BOYARSKY, G. & BORON, W.F. (1999). Shrinkage-induced activation of Na^+/H^+ exchange in rat renal mesangial cells. *Am J Physiol*, 276, C674-83.

BEVENSEE, M.O., SCHMITT, B.M., CHOI, I., ROMERO, M.F. & BORON, W.F. (2000). An electrogenic Na^+-HCO_3^- cotransporter (NBC) with a novel COOH-terminus, cloned from rat brain. *Am J Physiol Cell Physiol*, 278, C1200-11.

BIALER, M., JOHANNESSEN, S.I., KUPFERBERG, H.J., LEVY, R.H., LOISEAU, P. & PERUCCA, E. (1999). Progress report on new antiepileptic drugs: a summary of the fourth Eilat conference (EILAT IV). *Epilepsy Res*, 34, 1-41.

BIANCHINI, L., L'ALLEMAIN, G. & POUYSSEGUR, J. (1997). The p42/p44 mitogen-activated protein kinase cascade is determinant in mediating activation of the Na^+/H^+ exchanger (NHE1 isoform) in response to growth factors. *J Biol Chem*, 272, 271-9.

BICKLING, J.E., MASON, J.W., WOLTERSDORFF, O.W., JONES, J.H., KWON, S.F., ROBB, C.M. & CRAGOE, E.J. (1965). Pyrazine diuretic.I. N-amidino-3-amino-6-halopyrazine-carboxamides. *Journal of Medical Chemistry* 8, 638-642.

BLANCHARD, E.M., PAN, B.S. & SOLARO, R.J. (1984). The effect of acidic pH on the ATPase activity and troponin Ca^{2+} binding of rabbit skeletal myofilaments. *J Biol Chem*, 259, 3181-6.

BLANCHARD, E.M. & SOLARO, R.J. (1984). Inhibition of the activation and troponin calcium binding of dog cardiac myofibrils by acidic pH. *Circ Res*, 55, 382-91.

BLATZ, A.L. (1984). Asymmetric proton block of inward rectifier K^+ channels in skeletal muscle. *Pflugers Arch*, 401, 402-7.

BOCK, P.E. & FRIEDEN, C. (1976a). Phosphofructokinase. I. Mechanism of the pH-dependent inactivation and reactivation of the rabbit muscle enzyme. *J Biol Chem*, 251, 5630-6.

BOCK, P.E. & FRIEDEN, C. (1976b). Phosphofructokinase. II. Role of ligands in pH-dependent structural changes of the rabbit muscle enzyme. *J Biol Chem*, 251, 5637-43.

BORON, W.F. & BOULPAEP, E.L. (1983). Intracellular pH regulation in the renal proximal tubule of the salamander. Basolateral HCO_3^- transport. *J Gen Physiol*, 81, 53-94.

BOUNTRA, C., KAILA, K. & VAUGHAN-JONES, R.D. (1988). Effect of repetitive activity upon intracellular pH, sodium and contraction in sheep cardiac Purkinje fibres. *J Physiol*, 398, 341-60.

BRETT, C.L., DONOWITZ, M. & RAO, R. (2005). Evolutionary origins of eukaryotic sodium/proton exchangers. *Am J Physiol Cell Physiol*, 288, C223-39.

BRETT, C.L., WEI, Y., DONOWITZ, M. & RAO, R. (2002). Human Na^+/H^+ exchanger isoform 6 is found in recycling endosomes of cells, not in mitochondria. *Am J Physiol Cell Physiol*, 282, C1031-41.

BRIGANTI, F., MANGANI, S., SCOZZAFAVA, A., VERNAGLIONE, G. & SUPURAN, C.T. (1999). Carbonic anhydrase catalyzes cyanamide hydration to urea: is it mimicking the physiological reaction? *J Biol Inorg Chem*, 4, 528-36.

BRUNE, T., FETZER, S., BACKUS, K.H. & DEITMER, J.W. (1994). Evidence for electrogenic sodium-bicarbonate cotransport in cultured rat cerebellar astrocytes. *Pflugers Arch*, 429, 64-71.

BRUNS, W. & GROS, G. (1992). Membrane-bound carbonic anhydrase in the heart. *Am J Physiol*, 262, H577-84.

BUCKLER, K.J. & VAUGHAN-JONES, R.D. (1990). Application of a new pH-sensitive fluoroprobe (carboxy-SNARF-1) for intracellular pH measurement in small, isolated cells. *Pflugers Arch*, 417, 234-9.

BURNHAM, C.E., AMLAL, H., WANG, Z., SHULL, G.E. & SOLEIMANI, M. (1997). Cloning and functional expression of a human kidney Na^+:HCO_3^- cotransporter. *J Biol Chem*, 272, 19111-4.

BUSA, W.B. & NUCCITELLI, R. (1984). Metabolic regulation via intracellular pH. *Am J Physiol*, 246, R409-38.

BUTLER, T.L., AU, C.G., YANG, B., EGAN, J.R., TAN, Y.M., HARDEMAN, E.C., NORTH, K.N., VERKMAN, A.S. & WINLAW, D.S. (2006). Cardiac aquaporin expression in humans, rats, and mice. *Am J Physiol Heart Circ Physiol*, 291, H705-13.

CABANTCHIK, Z.I. & GREGER, R. (1992). Chemical probes for anion transporters of mammalian cell membranes. *Am J Physiol*, 262, C803-27.

CASINI, A., ANTEL, J., ABBATE, F., SCOZZAFAVA, A., DAVID, S., WALDECK, H., SCHAFER, S. & SUPURAN, C.T. (2003). Carbonic anhydrase inhibitors: SAR and X-ray crystallographic study for the interaction of sugar sulfamates/sulfamides with isozymes I, II and IV. *Bioorg Med Chem Lett*, 13, 841-5.

CH'EN, F.F., DILWORTH, E., SWIETACH, P., GODDARD, R.S. & VAUGHAN-JONES, R.D. (2003). Temperature dependence of Na^+-H^+ exchange, Na^+-HCO_3^- co-transport, intracellular buffering and intracellular pH in guinea-pig ventricular myocytes. *J Physiol*, 552, 715-26.

CH'EN, F.T. & VAUGHAN-JONES, R.D. (2001). Na^+-HCO_3^- cotransport is instructed by pH and not bicarbonate or Na^+. *Biophys J*, 80, 74 (Abstract).

CH'EN, F.T., VILLAFUERTE, F.C., SWIETACH, P., COBDEN, P.M., KLEEMAN, H.W. & VAUGHAN-JONES, R.D. (2008). S0859, an N-Cyanosulphonamide inhibitor of sodium-bicarbonate co-transport in the heart *Br. J. Pharm. 2008 Jan 21; [Epub ahead of print]. PMID: 18204485*

CHEGWIDDEN, W., DODGSON, S. & SPENCER, I. (2000). The roles of carbonic anhydrase in metabolism, cell growth and cancer in animals. In *The Carbonic Anhydrases: New Horizons*. eds Chegwidden, W., Edwards, Y. & Carter, N. Basel: Birkhauser Verlag.

CHEGWIDDEN, W.R. & CARTER, N.D. (2000). Introduction to the carbonic anhydrases. In *The Carbonic Anhydrases: New Horizons*. eds Chegwidden, W.R., Carter, N.D. & Edwards, Y.H. pp. 13-27. Basel/Switzerland: Birkhauser Verlag.

CHOI, H.S., TRAFFORD, A.W., ORCHARD, C.H. & EISNER, D.A. (2000a). The effect of acidosis on systolic Ca^{2+} and sarcoplasmic reticulum calcium content in isolated rat ventricular myocytes. *J Physiol*, 529 Pt 3, 661-8.

CHOI, I., AALKJAER, C., BOULPAEP, E.L. & BORON, W.F. (2000b). An electroneutral sodium/bicarbonate cotransporter NBCn1 and associated sodium channel. *Nature*, 405, 571-5.

CHOI, I., ROMERO, M.F., KHANDOUDI, N., BRIL, A. & BORON, W.F. (1999). Cloning and characterization of a human electrogenic Na^+-HCO_3^- cotransporter isoform (hhNBC). *Am J Physiol*, 276, C576-84.

CHRISTIANSON, D.W. & ALEXANDER, R.S. (1989). Carboxylate-histidine-zinc interactions in protein structure and function. *J Am Chem Soc*, 111, 6412-6419.

CHRISTIANSON, D.W. & FIERKE, C.A. (1996). Carbonic anhydrase: evolution of the zinc binding site by nature and by design. *Accounts of Chemical Research*, 29, 331-339.

CLEMENTS-JEWERY, H., SUTHERLAND, F.J., ALLEN, M.C., TRACEY, W.R. & AVKIRAN, M. (2004). Cardioprotective efficacy of zoniporide, a potent and selective inhibitor of Na^+/H^+ exchanger isoform 1, in an experimental model of cardiopulmonary bypass. *Br J Pharmacol*, 142, 57-66.

COHEN, J.P., HOFFER, A.P. & ROSEN, S. (1976). Carbonic anhydrase localization in the epidimymis and testis of the rat: histochemical and biochemical analysis. *Biol Reprod*, 14, 339-46.

COLEMAN, J.E. (1975). Chemical reactions of sulfonamides with carbonic anhydrase. *Annu Rev Pharmacol*, 15, 221-42.

COOPER, G.J. & BORON, W.F. (1998). Effect of PCMBS on CO_2 permeability of Xenopus oocytes expressing aquaporin 1 or its C189S mutant. *Am J Physiol*, 275, C1481-6.

COOPER, G.J., ZHOU, Y., BOUYER, P., GRICHTCHENKO, II & BORON, W.F. (2002). Transport of volatile solutes through AQP1. *J Physiol*, 542, 17-29.

COUNILLON, L. & POUYSSEGUR, J. (2000). The expanding family of eucaryotic Na^+/H^+ exchangers. *J Biol Chem*, 275, 1-4.

COUNILLON, L., SCHOLZ, W., LANG, H.J. & POUYSSEGUR, J. (1993). Pharmacological characterization of stably transfected Na^+/H^+ antiporter isoforms using amiloride analogs and a new inhibitor exhibiting anti-ischemic properties. *Mol Pharmacol*, 44, 1041-5.

DART, C. & VAUGHAN-JONES, R.D. (1992). Na^+-HCO_3^- symport in the sheep cardiac Purkinje fibre. *J Physiol*, 451, 365-85.

DE BRABANDER, M., GEUENS, G., NUYDENS, R., WILLEBRORDS, R. & DE MEY, J. (1982). Microtubule stability and assembly in living cells: the influence of metabolic inhibitors, taxol and pH. *Cold Spring Harb Symp Quant Biol*, 46 Pt 1, 227-40.

DEITMER, J.W. (1991). Electrogenic sodium-dependent bicarbonate secretion by glial cells of the leech central nervous system. *J Gen Physiol*, 98, 637-55.

DEITMER, J.W. & SCHLUE, W.R. (1989). An inwardly directed electrogenic sodium-bicarbonate co-transport in leech glial cells. *J Physiol*, 411, 179-94.

DEITMER, J.W. & SCHNEIDER, H.P. (1998). Acid/base transport across the leech giant glial cell membrane at low external bicarbonate concentration. *J Physiol*, 512 (Pt 2), 459-69.

DILWORTH, E.L., SWIETACH, P. & VAUGHAN-JONES, R.D. (2006). Local control of ventricular Ca^{2+}-signalling by intracellular pH. *Biophysical Society 50th Annual Meeting 2006*, 1552.

DOBSON, G.P., YAMAMOTO, E. & HOCHACHKA, P.W. (1986). Phosphofructokinase control in muscle: nature and reversal of pH-dependent ATP inhibition. *Am J Physiol*, 250, R71-6.

DODGSON, S. (1991). Liver Mitochondrial carbonic anhydrase (CA V), gluconeogenesis, and ureagenesis in the hepatocyte. In *The Carbonic Anhydrases: Cellular Physiology and Molecular Genetics*. eds Dodgson, S., Tashian, R., Gros, G. & Carter, N. pp. 297-306. London: Plenum Press.

DODGSON, S.J. (1987). Inhibition of mitochondrial carbonic anhydrase and ureagenesis: a discrepancy examined. *J Appl Physiol*, 63, 2134-41.

DODGSON, S.J. & CHERIAN, K. (1989). Mitochondrial carbonic anhydrase is involved in rat renal glucose synthesis. *Am J Physiol*, 257, E791-6.

DODGSON, S.J. & FORSTER, R.E., 2ND (1986a). Carbonic anhydrase: inhibition results in decreased urea production by hepatocytes. *J Appl Physiol*, 60, 646-52.

DODGSON, S.J. & FORSTER, R.E., 2ND (1986b). Inhibition of CA V decreases glucose synthesis from pyruvate. *Arch Biochem Biophys*, 251, 198-204.

DODGSON, S.J., FORSTER, R.E., 2ND, SCHWED, D.A. & STOREY, B.T. (1983). Contribution of matrix carbonic anhydrase to citrulline synthesis in isolated guinea pig liver mitochondria. *J Biol Chem*, 258, 7696-701.

DODGSON, S.J., FORSTER, R.E., 2ND & STOREY, B.T. (1984). The role of carbonic anhydrase in hepatocyte metabolism. *Ann N Y Acad Sci*, 429, 516-24.

DODGSON, S.J., QUISTORFF, B. & RIDDERSTRALE, Y. (1993). Carbonic anhydrases in cytosol, nucleus, and membranes of rat liver. *J Appl Physiol*, 75, 1186-93.

DODGSON, S.J., SHANK, R.P. & MARYANOFF, B.E. (2000). Topiramate as an inhibitor of carbonic anhydrase isoenzymes. *Epilepsia*, 41 Suppl 1, S35-9.

DONALDSON, T.L. & QUINN, J.A. (1974). Kinetic constants determined from membrane transport measurements: carbonic anhydrase activity at high concentrations. *Proc Natl Acad Sci U S A*, 71, 4995-9.

DORAI, T., SAWCZUK, I.S., PASTOREK, J., WIERNIK, P.H. & DUTCHER, J.P. (2005). The role of carbonic anhydrase IX overexpression in kidney cancer. *Eur J Cancer*, 41, 2935-47.

EIAM-ONG, S., HILDEN, S.A., KING, A.J., JOHNS, C.A. & MADIAS, N.E. (1992). Endothelin-1 stimulates the Na^+/H^+ and Na^+/HCO_3^- transporters in rabbit renal cortex. *Kidney Int*, 42, 18-24.

ELADARI, D., BLANCHARD, A., LEVIEL, F., PAILLARD, M., STUART-TILLEY, A.K., ALPER, S.L. & PODEVIN, R.A. (1998). Functional and molecular characterization of luminal and basolateral Cl^-/HCO_3^- exchangers of rat thick limbs. *Am J Physiol*, 275, F334-42.

ELLIOTT, A.C., SMITH, G.L. & ALLEN, D.G. (1994). The metabolic consequences of an increase in the frequency of stimulation in isolated ferret hearts. *J Physiol*, 474, 147-59.

ELLIS, D. & THOMAS, R.C. (1976). Microelectrode measurement of the intracellular pH of mammalian heart cells. *Nature*, 262, 224-5.

ENDEWARD, V., MUSA-AZIZ, R., COOPER, G.J., CHEN, L.M., PELLETIER, M.F., VIRKKI, L.V., SUPURAN, C.T., KING, L.S., BORON, W.F. & GROS, G. (2006). Evidence that aquaporin 1 is a major pathway for CO_2 transport across the human erythrocyte membrane. *Faseb J*, 20, 1974-81.

ENGBERG, P. & LINDSKOG, S. (1984). Effects of pH and inhibitors on the absorption spectrum of cobalt(II)-substituted carbonic anhydrase III from bovine skeletal muscle. *FEBS Lett*, 170, 326-30.

ERECINSKA, M., DEAS, J. & SILVER, I.A. (1995). The effect of pH on glycolysis and phosphofructokinase activity in cultured cells and synaptosomes. *J Neurochem*, 65, 2765-72.

ERIKSSON, A.E., KYLSTEN, P.M., JONES, T.A. & LILJAS, A. (1988). Crystallographic studies of inhibitor binding sites in human carbonic anhydrase II: a pentacoordinated binding of the SCN^- ion to the zinc at high pH. *Proteins*, 4, 283-93.

ERIKSSON, A.E. & LILJAS, A. (1991). X-Ray crystallographic studies of carbonic anhydrase isozymes I, II and III. In *The carbonic anhydrases: cellular physiology and molecular genetics*. eds Dodgson, S., Tashian, R., Gros, G. & Carter, N. pp. 33-48. New York: Plenum Press.

FABIATO, A. & FABIATO, F. (1978). Effects of pH on the myofilaments and the sarcoplasmic reticulum of skinned cells from cardiace and skeletal muscles. *J Physiol*, 276, 233-55.

FLEMING, R.E., PARKKILA, S., PARKKILA, A.K., RAJANIEMI, H., WAHEED, A. & SLY, W.S. (1995). Carbonic anhydrase IV expression in rat and human gastrointestinal tract regional, cellular, and subcellular localization. *J Clin Invest*, 96, 2907-13.

FLIEGEL, L. & FROHLICH, O. (1993). The Na^+/H^+ exchanger: an update on structure, regulation and cardiac physiology. *Biochem J*, 296 (Pt 2), 273-85.

FORSTER, R.E. (1991). Methods for the measurement of carbonic anhydrase activity. In *The Carbonic Anhydrases: Cellular Physiology and Molecular Genetics*. eds Dodgson, S., Tashian, R., Gros, G. & Carter, N. pp. 79-97. London: Plenum Press.

FORSTER, R.E. (1969). The rate of CO_2 equilibrium between red cells and plasma. In *CO_2: Chemical, Biological, and Physiological Aspects*. eds Forster, R.E., Edsall, J.T., Otis, A.B. & Roughton, F. pp. 275-286. Washington: NASA SP-188.

FORSTER, R.E., 2ND, DODGSON, S.J., STOREY, B.T. & LIN, L. (1984). Measurement of carbonic anhydrase activity inside cells and subcellular particles. *Ann N Y Acad Sci*, 429, 415-29.

FRANCIS, D., STERGIOPOULOS, K., EK-VITORIN, J.F., CAO, F.L., TAFFET, S.M. & DELMAR, M. (1999). Connexin diversity and gap junction regulation by pH_i. *Dev Genet*, 24, 123-36.

FUJIKAWA-ADACHI, K., NISHIMORI, I., TAGUCHI, T. & ONISHI, S. (1999). Human mitochondrial carbonic anhydrase VB. cDNA cloning, mRNA expression, subcellular localization, and mapping to chromosome x. *J Biol Chem*, 274, 21228-33.

GEERS, C. & GROS, G. (2000). Carbon dioxide transport and carbonic anhydrase in blood and muscle. *Physiol Rev*, 80, 681-715.

GEERS, C., KRUGER, D., SIFFERT, W., SCHMID, A., BRUNS, W. & GRO, G. (1992). Carbonic anhydrase in skeletal and cardiac muscle from rabbit and rat. *Biochem J*, 282 (Pt 1), 165-71.

GEVANTMAN, L.H. (1995). Solubility of Selected Gases in Water. In *CRC Handbook of Chemistry and Physics*. eds Lide, D.R. & Frederikse, H.P.R. New York: CRC Press.

GOSS, G.G., WOODSIDE, M., WAKABAYASHI, S., POUYSSEGUR, J., WADDELL, T., DOWNEY, G.P. & GRINSTEIN, S. (1994). ATP dependence of NHE-1, the ubiquitous isoform of the Na^+/H^+ antiporter. Analysis of phosphorylation and subcellular localization. *J Biol Chem*, 269, 8741-8.

GOYAL, H.O., FERGUSON, J.G. & HRUDKA, F. (1980). Histochemical activity of carbonic anhydrase in testicular and excurrent ducts of immature, mature intact and androgen-deprived bulls. *Biol Reprod*, 22, 991-7.

GREEN, J., YAMAGUCHI, D.T., KLEEMAN, C.R. & MUALLEM, S. (1988). Cytosolic pH regulation in osteoblasts. Interaction of Na^+ and H^+ with the extracellular and intracellular faces of the Na^+/H^+ exchanger. *J Gen Physiol*, 92, 239-61.

GRESZ, V., KWON, T.H., VORUM, H., ZELLES, T., KURTZ, I., STEWARD, M.C., AALKJAER, C. & NIELSEN, S. (2002). Immunolocalization of electroneutral Na^+-HCO_3^- cotransporters in human and rat salivary glands. *Am J Physiol Gastrointest Liver Physiol*, 283, G473-80.

GRICHTCHENKO, II, ROMERO, M.F. & BORON, W.F. (2000). Extracellular HCO_3^- dependence of electrogenic Na^+/HCO_3^- cotransporters cloned from salamander and rat kidney. *J Gen Physiol*, 115, 533-46.

GRINSTEIN, S., COHEN, S. & ROTHSTEIN, A. (1984). Cytoplasmic pH regulation in thymic lymphocytes by an amiloride-sensitive Na^+/H^+ antiport. *J Gen Physiol*, 83, 341-69.

GRINSTEIN, S. & FURUYA, W. (1986). Characterization of the amiloride-sensitive Na^+-H^+ antiport of human neutrophils. *Am J Physiol*, 250, C283-91.

GRINSTEIN, S., WOODSIDE, M., SARDET, C., POUYSSEGUR, J. & ROTIN, D. (1992). Activation of the Na^+/H^+ antiporter during cell volume regulation. Evidence for a phosphorylation-independent mechanism. *J Biol Chem*, 267, 23823-8.

GROSS, E., PUSHKIN, A., ABULADZE, N., FEDOTOFF, O. & KURTZ, I. (2002). Regulation of the sodium bicarbonate cotransporter kNBC1 function: role of Asp(986), Asp(988) and kNBC1-carbonic anhydrase II binding. *J Physiol*, 544, 679-85.

GUMINA, R.J., BUERGER, E., EICKMEIER, C., MOORE, J., DAEMMGEN, J. & GROSS, G.J. (1999). Inhibition of the Na^+/H^+ exchanger confers greater cardioprotection against 90 minutes of myocardial ischemia than ischemic preconditioning in dogs. *Circulation*, 100, 2519-26; discussion 2469-72.

GUZMAN-PEREZ, A., WESTER, R.T., ALLEN, M.C., BROWN, J.A., BUCHHOLZ, A.R., COOK, E.R., DAY, W.W., HAMANAKA, E.S., KENNEDY, S.P., KNIGHT, D.R., KOWALCZYK, P.J., MARALA, R.B., MULARSKI, C.J., NOVOMISLE, W.A., RUGGERI, R.B., TRACEY, W.R. & HILL, R.J. (2001). Discovery of zoniporide: a potent and selective sodium-hydrogen exchanger type 1 (NHE-1) inhibitor with high aqueous solubility. *Bioorg Med Chem Lett*, 11, 803-7.

HACKETT, P.H. & ROACH, R.C. (2001). High-altitude illness. *N Engl J Med*, 345, 107-14.

HAKANSSON, K., CARLSSON, M., SVENSSON, L.A. & LILJAS, A. (1992). Structure of native and apo carbonic anhydrase II and structure of some of its anion-ligand complexes. *J Mol Biol*, 227, 1192-204.

HALESTRAP, A.P., WANG, X., POOLE, R.C., JACKSON, V.N. & PRICE, N.T. (1997). Lactate transport in heart in relation to myocardial ischemia. *Am J Cardiol*, 80, 17A-25A.

HAUGLAND, R.P. (2002). pH Indicators. In *Handbokk of Fluorescent Probes and Research Products*. pp. 834-835. Eugene, OR: Molecular Probes.

HECK, R.W., TANHAUSER, S.M., MANDA, R., TU, C., LAIPIS, P.J. & SILVERMAN, D.N. (1994). Catalytic properties of mouse carbonic anhydrase V. *J Biol Chem*, 269, 24742-6.

HEWETT-EMMETT, D. (2000). Evolution and distribution of the carbonic anhydrase families. In *The Carbonic Anhydrases: New Horizons*. eds Chegwidden, W., Carter, N. & Edwards, Y.H. Basel: Birkhauser Verlag.

HO, Y.T., PUROHIT, A., VICKER, N., NEWMAN, S.P., ROBINSON, J.J., LEESE, M.P., GANESHAPILLAI, D., WOO, L.W., POTTER, B.V. & REED, M.J. (2003). Inhibition of carbonic anhydrase II by steroidal and non-steroidal sulphamates. *Biochem Biophys Res Commun*, 305, 909-14.

HOCHACHKA, P.W. & MOMMSEN, T.P. (1983). Protons and anaerobiosis. *Science*, 219, 1391-7.

HYNNINEN, P., VASKIVUO, L., SAARNIO, J., HAAPASALO, H., KIVELA, J., PASTOREKOVA, S., PASTOREK, J., WAHEED, A., SLY, W.S., PUISTOLA, U. & PARKKILA, S. (2006). Expression of transmembrane carbonic anhydrases IX and XII in ovarian tumours. *Histopathology*, 49, 594-602.

ICHIHARA, N., ASARI, M., KASUYA, T., SUSAKI, E., MATSUI, K., NISHITA, T. & AMASAKI, H. (2003). Immunohistolocalization of carbonic anhydrase isozyme (CA-VI) in bovine mammary glands. *J Vet Med Sci*, 65, 1167-70.

ILIES, M.A. & BANCIU, M.D. (2004a). Nonsulfonamide carbonic anhydrase inhibitors In *Carbonic anhydrase: its inhibitors and activators*. eds Supuran, C.T., Scozzafava, A. & Conway, J. pp. 209-241. London: CRC Press.

ILIES, M.A. & BANCIU, M.D. (2004b). Nonsulfonamide carbonic anhydrase inhibitors. In *Carbonic Anhydrase. Its Activators and Inhibitors*. eds Supuran, C., Scozzafava, A. & Conway, J. FL: CRC Press

INNOCENTI, A., ANTEL, J., WURL, M., VULLO, D., FIRNGES, M.A., SCOZZAFAVA, A. & SUPURAN, C.T. (2005). Carbonic anhydrase inhibitors. Inhibition of isozymes I, II, IV, V and IX with complex fluorides, chlorides and cyanides. *Bioorg Med Chem Lett*, 15, 1909-13.

IPPOLITO, J.A. & CHRISTIANSON, D.W. (1994). Structural consequences of redesigning a protein-zinc binding site. *Biochemistry*, 33, 15241-9.

IRISAWA, H. & SATO, R. (1986). Intra- and extracellular actions of proton on the calcium current of isolated guinea pig ventricular cells. *Circ Res*, 59, 348-55.

ISFORT, R.J., CODY, D.B., ASQUITH, T.N., RIDDER, G.M., STUARD, S.B. & LEBOEUF, R.A. (1993). Induction of protein phosphorylation, protein synthesis, immediate-early-gene expression and cellular proliferation by intracellular pH modulation. Implications for the role of hydrogen ions in signal transduction. *Eur J Biochem*, 213, 349-57.

ISHIBASHI, K., SASAKI, S. & MARUMO, F. (1998). Molecular cloning of a new sodium bicarbonate cotransporter cDNA from human retina. *Biochem Biophys Res Commun*, 246, 535-8.

ITADA, N. & FORSTER, R.E. (1977). Carbonic anhydrase activity in intact red blood cells measured with 18O exchange. *J Biol Chem*, 252, 3881-90.

JANSE, M.J. & WIT, A.L. (1989). Electrophysiological mechanisms of ventricular arrhythmias resulting from myocardial ischemia and infarction. *Physiol Rev*, 69, 1049-169.

JENSEN, L.J., SCHMITT, B.M., BERGER, U.V., NSUMU, N.N., BORON, W.F., HEDIGER, M.A., BROWN, D. & BRETON, S. (1999a). Localization of sodium bicarbonate cotransporter (NBC) protein and messenger ribonucleic acid in rat epididymis. *Biol Reprod*, 60, 573-9.

JENSEN, L.J., STUART-TILLEY, A.K., PETERS, L.L., LUX, S.E., ALPER, S.L. & BRETON, S. (1999b). Immunolocalization of AE2 anion exchanger in rat and mouse epididymis. *Biol Reprod*, 61, 973-80.

KACZOROWSKI, G.J., BARROS, F., DETHMERS, J.K., TRUMBLE, M.J. & CRAGOE, E.J., JR. (1985). Inhibition of Na^+/Ca^{2+} exchange in pituitary plasma membrane vesicles by analogues of amiloride. *Biochemistry*, 24, 1394-403.

KADOYA, Y., KUWAHARA, H., SHIMAZAKI, M., OGAWA, Y. & YAGI, T. (1987). Isolation of a novel carbonic anhydrase from human saliva and immunohistochemical demonstration of its related isozymes in salivary gland. *Osaka City Med J*, 33, 99-109.

KARHUMAA, P., LEINONEN, J., PARKKILA, S., KAUNISTO, K., TAPANAINEN, J. & RAJANIEMI, H. (2001). The identification of secreted carbonic anhydrase VI as a constitutive glycoprotein of human and rat milk. *Proc Natl Acad Sci U S A*, 98, 11604-8.

KARHUMAA, P., PARKKILA, S., TURECI, O., WAHEED, A., GRUBB, J.H., SHAH, G., PARKKILA, A., KAUNISTO, K., TAPANAINEN, J., SLY, W.S. & RAJANIEMI, H. (2000). Identification of carbonic anhydrase XII as the membrane isozyme expressed in the normal human endometrial epithelium. *Mol Hum Reprod*, 6, 68-74.

KARMAZYN, M., GAN, X.T., HUMPHREYS, R.A., YOSHIDA, H. & KUSUMOTO, K. (1999). The myocardial Na^+-H^+ exchange: structure, regulation, and its role in heart disease. *Circ Res*, 85, 777-86.

KAUNISTO, K., PARKKILA, S., PARKKILA, A.K., WAHEED, A., SLY, W.S. & RAJANIEMI, H. (1995). Expression of carbonic anhydrase isoenzymes IV and II in rat epididymal duct. *Biol Reprod*, 52, 1350-7.

KAUNISTO, K., PARKKILA, S., TAMMELA, T., RONNBERG, L. & RAJANIEMI, H. (1990). Immunohistochemical localization of carbonic anhydrase isoenzymes in the human male reproductive tract. *Histochemistry*, 94, 381-6.

KENTISH, J.C. & NAYLER, W.G. (1979). The influence of pH on the Ca^{2+}-regulated ATPase of cardiac and white skeletal myofibrils. *J Mol Cell Cardiol*, 11, 611-7.

KERNOHAN, J.C. (1965). The pH-Activity Curve of Bovine Carbonic Anhydrase and its Relationship to the Inhibition of the Enzyme by Anions. *Biochim Biophys Acta*, 96, 304-17.

KHADILKAR, A., IANNUZZI, P. & ORLOWSKI, J. (2001). Identification of sites in the second exomembrane loop and ninth transmembrane helix of the mammalian Na^+/H^+ exchanger important for drug recognition and cation translocation. *J Biol Chem*, 276, 43792-800.

KHALIFAH, R.G. (1971). The carbon dioxide hydration activity of carbonic anhydrase. I. Stop-flow kinetic studies on the native human isoenzymes B and C. *J Biol Chem*, 246, 2561-73.

KHALIFAH, R.G. (1973). Carbon dioxide hydration activity of carbonic anhydrase: paradoxical consequences of the unusually rapid catalysis. *Proc Natl Acad Sci U S A*, 70, 1986-9.

KHALIFAH, R.G. & SILVERMAN, D.N. (1991). Carbonic anhydrase kinetics and molecular function. In *The carbonic anhydrases: cellular physiology and molecular genetics*. eds Dodgson, S., Tashian, R., Gros, G. & Carter, N. pp. 49-70. New York: Plenum Press.

KHANDOUDI, N., HO, J. & KARMAZYN, M. (1994). Role of Na^+-H^+ exchange in mediating effects of endothelin-1 on normal and ischemic/reperfused hearts. *Circ Res*, 75, 369-78.

KHOBZAOUI, M., TILLEKERATNE, L.M. & HUDSON, R.A. (2004). Potent isothiocyanate inhibitors of carbonic anhydrase: synthesis and evaluation. *Biochem Biophys Res Commun*, 318, 1-3.

KIEFER, L.L. & FIERKE, C.A. (1994). Functional characterization of human carbonic anhydrase II variants with altered zinc binding sites. *Biochemistry*, 33, 15233-40.

KIMOTO, M., IWAI, S., MAEDA, T., YURA, Y., FERNLEY, R.T. & OGAWA, Y. (2004). Carbonic anhydrase VI in the mouse nasal gland. *J Histochem Cytochem*, 52, 1057-62.

KINSELLA, J.L. & ARONSON, P.S. (1981). Amiloride inhibition of the Na^+-H^+ exchanger in renal microvillus membrane vesicles. *Am J Physiol*, 241, F374-9.

KNIGHT, D.R., SMITH, A.H., FLYNN, D.M., MACANDREW, J.T., ELLERY, S.S., KONG, J.X., MARALA, R.B., WESTER, R.T., GUZMAN-PEREZ, A., HILL, R.J., MAGEE, W.P. & TRACEY, W.R. (2001). A novel sodium-hydrogen exchanger isoform-1 inhibitor, zoniporide, reduces ischemic myocardial injury in vitro and in vivo. *J Pharmacol Exp Ther*, 297, 254-9.

KNUPPEL-RUPPERT, A.S., GROS, G., HARRINGER, W. & KUBIS, H.P. (2000). Immunochemical evidence for a unique GPI-anchored carbonic anhydrase isozyme in human cardiomyocytes. *Am J Physiol Heart Circ Physiol*, 278, H1335-44.

KOHOUT, T.A. & ROGERS, T.B. (1995). Angiotensin II activates the Na^+/HCO_3^- symport through a phosphoinositide-independent mechanism in cardiac cells. *J Biol Chem*, 270, 20432-8.

KOMUKAI, K., BRETTE, F., PASCAREL, C. & ORCHARD, C.H. (2002). Electrophysiological response of rat ventricular myocytes to acidosis. *Am J Physiol Heart Circ Physiol*, 283, H412-22.

KREBS, J.F., RANA, F., DLUHY, R.A. & FIERKE, C.A. (1993). Kinetic and spectroscopic studies of hydrophilic amino acid substitutions in the hydrophobic pocket of human carbonic anhydrase II. *Biochemistry*, 32, 4496-505.

KWON, T.H., PUSHKIN, A., ABULADZE, N., NIELSEN, S. & KURTZ, I. (2000). Immunoelectron microscopic localization of NBC3 sodium-bicarbonate cotransporter in rat kidney. *Am J Physiol Renal Physiol*, 278, F327-36.

LAGADIC-GOSSMANN, D., BUCKLER, K.J. & VAUGHAN-JONES, R.D. (1992). Role of bicarbonate in pH recovery from intracellular acidosis in the guinea-pig ventricular myocyte. *J Physiol*, 458, 361-84.

LAGADIC-GOSSMANN, D. & VAUGHAN-JONES, R.D. (1993). Coupling of dual acid extrusion in the guinea-pig isolated ventricular myocyte to alpha 1- and beta-adrenoceptors. *J Physiol*, 464, 49-73.

LEAF, D.E. & GOLDFARB, D.S. (2007). Mechanisms of action of acetazolamide in the prophylaxis and treatment of acute mountain sickness. *J Appl Physiol*, 102, 1313-22.

LEEM, C.H., LAGADIC-GOSSMANN, D. & VAUGHAN-JONES, R.D. (1999). Characterization of intracellular pH regulation in the guinea-pig ventricular myocyte. *J Physiol*, 517 (Pt 1), 159-80.

LEEM, C.H. & VAUGHAN-JONES, R.D. (1998a). Out-of-equilibrium pH transients in the guinea-pig ventricular myocyte. *J Physiol*, 509 (Pt 2), 471-85.

LEEM, C.H. & VAUGHAN-JONES, R.D. (1998b). Sarcolemmal mechanisms for pH_i recovery from alkalosis in the guinea-pig ventricular myocyte. *J Physiol*, 509 (Pt 2), 487-96.

LEINONEN, J.S., SAARI, K.A., SEPPANEN, J.M., MYLLYLA, H.M. & RAJANIEMI, H.J. (2004). Immunohistochemical demonstration of carbonic anhydrase isoenzyme VI (CA VI) expression in rat lower airways and lung. *J Histochem Cytochem*, 52, 1107-12.

LEPPILAMPI, M., SAARNIO, J., KARTTUNEN, T.J., KIVELA, J., PASTOREKOVA, S., PASTOREK, J., WAHEED, A., SLY, W.S. & PARKKILA, S. (2003). Carbonic anhydrase isozymes IX and XII in gastric tumors. *World J Gastroenterol*, 9, 1398-403.

LEVINE, S.A., MONTROSE, M.H., TSE, C.M. & DONOWITZ, M. (1993). Kinetics and regulation of three cloned mammalian Na^+/H^+ exchangers stably expressed in a fibroblast cell line. *J Biol Chem*, 268, 25527-35.

LI, X., ALVAREZ, B., CASEY, J.R., REITHMEIER, R.A. & FLIEGEL, L. (2002). Carbonic anhydrase II binds to and enhances activity of the Na^+/H^+ exchanger. *J Biol Chem*, 277, 36085-91.

LIANG, J.Y. & LIPSCOMB, W.N. (1990). Binding of substrate CO_2 to the active site of human carbonic anhydrase II: a molecular dynamics study. *Proc Natl Acad Sci U S A*, 87, 3675-9.

LILJAS, A., HAKANSSON, K., JONSSON, B.H. & XUE, Y. (1994). Inhibition and catalysis of carbonic anhydrase. Recent crystallographic analyses. *Eur J Biochem*, 219, 1-10.

LILJAS, A., KANNAN, K.K., BERGSTEN, P.C., WAARA, I., FRIDBORG, K., STRANDBERG, B., CARLBOM, U., JARUP, L., LOVGREN, S. & PETEF, M. (1972). Crystal structure of human carbonic anhydrase C. *Nat New Biol*, 235, 131-7.

LINDAHL, M., SVENSSON, L.A. & LILJAS, A. (1993). Metal poison inhibition of carbonic anhydrase. *Proteins*, 15, 177-82.

LINDSKOG, S. (1963). Effects of pH and inhibitors on some properties related to metal binding in bovine carbonic anhydrase. *J Biol Chem*, 238, 945-51.

LINDSKOG, S. (1986). The structural basis if kinetic differences between carbonic anydrase isoforms. In *Zinc Enzymes*. eds Bertini, I., Luchinat, C., Maret, W. & Zeppezauer, M. Boston: Birkhauser.

LINDSKOG, S. (1997). Structure and mechanism of carbonic anhydrase. *Pharmacol. Ther.*, 74, 1-20.

LINDSKOG, S. & COLEMAN, J.E. (1973). The catalytic mechanism of carbonic anhydrase. *Proc Natl Acad Sci U S A*, 70, 2505-8.

LINDSKOG, S., HENDERSON, L., KANNAN, K., LILJAS, A., NYMAN, P. & STRANDBERG, B. (1971). *Carbonic anhydrase enzymes*. New York: Academic Press.

LINDSKOG, S. & LILJAS, A. (1993). Carbonic anhydrase and the role of orientation in catalysis. *Curr Opin Struct Biol*, 3, 915-920.

LINDSKOG, S. & SILVERMAN, D.N. (2000). The catalytic mechanism of mammalian carbonic anhydrases. In *The carbonic anhydrases: New horizons*. eds Chegwidden, W., Carter, N. & Edwards, Y.H. pp. 175-194. Basel/Switzerland: Birkhauser Verlag.

LOH, S.H., SUN, B. & VAUGHAN-JONES, R.D. (1996). Effect of Hoe 694, a novel Na^+-H^+ exchange inhibitor, on intracellular pH regulation in the guinea-pig ventricular myocyte. *Br J Pharmacol*, 118, 1905-12.

LOISELLE, F.B., JASCHKE, P. & CASEY, J.R. (2003). Structural and functional characterization of the human NBC3 sodium/bicarbonate co-transporter carboxyl-terminal cytoplasmic domain. *Mol Membr Biol*, 20, 307-17.

LOISELLE, F.B., MORGAN, P.E., ALVAREZ, B.V. & CASEY, J.R. (2004). Regulation of the human NBC3 Na^+/HCO_3^- cotransporter by carbonic anhydrase II and PKA. *Am J Physiol Cell Physiol*, 286, C1423-33.

LU, J., DALY, C.M., PARKER, M.D., GILL, H.S., PIERMARINI, P.M., PELLETIER, M.F. & BORON, W.F. (2006). Effect of human carbonic anhydrase II on the activity of the human electrogenic Na^+/HCO_3^- cotransporter NBCe1-A in Xenopus oocytes. *J Biol Chem*, 281, 19241-50.

LUO, X., CHOI, J.Y., KO, S.B., PUSHKIN, A., KURTZ, I., AHN, W., LEE, M.G. & MUALLEM, S. (2001). HCO_3^- salvage mechanisms in the submandibular gland acinar and duct cells. *J Biol Chem*, 276, 9808-16.

LYSENG-WILLIAMSON, K.A. & YANG, L.P. (2007). Topiramate: a review of its use in the treatment of epilepsy. *Drugs*, 67, 2231-56.

MADDY, A.H. (1964). A fluorescent label for the outer component of the plasma membrane. *Biochim. Biophys. Acta*, 88, 390-399.

MANGANI, S. & HAKANSSON, K. (1992). Crystallographic studies of the binding of protonated and unprotonated inhibitors to carbonic anhydrase using hydrogen sulphide and nitrate anions. *Eur J Biochem*, 210, 867-71.

MANGANI, S. & LILJAS, A. (1993). Crystal structure of the complex between human carbonic anhydrase II and the aromatic inhibitor 1,2,4-triazole. *J Mol Biol*, 232, 9-14.

MANN, T. & KEILIN, D. (1940). Sulphamilamide as a specific carbonic anhydrase inhibitor. *Nature*, 146, 164-165.

MANSOOR, U.F., ZHANG, X.R. & BLACKBURN, G.M. (2000). The design of new carbonic anhydrase inhibitors. In *The Carbonic Anhydrases: New Horizons*. eds Chegwidden, W.R., Carter, N.D. & Edwards, Y.H. pp. 437-459. Basel: Birkhauser Verlag.

MARCHESE, A.C., HILL, J.A., XIE, P. & STRAUSS, H.C. (1984). Electrophysiologic effects of amiloride in canine purkinje fibres: evidence for a delayed effect of repolarisation. *Journal of Pharmacology and Experimental Therapeutics* 232, 485-491

MAREN, T.H. (1967). Carbonic anhydrase: chemistry, physiology, and inhibition. *Physiol Rev*, 47, 595-781.

MAREN, T.H. & CONROY, C.W. (1993). A new class of carbonic anhydrase inhibitor. *J Biol Chem*, 268, 26233-9.

MAREN, T.H., RAYBURN, C.S. & LIDDELL, N.E. (1976). Inhibition by anions of human red cell carbonic anhydrase B: physiological and biochemical implications. *Science*, 191, 469-72.

MAREN, T.H. & SANYAL, G. (1983). The activity of sulfonamides and anions against the carbonic anhydrases of animals, plants, and bacteria. *Annu Rev Pharmacol Toxicol*, 23, 439-59.

MAREN, T.H., WYNNS, G.C. & WISTRAND, P.J. (1993). Chemical properties of carbonic anhydrase IV, the membrane-bound enzyme. *Mol Pharmacol*, 44, 901-5.

MARINO, C.R., JEANES, V., BORON, W.F. & SCHMITT, B.M. (1999). Expression and distribution of the Na^+-HCO_3^- cotransporter in human pancreas. *Am J Physiol*, 277, G487-94.

MARYANOFF, B.E., MCCOMSEY, D.F., COSTANZO, M.J., HOCHMAN, C., SMITH-SWINTOSKY, V. & SHANK, R.P. (2005). Comparison of sulfamate and sulfamide groups for the inhibition of carbonic anhydrase-II by using topiramate as a structural platform. *J Med Chem*, 48, 1941-7.

MASEREEL, B., POCHET, L. & LAECKMANN, D. (2003). An overview of inhibitors of Na^+/H^+ exchanger. *Eur J Med Chem*, 38, 547-54.

MATSUI, H., BARRY, W.H., LIVSEY, C. & SPITZER, K.W. (1995). Angiotensin II stimulates sodium-hydrogen exchange in adult rabbit ventricular myocytes. *Cardiovasc Res*, 29, 215-21.

MCMURTRIE, H.L., CLEARY, H.J., ALVAREZ, B.V., LOISELLE, F.B., STERLING, D., MORGAN, P.E., JOHNSON, D.E. & CASEY, J.R. (2004). The bicarbonate transport metabolon. *J Enzyme Inhib Med Chem*, 19, 231-6.

MELDRUM, N.U. & ROUGHTON, F.J. (1933). Carbonic anhydrase. Its preparation and properties. *J Physiol*, 80, 113-42.

MERZ, K. (1991). CO_2 binding to human carbonic anhydrase II. *J Am Chem Soc*, 406-411.

MERZ, K.M., JR. (1990). Insights into the function of the zinc hydroxide-Thr199-Glu106 hydrogen bonding network in carbonic anhydrases. *J Mol Biol*, 214, 799-802.

MICCOLI, L., OUDARD, S., SUREAU, F., POIRSON, F., DUTRILLAUX, B. & POUPON, M.F. (1996). Intracellular pH governs the subcellular distribution of hexokinase in a glioma cell line. *Biochem J*, 313 (Pt 3), 957-62.

MORGAN, P.E., PASTOREKOVA, S., STUART-TILLEY, A.K., ALPER, S.L. & CASEY, J.R. (2007). Interactions of transmembrane carbonic anhydrase, CAIX, with bicarbonate transporters. *Am J Physiol Cell Physiol*, 293, C738-48.

MORGAN, P.E., SUPURAN, C.T. & CASEY, J.R. (2004). Carbonic anhydrase inhibitors that directly inhibit anion transport by the human Cl^-/HCO_3^- exchanger, AE1. *Mol Membr Biol*, 21, 423-33.

MUNSCH, T. & DEITMER, J.W. (1994). Sodium-bicarbonate cotransport current in identified leech glial cells. *J Physiol*, 474, 43-53.

MURAKAMI, H. & SLY, W.S. (1987). Purification and characterization of human salivary carbonic anhydrase. *J Biol Chem*, 262, 1382-8.

NAKAMURA, N., TANAKA, S., TEKO, Y., MITSUI, K. & KANAZAWA, H. (2005). Four Na^+/H^+ exchanger isoforms are distributed to Golgi and post-Golgi compartments and are involved in organelle pH regulation. *J Biol Chem*, 280, 1561-72.

NISHITA, T., TANAKA, Y., WADA, Y., MURAKAMI, M., KASUYA, T., ICHIHARA, N., MATSUI, K. & ASARI, M. (2007). Measurement of Carbonic Anhydrase Isozyme VI (CA-VI) in Bovine Sera, Saliva, Milk and Tissues. *Vet Res Commun*, 31, 83-92.

NOEL, J., ROUX, D. & POUYSSEGUR, J. (1996). Differential localization of Na^+/H^+ exchanger isoforms (NHE1 and NHE3) in polarized epithelial cell lines. *J Cell Sci*, 109 (Pt 5), 929-39.

NUMATA, M. & ORLOWSKI, J. (2001). Molecular cloning and characterization of a novel $(Na^+,K^+)/H^+$ exchanger localized to the trans-Golgi network. *J Biol Chem*, 276, 17387-94.

ODGAARD, E., JAKOBSEN, J.K., FRISCHE, S., PRAETORIUS, J., NIELSEN, S., AALKJAER, C. & LEIPZIGER, J. (2004). Basolateral Na^+-dependent HCO_3^- transporter NBCn1-mediated HCO_3^- influx in rat medullary thick ascending limb. *J Physiol*, 555, 205-18.

OGAWA, Y., CHANG, C.K., KUWAHARA, H., HONG, S.S., TOYOSAWA, S. & YAGI, T. (1992). Immunoelectron microscopy of carbonic anhydrase isozyme VI in rat submandibular gland: comparison with isozymes I and II. *J Histochem Cytochem*, 40, 807-17.

OGAWA, Y., HONG, S.S., TOYOSAWA, S., KUWAHARA, H., SHIMAZAKI, M. & YAGI, T. (1993). Immunoelectron microscopy of carbonic anhydrase isozyme VI in human submandibular gland: comparison with isozymes I and II. *J Histochem Cytochem*, 41, 343-51.

ORCHARD, C.H. & CINGOLANI, H.E. (1994). Acidosis and arrhythmias in cardiac muscle. *Cardiovasc Res*, 28, 1312-9.

ORCHARD, C.H. & KENTISH, J.C. (1990). Effects of changes of pH on the contractile function of cardiac muscle. *Am J Physiol*, 258, C967-81.

ORLOWSKI, J. (1993). Heterologous expression and functional properties of amiloride high affinity (NHE-1) and low affinity (NHE-3) isoforms of the rat Na^+/H^+ exchanger. *J Biol Chem*, 268, 16369-77.

ORLOWSKI, J. & GRINSTEIN, S. (2004). Diversity of the mammalian sodium/proton exchanger SLC9 gene family. *Pflugers Arch*, 447, 549-65.

ORLOWSKI, J. & GRINSTEIN, S. (1997). Na^+/H^+ exchangers of mammalian cells. *J Biol Chem*, 272, 22373-6.

ORLOWSKI, J., KANDASAMY, R.A. & SHULL, G.E. (1992). Molecular cloning of putative members of the Na/H exchanger gene family. cDNA cloning, deduced amino acid sequence, and mRNA tissue expression of the rat Na^+/H^+ exchanger NHE-1 and two structurally related proteins. *J Biol Chem*, 267, 9331-9.

OVADI, J. & SRERE, P.A. (2000). Macromolecular compartmentation and channeling. *Int Rev Cytol*, 192, 255-80.

PARKKILA, A.K., SCARIM, A.L., PARKKILA, S., WAHEED, A., CORBETT, J.A. & SLY, W.S. (1998). Expression of carbonic anhydrase V in pancreatic beta cells suggests role for mitochondrial carbonic anhydrase in insulin secretion. *J Biol Chem*, 273, 24620-3.

PARKKILA, S. (2000). An overview of the distribution and function of carbonic anhydrase in mammals. In *The Carbonic Anhydrases: New Horizons*. eds Chegwidden, W., Carter, N. & Edwards, Y.H. Basel: Birkhauser Verlag.

PARKKILA, S., KAUNISTO, K., RAJANIEMI, L., KUMPULAINEN, T., JOKINEN, K. & RAJANIEMI, H. (1990). Immunohistochemical localization of carbonic anhydrase isoenzymes VI, II, and I in human parotid and submandibular glands. *J Histochem Cytochem*, 38, 941-7.

PARKKILA, S. & PARKKILA, A.K. (1996). Carbonic anhydrase in the alimentary tract. Roles of the different isozymes and salivary factors in the maintenance of optimal conditions in the gastrointestinal canal. *Scand J Gastroenterol*, 31, 305-17.

PARKKILA, S., PARKKILA, A.K., JUVONEN, T. & RAJANIEMI, H. (1994). Distribution of the carbonic anhydrase isoenzymes I, II, and VI in the human alimentary tract. *Gut*, 35, 646-50.

PARKKILA, S., PARKKILA, A.K., KAUNISTO, K., WAHEED, A., SLY, W.S. & RAJANIEMI, H. (1993). Location of a membrane-bound carbonic anhydrase isoenzyme (CA IV) in the human male reproductive tract. *J Histochem Cytochem*, 41, 751-7.

PARKKILA, S., PARKKILA, A.K., SAARNIO, J., KIVELA, J., KARTTUNEN, T.J., KAUNISTO, K., WAHEED, A., SLY, W.S., TURECI, O., VIRTANEN, I. & RAJANIEMI, H. (2000). Expression of the membrane-associated carbonic anhydrase isozyme XII in the human kidney and renal tumors. *J Histochem Cytochem*, 48, 1601-8.

PASTOR-SOLER, N., PIETREMENT, C. & BRETON, S. (2005). Role of acid/base transporters in the male reproductive tract and potential consequences of their malfunction. *Physiology (Bethesda)*, 20, 417-28.

PASTOREK, J., PASTOREKOVA, S., CALLEBAUT, I., MORNON, J.P., ZELNIK, V., OPAVSKY, R., ZAT'OVICOVA, M., LIAO, S., PORTETELLE, D., STANBRIDGE, E.J. & ET AL. (1994). Cloning and characterization of MN, a human tumor-associated protein with a domain homologous to carbonic anhydrase and a putative helix-loop-helix DNA binding segment. *Oncogene*, 9, 2877-88.

PASTOREKOVA, S., ZAVADOVA, Z., KOSTAL, M., BABUSIKOVA, O. & ZAVADA, J. (1992). A novel quasi-viral agent, MaTu, is a two-component system. *Virology*, 187, 620-6.

PIERMARINI, P.M., CHOI, I. & BORON, W.F. (2007a). Cloning and characterization of an electrogenic Na^+/HCO_3^- cotransporter from the squid giant fiber lobe. *Am J Physiol Cell Physiol*, 292, C2032-45.

PIERMARINI, P.M., KIM, E.Y. & BORON, W.F. (2007b). Evidence against a direct interaction between intracellular carbonic anhydrase II and pure C-terminal domains of SLC4 bicarbonate transporters. *J Biol Chem*, 282, 1409-21.

POCKER, Y. & STONE, J.T. (1968). The catalytic versatility of erythrocyte carbonic anhydrase. VI. Kinetic studies of noncompetitive inhibition of enzyme-catalyzed hydrolysis of p-nitrophenyl acetate. *Biochemistry*, 7, 2936-45.

POCKER, Y. & STORM, D.R. (1968). The catalytic versatility of erythrocyte carbonic anhydrase. IV. Kinetic studies of enzyme-catalyzed hydrolyses of para-nitrophenly esters. *Biochemistry*, 7, 1202-14.

POTTER, C. & HARRIS, A.L. (2004). Hypoxia inducible carbonic anhydrase IX, marker of tumour hypoxia, survival pathway and therapy target. *Cell Cycle*, 3, 164-7.

PRAETORIUS, J., HAGER, H., NIELSEN, S., AALKJAER, C., FRIIS, U.G., AINSWORTH, M.A. & JOHANSEN, T. (2001). Molecular and functional evidence for electrogenic and electroneutral Na^+-HCO_3^- cotransporters in murine duodenum. *Am J Physiol Gastrointest Liver Physiol*, 280, G332-43.

PRAETORIUS, J., KIM, Y.H., BOUZINOVA, E.V., FRISCHE, S., ROJEK, A., AALKJAER, C. & NIELSEN, S. (2004a). NBCn1 is a basolateral Na^+-HCO_3^- cotransporter in rat kidney inner medullary collecting ducts. *Am J Physiol Renal Physiol*, 286, F903-12.

PRAETORIUS, J., NEJSUM, L.N. & NIELSEN, S. (2004b). A SCL4A10 gene product maps selectively to the basolateral plasma membrane of choroid plexus epithelial cells. *Am J Physiol Cell Physiol*, 286, C601-10.

PURKERSON, J.M. & SCHWARTZ, G.J. (2005). Expression of membrane-associated carbonic anhydrase isoforms IV, IX, XII, and XIV in the rabbit: induction of CA IV and IX during maturation. *Am J Physiol Regul Integr Comp Physiol*, 288, R1256-63.

PUSHKIN, A., ABULADZE, N., GROSS, E., NEWMAN, D., TATISHCHEV, S., LEE, I., FEDOTOFF, O., BONDAR, G., AZIMOV, R., NGYUEN, M. & KURTZ, I. (2004). Molecular mechanism of kNBC1-carbonic anhydrase II interaction in proximal tubule cells. *J Physiol*, 559, 55-65.

PUSHKIN, A., ABULADZE, N., LEE, I., NEWMAN, D., HWANG, J. & KURTZ, I. (1999a). Cloning, tissue distribution, genomic organization, and functional characterization of NBC3, a new member of the sodium bicarbonate cotransporter family. *J Biol Chem*, 274, 16569-75.

PUSHKIN, A., ABULADZE, N., NEWMAN, D., LEE, I., XU, G. & KURTZ, I. (2000a). Cloning, characterization and chromosomal assignment of NBC4, a new member of the sodium bicarbonate cotransporter family. *Biochim Biophys Acta*, 1493, 215-8.

PUSHKIN, A., CLARK, I., KWON, T.H., NIELSEN, S. & KURTZ, I. (2000b). Immunolocalization of NBC3 and NHE3 in the rat epididymis: colocalization of NBC3 and the vacuolar H^+-ATPase. *J Androl*, 21, 708-20.

PUSHKIN, A., YIP, K.P., CLARK, I., ABULADZE, N., KWON, T.H., TSURUOKA, S., SCHWARTZ, G.J., NIELSEN, S. & KURTZ, I. (1999b). NBC3 expression in rabbit collecting duct: colocalization with vacuolar H^+-ATPase. *Am J Physiol*, 277, F974-81.

PUTNEY, L.K., DENKER, S.P. & BARBER, D.L. (2002). The changing face of the Na^+/H^+ exchanger, NHE1: structure, regulation, and cellular actions. *Annu Rev Pharmacol Toxicol*, 42, 527-52.

RAMSAY, L.E., HETTIARACHCHI, J., FRASER, R. & MORTON, J.J. (1980). Amiloride, spironolactone, and potassium chloride in thiazide-treated hypertensive patients. *Clin Pharmacol Ther*, 27, 533-43.

REISS, W.G. & OLES, K.S. (1996). Acetazolamide in the treatment of seizures. *Ann Pharmacother*, 30, 514-9.

RICHALET, J.P., RIVERA, M., BOUCHET, P., CHIRINOS, E., ONNEN, I., PETITJEAN, O., BIENVENU, A., LASNE, F., MOUTEREAU, S. & LEON-VELARDE, F. (2005). Acetazolamide: a treatment for chronic mountain sickness. *Am J Respir Crit Care Med*, 172, 1427-33.

RICHMOND, P.H. & VAUGHAN-JONES, R.D. (1997). Assessment of evidence for K^+-H^+ exchange in isolated type-1 cells of neonatal rat carotid body. *Pflugers Arch*, 434, 429-37.

RIVERA-CH, M., LEON-VELARDE, F. & HUICHO, L. (2007). Treatment of chronic mountain sickness: Critical reappraisal of an old problem. *Respir Physiol Neurobiol*, 158, 251-65.

ROBERTS, S.B., LANE, T.W. & MOREL, F.M. (1997). Carbonic anhydrase in the marine diatom Thalassiosira weissflogii (Bacillariophyceae). *J Phycol*, 33, 845-850.

ROMERO, M.F. & BORON, W.F. (1999). Electrogenic Na^+/HCO_3^- cotransporters: cloning and physiology. *Annu Rev Physiol*, 61, 699-723.

ROMERO, M.F., FULTON, C.M. & BORON, W.F. (2004). The SLC4 family of HCO_3^- transporters. *Pflugers Arch*, 447, 495-509.

ROMERO, M.F., HEDIGER, M.A., BOULPAEP, E.L. & BORON, W.F. (1997). Expression cloning and characterization of a renal electrogenic Na^+/HCO_3^- cotransporter. *Nature*, 387, 409-13.

ROOS, A. & BORON, W.F. (1981). Intracellular pH. *Physiol Rev*, 61, 296-434.

ROSOFF, P.M., STEIN, L.F. & CANTLEY, L.C. (1984). Phorbol esters induce differentiation in a pre-B-lymphocyte cell line by enhancing Na^+/H^+ exchange. *J Biol Chem*, 259, 7056-60.

ROWLETT, R.S., GARGIULO, N.J., 3RD, SANTOLI, F.A., JACKSON, J.M. & CORBETT, A.H. (1991). Activation and inhibition of bovine carbonic anhydrase III by dianions. *J Biol Chem*, 266, 933-41.

RUIZ, O.S. & ARRUDA, J.A. (1992). Regulation of the renal Na^+-HCO_3^- cotransporter by cAMP and Ca-dependent protein kinases. *Am J Physiol*, 262, F560-5.

RUIZ, O.S., QIU, Y.Y., CARDOSO, L.R. & ARRUDA, J.A. (1997). Regulation of the renal Na^+-HCO_3^- cotransporter: VII. Mechanism of the cholinergic stimulation. *Kidney Int*, 51, 1069-77.

RUIZ, O.S., QIU, Y.Y., WANG, L.J. & ARRUDA, J.A. (1995). Regulation of the renal Na^+-HCO_3^- cotransporter: IV. Mechanisms of the stimulatory effect of angiotensin II. *J Am Soc Nephrol*, 6, 1202-8.

RUIZ, O.S., QIU, Y.Y., WANG, L.J. & ARRUDA, J.A. (1996a). Regulation of the renal Na^+-HCO_3^- cotransporter: V. mechanism of the inhibitory effect of parathyroid hormone. *Kidney Int*, 49, 396-402.

RUIZ, O.S., WANG, L.J., QIU, Y.Y., KEAR, F., BERNARDO, A. & ARRUDA, J.A. (1996b). Regulation of the renal Na-HCO3 cotransporter: VI. Mechanism of the stimulatory effect of protein kinase C. *Kidney Int*, 49, 696-704.

RUSS, U., BALSER, C., SCHOLZ, W., ALBUS, U., LANG, H.J., WEICHERT, A., SCHOLKENS, B.A. & GOGELEIN, H. (1996). Effects of the Na^+/H^+-exchange inhibitor Hoe 642 on intracellular pH, calcium and sodium in isolated rat ventricular myocytes. *Pflugers Arch*, 433, 26-34.

SAMPATH, P. & POLLARD, T.D. (1991). Effects of cytochalasin, phalloidin, and pH on the elongation of actin filaments. *Biochemistry*, 30, 1973-80.

SANYAL, G. & MAREN, T.H. (1981). Thermodynamics of carbonic anhydrase catalysis. A comparison between human isoenzymes B and C. *J Biol Chem*, 256, 608-12.

SATO, R., NOMA, A., KURACHI, Y. & IRISAWA, H. (1985). Effects of intracellular acidification on membrane currents in ventricular cells of the guinea pig. *Circ Res*, 57, 553-61.

SCHEIBE, R.J., GROS, G., PARKKILA, S., WAHEED, A., GRUBB, J.H., SHAH, G.N., SLY, W.S. & WETZEL, P. (2006). Expression of Membrane-bound Carbonic Anhydrases IV, IX, and XIV in the Mouse Heart. *J Histochem Cytochem*.

SCHMITT, B.M., BERGER, U.V., DOUGLAS, R.M., BEVENSEE, M.O., HEDIGER, M.A., HADDAD, G.G. & BORON, W.F. (2000). Na^+/HCO_3^- cotransporters in rat brain: expression in glia, neurons, and choroid plexus. *J Neurosci*, 20, 6839-48.

SCHMITT, B.M., BIEMESDERFER, D., ROMERO, M.F., BOULPAEP, E.L. & BORON, W.F. (1999). Immunolocalization of the electrogenic Na^+-HCO_3^- cotransporter in mammalian and amphibian kidney. *Am J Physiol*, 276, F27-38.

SCHOLZ, W., ALBUS, U., COUNILLON, L., GOGELEIN, H., LANG, H.J., LINZ, W., WEICHERT, A. & SCHOLKENS, B.A. (1995). Protective effects of HOE642, a selective sodium-hydrogen exchange subtype 1 inhibitor, on cardiac ischaemia and reperfusion. *Cardiovasc Res*, 29, 260-8.

SCHOLZ, W., ALBUS, U., LANG, H.J., LINZ, W., MARTORANA, P.A., ENGLERT, H.C. & SCHOLKENS, B.A. (1993). Hoe 694, a new Na^+/H^+ exchange inhibitor and its effects in cardiac ischaemia. *Br J Pharmacol*, 109, 562-8.

SCHOLZ, W., JESSEL, A. & ALBUS, U. (1999). Development of the Na^+/H^+ exchange inhibitor cariporide as a cardioprotective drug: from the laboratory to the GUARDIAN trial. *J Thromb Thrombolysis*, 8, 61-70.

SCHWAB, A., ROSSMANN, H., KLEIN, M., DIETERICH, P., GASSNER, B., NEFF, C., STOCK, C. & SEIDLER, U. (2005). Functional role of Na^+-HCO_3^- cotransport in migration of transformed renal epithelial cells. *J Physiol*, 568, 445-58.

SCHWIENING, C.J. & BORON, W.F. (1994). Regulation of intracellular pH in pyramidal neurones from the rat hippocampus by Na^+-dependent Cl^--HCO_3^- exchange. *J Physiol*, 475, 59-67.

SCIORTINO, C.M. & ROMERO, M.F. (1999). Cation and voltage dependence of rat kidney electrogenic Na^+-HCO_3^- cotransporter, rkNBC, expressed in oocytes. *Am J Physiol*, 277, F611-23.

SCOZZAFAVA, A., BRIGANTI, F., ILIES, M.A. & SUPURAN, C.T. (2000). Carbonic anhydrase inhibitors: synthesis of membrane-impermeant low molecular weight sulfonamides possessing in vivo selectivity for the membrane-bound versus cytosolic isozymes. *J Med Chem*, 43, 292-300.

SENDER, S., DECKER, B., FENSKE, C.D., SLY, W.S., CARTER, N.D. & GROS, G. (1998). Localization of carbonic anhydrase IV in rat and human heart muscle. *J Histochem Cytochem*, 46, 855-61.

SHAH, G.N., HEWETT-EMMETT, D., GRUBB, J.H., MIGAS, M.C., FLEMING, R.E., WAHEED, A. & SLY, W.S. (2000). Mitochondrial carbonic anhydrase CA VB: differences in tissue distribution and pattern of evolution from those of CA VA suggest distinct physiological roles. *Proc Natl Acad Sci U S A*, 97, 1677-82.

SHRODE, L.D., TAPPER, H. & GRINSTEIN, S. (1997). Role of intracellular pH in proliferation, transformation, and apoptosis. *J Bioenerg Biomembr*, 29, 393-9.

SILVER, L.H. (2000). Dose-response evaluation of the ocular hypotensive effect of brinzolamide ophthalmic suspension (Azopt). Brinzolamide Dose-Response Study Group. *Surv Ophthalmol*, 44 Suppl 2, S147-53.

SILVERMAN, D.N. (1995). Proton transfer in carbonic anhydrase measured by equilibrium isotope exchange. *Methods Enzymol*, 249, 479-503.

SILVERMAN, D.N. & LINDSKOG, S. (1988). The catalytic mechanism of carbonic anhydrase: implications of a rate-limiting protolysis of water. *Accounts of Chemical Research*, 21, 30-36.

SILVERMAN, D.N. & VINCENT, S.H. (1983). Proton transfer in the catalytic mechanism of carbonic anhydrase. *CRC Crit Rev Biochem*, 14, 207-55.

SILVERTON, S.F. (1991). Carbonic anhydrase and skeletogenesis. In *The Carbonic Anhydrases: Cellular Physiology and Molecular Genetics*. eds Dodgson, S., Tashian, R., Gros, G. & Carter, N. pp. 357-363. London: Plenum Press.

SLEPKOV, E.R., RAINEY, J.K., SYKES, B.D. & FLIEGEL, L. (2007). Structural and functional analysis of the Na^+/H^+ exchanger. *Biochem J*, 401, 623-33.

SLY, W.S. & HU, P.Y. (1995). Human carbonic anhydrases and carbonic anhydrase deficiencies. *Annu Rev Biochem*, 64, 375-401.

SOLEIMANI, M., BERGMAN, J.A., HOSFORD, M.A. & MCKINNEY, T.D. (1990). Potassium depletion increases luminal Na^+/H^+ exchange and basolateral $Na^+:CO_3^{2-}:HCO_3^-$ cotransport in rat renal cortex. *J Clin Invest*, 86, 1076-83.

SOLEIMANI, M., LESOINE, G.A., BERGMAN, J.A. & ARONSON, P.S. (1991). Cation specificity and modes of the $Na^+:CO_3^{2-}:HCO_3^-$ cotransporter in renal basolateral membrane vesicles. *J Biol Chem*, 266, 8706-10.

SORGEN, P.L., DUFFY, H.S., SPRAY, D.C. & DELMAR, M. (2004). pH-dependent dimerization of the carboxyl terminal domain of Cx43. *Biophys J*, 87, 574-81.

SPITZER, K.W., ERSHLER, P.R., SKOLNICK, R.L. & VAUGHAN-JONES, R.D. (2000). Generation of intracellular pH gradients in single cardiac myocytes with a microperfusion system. *Am J Physiol Heart Circ Physiol*, 278, H1371-82.

SPITZER, K.W., SKOLNICK, R.L., PEERCY, B.E., KEENER, J.P. & VAUGHAN-JONES, R.D. (2002). Facilitation of intracellular H^+ ion mobility by CO_2/HCO_3^- in rabbit ventricular myocytes is regulated by carbonic anhydrase. *J Physiol*, 541, 159-67.

SPITZER, K.W. & VAUGHAN-JONES, R.D. (2006). Regional intracellular acidosis in ventricular myocytes creates spatial gradients of Ca^{2+} transients. *Biophysical Society 50th Annual Meeting 2006*, 73A.

SPRAY, D.C. & BURT, J.M. (1990). Structure-activity relations of the cardiac gap junction channel. *Am J Physiol*, 258, C195-205.

SPRAY, D.C., WHITE, R.L., MAZET, F. & BENNETT, M.V. (1985). Regulation of gap junctional conductance. *Am J Physiol*, 248, H753-64.

SRERE, P.A. (1987). Complexes of sequential metabolic enzymes. *Annu Rev Biochem*, 56, 89-124.

SRERE, P.A. (2000). Macromolecular interactions: tracing the roots. *Trends Biochem Sci*, 25, 150-3.

STAMS, T. & CHRISTIANSON, D.W. (2000). X-ray crystallographic studies of mammalian carbonic anhydrase isozymes. In *The Carbonic Anhydrases: New Horizons*. eds Chegwidden, W.R., Carter, N.D. & Edwards, Y.H. Basel/Switzerland: Birkhauser Verlag

STERLING, D., ALVAREZ, B.V. & CASEY, J.R. (2002). The extracellular component of a transport metabolon. Extracellular loop 4 of the human AE1 Cl^-/HCO_3^- exchanger binds carbonic anhydrase IV. *J Biol Chem*, 277, 25239-46.

STERLING, D. & CASEY, J.R. (2002). Bicarbonate transport proteins. *Biochem Cell Biol*, 80, 483-97.

STERLING, D., REITHMEIER, R.A. & CASEY, J.R. (2001a). Carbonic anhydrase: in the driver's seat for bicarbonate transport. *Jop*, 2, 165-70.

STERLING, D., REITHMEIER, R.A. & CASEY, J.R. (2001b). A transport metabolon. Functional interaction of carbonic anhydrase II and chloride/bicarbonate exchangers. *J Biol Chem*, 276, 47886-94.

STEWART, A.K., BOYD, C.A. & VAUGHAN-JONES, R.D. (1999). A novel role for carbonic anhydrase: cytoplasmic pH gradient dissipation in mouse small intestinal enterocytes. *J Physiol*, 516 (Pt 1), 209-17.

STIM, J., BERNARDO, A.A., KEAR, F.T., QIU, Y.Y. & ARRUDA, J.A. (1994). Renal cortical basolateral Na^+/HCO_3^- cotransporter: II. Detection of conformational changes with fluorescein isothiocyanate labeling. *J Membr Biol*, 140, 39-46.

STUWE, L., MULLER, M., FABIAN, A., WANING, J., MALLY, S., NOEL, J., SCHWAB, A. & STOCK, C. (2007). pH dependence of melanoma cell migration: protons extruded by NHE1 dominate protons of the bulk solution. *J Physiol*, 585, 351-60.

SUGRUE, M.F. (2000). Pharmacological and ocular hypotensive properties of topical carbonic anhydrase inhibitors. *Prog Retin Eye Res*, 19, 87-112.

SUN, B., LEEM, C.H. & VAUGHAN-JONES, R.D. (1996). Novel chloride-dependent acid loader in the guinea-pig ventricular myocyte: part of a dual acid-loading mechanism. *J Physiol*, 495 (Pt 1), 65-82.

SUPURAN, C., CASINI, A. & SCOZZAFAVA, A. (2004). Development of Sulfonamide Carbonic Anhydrase Inhibitors. In *Carbonic Anhydrase. Its Activators and Inhibitors*. eds Supuran, C., Scozzafava, A. & Conway, J. FL: CRC Press.

SUPURAN, C.T. (2004). Carbonic anhydrases: catalytic and inhibition mechanisms, distribution and physiological roles. In *Carbonic anhydrases: its inhibitors and activators*. eds Supuran, C.T., Scozzafava, A. & Conway, J. pp. 1-23. London: CRC Press.

SUPURAN, C.T. & SCOZZAFAVA, A. (2000). Carbonic anhydrase inhibitors and their therapeutic potential. *Expert Opinion on Therapeutic Patents*, 10, 575-600.

SUPURAN, C.T., SCOZZAFAVA, A. & CASINI, A. (2003). Carbonic anhydrase inhibitors. *Med Res Rev*, 23, 146-89.

SWARTZ, D.R., ZHANG, D. & YANCEY, K.W. (1999). Cross bridge-dependent activation of contraction in cardiac myofibrils at low pH. *Am J Physiol*, 276, H1460-7.

SWENSON, E.R. (1991). Distribution and functions of carbonic anhydrase in the gastrointestinal tract. In *The Carbonic Anhydrases: Cellular Physiology and Molecular Genetics*. eds Dodgson, S., Tashian, R., Gros, G. & Carter, N. pp. 265-287. London: Plenum Press.

SWIETACH, P., ROSSINI, A., SPITZER, K.W. & VAUGHAN-JONES, R.D. (2007a). H^+ ion activation and inactivation of the ventricular gap junction: a basis for spatial regulation of intracellular pH. *Circ Res*, 100, 1045-54.

SWIETACH, P., SPITZER, K.W. & VAUGHAN-JONES, R.D. (2007b). pH-Dependence of Extrinsic and Intrinsic H^+-Ion Mobility in the Rat Ventricular Myocyte, Investigated Using Flash Photolysis of a Caged-H^+ Compound. *Biophys J*, 92, 641-53.

SWIETACH, P. & VAUGHAN-JONES, R.D. (2005a). Relationship between intracellular pH and proton mobility in rat and guinea-pig ventricular myocytes. *J Physiol*, 566, 793-806.

SWIETACH, P. & VAUGHAN-JONES, R.D. (2005b). Spatial regulation of intracellular pH in the ventricular myocyte. *Ann N Y Acad Sci*, 1047, 271-82.

SWIETACH, P., VAUGHAN-JONES, R.D. & HARRIS, A.L. (2007c). Regulation of tumor pH and the role of carbonic anhydrase 9. *Cancer Metastasis Rev*, 26, 299-310.

TAKAHASHI, K., WAKAMORI, M. & AKAIKE, N. (1989). Hippocampal CA1 pyramidal cells of rats have four voltage-dependent calcium conductances. *Neurosci Lett*, 104, 229-34.

TASHIAN, R., HEWLETT-EMMETT, D., CARTER, N.D. & BERGENHEM, N. (2000). Carbonic anhydrase (CA)-related proteins (CA-RPs), and trasmembrane proteins with CA or CA-RP domains. In *The Carbonic Anhydrases: New Horizons*. eds Chegwidden, W., Edwards, Y.H. & Carter, N. Basel: Birkhauser Verlag.

TATISHCHEV, S., ABULADZE, N., PUSHKIN, A., NEWMAN, D., LIU, W., WEEKS, D., SACHS, G. & KURTZ, I. (2003). Identification of membrane topography of the electrogenic sodium bicarbonate cotransporter pNBC1 by in vitro transcription/translation. *Biochemistry*, 42, 755-65.

THEROUX, P., CHAITMAN, B.R., DANCHIN, N., ERHARDT, L., MEINERTZ, T., SCHROEDER, J.S., TOGNONI, G., WHITE, H.D., WILLERSON, J.T. & JESSEL, A. (2000). Inhibition of the sodium-hydrogen exchanger with cariporide to prevent myocardial infarction in high-risk ischemic situations. Main results of the GUARDIAN trial. Guard during ischemia against necrosis (GUARDIAN) Investigators. *Circulation*, 102, 3032-8.

THOMAS, J.A., BUCHSBAUM, R.N., ZIMNIAK, A. & RACKER, E. (1979). Intracellular pH measurements in Ehrlich ascites tumor cells utilizing spectroscopic probes generated in situ. *Biochemistry*, 18, 2210-8.

TILANDER, B., STRANDEBERG, B. & FRIDBORG, K. (1965). Crystal structure studies on human erythrocyte carbonic anhydrase C. (II). *J Mol Biol*, 12, 740-60.

TRIPP, B.C., SMITH, K. & FERRY, J.G. (2001). Carbonic anhydrase: new insights for an ancient enzyme. *J Biol Chem*, 276, 48615-8.

TSAI, S.T., ZHANG, R.B. & VERKMAN, A.S. (1991). High channel-mediated water permeability in rabbit erythrocytes: characterization in native cells and expression in Xenopus oocytes. *Biochemistry*, 30, 2087-92.

TU, C., SANYAL, G., WYNNS, G.C. & SILVERMAN, D.N. (1983). The pH dependence of the hydration of CO_2 catalyzed by carbonic anhydrase III from skeletal muscle of the cat. Steady state and equilibrium studies. *J Biol Chem*, 258, 8867-71.

TU, C., WYNNS, G.C. & SILVERMAN, D.N. (1981). Inhibition by cupric ions of ^{18}O exchange catalyzed by human carbonic anhydrase II. Relation to the interaction between carbonic anhydrase and hemoglobin. *J Biol Chem*, 256, 9466-70.

TU, C.K., SILVERMAN, D.N., FORSMAN, C., JONSSON, B.H. & LINDSKOG, S. (1989). Role of histidine 64 in the catalytic mechanism of human carbonic anhydrase II studied with a site-specific mutant. *Biochemistry*, 28, 7913-8.

ULMASOV, B., WAHEED, A., SHAH, G.N., GRUBB, J.H., SLY, W.S., TU, C. & SILVERMAN, D.N. (2000). Purification and kinetic analysis of recombinant CA XII, a membrane carbonic anhydrase overexpressed in certain cancers. *Proc Natl Acad Sci U S A*, 97, 14212-7.

VAANANEN, H.K. & PARVINEN, E.K. (1991). Localization of carbonic anhydrase isozymes in calcified tissues. In *The Carbonic Anhydrases: Cellular Physiology and Molecular Genetics*. eds Dodgson, S., Tashian, R., Gros, G. & Carter, N. pp. 351-355. London: Plenum Press.

VANDENBERG, J.I., CARTER, N.D., BETHELL, H.W., NOGRADI, A., RIDDERSTRALE, Y., METCALFE, J.C. & GRACE, A.A. (1996). Carbonic anhydrase and cardiac pH regulation. *Am J Physiol*, 271, C1838-46.

VANDENBERG, J.I., METCALFE, J.C. & GRACE, A.A. (1993). Mechanisms of pH_i recovery after global ischemia in the perfused heart. *Circ Res*, 72, 993-1003.

VANHEEL, B., DE HEMPTINNE, A. & LEUSEN, I. (1986). Influence of surface pH on intracellular pH regulation in cardiac and skeletal muscle. *Am J Physiol*, 250, C748-60.

VAUGHAN-JONES, R.D. (1986). An investigation of chloride-bicarbonate exchange in the sheep cardiac Purkinje fibre. *J Physiol*, 379, 377-406.

VAUGHAN-JONES, R.D. (1979). Regulation of chloride in quiescent sheep-heart Purkinje fibres studied using intracellular chloride and pH-sensitive micro-electrodes. *J Physiol*, 295, 111-37.

VAUGHAN-JONES, R.D., PEERCY, B.E., KEENER, J.P. & SPITZER, K.W. (2002). Intrinsic H(+) ion mobility in the rabbit ventricular myocyte. *J Physiol*, 541, 139-58.

VAUGHAN-JONES, R.D., SPITZER, K.W. & SWIETACH, P. (2006). Spatial aspects of intracellular pH regulation in heart muscle. *Prog Biophys Mol Biol*, 90, 207-24.

VICKER, N., HO, Y., ROBINSON, J., WOO, L.L., PUROHIT, A., REED, M.J. & POTTER, B.V. (2003). Docking studies of sulphamate inhibitors of estrone sulphatase in human carbonic anhydrase II. *Bioorg Med Chem Lett*, 13, 863-5.

VINCE, J.W., CARLSSON, U. & REITHMEIER, R.A. (2000). Localization of the Cl^-/HCO_3^- anion exchanger binding site to the amino-terminal region of carbonic anhydrase II. *Biochemistry*, 39, 13344-9.

VINCE, J.W. & REITHMEIER, R.A. (1998). Carbonic anhydrase II binds to the carboxyl terminus of human band 3, the erythrocyte C1-/HCO3- exchanger. *J Biol Chem*, 273, 28430-7.

VINCE, J.W. & REITHMEIER, R.A. (2000). Identification of the carbonic anhydrase II binding site in the Cl^-/HCO_3^- anion exchanger AE1. *Biochemistry*, 39, 5527-33.

VIRKKI, L.V., WILSON, D.A., VAUGHAN-JONES, R.D. & BORON, W.F. (2002). Functional characterization of human NBC4 as an electrogenic Na^+-HCO_3^- cotransporter (NBCe2). *Am J Physiol Cell Physiol*, 282, C1278-89.

VORUM, H., KWON, T.H., FULTON, C., SIMONSEN, B., CHOI, I., BORON, W., MAUNSBACH, A.B., NIELSEN, S. & AALKJAER, C. (2000). Immunolocalization of electroneutral Na^+-HCO_3^- cotransporter in rat kidney. *Am J Physiol Renal Physiol*, 279, F901-9.

WAJIMA, T., BEGUIER, B. & YAGUCHI, M. (2004). Effects of cariporide (HOE642) on myocardial infarct size and ventricular arrhythmias in a rat ischemia/reperfusion model: comparison with other drugs. *Pharmacology*, 70, 68-73.

WAKABAYASHI, S., BERTRAND, B., SHIGEKAWA, M., FAFOURNOUX, P. & POUYSSEGUR, J. (1994). Growth factor activation and "H^+-sensing" of the Na^+/H^+ exchanger isoform 1 (NHE1). Evidence for an additional mechanism not requiring direct phosphorylation. *J Biol Chem*, 269, 5583-8.

WAKABAYASHI, S., FAFOURNOUX, P., SARDET, C. & POUYSSEGUR, J. (1992). The Na^+/H^+ antiporter cytoplasmic domain mediates growth factor signals and controls "H^+-sensing". *Proc Natl Acad Sci U S A*, 89, 2424-8.

WAKABAYASHI, S., PANG, T., SU, X. & SHIGEKAWA, M. (2000). A novel topology model of the human Na^+/H^+ exchanger isoform 1. *J Biol Chem*, 275, 7942-9.

WAKABAYASHI, S., SHIGEKAWA, M. & POUYSSEGUR, J. (1997). Molecular physiology of vertebrate Na^+/H^+ exchangers. *Physiol Rev*, 77, 51-74.

WALLERT, M.A. & FROHLICH, O. (1992). Alpha 1-adrenergic stimulation of Na^+-H^+ exchange in cardiac myocytes. *Am J Physiol*, 263, C1096-102.

WANG, X., LEVI, A.J. & HALESTRAP, A.P. (1996). Substrate and inhibitor specificities of the monocarboxylate transporters of single rat heart cells. *Am J Physiol*, 270, H476-84.

WANG, Z., CONFORTI, L., PETROVIC, S., AMLAL, H., BURNHAM, C.E. & SOLEIMANI, M. (2001). Mouse Na^+: HCO_3^- cotransporter isoform NBC-3 (kNBC-3): cloning, expression, and renal distribution. *Kidney Int*, 59, 1405-14.

WEBER, A., CASINI, A., HEINE, A., KUHN, D., SUPURAN, C.T., SCOZZAFAVA, A. & KLEBE, G. (2004). Unexpected nanomolar inhibition of carbonic anhydrase by COX-2-selective celecoxib: new pharmacological opportunities due to related binding site recognition. *J Med Chem*, 47, 550-7.

WEISE, A., BECKER, H.M. & DEITMER, J.W. (2007). Enzymatic suppression of the membrane conductance associated with the glutamine transporter SNAT3 expressed in Xenopus oocytes by carbonic anhydrase II. *J Gen Physiol*, 130, 203-15.

WETZEL, P. & GROS, G. (2000). Carbonic anhydrases in striated muscle In *The Carbonic Anhydrases: New Horizons*. eds Chegwidden, W.R., Carter, N.D. & Edwards, Y.H. pp. 375-399. Basel/Switzerland: Birkhauser Verlag.

WETZEL, P., HASSE, A., PAPADOPOULOS, S., VOIPIO, J., KAILA, K. & GROS, G. (2001). Extracellular carbonic anhydrase activity facilitates lactic acid transport in rat skeletal muscle fibres. *J Physiol*, 531, 743-56.

WHITTINGTON, D.A., GRUBB, J.H., WAHEED, A., SHAH, G.N., SLY, W.S. & CHRISTIANSON, D.W. (2004). Expression, assay, and structure of the extracellular domain of murine carbonic anhydrase XIV: implications for selective inhibition of membrane-associated isozymes. *J Biol Chem*, 279, 7223-8.

WHITTINGTON, D.A., WAHEED, A., ULMASOV, B., SHAH, G.N., GRUBB, J.H., SLY, W.S. & CHRISTIANSON, D.W. (2001). Crystal structure of the dimeric extracellular domain of human carbonic anhydrase XII, a bitopic membrane protein overexpressed in certain cancer tumor cells. *Proc Natl Acad Sci U S A*, 98, 9545-50.

WINGO, T., TU, C., LAIPIS, P.J. & SILVERMAN, D.N. (2001). The catalytic properties of human carbonic anhydrase IX. *Biochem Biophys Res Commun*, 288, 666-9.

WU, M.L. & VAUGHAN-JONES, R.D. (1994). Effect of metabolic inhibitors and second messengers upon Na^+-H^+ exchange in the sheep cardiac Purkinje fibre. *J Physiol*, 478 (Pt 2), 301-13.

WU, M.L. & VAUGHAN-JONES, R.D. (1997). Interaction between Na^+ and H^+ ions on Na^+-H^+ exchange in sheep cardiac Purkinje fibers. *J Mol Cell Cardiol*, 29, 1131-40.

XU, L., MANN, G. & MEISSNER, G. (1996). Regulation of cardiac Ca^{2+} release channel (ryanodine receptor) by Ca^{2+}, H^{+}, Mg^{2+}, and adenine nucleotides under normal and simulated ischemic conditions. *Circ Res*, 79, 1100-9.

XUE, Y., VIDGREN, J., SVENSSON, L.A., LILJAS, A., JONSSON, B.H. & LINDSKOG, S. (1993). Crystallographic analysis of Thr-200-->His human carbonic anhydrase II and its complex with the substrate, HCO3. *Proteins*, 15, 80-7.

YAMAMOTO, T., SHIRAYAMA, T., SAKATANI, T., TAKAHASHI, T., TANAKA, H., TAKAMATSU, T., SPITZER, K.W. & MATSUBARA, H. (2007). Enhanced activity of ventricular Na^{+}-HCO_3^{-} cotransport in pressure overload hypertrophy. *Am J Physiol Heart Circ Physiol*, 293, H1254-64.

YAMAMOTO, T., SWIETACH, P., ROSSINI, A., LOH, S.H., VAUGHAN-JONES, R.D. & SPITZER, K.W. (2005). Functional diversity of electrogenic Na^{+}-HCO_3^{-} cotransport in ventricular myocytes from rat, rabbit and guinea pig. *J Physiol*, 562, 455-75.

YASUTAKE, M., HAWORTH, R.S., KING, A. & AVKIRAN, M. (1996). Thrombin activates the sarcolemmal Na^{+}-H^{+} exchanger. Evidence for a receptor-mediated mechanism involving protein kinase C. *Circ Res*, 79, 705-15.

YOSHIDA, H. & KARMAZYN, M. (2000). Na^{+}/H^{+} exchange inhibition attenuates hypertrophy and heart failure in 1-wk postinfarction rat myocardium. *Am J Physiol Heart Circ Physiol*, 278, H300-4.

ZANIBONI, M., SWIETACH, P., ROSSINI, A., YAMAMOTO, T., SPITZER, K.W. & VAUGHAN-JONES, R.D. (2003). Intracellular proton mobility and buffering power in cardiac ventricular myocytes from rat, rabbit, and guinea pig. *Am J Physiol Heart Circ Physiol*, 285, H1236-46.

ZHANG, J.F. & SIEGELBAUM, S.A. (1991). Effects of external protons on single cardiac sodium channels from guinea pig ventricular myocytes. *J Gen Physiol*, 98, 1065-83.